

# **Application of Engineered Amine Oxidases for the Synthesis of Chiral Amines**

A thesis submitted to the University of Manchester  
for the degree of Doctor of Philosophy (PhD)  
in the Faculty of Engineering and Physical Sciences

**2013**

**Diego Ghislieri**

**School of Chemistry**

## Contents

DECLARATION .....	3
COPYRIGHT.....	4
ACKNOWLEDGEMENTS .....	5
THESIS STRUCTURE.....	6
ABSTRACT.....	7
INTRODUCTION .....	9
THESIS OBJECTIVES .....	36
ENGINEERING AN ENANTIOSELECTIVE AMINE OXIDASE FOR THE SYNTHESIS OF ALKALOIDS NATURAL PRODUCTS AND PHARMACEUTICAL BUILDING BLOCK.....	37
Supplementary information .....	56
MAO-N CATALYSED DERACEMISATION OF TETRAHYDRO- $\beta$ -CARBOLINES .....	95
Supplementary information .....	103
DERACEMISATION OF BENZYLISOQUINOLINE ALKALOIDS EMPLOYING MONOAMINE OXIDASE VARIANTS.....	132
Supplementary information .....	146
ASYMMETRIC REDUCTION OF CYCLIC IMINES CATALYSED BY A WHOLE CELL BIOCATALYST PRODUCING AN ( <i>S</i> )-IMINE REDUCTASE.....	151
Supplementary information .....	159
SYNTHETIC CASCADES ARE ENABLED BY COMBINING BIOCATALYST WITH ARTIFICIAL METALLOENZYMES .....	178
Supplementary information .....	196
CHEMO/BI-ENZYMATIC REDOX CASCADE FOR THE ENANTIOCONVERGENT TRANSFORMATION OF ( $\pm$ )-BENZYLISOQUINOLINES INTO ( <i>S</i> )-BERBINES .....	207
Supplementary information .....	219
TRANSAMINASES/MONOAMINE OXIDASES BIOCATALYTIC CASCADE FOR THE SYNTHESIS OF CHIRAL PYRROLIDINES .....	222
Supplementary information .....	226
METHODS .....	239
CONCLUSIONS AND OUTLOOK.....	246
Conclusions.....	246
Outlook .....	248

# DECLARATION

**The University of Manchester**  
**PhD by published work Candidate Declaration**

**Candidate Name:** Diego Ghislieri

**Faculty:** Engineering and Physical Sciences

**Thesis Title:** Application of Engineered Amine Oxidases for the Synthesis of Chiral Amines

Declaration to be completed by the candidate:

I declare that no portion of this work referred to in this thesis has been submitted in support of an application for another degree or qualification of this or any other university or other institute of learning.

## **COPYRIGHT**

The author of this thesis (including any appendices and/or schedules to this thesis) owns any copyright in it (the "Copyright")<sup>1</sup> and he has given The University of Manchester the right to use such Copyright for any administrative, promotional, educational and/or teaching purposes.

Copies of this thesis, either in full or in extracts, may be made only in accordance with the regulations of the John Rylands University Library of Manchester. Details of these regulations may be obtained from the Librarian. This page must form part of any such copies made.

The ownership of any patents, designs, trademarks and any and all other intellectual property rights except for the Copyright (the "Intellectual Property Rights") and any reproductions of copyright works, for example graphs and tables ("Reproductions"), which may be described in this thesis, may not be owned by the author and may be owned by third parties. Such Intellectual Property Rights and Reproductions cannot and must not be made available for use without the prior written permission of the owner(s) of the relevant Intellectual Property Rights and/or Reproductions.

Further information on the conditions under which disclosure, publication and exploitation of this thesis, the Copyright and any Intellectual Property Rights and/or Reproductions described in it may take place is available from the Head of School of Chemistry (or the Vice-President) and the Dean of the Faculty of Engineering and Physical Sciences, for Faculty of Engineering and Physical Sciences candidates.

<sup>1</sup>This excludes material already printed in academic journals, for which the copyright belongs to said journal and publisher. Pages for which the author does not own the copyright are numbered differently from the rest of the thesis.

## ACKNOWLEDGEMENTS

First and foremost I would like to thank my supervisor, Prof Nick Turner, for giving me the opportunity to work on this interesting project in a fascinating and highly interdisciplinary environment.

I am also grateful for the generous support from the Marie Curie research fellowship which made many of the collaborations possible.

I am also very happy of being a part of the Turner/Flitsch group. It was great to work in such a nice atmosphere in the lab as well as in the pub afterwards. Thanks to the colleagues that collaborated on my projects (in alphabetic order) Marcos Diaz Muñoz, Dr Anthony Green, Deborah Houghton, Dr Valentin Köhler, Dr Jennifer Hopwood, Dr Friedemann Leipold, Dr Marta Pontini, Dr Joerg Schrittwieser and Dr Simon Willies. I would also like to thank Dr Mark Corbett and Dr Bas Groenendaal for their fantastic and numerous proof readings.

Finally, I want to thank the Italian community of the Turner/Flitsch group, with them I have always felt at home...

## THESIS STRUCTURE

This thesis describes my work on the development of new variants of MAO-N and their application in deracemisation processes or in combination with other chemo- and biocatalysts.

An introduction to the work highlights the role of amines as building blocks for drugs and the different methods to synthesise them, in particular using monoamine oxidase will be discussed in detail.

The objectives of the thesis are then discussed in a separate chapter.

The main body of the thesis consists of six publications which have either already been published or the manuscripts have been submitted or are ready to be submitted. The format of these papers is modified to fit in the template of the thesis, but no modifications are made to the main text. The supplementary information has been edited so that it contains only the experiments that were performed by Diego Ghislieri. References for the paper are at the end of each manuscript numbered as in the submitted version. Initially, there are four papers discussing different enzymes (MAO-N and IRED) used independently. Then, another two papers follow discussing the combination of monoamine oxidase-N with chemocatalysts (Ir-SAV system) and biocatalysts (Berberine Bridge Enzyme) in order to complete a cascade of enzymatic reactions.

Another two small chapters follow the first covers the results that have not been published and the second describes the methods not discussed in the papers supplementary information.

The last chapter is a conclusion and an overview of the further development of this project.

## ABSTRACT

The development of cost-effective and sustainable catalytic methods for the production of enantiomerically pure chiral amines is a key challenge facing the pharmaceutical and fine chemical industries. There is an increasing demand for broadly applicable synthetic methods which deliver the desired amine product in high yield and enantiomeric excess (e.e.).

Previously we have described the development of variants of monoamine oxidase from *Aspergillus niger* (MAO-N) which are able to mediate the complete conversion of racemic amines to the corresponding enantiomerically pure products in a single step. In this thesis we report a panel of MAO-N variants (D5, D9 and D11) developed in our laboratory, which are able to mediate the deracemisation of primary, secondary and tertiary amines with broad structural features. In particular, we have synthesized and subjected to deracemisation a broad range of tetrahydroisoquinolines and tetrahydro- $\beta$ -carbolines checking enantioselectivity and enantiopreference of our biocatalysts. A relation between lipophilicity of the substituents and enantiopreference of the enzyme has been identified. We have also engineered a new MAO-N variant (D11) with a greatly increased substrate scope and enhanced tolerance for bulky substrates. Application of this engineered biocatalyst is highlighted by the asymmetric synthesis of the generic drugs Solifenacin and Levocetirizine as well as a number of important classes of biologically active alkaloid natural products. We also report a novel MAO-N mediated asymmetric oxidative Pictet-Spengler approach to the synthesis of (*R*)-harmicine.

Another challenge facing the chemist in the new millennium is the development of cleaner and more efficient chemical processes. To this aim the combination of two or more catalytic systems to complete a series of cascade reactions is considered particularly appealing. We have reported a concurrent redox cascade for the deracemisation of pyrrolidines and tetrahydroisoquinolines using our monoamine oxidase-N with a biotinylated Ir-complex within streptavidin (SAV). To achieve the final goal it is necessary to shield the metal inside a host to avoid the mutual inactivation of the two catalysts. We have also described the combination of MAO-N with berberine bridge enzyme (BBE) for the synthesis of berbines (tetrahydroprotoberberines), which represent a sub-class of tetrahydro-isoquinoline

alkaloids found in various plants. This bi-enzymatic cascade allows the synthesis of these structures achieving a theoretical 100% yield instead of the 50% given by the kinetic resolution using BBE itself.

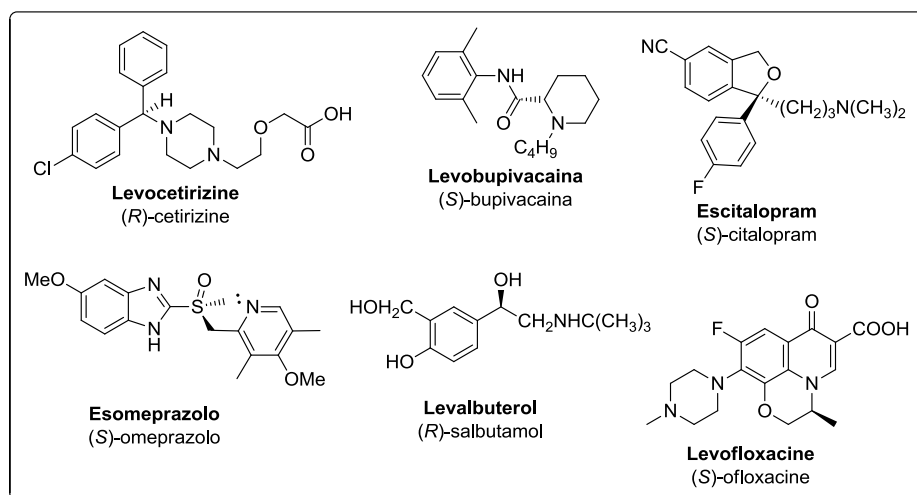


## INTRODUCTION

### Synthesis of chiral bioactive molecules

Enantiomerically pure amines, amino acids, amino alcohols and alcohols are playing an increasingly important role as building blocks in the pharmaceutical and agrochemical industry, where high purity (usually >99.5%) and relative large quantities of compounds are required.

The life-science sector is one of the most important markets served by the chemical industry. Enantiomerically pure intermediates which can be used as building blocks, chiral auxiliaries, or advanced intermediates constitute 15% of the market. At the beginning of the new millennium, the total revenue from sales of these special intermediates in life-science industries was estimated to exceed 20 billion pounds with an annual increasing rate of about 7–8%. [1]



**Figure 1.** Selected examples of marketed single enantiomers of drugs which have been previously sold as racemic mixture.

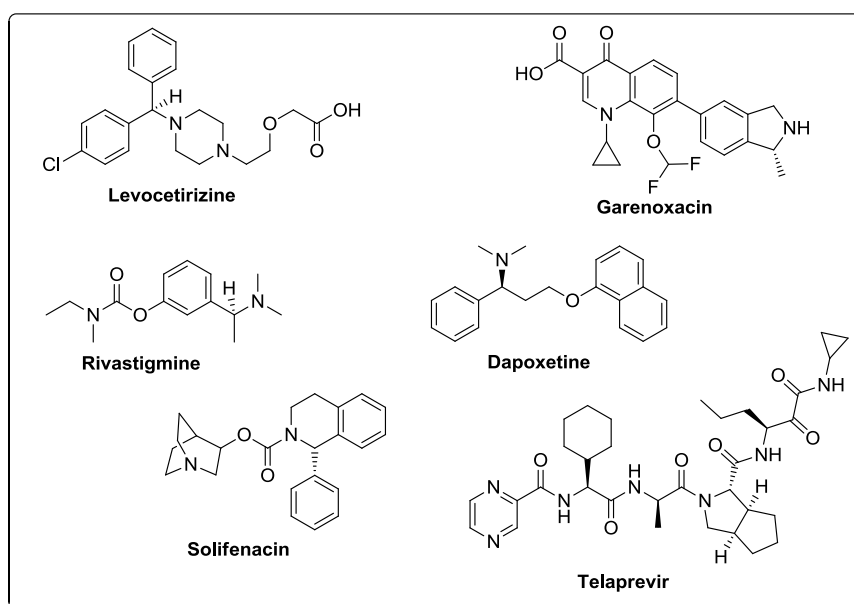
An important boost to the chiral molecules market was given by the US Food and Drug Administration (FDA) and the European Committee for Proprietary Medicinal Products after the discovery that the enantiomers of a pharmaceutically active molecules, upon different interaction with bioreceptors, could produce different biological responses; the most famous example was the Thalidomide<sup>®</sup> where only the (R)-enantiomer of this molecule has a sedative property while the opposite (S)-enantiomer has teratogenic effects. As a result of this, the two agencies introduced strict regulations which came into effect in 1992, requiring the targeted synthesis of

one stereoisomer. In particular they have stated that the pharmaceutical action of each enantiomer of a product must be characterised and since 1997 the introduction of the fast-track, the single-isomer program of the FDA has allowed pharmaceutical companies to shorten registration times with the development of a single enantiomer drug from a previously marketed racemate. This so-called “chiral switch”, which allows the companies the extension of patent term in addition to lower dosages and improved efficacy, was also a driving force to convert racemic active compound into the enantiomerically pure form (Figure 1). Following the introduction of these rules, the demand for drugs as well as many other synthetic products in an enantiopure form has continuously increased and the development of different and successful methods to obtain molecules in a non-racemic form have become crucial.

The same trend was followed in the agrochemicals industry whereas enantiomerically pure active compounds can reduce the quantities necessary improving the economics of the project and reducing the environmental impact.

### Chiral amines, importance and synthesis

Enantiomerically pure amines were widely used as chiral auxiliaries and resolving agents and are now increasing in importance as well as monetary value especially as building blocks for the synthesis of pharmaceuticals and agrochemicals (Figure 2).[2]

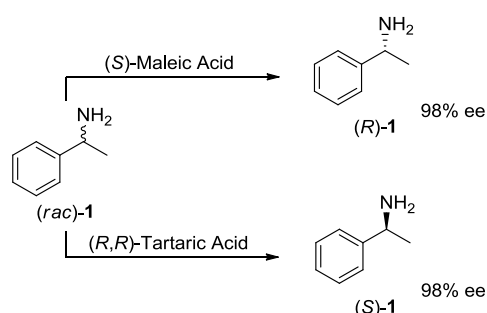


**Figure 2.** Pharmaceutical drugs in development or in the clinic that contain chiral amine building blocks

Classical methods to obtain enantiopure amine include crystallisation of the

diastereoisomeric salt, enantioselective synthesis via a reduction of the corresponding enamine or imine using a optically-active auxiliary and asymmetric reductive amination.[3]

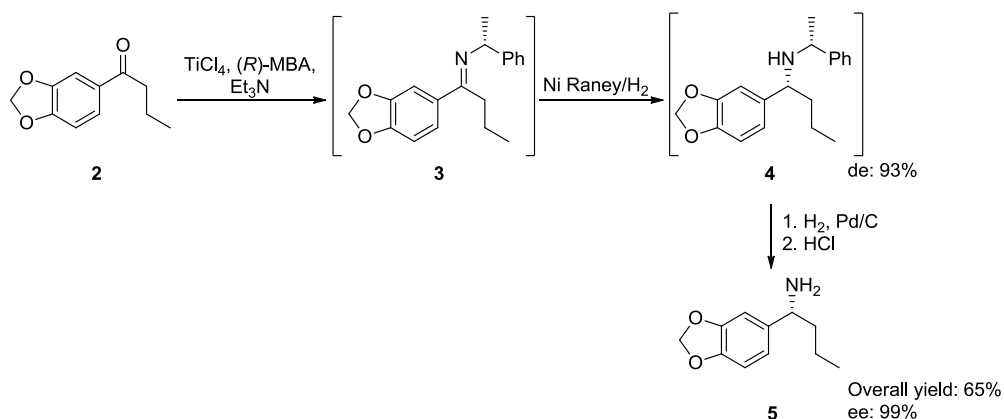
The diastereomeric crystallisation of enantiopure amine salts with chiral carboxylic acids is currently still of considerable importance for the isolation of enantiopure amines. However, this technique suffers from an important drawback, since the maximum yield from the starting racemate of the desired enantiomerically pure product is 50%, while the other 50% generally is discarded. Industrially, diastereomeric crystallisation has been used to obtain optically pure (*R* or *S*)-methyl benzylamine (**1**) using either (*S*)-maleic[4] or (*R,R*)-tartaric acid (Scheme 1).[5]



**Scheme 1.** Diastereomeric crystallisation of (*R* or *S*)-**1** using (*S*)-maleic or (*R,R*)-tartaric acid

A different approach for the synthesis of enantiopure amines is the asymmetric hydrogenation of the corresponding imine and the main strategy is the use of transition metal catalyst. The problem lies in the fact that is usually necessary to activate the imine (using groups such as phenyl, benzyl, substituted phenyl, phosphinoyl or sulfonyl) and then cleavage of the auxiliary group to give the free amine. Acyclic imines undergo asymmetric hydrogenation with various transition metals such as Rh, Ru, Ir and Ti. Currently, iridium is the most useful metal for acyclic imine reduction but its high price limits the applicability on an industrial scale.[3]

Bristol-Myers researcher developed a synthetic route, without isolating any intermediate, to make the leukocyte elastase inhibitor **5**. They reacted ketone **2** with (*R*)-**1** to obtain the Schiff base **3** which is enantioselectively reduced to the amine **4** with a good diastereoisomeric excess, subsequent cleavage and crystallisation of the hydrochloric salt led to **5** in optically pure form (Scheme 2).[6]

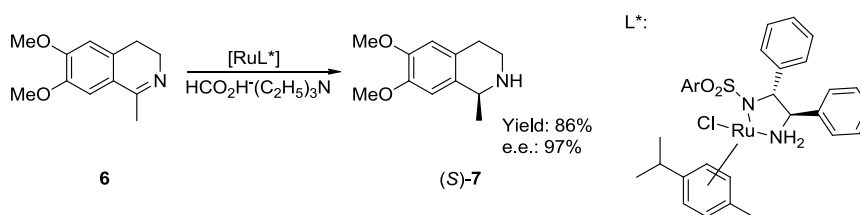


**Scheme 2.** Synthesis of **5** using a Ni Raney catalysed enantioselective reduction of the Schiff base **3**

A similar approach for the synthesis of enantiopure amines is the enantioselective reduction of prochiral molecules containing cyclic C-N double bonds via organometallic or organocatalytic systems.

In 2008, Xiao and co-worker developed the enantioselective reduction of cyclic imines as dihydroisoquinolines and dihydro- $\beta$ -carbolines using a Rh-diamine catalyst, which affords excellent enantiomeric excess in the asymmetric hydrogenation.[7]

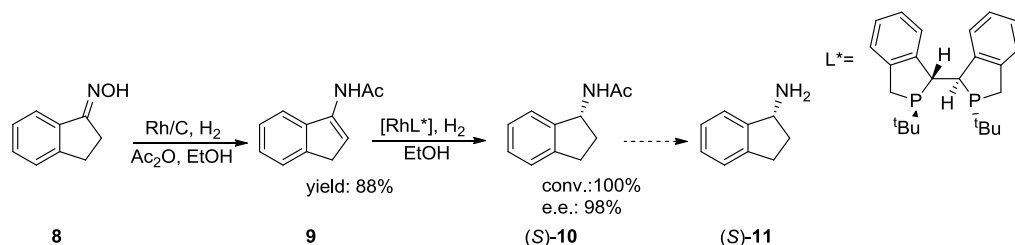
Concurrently, several groups developed a transfer hydrogenation system which uses stable organic hydrogen donors and it is an attractive alternative to the classical hydrogenation in view of the less hazardous properties of the reducing agents as well as the operational simplicity. The enantioselective reduction is carried on under classical Noyori conditions (diamino ligand and Ru catalyst)[8] either in the classical organic solvent[9] or in aqueous media.[10]



**Scheme 3.** Ru-catalysed enantioselective reduction of **6** to obtain (*S*)-Salsolidine (**7**)

Another approach to the synthesis of chiral amines is the hydrogenation of the corresponding enamide. Commonly, N-acetylenamides are synthesised via one-pot reactions of aromatic nitriles with a Grignard reagent followed by addition of acetic anhydride (Blaise reaction); other approaches involve the formation of oximes from

ketones followed by acetylation in presence of Et<sub>3</sub>P. Hydrogenations of enamines are usually carried on in presence of chiral phosphorous ligands and transition metal catalyst. Recently, Zhang developed a catalytic process for the Rh-catalyzed reduction of N-acetylenamides, involving a hydroacylation of ketoximes followed by enantioselective reduction.[11]



**Scheme 4.** Rh-catalyzed reduction of N-acetylenamide (**9**) for the synthesis of enantiopure (*S*)-**11**

Besides the synthesis of chiral intermediates and products using established chemical methods, in the last 20 years, the development of new technologies such as recombinant DNA, expression systems, genome sequencing and gene synthesis, has allowed the rapid identification and production of novel enzymes. In particular, recombinant DNA technology allowed the development of enzyme engineering; a powerful tool to make more stable and tuneable biocatalysts and address enzyme limitations for synthetic chemistry. The implementations of these advances for biocatalysis in large-scale industrial processes opened up new perspectives and economically more attractive methods for the production of active compounds.[12]

The greatest advantage of biocatalysis is that enzymes are often able to differentiate between enantiomers of a racemic substrate giving high chemical selectivity or regioselectivity to the transformation. With the use of enzymes, enantiopure compounds (e.e. >99%) can be routinely achieved, although it is not possible in every case. The importance of obtaining enantiopure molecules as well as sustainable development with “environmentally benign manufacturing” and “green chemistry” in the pharmaceutical industry increased the interest in the use of biocatalysts in the synthesis of advanced drugs intermediates.

Compared with other kinds of catalysts, as homogeneous catalysts, the enzymes have different characteristic which could be either advantages or disadvantages. Enzymes usually work at mild conditions (near-ambient temperature and pH) and in aqueous media, which nowadays is considered as an advantage rather than a drawback.

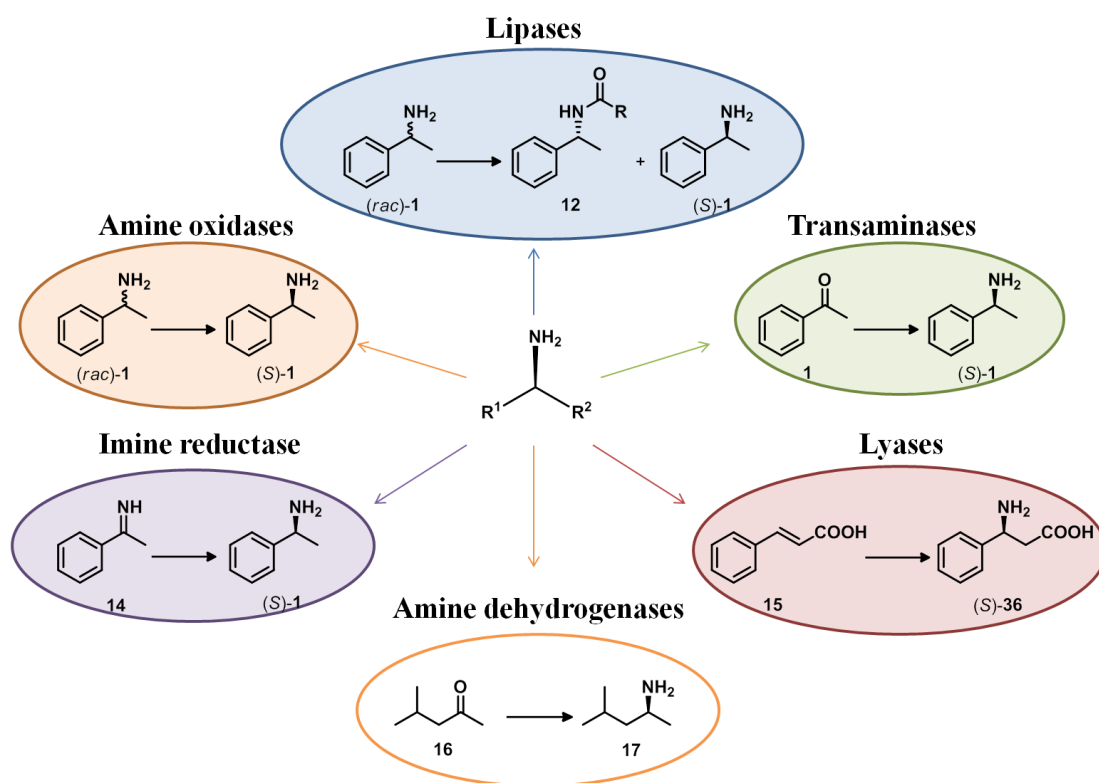
A major disadvantage of enzymes is that, despite their great benefits in terms of selectivity, usually their stability is not sufficient for an intensive use. Additionally, an insufficient base knowledge of biocatalysis and biotechnology in the big industry remains a problem as well as a challenge and this lead to long development times to find more tuneable, active and stable enzymes. The advantages and disadvantages of using enzymes as catalysts in organic reactions are shown below in Table 1.

<b>Advantages</b>	<b>Disadvantages</b>
Very high enantioselectivity	Often low specific activity
Very high regioselectivity	Instability at extremes of T and pH
Transformation under mild conditions	Availability for selected reactions only
Solvent often water	Long development times for new enzymes

**Table 1.** Advantages and disadvantages of biocatalysts and enzymes.

Only in the last decade, biocatalysts have been intensively studied and new enzymes have been found able to catalyse an increasing number of reactions. This translates into an increasing range of applications for biocatalysis on an industrial scale. Moreover, biocatalysts have been combined with chemical catalysts or utilised in a network of reactions in the cell[13] and the main challenge over the coming years will be the combination of different enzymes to complete a cascade of enzymatic reactions.[14]

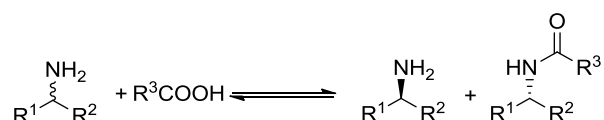
In the next part of the introduction the enzymes employed in the synthesis of chiral amines will be discussed in detail (Figure 3).



**Figure 3.** Classes of enzymes that catalyse the enantioselective synthesis of amines

### Lipases

Lipases are enzymes belonging to the esterase, which catalyse the formation or the cleavage of esters, in particular fats (Scheme 5).

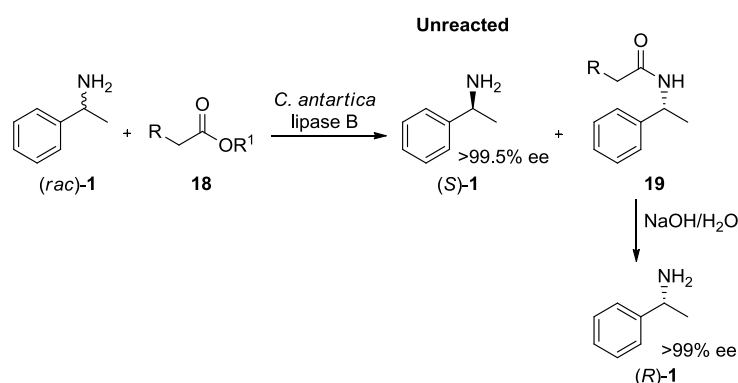


**Scheme 5.** General scheme for a lipase-catalysed biotransformation

These enzymes started to be used industrially at the beginning of the '90s when different companies explored biocatalysis as a route for the enantioselective hydrolysis of racemic amides. In the mid-'90s Bayer developed the kinetic resolution of  $\alpha$ -methylbenzylamine (**1**) using a lipase B from *Candida Antartica*. Despite the high enantiomeric excess that was achieved this process required unacceptably high catalyst concentrations, making it industrially inviable.

At the end of the '90s the immobilisation of these enzymes gave higher stability and the possibility to recycle the catalyst leading to a more efficient process. After some development BASF patented and started to produce in tons scale the lipases

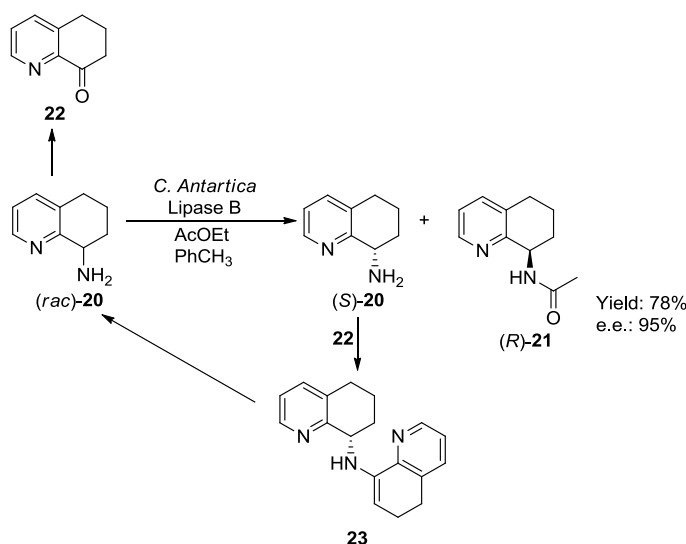
catalysed kinetic resolution of racemic amines. In this process the amide (*R*)-**19** was produced in a single step along with the unreacted (*S*)-**1** in nearly optically pure form. After separation of **19** via distillation or extraction, (*R*)-**1** was released through a basic hydrolysis of the amide (Scheme 6). Another remarkable feature of the enzymology used for this kinetic resolution was the broad substrate spectrum of the catalyst, which allows the use of the same process for the resolution of other amines.



**Scheme 6.** Synthetic route for the resolution of (*S*)-**1** and (*R*)-**1** using *C. Antartica* lipase B patented by BASF

In some cases, in order to increase the final yield of the kinetic resolution it is possible to transform this type of process into a dynamic kinetic resolution (DKR), in which case it is possible to convert the reactant with 100% completion because both (reactant) enantiomers engage in a chemical equilibrium and exchange. An example of DKR is the acetylation of a racemic 8-aminotetrahydroquinoline (**20**) using *Candida antartica* Lipase B; in this case, the enzyme only converts the (*R*)-enantiomer into the acetamide **21** and, in regular kinetic resolution, a 50:50 mixture of unreacted (*S*)-amine (**20**) and (*R*)-acetamide (**21**) would be obtained. However, a catalytic amount of the ketone **22** allows the racemisation of (*S*)-**20**, thus increasing the yield of (*R*)-**21** beyond 50% and turning the process into a DKR (Scheme 7).[15]



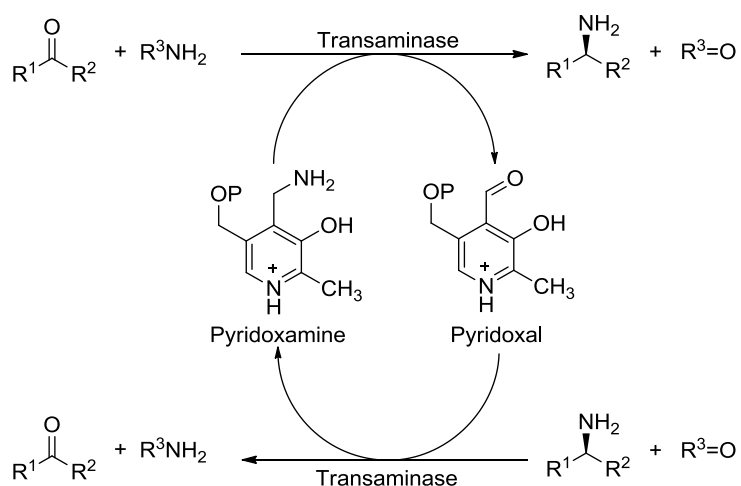


**Scheme 7.** Dynamic kinetic resolution of 8-aminotetrahydroquinoline (**20**) with *C. antartica* Lipase *B*.

The use of lipases for the kinetic resolution of amines is state of the art technique and until now many results obtained through the combination of biocatalyst and acylating agents cannot be surpassed.

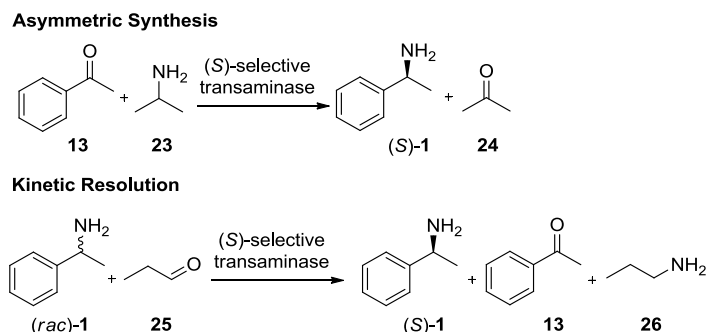
### Transaminases

$\omega$ -Transaminases (TA) are enzymes which transfer an amino group from an amino donor to a carbonyl moiety. The reaction is readily reversible and the direction is determined by the reactant in excess. Transaminases require pyridoxal-phosphate as coenzyme, which is converted into pyridoxamine when the amino group is converted into a ketone in the deamination reaction and *vice versa* in the amination reaction (Scheme 8).



**Scheme 8.** General scheme for transamination reactions

As biocatalysts, TAs can be applied either for the asymmetric synthesis of amines starting from the corresponding ketones or for the kinetic resolution of racemic amines. The first of these processes is more commonly employed, offering the advantage of 100% product yields (Scheme 9).[16]



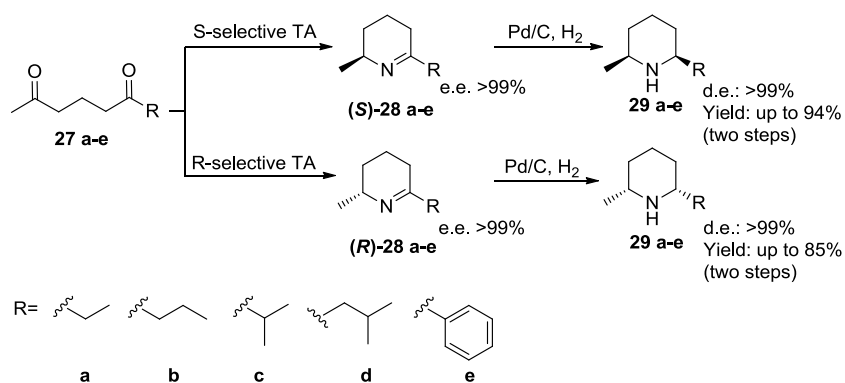
**Scheme 9.** Transaminases can be applied either for the asymmetric synthesis of amines starting from the corresponding ketones or for the kinetic resolution of racemic amines.

At the beginning of the '90s Celgene researchers developed both (*R*)- and (*S*)-selective transaminases able to aminate prochiral ketones to synthesise a number of phenyl methylamines in more than 90% yield.

Despite their great potentials TA's started to be used in organic synthesis only recently, mainly because of three big limitations: product inhibition, limited applicability only to the synthesis of primary amines and narrow wild type substrate scope.[17]

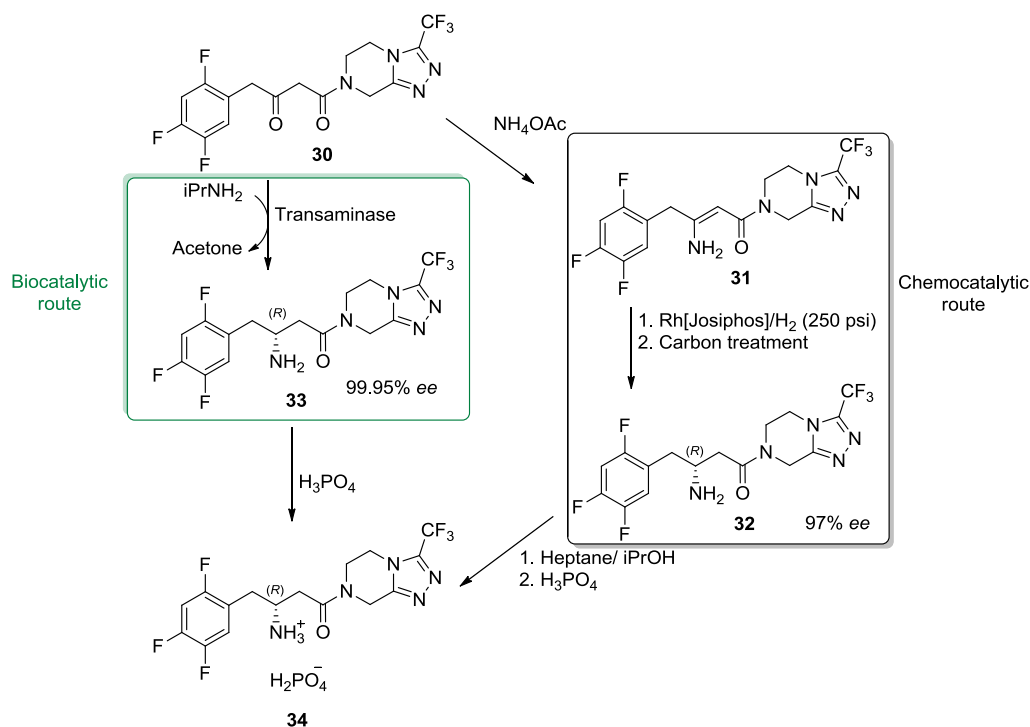
A number of techniques have been developed to prevent product inhibition. In particular it is possible to extract the inhibitory ketone from the aqueous phase using a ketone removal solvent[18], or using a low molecular weight amine donor such as *isopropyl* amine yielding the volatile ketone acetone as co-product which can then be removed under reduced pressure.[19]

Due to the enzyme mechanism it is possible to directly synthesise only primary amines (see Scheme 8). To address this limitation, recently the Kroutil group in collaboration with Sandoz researcher have reported the first synthesis of cyclic secondary amines via a transamination reaction followed by intramolecular imine formation, in particular they described the regio- and enantioselective amination of 1,5 diketones (**27a-e**) for the synthesis of 2,6 disubstituted piperidines (**29a-e**) (Scheme 10).[20]



**Scheme 10.** Enantioselective synthesis of 2,6 disubstituted piperidines starting from 1,5 diketones using  $\omega$ -transaminases

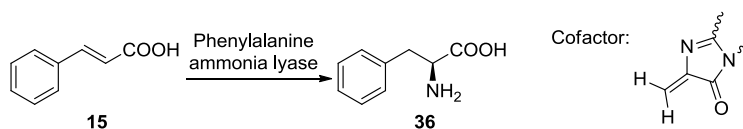
The most successful example of using TA in industrial application is the engineering of ATA-117 transaminase for the synthesis of Januvia<sup>®</sup> (Sitagliptin phosphate **34**, Scheme 11) process. Codexis researchers, in collaboration with Merck, started from a (*R*)-selective  $\omega$ -TA (ATA-117) with activity toward small substrates related to their target molecule and they used semi-rational design to improve the activity toward a truncated substrate; then, after several more rounds of random and targeted mutagenesis, they ended up with the development of a new enzyme designed for industrial yields and operating conditions. Moreover they showed that the biocatalytic process not only reduced the total waste and eliminated all need for heavy metals, but even increased the overall yield by 10% and the productivity (kg/L per day) by 53% compared to the previous Rh-catalysed process.[19]



**Scheme 11.** Different routes for the synthesis of Sitagliptin. Biocatalytic route (left) provides Sitagliptin in 99.9% e.e., chemocatalytic route provides Sitagliptin in 97% e.e.

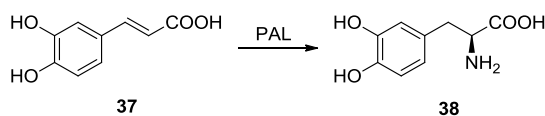
## Lyases

Lyases are a class of enzymes that catalyzed the reversible addition or removal of ammonia to a C-C bond using methyldiene-imidazolone (MIO) as electrophilic prosthetic group. For biocatalytic applications, the synthetic mode (the addition of ammonia) to the unsaturated substrate is the interesting reaction (Scheme 12).



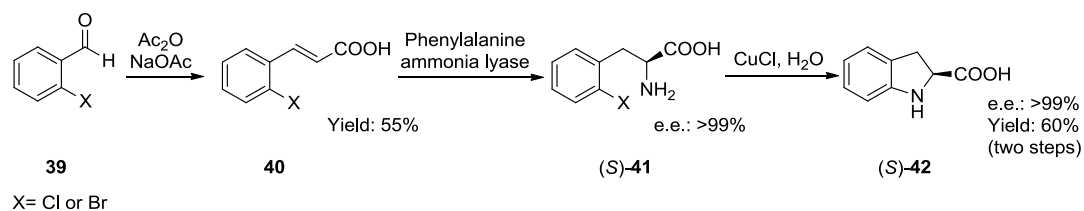
**Scheme 12.** General scheme for a PAL-catalysed biotransformation

For example, the phenylalanine ammonia lyase (PAL) catalyzed the formation of the enantiopure L-DOPA (38) and this transformation is industrially used at ton scale (Scheme 8).



**Scheme 13.** Phenylalanine ammonia lyase (PAL) catalysed formation of the enantiopure L-DOPA

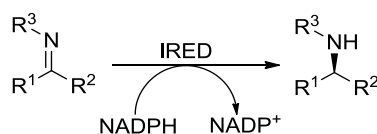
The activity of wild-type PAL enzymes was limited to the substrate phenylalanine but recently DSM have claimed that it was necessary to clone and express novel ammonia lyases mutants with enhanced operational stability and broader activity to match the challenge of the industrialisation of the process.[21] In particular they developed a new procedure currently used for ton-scale production of (*S*)-indolinecarboxylic acid (**42**) starting from substituted benzaldehydes (**39**) combining chemo- and biocatalysis.[22]



**Scheme 14.** Synthetic route for the industrial production of (*S*)-**42** combining biocatalysis with chemocatalysis

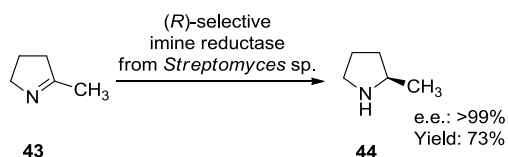
### Imine reductases

Imine reductase (IRED) is a class of enzymes catalysing the NADPH-dependent enantioselective reduction of imines to the corresponding amine (Scheme 15).



**Scheme 15.** General scheme for an IRED-catalysed biotransformation

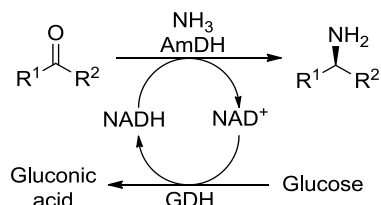
Recently, Mitsukura and co-workers, after the screening of different yeasts, bacteria and fungi strains, discovered an (*R*)-selective imine reductase from *Streptomyces* sp. GF3587.[23] After screening of a broad range of substrates they found that it was only able to reduce the substrate 2-methyl pyrroline (**43**) with high enantioselectivity (Scheme 16).[24]



**Scheme 16.** Enantioselective reduction of **31** using an (*R*)-selective imine reductase from *Streptomyces* sp. GF3587

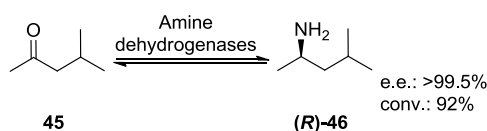
## Amine dehydrogenases

Amine dehydrogenases (AmDHs) are a class of enzymes that catalyse the enantioselective reductive amination of ketones. Specifically, AmDHs are NADH-dependent enzymes that, if combined with a cofactor recycling system, such as formate dehydrogenase (FDH) or glucose dehydrogenase (GDH), allow the direct production of chiral amines only using an inexpensive reducing agent, such as formate or glucose, and ammonia (Scheme 17).



**Scheme 17.** General scheme for an AmDH-catalysed biotransformation

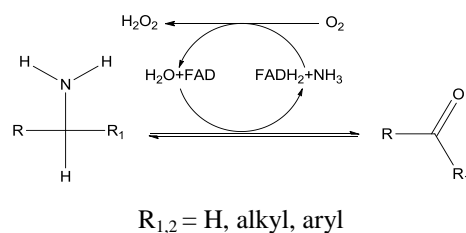
At the beginning of 2000, Itoh *et al.* characterised a new AmDHs from *Streptomyces virginiae* able to catalyse the reductive amination of a range of aliphatic and aromatic ketones. The main drawback of this enzyme was the lack of selectivity that limited the applicability.[25] Abrahamson *et al.* have recently reported the development of a new variant of AmDH for the enantioselective reductive amination of methyl isobutyl ketone (**45**), starting from a Leucine dehydrogenase from *Bacillus stercorophilus*. Using the CASTing approach they found an (*R*)-selective mutant with good substrate specificity (Scheme 18).[26]



**Scheme 18.** AmDH catalysed reductive amination of ketones.

## Amine oxidases

Amine oxidase (AO) is a member of the oxidoreductase-class of enzymes (EC 1.4.3.4.). Enzymes of this class catalyse oxidoreduction reactions, particularly monoamine oxidases (MAOs) are able to oxidize amines to imines, which, in the case of primary amines, are hydrolyzed in water to give aldehydes or ketones, with simultaneous reduction of oxygen to hydrogen peroxide (Scheme 19).



**Scheme 19.** General reaction scheme for oxidative deamination using amine oxidase

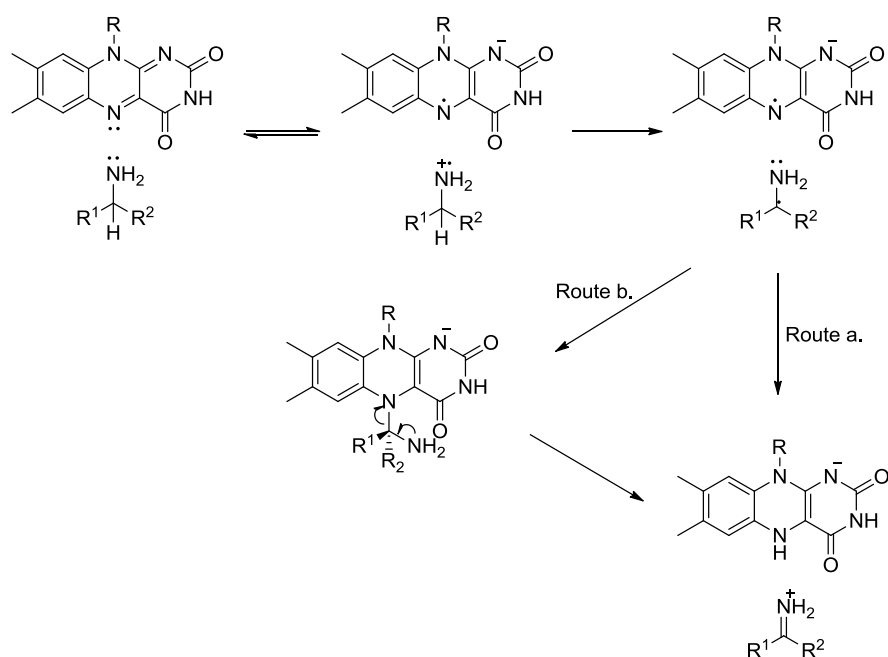
Amine oxidases have been classified into two groups: Type I and Type II Amine Oxidase. Type I are copper dependent enzymes and Type II are flavin dependent enzymes. Copper dependent AOs contain two cofactors: copper and PQQ (Pyrroloquinoline quinone); they are found in bacteria, fungi, plants, animals and are involved in several metabolic pathways including amino acid metabolisms and alkaloids biosynthesis. Flavin-dependent amine oxidases, primarily comprising monoamine oxidase (MAO), are found in mammals, fungi and bacteria. In humans the amine oxidases are membrane bound and catalyse the inactivation of neurotransmitters such as serotonin and dopamine and the catabolism of monoamines ingested in food. Amino oxidases characterised in lower eukaryotes are not membrane proteins and principally have a role in providing the cell with nitrogen to assimilate in the form of ammonia. For biocatalytic applications, monoamine oxidases from the fungus *Aspergillus niger* (MAO-N) have attracted many attentions in the last decade. These enzymes contain both the two types of amine oxidase: the Type I copper-dependent and the Type II flavin-dependent. Type I enzymes, in their catalytic cycle, form an intermediate imine which remains covalently bound to the protein and consequently these enzymes were deemed unsuitable for biocatalytic purpose. On the contrary, Type II enzymes generate free imines that can be substrates for further chemical reactions allowing their use as biocatalysts.

**Mechanism of monoamine oxidase**

A number of mechanisms for Type II MAO-catalysed amine oxidation have been proposed over the years and several reviews are available.[27] There are currently three main mechanistic proposals for MAO catalysis. These comprise: 1) the concerted polar nucleophilic mechanism; 2) the direct hydride transfer mechanism; and 3) the single electron transfer mechanism.

At the beginning of the '80s, Silverman proposed an aminyl radical cation mechanism, which involves single electron transfer (SET), applied to the MAO-

catalyzed oxidation. According to his studies, a non-bonded electron of the amine nitrogen is transferred, in a slow step, to the flavin giving the flavin semiquinone radical and the amine radical cation. This makes the  $\alpha$ -proton of the amine more acidic and consequently the proton loss would be easier. The proton loss generates a radical which undergoes decomposition by two possible routes: a second transfer of one electron to the flavin (route a); radical combination of radicals followed by two-electron transfer to the flavin (route b). Both the mechanisms generate the same products, the reduced flavin and the iminium ion (Scheme 20).[28]

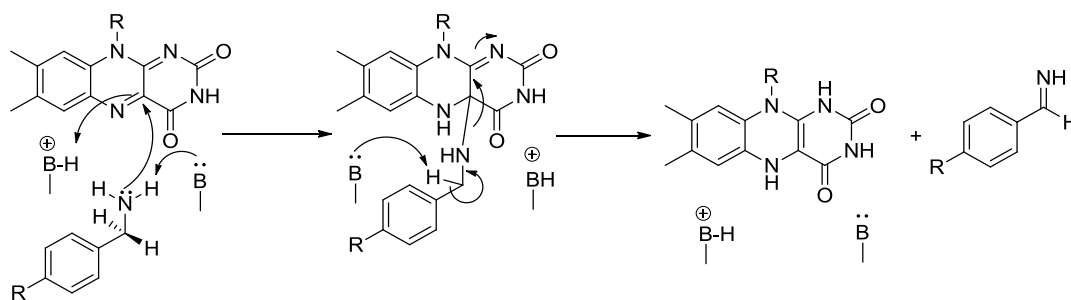


**Scheme 20.** MAO catalysed oxidation of amines by the aminyl radical cation mechanism

In this study, the *Aspergillus niger* flavin-dependent monoamine oxidase MAO-N was used. Millers and Edmondson proposed a polar nucleophilic mechanism for mammalian MAO-A and MAO-B[29] and, based on their studies, we propose a similar mechanism for MAO-N.[30] The FAD is non-covalently attached to the enzyme but there are several H-bonding and electrostatic interactions between the isoalloxazine ring and the protein.[30] No basic active site residue was identified that could facilitate the proton abstraction from the  $\alpha$ -C of the amine. Instead, the N<sub>5</sub> atom of the flavin is proposed to function as a base and abstract the  $\alpha$ -proton of the amine. The amine oxidation is initiated by the nucleophilic attack of the amine nitrogen on the flavin. The amine moiety of the bound substrate is in its deprotonated form and attacks the C<sub>4a</sub> position of the flavin to form a flavin C<sub>4a</sub> adduct. The formation of the



adduct results in the generation of a basic N<sub>5</sub> position, which subsequently abstracts the pro-*R*-H from the substrate (Scheme 21).

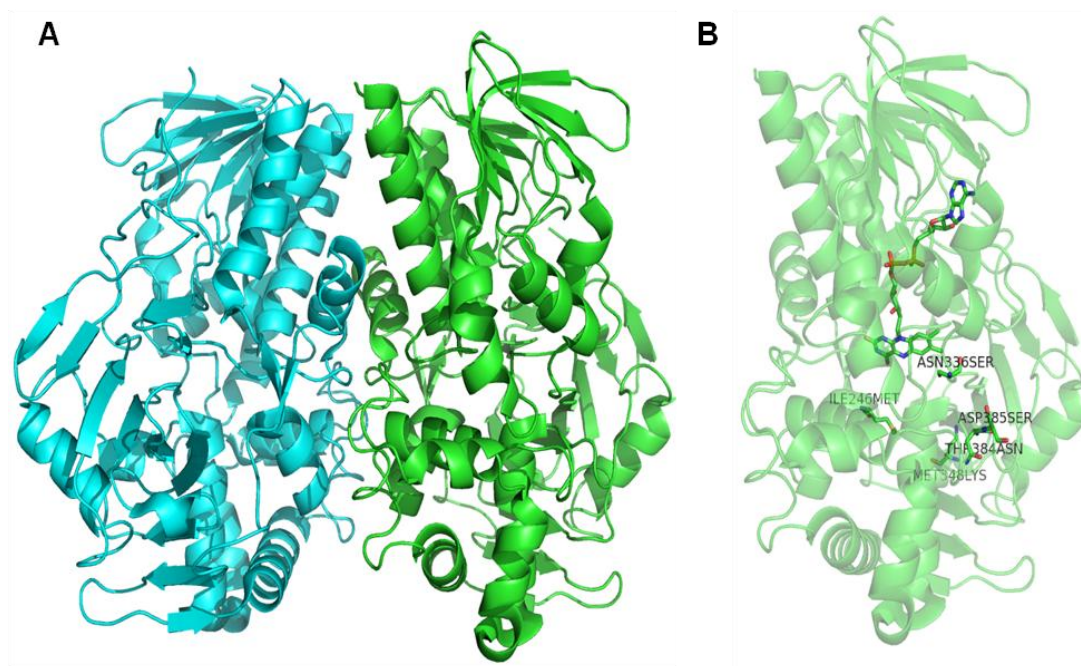


**Scheme 21.** Hypothesis of nucleophilic mechanism scheme for the reductive half reaction of MAO-N catalysis where the products of amine oxidation are the protonated imine and the flavin hydroquinone. The FAD is non-covalently attached to the enzyme but there are several H-bonding and electrostatic interactions between the isoalloxazine ring and the protein.[30]

### X-ray crystal structure

The first MAO-N crystal structure was solved in 2008 by Atkin *et al.*[31] which reported the X-ray diffraction analysis of MAO-N mutant D5 and subsequent structure solution.

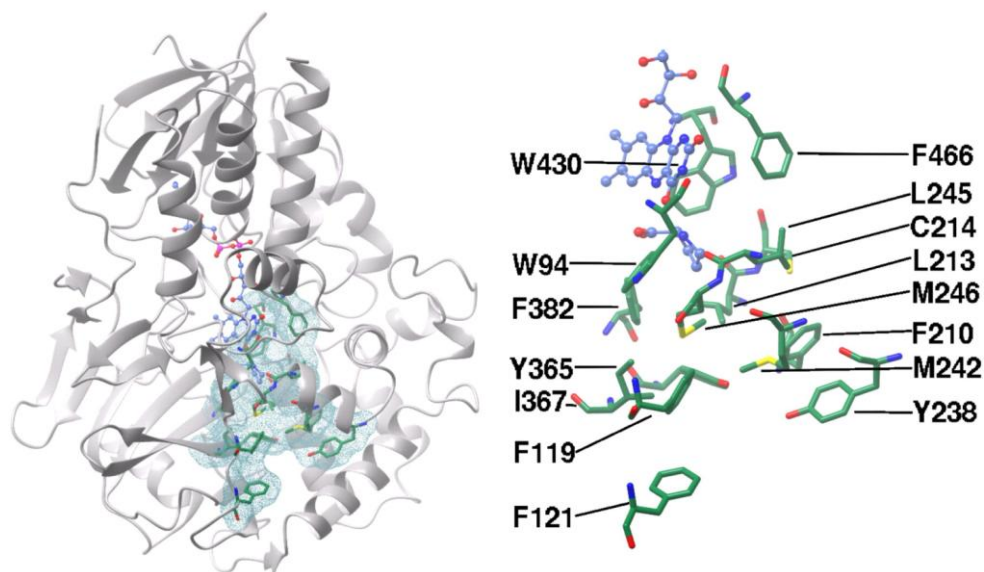
MAO-N D5 contains five amino acid substitutions from the wild type. N336S, I246M and M348L, which were present in the MAO-N D3 mutant, confer the ability to catalyse the oxidation of secondary amines. In particular N336S reduces the steric bulk behind the amino acid W430 of the aromatic cage and I246M gives greater flexibility within the substrate binding site. In the MAO-N D5 variant, the two additional mutations, T384N and D385S, were added leading to a new variant able to oxidise tertiary amines. These mutations appear to remotely influence the active-site environment through modifications in tertiary structure that moves the side chain of F382 altering electronic and steric character of the active site near the flavin (Figure 4).



**Figure 4.** a) Dimeric structure of MAO-N D5 variant (PDB code 2VVM). b) Monomer of MAO-N D5 with the flavin cofactor and mutations highlighted.[31]

### Active site

The active site cavity in human MAO-B consists of a hydrophobic cavity on the *re* face of the isoalloxazine ring of the FAD. In MAO-N 15 residues were identified, forming a mainly hydrophobic cavity likewise on the *re* face of the isoalloxazine ring of the FAD, which is located close to the protein surface and not buried deeply within the protein.[31]



**Figure 5.** Proposed hydrophobic cavity in MAO-N-D5.[29] The flavin cofactor is shown in blue, residues W430 and F466 are part of the aromatic cage, residues

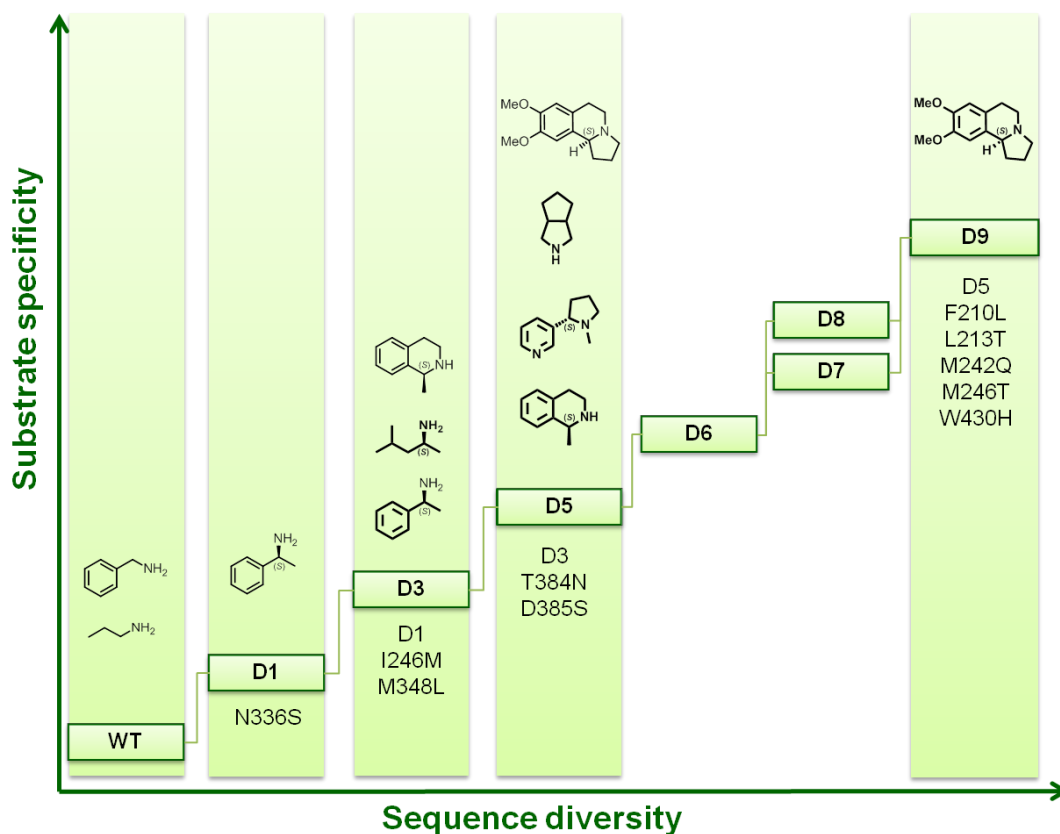
M242, M246, L213 and F210 form the entrance channel to the aromatic cage

An important feature of the MAO-N active site is the presence of residues forming the sides of an ‘aromatic cage’ with the FAD, very similar to those observed in human MAO. The cage in MAO-N is formed by W430 and F466 (Figure 5), which are positioned at an approximately perpendicular angle to the re face of the isoalloxazine ring. Residue W430 was found positioned further back from the FAD and modelling studies highlighted that it may therefore be involved in substrate stabilisation. In particular, docking of  $\alpha$ -methyl benzylamine showed a theoretical alignment of the substrate with W430.

The conservation of aromatic residues at this position in a number of amine oxidases, such as polyamine oxidase and both human MAO-A and MAO-B, suggests that these residues, as part of the aromatic cage, play an important role in the function of the enzyme. In 2006, the possible role of the aromatic cage was explored in depth by Li *et al.*[32], who performed detailed mechanistic studies that suggested both electronic and steric functions for the cage in MAO-B. Furthermore in the MAO-N crystal structure an entrance channel was identified within the substrate cavity and consists of M242, M246, L213 and F210. These amino acids were identified as target for further round of mutagenesis in order to increase the specific activity toward bulky substrates as Crispine A. Therefore, a rational design approach yielded a new MAO-N variant with enhanced activity but its crystal structure is not been solved yet.[33]

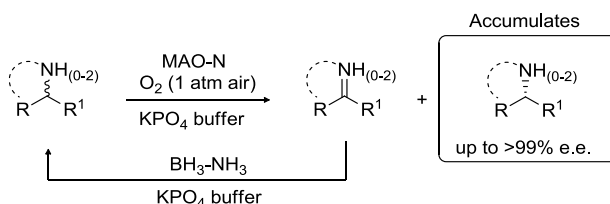
### **MAO-N previous work**

At the beginning of 2000, Turner’s group started using monoamine oxidase from *Aspergillus Niger* (MAO-N) in biotransformations as a good alternative to transaminases to obtain enantiopure amines.[34] Over the course of the past decade, a combination of directed evolution, rational design and high-throughput screening methods were used to develop a ‘toolbox’ of MAO-N variants which display complementary activity and are able to mediate the synthesis of enantiomerically pure chiral amines with diverse structural architectures (Figure 6).



**Figure 6.** Evolution of MAO-N variants from *Aspergillus Niger*. After numbers of cycle of random mutagenesis and directed evolution combined with rational design the panel of MAO-N variants have been developed in our laboratory over the last decade. Starting from the MAO-N wild type able to oxidise only simple primary amines, the MAO-N variants (from D3 to the new D9) are able to mediate the deracemisation of primary, secondary and tertiary amines with broad structural features.

In particular, after finding new mutants with enhanced activity and selectivity, they developed the deracemisation process: a biotransformation where the MAO-N catalysed enantioselective oxidation of primary, secondary and tertiary amines is followed by a non-selective chemical reduction of the achiral imine (Scheme 22).



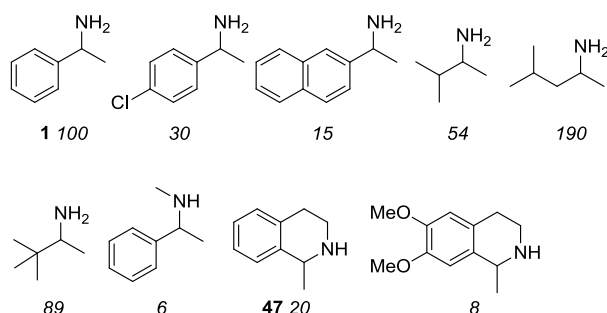
**Scheme 22.** General scheme of a deracemisation process: the MAO-N catalysed the enantioselective oxidation of amines, followed by a non-selective chemical reduction of the achiral imine.

The MAO-N gene from *A. niger* was obtained from Schilling and Lerch,[35] who

previously reported cloning and expression of this enzyme. Subsequently, Sablin *et al.* purified the enzyme and carried out substrate-specificity studies highlighting high activity towards simple aliphatic primary amines e.g. amylamine, butylamine, but was also towards benzylamine (even though at low rate).[36]

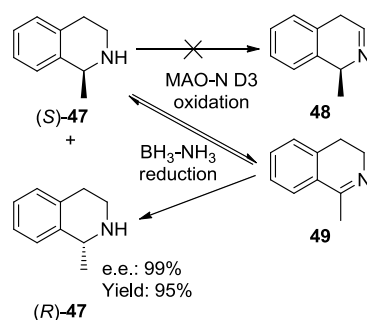
Considering these pioneering studies, in 2002, Alexeeva *et al.*, starting from the MAO-N wild-type used directed evolution to find a mutant with increased activity toward  $\alpha$ -methylbenzylamine **1**. A solid phase screening based upon the capture of hydrogen peroxide by a peroxidase and the use of a dye to detect the positive hits allowed the screening of about 150000 colonies. The catalytic activity of the best mutant (N336S or MAO-N D1) was significantly improved (47-fold higher) and the selectivity for the (*S*)-**1** versus (*R*)-**1** (100:1) had also increased (6-fold) relative to the wild-type enzyme.[37]

Subsequently, Carr *et al.* explored the substrate scope of the new MAO-N D1 mutant (with the addition of M348L mutation) finding high activity toward classes of chiral primary amines, such as substituted phenethylamines, aliphatic ethylamines and cyclic secondary amines (Scheme 23).[38]



**Scheme 23.** Panel of amines used in the screening experiments. Numbers in italics beneath the structures refer to relative rates of oxidation for MAO-N D3 mutant compared to  $\alpha$ -methylbenzylamine.[38]

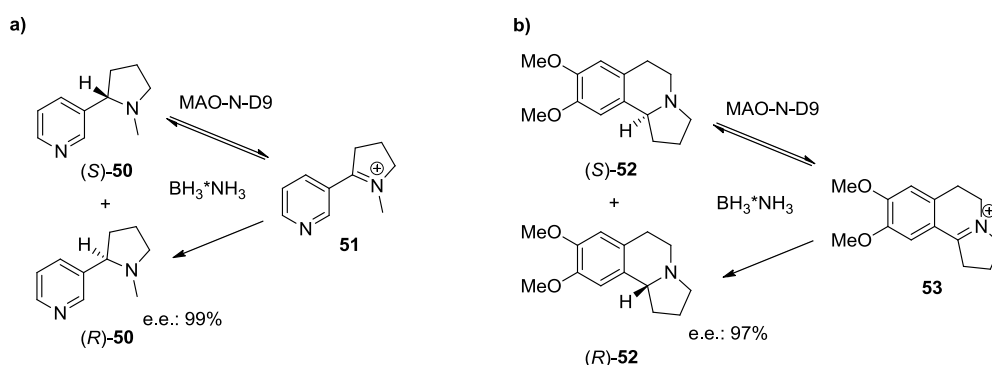
Although this mutant displayed lower activity towards cyclic secondary amines compared to the corresponding primary amines (**47** was oxidized 5 times slower than **1**), this mutant was used to mediate the stereoinversion of (*S*)-**47** in high yield and enantiomeric excess without formation of the intermediate **48** (Scheme 24).[39]



**Scheme 24.** Stereoinversion of (*S*)-**47** using MAO-N D3 in combination with  $\text{BH}_3\text{-NH}_3$ [39]

To increase the activity of the MAO-N D1 mutant, the gene was subjected to random mutagenesis and the library screened against (*R/S*)-**47**. A new mutant with an additional amino acid substitution (I246M; MAO-N D3) located in the entrance channel (Fig. 5) led to a 5.5 fold higher activity if compared with the parent D1 toward the oxidation of **47**. [39]

Further rounds of directed evolution identified another MAO-N mutant (N336S/I246M /M348L/T384N/D385S; D5) with increased activity in comparison with the previous D3 mutant. This variant showed a good activity toward a number of tertiary amines.[40] Therefore, the D5 mutant was used for the stereoinversion of (*S*)-nicotine (**50**) via the intermediate iminium ion **51**, yielding (*R*)-**50** in enantiopure form and for the deracemisation of Crispine A (**52**), an alkaloid which has been shown to possess certain anticancer activity, giving (*R*)-**52** in 97% enantiomeric excess (Scheme 25).[41] This MAO-N mutant was also crystallised in order to better understand the insight of the enzyme and planning further rounds of mutagenesis using a rational design approach (Fig. 4).

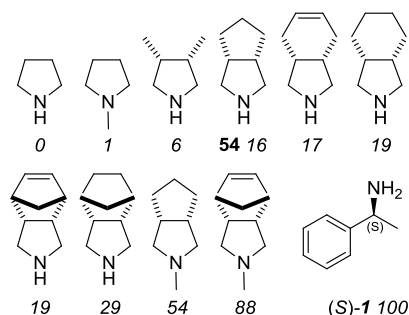


**Scheme 25.** a) Deracemisation of (*R*)-nicotine (**50**) b) Deracemisation of (*R*)-crispine A (**52**).[41]

Compound **52** has also been used as a model substrate for the development of a more

active mutant. Rowles *et al.* modelled the substrate in the active site identifying four amino acids (F210, L213, M242, M246) located in the entrance channel as target residues for site-directed mutagenesis. It was proposed that mutation of these residues could reduce steric interactions with catalytic residues within the active site. To optimise these residues, they created two randomised libraries: library D7 (F210 and L213) and library D8 (M242 and M246). Both libraries were screened against compound **52** and the two most active mutants from each of the four mutations were picked and replicated in combination to produce the synthetic MAO-N variants (D9A-D). The D9C mutant showed the highest activity toward **52** with a 1000 fold improvement in comparison with the parent MAO-N D5 mutant.[33]

To illustrate the potential of using MAO-N in the synthesis of building blocks for pharmaceutical drug, the D5 variant has been applied in the desymmetrisation of a range of 3,4-substituted *meso*-pyrrolidines obtaining the enantiopure imine (*S*-**1**) (Scheme 26).[42]

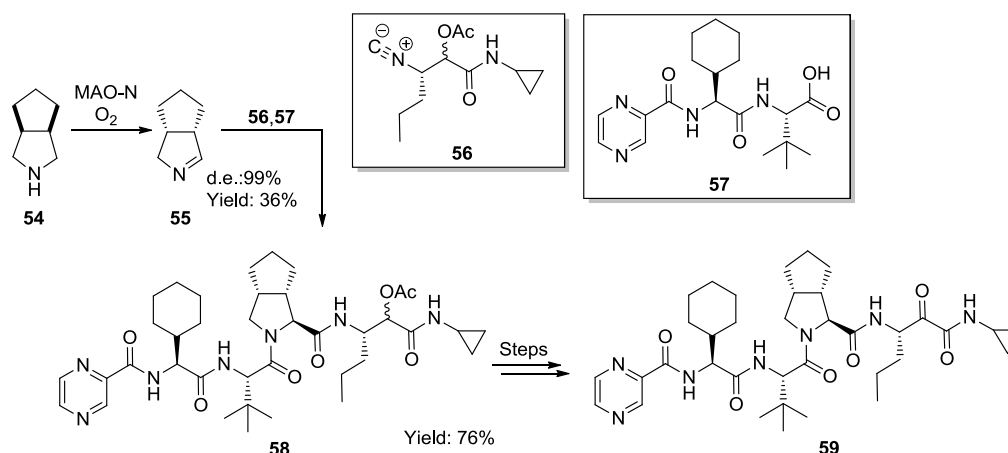


**Scheme 26.** Panel of pyrrolidines used in the screening experiments. Numbers in italics beneath the structures refer to relative rates of oxidation for MAO-N D5 mutant compared to (*S*-**1**).[42]

The corresponding  $\Delta^1$ -pyrrolines, obtained in most cases with enantiomeric excess greater than 98%, were found to serve as useful building block for the synthesis of L-proline analogues and (*R*)-amino nitriles of high enantiomeric purity. In particular **54** was subjected to addition of HCN to form the amino nitrile, which was then hydrolysed to the corresponding proline analogue with high diastereoisomeric excess. Such bicyclic proline analogues are building blocks of the hepatitis C viral protease inhibitors such as Telaprevir (**59**) and Boceprevir (**67**).

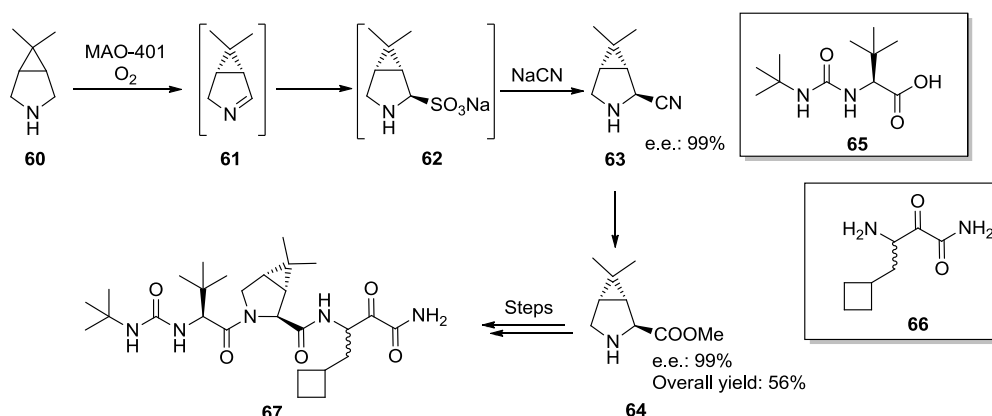
An alternative synthesis of Telaprevir has been developed by Znabet *et al.* using **55** as a substrate in a 3-component Ugi reaction.[43] The enantiopure imine **55** is reacted with the acid **57**, easily made with standard peptide synthesis, and the

isocyanide **56**, synthesised via a Passerini reaction, to give intermediate **58**. Cleavage of the acetyl group and subsequent oxidation of the alcohol gave Telaprevir (**59**) (Scheme 27).



**Scheme 27.** MAO-N catalysed desymmetrisation of **54** and 3-component Ugi reaction for the synthesis of Telaprevir.[43]

Recently, researchers from Codexis proved the applicability of MAO on an industrial scale. Using a family shuffling approach, using monoamine oxidase from *A. niger* and *A. oryzae*, over consecutive rounds of evolution, they managed to obtain a new mutant (MAO-401) with increased thermostability and activity towards bicyclic pyrrolidines. This new mutant was used for the desymmetrisation of **60** to give the enantiopure imine **61**, substrate for cynde addition and subsequent Strecker reaction to obtain the methyl ester **63**, important intermediate to finish the synthesis of Boceprevir (**67**)(Scheme 28).[44]



**Scheme 28.** MAO-N catalysed desymmetrisation of **60** to make the imine **61** substrate for the cynde addition and subsequent Strecker reaction to obtain intermediate **63** building block for the synthesis of Boceprevir[44]



Monoamine oxidases from *Aspergillus Niger* have shown a broad applicability both in terms of substrate scope and industrial uses. Nonetheless further efforts could be made in trying to identify new mutants with enhanced activity toward commercially relevant amines such as building blocks for drugs or alkaloid natural products. Since currently only (*S*)-selective mutants of MAO-N have been found, another important challenge would be the identification of an enantiocomplementary amine oxidase which could give access to both enantiomers and further enhance the applicability of this biocatalyst.

## References

- [1] M. Breuer, K. Ditrich, T. Habicher, B. Hauer, M. Kessler, R. Sturmer, T. Zelinski, *Angew. Chem. Int. Ed.* **2004**, *43*, 788-824.
- [2] N. J. Turner, *Nature Chem. Biol.* **2009**, *5*, 568-574.
- [3] T. C. Nugent, M. El-Shazly, *Adv. Synth. Catal.* **2010**, *352*, 753-819.
- [4] A. W. Ingersoll, *Org. Synth.* **1937**, *17*, 80-83.
- [5] A. Ault, *J. Chem. Ed.* **1965**, *42*, 269-270.
- [6] L. Storace, L. Anzalone, P. N. Confalone, W. P. Davis, J. M. Fortunak, M. Giangiordano, J. J. Haley, K. Kamholz, H. Y. Li, P. Ma, W. A. Nugent, R. L. Parsons, P. J. Sheeran, C. E. Silverman, R. E. Waltermire, C. C. Wood, *Org. Proc. Res. Dev.* **2002**, *6*, 54-63.
- [7] C. Li, J. Xiao, *J. Am. Chem. Soc.* **2008**, *130*, 13208-13209.
- [8] N. Uematsu, A. Fujii, S. Hashiguchi, T. Ikariya, R. Noyori, *J. Am. Chem. Soc.* **1996**, *118*, 4916-4917.
- [9] P. Roszkowski, J. K. Maurin, Z. Czarnocki, *Tetrahedron:Asymmetry* **2006**, *17*, 1415-1419.
- [10] J. S. Wu, F. Wang, Y. P. Ma, X. C. Cui, L. F. Cun, J. Zhu, J. G. Deng, B. L. Yu, *Chem. Commun.* **2006**, 1766-1768.
- [11] Z. H. Guan, K. Huang, S. Yu, X. Zhang, *Org. Lett.* **2009**, *11*, 481-483.
- [12] G. A. Strohmeier, H. Pichler, O. May, M. Gruber-Khadjawi, *Chem. Rev.* **2011**, *111*, 4141-4164.
- [13] J. M. Foulkes, K. J. Malone, V. S. Coker, N. J. Turner, J. R. Lloyd, *Acs Catal.* **2011**, *1*, 1589-1594.
- [14] E. Ricca, B. Brucher, J. H. Schrittwieser, *Adv. Synth. Catal.* **2011**, *353*, 2239-2262.
- [15] J. B. Crawford, R. T. Skerlj, G. J. Bridger, *J. Org. Chem.* **2007**, *72*, 669-671.

- [16] D. Koszelewski, K. Tauber, K. Faber, W. Kroutil, *Trends Biotechnol.* **2010**, 28, 324-332.
- [17] S. Mathew, H. Yun, *Acs Catal.* **2012**, 2, 993-1001.
- [18] J. S. Shin, B. G. Kim, A. Liese, C. Wandrey, *Biotechnol. Bioeng.* **2001**, 73, 179-187.
- [19] C. K. Savile, J. M. Janey, E. C. Mundorff, J. C. Moore, S. Tam, W. R. Jarvis, J. C. Colbeck, A. Krebber, F. J. Fleitz, J. Brands, P. N. Devine, G. W. Huisman, G. J. Hughes, *Science* **2010**, 329, 305-309.
- [20] R. C. Simon, B. Grischek, F. Zepeck, A. Steinreiber, F. Belaj, W. Kroutil, *Angew. Chem. Int. Ed.* **2012**, 51, 6713-6716.
- [21] P. Poechlauer, S. Braune, A. De Vries, O. May, *Chim. Oggi* **2010**, 28, 14-17.
- [22] B. de lange, D. J. Hyett, P. J. D. Maas, D. Mink, F. B. J. van Assema, N. Sereinig, A. H. M. de Vries, J. G. de Vries, *Chemcatchem* **2011**, 3, 289-292.
- [23] K. Mitsukura, M. Suzuki, K. Tada, T. Yoshida, T. Nagasawa, *Org. Biomol. Chem.* **2010**, 8, 4533-4535.
- [24] K. Mitsukura, M. Suzuki, S. Shinoda, T. Kuramoto, T. Yoshida, T. Nagasawa, *Biosc. Biotech. Biochem.* **2011**, 75, 1778-1782.
- [25] N. Itoh, C. Yachi, T. Kudome, *J. Mol. Catal. B:Enzym.* **2000**, 10, 281-290.
- [26] M. J. Abrahamson, E. Vazquez-Figueroa, N. B. Woodall, J. C. Moore, A. S. Bommarius, *Angew. Chem. Int. Ed.* **2012**, 51, 3969-3972.
- [27] a) D. E. Edmondson, C. Binda, A. Mattevi, *Arch. Biochem. Biophys.* **2007**, 464, 269-276; b) P. F. Fitzpatrick, *Arch. Biochem. Biophys.* **2010**, 493, 13-25; c) N. S. Scrutton, *Nat. Prod. Rep.* **2004**, 21, 722-730.
- [28] J. R. Miller, D. E. Edmondson, *Biochemistry* **1999**, 38, 13670-13683.
- [29] R. B. Silverman, S. J. Hoffman, W. B. Catus, *J. Am. Chem. Soc.* **1980**, 102, 7126-7128.
- [30] K. E. Atkin, R. Reiss, V. Koehler, K. R. Bailey, S. Hart, J. P. Turkenburg, N. J. Turner, A. M. Brzozowski, G. Grogan, *J. Mol. Biol.* **2008**, 384, 1218-1231.
- [31] R. Reiss, University of Manchester (Manchester), **2008**.
- [32] M. Li, C. Binda, A. Mattevi, D. E. Edmondson, *Biochemistry* **2006**, 45, 4775-4784.
- [33] I. Rowles, K. J. Malone, L. L. Etchells, S. C. Willies, N. J. Turner, *Chemcatchem* **2012**, 4, 1259-1261.
- [34] N. J. Turner, *Chem. Rev.* **2011**, 111, 4073-4087.
- [35] a) B. Schilling, K. Lerch, *Mol. Gen. Genet.* **1995**, 247, 430-438; b) B. Schilling, K. Lerch, *Biochim. Biophys. Acta: Gen. Subj.* **1995**, 1243, 529-537.

- [36] S. O. Sablin, V. Yankovskaya, S. Bernard, C. N. Cronin, T. P. Singer, *Eur. J. Biochem.* **1998**, *253*, 270-279.
- [37] M. Alexeeva, A. Enright, M. J. Dawson, M. Mahmoudian, N. J. Turner, *Angew. Chem. Int. Ed.* **2002**, *41*, 3177-3180.
- [38] R. Carr, M. Alexeeva, A. Enright, T. S. C. Eve, M. J. Dawson, N. J. Turner, *Angew. Chem. Int. Ed.* **2003**, *42*, 4807-4810.
- [39] R. Carr, M. Alexeeva, M. J. Dawson, V. Gotor-Fernandez, C. E. Humphrey, N. J. Turner, *Chembiochem* **2005**, *6*, 637-639.
- [40] C. J. Dunsmore, R. Carr, T. Fleming, N. J. Turner, *J. Am. Chem. Soc.* **2006**, *128*, 2224-2225.
- [41] K. R. Bailey, A. J. Ellis, R. Reiss, T. J. Snape, N. J. Turner, *Chem. Commun.* **2007**, 3640-3642.
- [42] V. Kohler, K. R. Bailey, A. Znabet, J. Raftery, M. Helliwell, N. J. Turner, *Angew. Chem. Int. Ed.* **2010**, *49*, 2182-2184.
- [43] A. Znabet, M. M. Polak, E. Janssen, F. J. J. de Kanter, N. J. Turner, R. V. A. Orru, E. Ruijter, *Chem. Commun.* **2010**, *46*, 7918-7920.
- [44] T. Li, J. Liang, A. Ambrogelly, T. Brennan, G. Gloor, G. Huisman, J. Lalonde, A. Lekhal, B. Mijts, S. Muley, L. Newman, M. Tobin, G. Wong, A. Zaks, X. Zhang, *J. Am. Chem. Soc.* **2012**, *134*, 6467-6472.

## THESIS OBJECTIVES

Enantiomerically pure chiral amines are of increasing value in organic synthesis, especially as resolving agents, chiral auxiliaries/chiral bases and building blocks for the synthesis of biologically active pharmaceutical drugs.

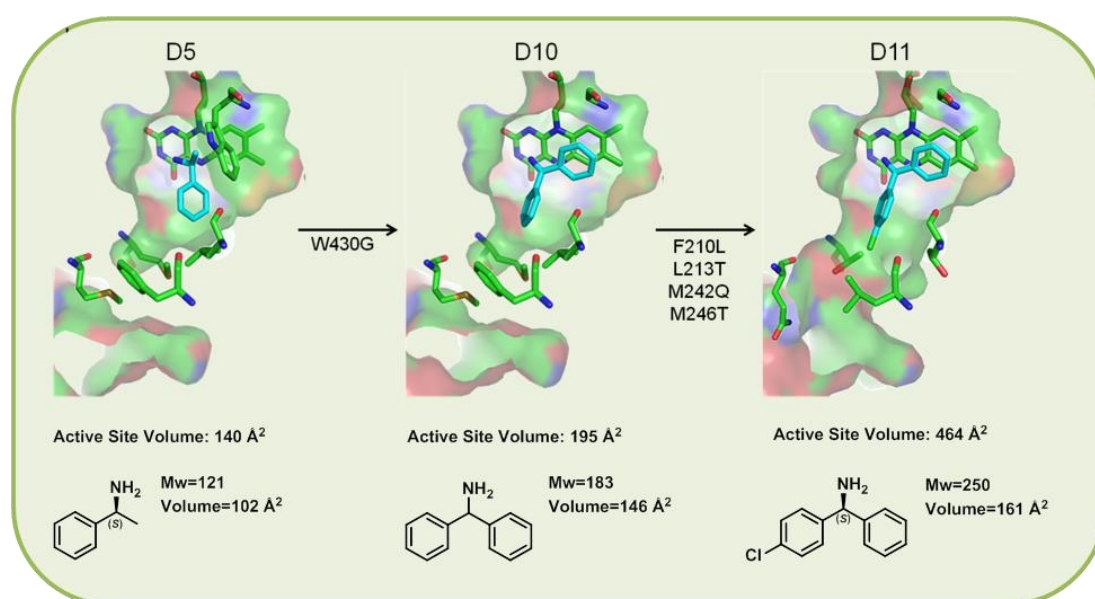
We have already reported the use of engineered variants of monoamine oxidases from *Aspergillus niger* (MAO-N) for the complete conversion of racemic primary, secondary and tertiary amines to the corresponding enantiomerically pure products in a single step.

The goal of this work was to use MAO-N as starting point for a number of different projects. In particular, we decided to screen the mutants already available in the lab to find activity toward novel classes of substrates which could be deracemised. Alongside this we wanted to address the limitation of MAO-N in substrate specificity developing a new generation of mutants with activity towards aminodiphenylmethane like structures. Then, with the idea in mind that the combination of a series of biocatalytic cascade reactions to achieve more efficient chemical processes is the natural development of the biocatalysis, we decide to combine MAO-N with other catalyst for the synthesis of chiral amines.

# ENGINEERING AN ENANTIOSELECTIVE AMINE OXIDASE FOR THE SYNTHESIS OF ALKALOIDS NATURAL PRODUCTS AND PHARMACEUTICAL BUILDING BLOCK

*Nature*, submitted

D.Ghislieri,<sup>1</sup> A. P. Green,<sup>1</sup> M. Pontini,<sup>1</sup> S. C. Willies,<sup>1</sup> I. Rowles,<sup>1</sup> A. Frank,<sup>2</sup> G.  
Grogan<sup>2</sup> and N. J. Turner\*<sup>1</sup>



A new engineered variant of monoamine oxidase from *Aspergillus niger* (MAO-N) displayed remarkable substrate scope and tolerance for sterically demanding motifs that are found in natural products and active pharmaceutical ingredients (APIs). Application of these engineered biocatalysts is highlighted by the asymmetric synthesis of the generic APIs as well as number of important representatives of the different classes of biologically active alkaloid natural products. We also report a novel MAO-N mediated asymmetric oxidative Pictet-Spengler approach to the synthesis of (*R*)-harmicine.

In this paper D.G. conceived the project, performed the chemical synthesis, mutagenesis (under the strict supervision of SCW) and biotransformations, analysed the data, co-wrote the paper and wrote the supplementary information.

# Engineering an Enantioselective Amine Oxidase for the Synthesis of Alkaloid Natural Products and Pharmaceutical Building Blocks

D.Ghislieri,<sup>1</sup> A. P. Green,<sup>1</sup> M. Pontini,<sup>1</sup> S. C. Willies,<sup>1</sup> I. Rowles,<sup>1</sup> A. Frank,<sup>2</sup> G. Grogan<sup>2</sup> and N. J. Turner\*<sup>1</sup>

<sup>1</sup>School of Chemistry, University of Manchester, Manchester Institute of Biotechnology, 131 Princess Street, Manchester, M1 7DN, UK.

<sup>2</sup>Structural Biology Laboratory, University of York, Department of Chemistry, Heslington, York, YO10 5YW, United Kingdom

*Nicholas.Turner@manchester.ac.uk*

## Abstract

The development of cost-effective and sustainable catalytic methods for the production of enantiomerically pure chiral amines is a key challenge facing the pharmaceutical and fine chemical industries. The proportion of drug candidates that contain a chiral amine is estimated to be between 40-45% and hence there is an increasing demand for broadly applicable synthetic methods which deliver the desired amine product in high yield and enantiomeric excess (e.e.). Herein, we describe a broadly applicable biocatalytic strategy for the conversion of racemic amines to the corresponding optically pure products in a single step. Engineering of monoamine oxidase from *Aspergillus niger* (MAO-N) has led to the development of a ‘toolbox’ of variants which display remarkable substrate scope and tolerance for sterically demanding motifs that are found in natural products and active pharmaceutical ingredients (APIs). Application of these engineered biocatalysts is highlighted by the asymmetric synthesis of the generic APIs Solifenacin<sup>®</sup> and Levocetirizine<sup>®</sup> as well as number of important representatives of the different classes of biologically active alkaloid natural products. We also report a novel MAO-N mediated asymmetric oxidative Pictet-Spengler approach to the synthesis of (*R*)-harmicine. These MAO-N biocatalysts have been made commercially available and

we anticipate their widespread application for chiral amine synthesis both in industrial and academic laboratories.

## **Introduction**

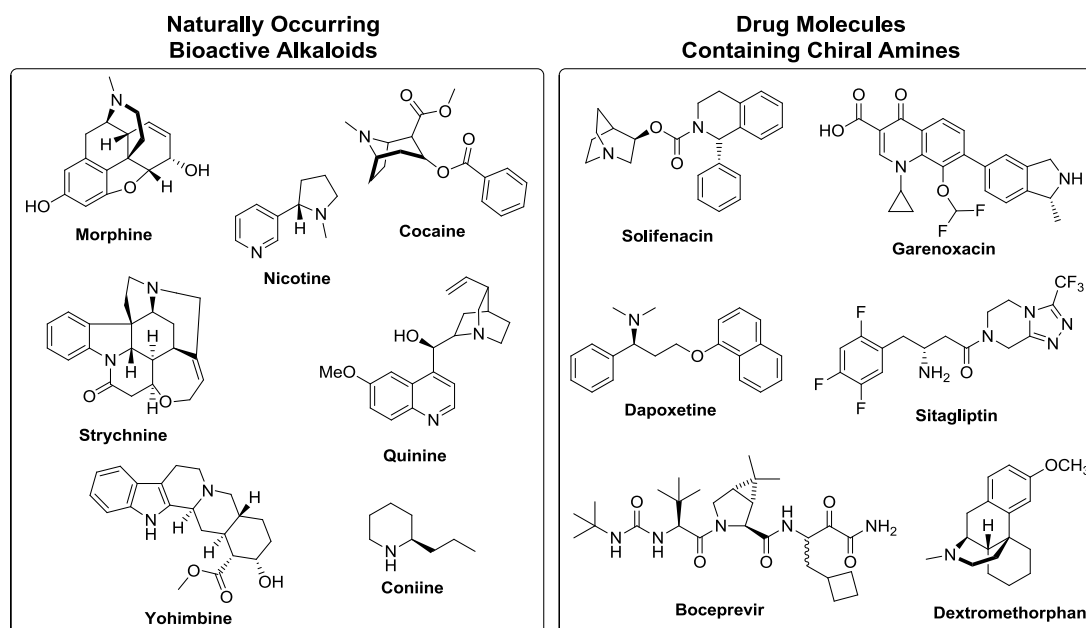
The alkaloids are a large family of natural products which display diverse structural architectures and possess a broad range of powerful biological activities leading to their widespread application as medicines, recreational drugs, poisons and in entheogenic rituals.[1] Prominent examples include the stimulants nicotine and cocaine, the anti-malarial quinine and the analgesic morphine (Figure 1). Natural alkaloids often serve as lead compounds for further development in the pharmaceutical industry in cases where structural modification is required to enhance their biological activity or to reduce undesired side-effects.[2,3] With few exceptions, alkaloid structures are based upon a template which includes one or more chiral amine moieties embedded within a heterocyclic ring. Although alkaloid natural products can appear extremely diverse in structure, they can be grouped into a relatively small number of classes based on their structural motifs or their biosynthetic origin.[4]

The complex molecular architectures and the wealth of biological activities associated with the alkaloids have attracted significant attention from the synthetic community, and numerous pioneering studies describing the total synthesis of these structures have been reported.[5-9] The increasing demand to access these structures as single enantiomers has driven the development of methodology for the asymmetric synthesis of key structural motifs. Although a number of impressive approaches have been reported, they often suffer from drawbacks such as the use of rare or toxic metal catalysts or the requirement for attachment and removal of (chiral) auxiliaries. Additionally, these strategies are generally only applicable to a small subset of chiral amines. As a result, classical resolution of racemic final products, or key intermediates, often remains the method of choice to produce enantiopure compounds on an industrial scale.[10] Unfortunately, the maximum theoretical yield of the desired enantiomer from this method is fifty percent, severely limiting the efficiency of this process, particularly in situations where synthesis of the racemic product in question requires a multi-step route.

We have previously described a chemoenzymatic method for the conversion of racemic amines to the corresponding enantiomerically pure form in a single step with

100% theoretical yield.[11] Monoamine oxidase from *Aspergillus niger* (MAO-N) is a flavin-dependent enzyme that catalyses the oxidation of amines to imines using molecular oxygen as the stoichiometric oxidant (Figure 2a). Employing this enzyme as a starting point for directed evolution, we were able to develop MAO-N variants capable of selectively oxidising a range of chiral amines with broad structural features. Although impressive advances have been made in the generation of non-enzyme based catalysts for the oxidation of amines to imines [16], to date there have been no reports of enantioselective catalysts that are generally synthetically applicable. When coupled with a non-selective chemical reducing agent, the MAO-N variants developed in our laboratory have been shown to mediate the deracemisation of simple chiral primary, secondary and tertiary amines.[12,13] We now demonstrate that the substrate range of MAO-N can be significantly increased, enabling new important classes of alkaloid natural products to be efficiently deracemised. In addition, the application of MAO-N in a cascade sequence leading to the efficient formation of (*R*)-harmicine is also described. Finally, the development of a new (D11) variant of MAO-N is described with increased tolerance for sterically demanding substrates. The activity of this new variant is highlighted by the asymmetric synthesis of two important drug molecules which are currently prepared industrially using classical resolution.[14,15] Overall, the work described highlights the potential of MAO-N as a highly tuneable biocatalyst for the production of a diverse range of alkaloid natural products and drug molecules in enantiomerically pure form.





**Figure 1. Examples of natural products and drug molecules containing chiral amines.** (Left) A selection of alkaloid natural products which display diverse structural features. The wealth of biological properties associated with the alkaloids has led to their widespread application as medicines, recreational drugs, poisons and or as lead compounds for further development in the pharmaceutical industry. (Right) A selection of pharmaceutical drug molecules that contain chiral amine moiety and are commercially available in enantiopure form.

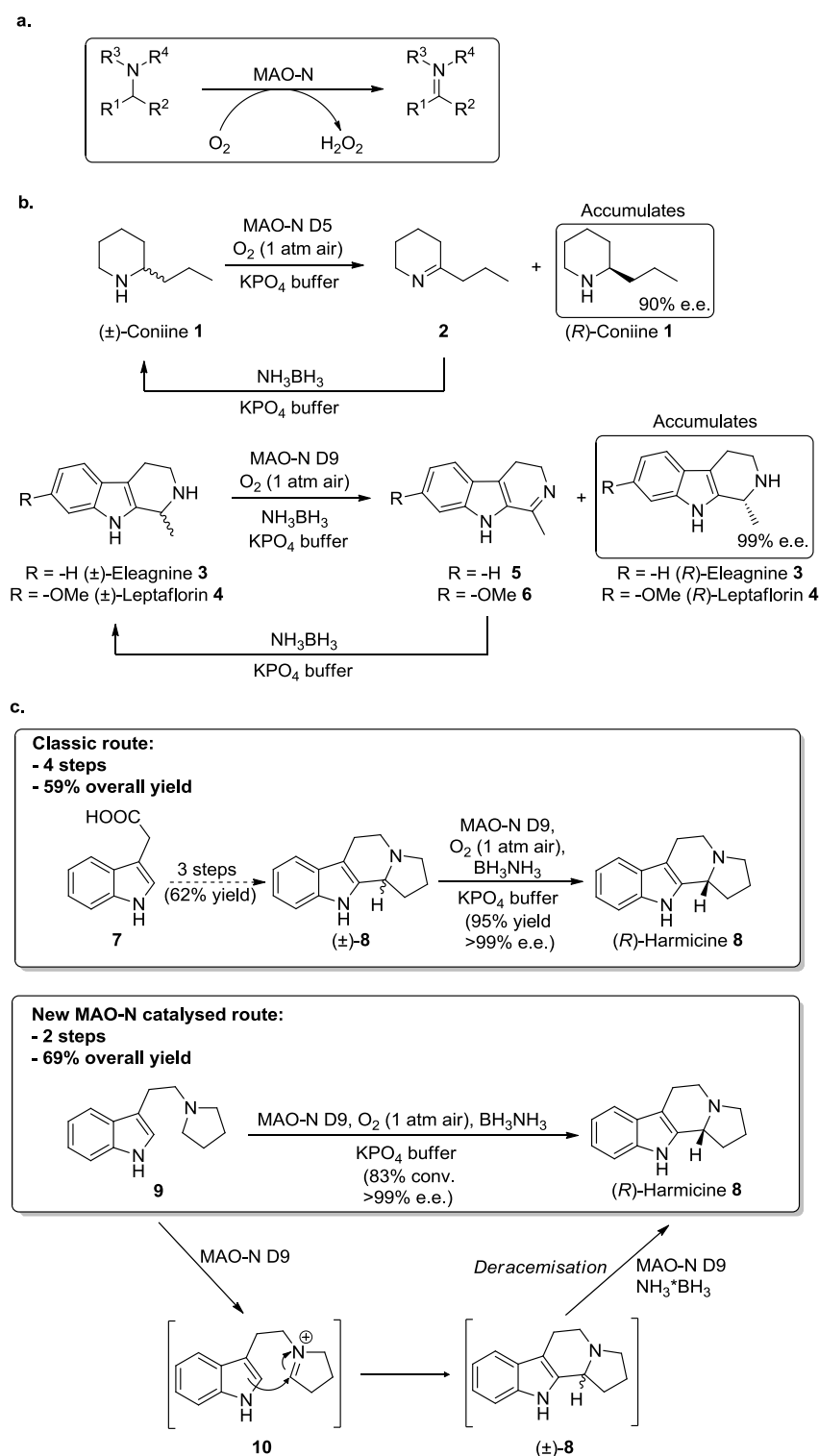
## Results

The piperidine alkaloid coniine (2-propylpiperidine) (**1**) is a potent neurotoxin which is isolated from the plant *Conium maculatum* (poison hemlock). Coniine was the first alkaloid to be chemically synthesised and is famous as the poison used to kill Socrates in 399 BC. Although both enantiomers of coniine are natural products, their biological properties are not identical.[17] Whilst the racemic form of this compound is commercially available, the single enantiomers are not. As a result, methods for the asymmetric synthesis of **1** are of interest, and a number of multi-step strategies have been reported.[18,19] The previously reported MAO-N D5 variant (see Table S3 in SI for sequences of all variants described in this manuscript) is able to mediate the efficient deracemisation of commercially available ( $\pm$ )-coniine. Repeated cycles of selective oxidation of the (*S*)-enantiomer followed by non-selective chemical reduction of the resulting imine with  $\text{BH}_3\text{-NH}_3$  leads to the accumulation of the (*R*)-enantiomer in 90% e.e. (Figure 2b). This represents the first reported example of the use of MAO-N for the oxidation of a 2-substituted piperidine, a common structural motif found in many alkaloid natural products.

The tetrahydro- $\beta$ -carboline (THBC) ring system is found in a large number of bioactive alkaloid natural products. Eleagnine (**3**) is an alkaloid isolated from *Chrysophyllum albidum* which displays potent analgesic, anti-inflammatory and weak antioxidant properties.[20] The asymmetric synthesis of this structure has previously been described *via* transition metal catalysed reduction of the corresponding imine.[21,22] Leptaflorin (**4**) has been isolated from *Peganum harmala* and from *Leptactina densiflora*, a stove shrub from central Africa which is a known psychedelic.[23] Leptaflorin possesses an additional methoxy substituent at the 7-position of the indole ring when compared with eleagnine, a modification commonly found in indole alkaloid natural products. The D9 variant of MAO-N[24] when combined with  $\text{BH}_3\text{-NH}_3$  was able to mediate the deracemisation of both eleagnine and leptaflorin leading to the formation of the (*R*)-enantiomers of these natural products in >99% e.e.

Harmicine (**7**) was isolated from the Malaysian plant *Kopsia griffithii* and displays strong *anti-Leishmania* activity.[25] Leishmaniasis is a disease spread by the bite of the phlebotomine sand fly and occurs in tropical and sub-tropical regions, affecting some 12 million people in 88 countries. Currently there are relatively few synthetic methods available for the enantioselective synthesis of naturally occurring (*R*)-harmicine (**8**), which include a diastereoselective Pictet–Spengler type cyclisation using tryptophan derivatives [26] or a thiourea catalysed asymmetric Pictet–Spengler reaction of an *N*-acyl iminium ion.[27]

We have developed two approaches to the synthesis of (*R*)-harmicine using the D9 variant of MAO-N (Figure 2c). The first relies on a MAO-N mediated deracemisation (>99% e.e.) of the racemate which was prepared in three steps from indole-3-acetic acid.[28]



**Figure 2. The application of MAO-N variants in the synthesis of biologically active alkaloid natural products.** a) MAO-N catalyses the oxidation of amines to imines using molecular oxygen as the stoichiometric oxidant. b) MAO-N D5 mediates the deracemisation of the neurotoxin coniine (**1**). Repeated cycles of selective oxidation of the (*S*)-enantiomer followed by non-selective chemical reduction of the resulting imine with  $\text{BH}_3\text{-NH}_3$  leads to the accumulation of the (*R*)-enantiomer. MAO-N D9 mediates the deracemisation of eleagnine (**3**) and leptaflorin (**4**). c) Two approaches to the synthesis of the naturally occurring (*R*)-harmicine (**8**).

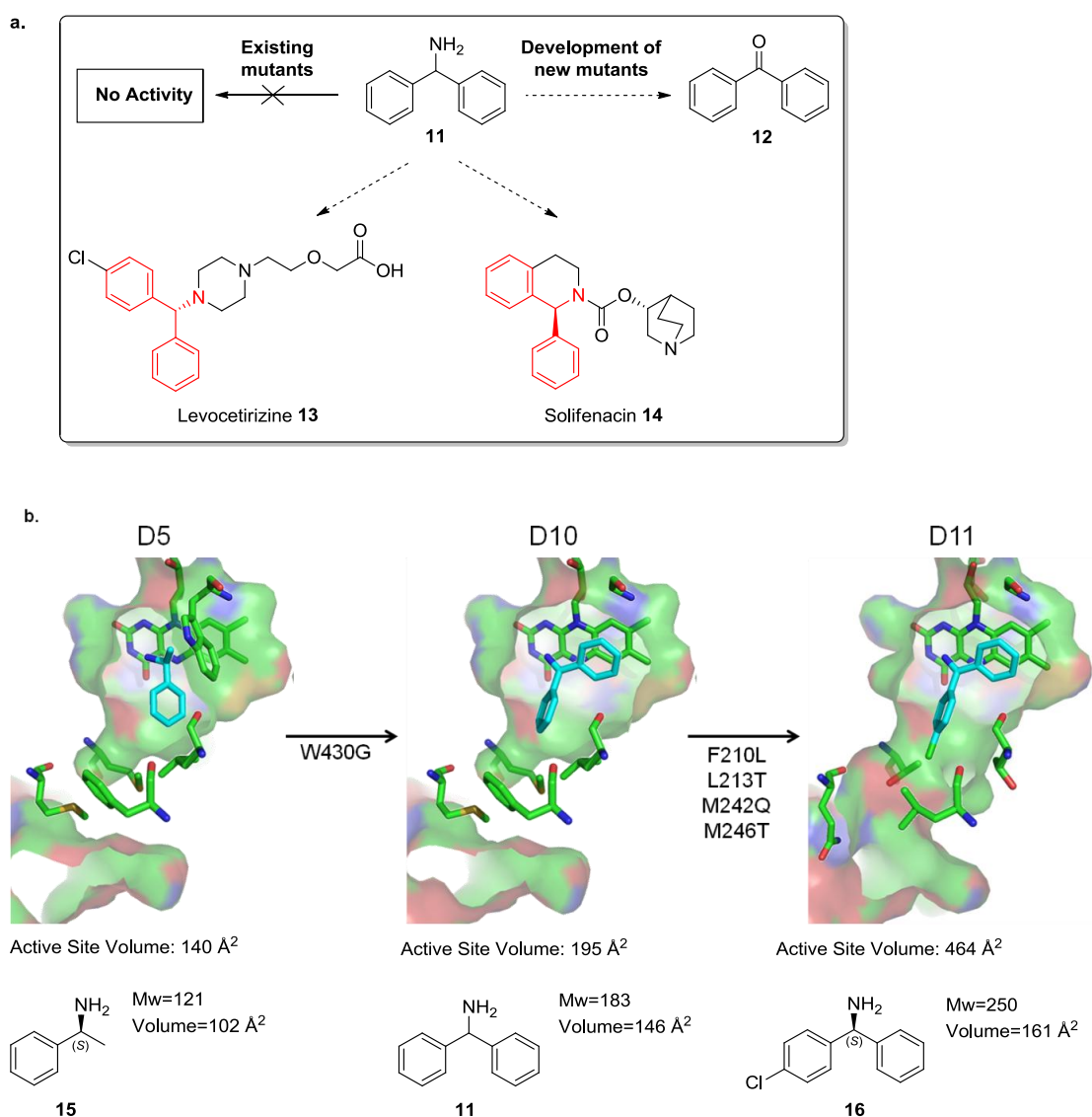
The first involves a MAO-N D9 mediated deracemisation of the racemate. The second approach involves the MAO-N mediated conversion of achiral pyrrolidine (**9**) to (*R*)-harmicine (**8**).

We also recognised the potential for using MAO-N as a biocatalyst for the oxidative generation of reactive iminium ions, thereby generating a conceptually new approach to this class of alkaloid. Pyrrolidine **9** is available in one step from tryptamine and 1,4-butanediol in high yield.[29] Incubation of **9** with MAO-N D9 resulted in generation of the intermediate iminium ion **10**, which underwent a non-stereoselective cyclisation to form harmicine as a mixture of enantiomers. The (*S*)-enantiomer was then further oxidised to the corresponding iminium ion, which upon reduction with BH<sub>3</sub>-NH<sub>3</sub> and further rounds of oxidation/reduction was fully converted to the desired (*R*)-enantiomer. The overall transformation from pyrrolidine **9** to (*R*)-harmicine occurs in >99% e.e. with an 83% conversion and formally represents an oxidative asymmetric Pictet-Spengler reaction under aqueous conditions using molecular oxygen as the stoichiometric oxidant. This synthesis of (*R*)-harmicine represents the shortest route reported to date and demonstrates the potential of variants of MAO-N in the development of novel synthetic strategies to access target molecules.

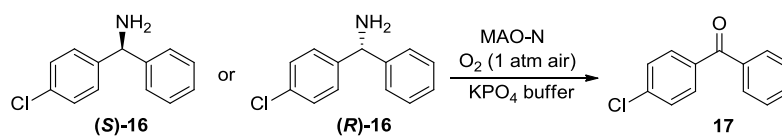
To date, an important structural unit that has eluded oxidation by MAO-N is the aminodiphenylmethane motif (Figure 3a). None of the previously described variants displays activity towards the parent compound **11** or towards derivatives such as 4-chloro-benzhydrylamine (**16**) and 1-phenyl-tetrahydroisoquinoline (**18**), which are motifs present in the commercially available drugs Levocetirizine (**13**) and Solifenacin (**14**) respectively. Such limitations present opportunities to develop new generations of MAO-N variants with the desired substrate scope.

We therefore selected the D5 variant of MAO-N for further rational engineering using the previously reported crystal structure to guide selection of residues for mutation.[30] We reasoned that increasing the volume of the active site pocket would allow the binding of larger substrates. Modelling of  $\alpha$ -methylbenzylamine (**15**) into the MAO-N D5 active site (Figure 3b) highlighted two residues (A429 and W430) as potential targets for site directed mutagenesis with the specific aim of increasing the size of the small cavity within the active site pocket to incorporate an additional phenyl group associated with the aminodiphenylmethane motif. Saturation mutagenesis was performed at amino acid positions A429 and W430 and the

resulting libraries of variants were screened against aminodiphenylmethane (**11**) using our previously reported solid phase assay.[11]



**Figure 3. The development of MAO-N variants with activity towards benzhydrylamines.** a) Existing variants of MAO-N display no activity towards aminodiphenylmethane (**11**) or towards derivatives such as 4-chlorobenzhydrylamine and 1-phenyl-tetrahydroisoquinoline, which are motifs present in the commercially available drugs Levocetirizine (**13**) and Solifenacin (**14**) respectively. b) Modelling (*S*)-**15** into the active site of the MAO-N D5 variant highlighted A429 and W430 as targets for site directed mutagenesis. After screening, a new MAO-N variant (D10) was identified with activity toward **11**. Further modifications in the active site entrance channel led to the development of a MAO-N variant (D11) with excellent activity and selectivity towards 4-chlorobenzhydrylamine.



MAO-N Variant	Mutation <sup>[a]</sup>	(S)-16 <sup>[b]</sup> (%)	(R)-16 <sup>[b]</sup> (%)	Time (h)
D5	I246M, N336S, M348K, T384N, D385S	0	0	48
D9	D5 + F210L, L213T, M242Q, I246T, W430H	0	0	48
D10	D5 + W430G	75	26	48
D11A	D10 + F210M, L213C, M242V, I246T	100	12	30
D11B	D10 + F210L, L213T, M242V, I246T	100	7	4
<b>D11C</b>	<b>D10 + F210L, L213T, M242Q, I246T</b>	<b>100</b>	<b>&lt;1</b>	<b>6</b>
D11D	D10 + F210M, L213C, M242Q, I246T	100	14	35

**Figure 4. Activity of MAO-N variants towards (R)-16 and (S)-16.** The oxidation of (R)-16 and (S)-16 was carried out with variants of MAO-N. The previously reported MAO-N D5 and D9[24] displayed no activity towards either enantiomer. The D10 and D11 variants all displayed activity towards **16** with varying degrees of selectivity. The MAO-N D11C variant displays a high degree of selectivity towards (S)-**16**, making it a promising candidate for production of the desired (R)-enantiomer. <sup>[a]</sup>Mutations relative to wild-type MAO-N. <sup>[b]</sup>Conversion was calculated by HPLC.

After screening, a variant of MAO-N (D10) was identified with the single amino acid substitution W430G which displayed activity towards aminodiphenylmethane (**11**). There was no change to the amino acid at position 429 (A429) in this variant. A homology model of the MAO-N D10 variant is shown in Figure 3b. This structure clearly demonstrates how the single mutation leads to an increase in volume of the small cavity within the active site, allowing the bulky substrate aminodiphenylmethane (**11**) to be accommodated. This D10 variant of MAO-N was screened against 4-chlorobenzhydramine (**16**) and was shown to display moderate activity and enantioselectivity towards this substrate (Figure 4). In an attempt to improve the activity further, our attention turned towards the modification of amino acid residues in the active site channel. We have previously described mutations in

this region of the enzyme during the development of the MAO-N D9 generation of variants, which displayed significantly enhanced activity towards the bulky tertiary amine Crispine A when compared with MAO-N D5.[24] The amino acid substitutions (in the active site channel) from MAO-N D9 (A-D) were combined with the W430G modification of MAO-N D10 to create the MAO-N D11A-D library of variants.

The activity and stereoselectivity of the MAO-N variants towards **16** was then determined by monitoring the conversion of enantiopure (*R*)-**16** and (*S*)-**16** to the corresponding ketones by HPLC. Biotransformations were carried out using *E. coli* whole cells expressing the relevant MAO-N variant in aqueous phosphate buffer (1 M, pH 7.7). The results of these transformations are illustrated in Figure 4. As anticipated, the existing D5 and the D9 variants displayed no activity towards (*R*)-**16** or (*S*)-**16** after incubation for 48 hours. Introduction of the W430G mutation to the MAO-N D5 led to the generation of a variant of MAO-N D10 which displayed significant activity but only moderate selectivity towards **16**. All MAO-N D11 variants displayed a high selectivity and reaction rate for (*S*)-**16** when compared with the MAO-N D10 variant. The most promising candidate for the deracemisation of ( $\pm$ )-**16** for the production of the desired (*R*)-enantiomer was the MAO-N D11C variant, which was shown to mediate the conversion of 100% of (*S*)-**16** to the corresponding ketone in 6 hours, with <1% of the corresponding (*R*)-enantiomer converted in the same reaction time.

The crystal structure of this MAO-N D11C variant, refined to a resolution of 2.55 Å, was solved (see supporting information). This structure superimposes well with that of the D5 variant described previously (2VVM) [29], with few significant movements in the peptide backbone (the rmsd between one subunit of the two structures was 0.23 Å over 478 residues). The anticipated increase in volume of the small cavity within the active site pocket as a result of the W430G modification was clearly visible in the maps for the D11C structure (Figure 3b). The modifications in the substrate access channel (F210L, L213T, M242Q, and I246T) result in a reduction in steric obstruction to the active site (Figure 3b) and have a significant effect on both activity and selectivity towards oxidation of **16** (Figure 4). Interestingly, the newly introduced Q242 residue forms new hydrogen bonds with D146. This interaction occurs as a result of rotation of the side-chain of D146 in comparison to the D5 mutant in which D146 forms a salt-bridge with R150. Q242

also forms a new H-bond with the phenolic hydroxyl of Y238, as does the newly positioned D146 residue. As a result of the new H-bonding interactions to Y238, this residue moves a distance of 2 Å out of the access channel, again relieving steric obstruction (supplementary Figure S1).

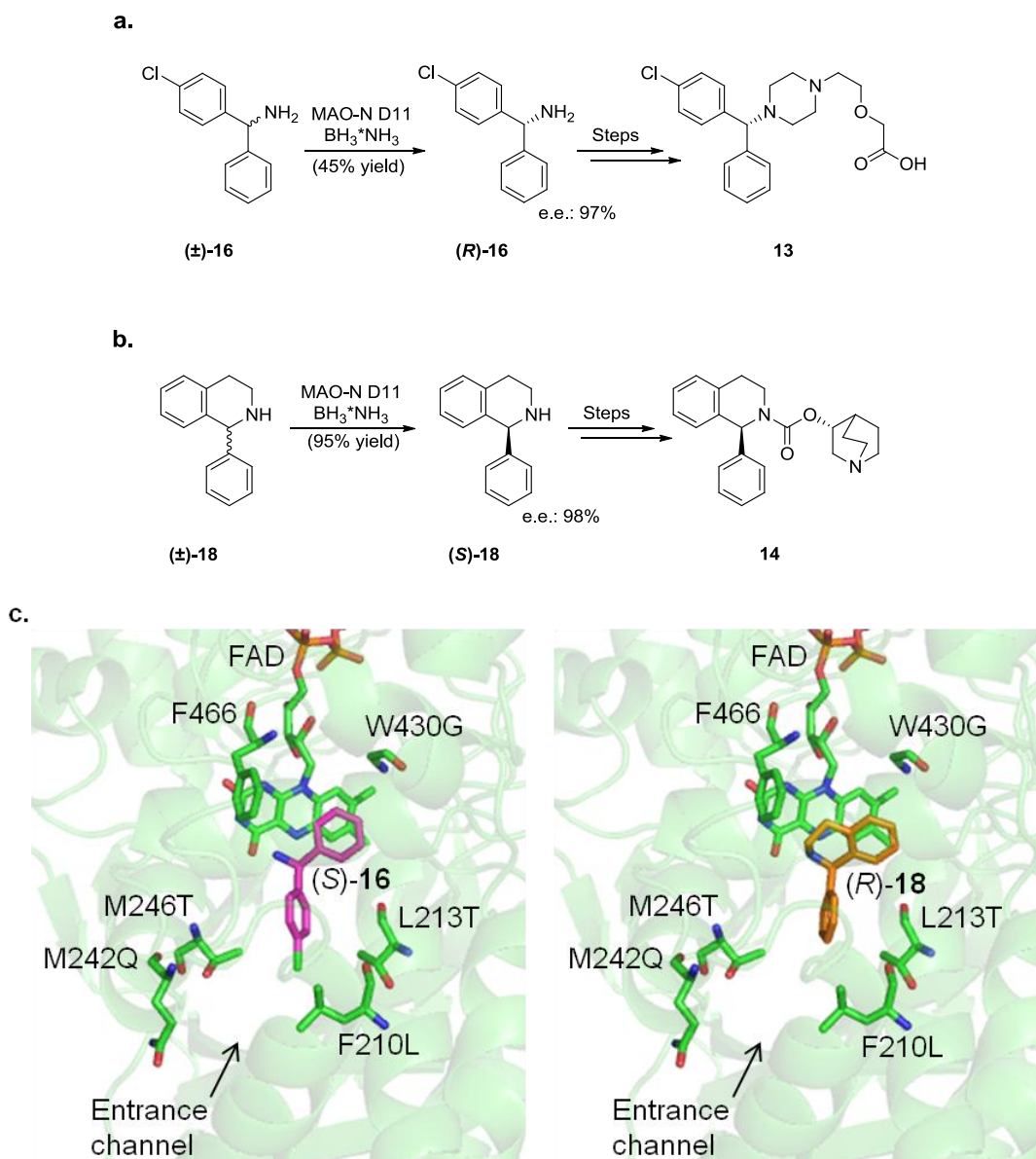
(*R*)-**16** is a key chiral building block for the synthesis of Levocetirizine (**13**), an antihistamine and a selective H1 receptor inverse agonist used in the treatment of allergies. (*R*)-**16** is commonly prepared *via* classical resolution of the tartrate salt of (±)-**16**.<sup>[31]</sup> Other syntheses include the asymmetric addition of a phenylzinc reagent to the *N*-formyl 4-chlorobenzylimine [32] or asymmetric transfer hydrogenation of an *ortho*-hydroxylated imine followed by subsequent removal of the hydroxyl auxiliary.<sup>[33]</sup>

Optimisation of conditions for the deracemisation of (±)-**16** on a 20 mM scale resulted in production of (*R*)-**16** in 97% enantiomeric excess (45% isolated yield) within 48 hours. Completion of the synthesis of Levocetirizine (**13**) was then carried out according to the previously described method (Figure 5a).<sup>[14]</sup>

We next examined the deracemisation of the structurally related 1-phenyltetrahydroisquinoline (**18**). After incubation for 24 hours, complete deracemisation was observed as judged by chiral HPLC. Interestingly, in this case the MAO-N D11C variant showed a preference for the oxidation of the (*R*)-enantiomer, leading to the production of (*S*)-**18** in 98% enantiomeric excess. This result is in contrast to the (*S*)-selectivity observed for all previously reported substrates for MAO-N, including the preferential oxidation of (*S*)-**16** using the same variant (D11). Modelling of the (*S*)-**16** and (*R*)-**18** into the active site of MAO-N D11 highlights the preferred modes of binding of these two substrates (Figure 5c). Attempts to dock (*S*)-**18** into the active site of the D11 variant failed to provide a reasonable productive binding mode for this substrate, providing an explanation for the observed switch in selectivity.

(*S*)-**18** is a key chiral intermediate in the synthesis of Solifenacin (**14**), a competitive muscarinic acetylcholine receptor antagonist used in the treatment of overactive bladder.<sup>[34]</sup> Using the MAO-N D11 variant, the deracemisation of (±)-**18** was carried out on a preparative scale (1 g, 15 mM), leading to the formation of (*S*)-**18** in 90% isolated yield and 98% enantiomeric excess after 48 hours (Figure 5b). Conversion of this product to Solifenacin (**14**) was carried out in two steps according to the previously reported procedure.<sup>[35]</sup>



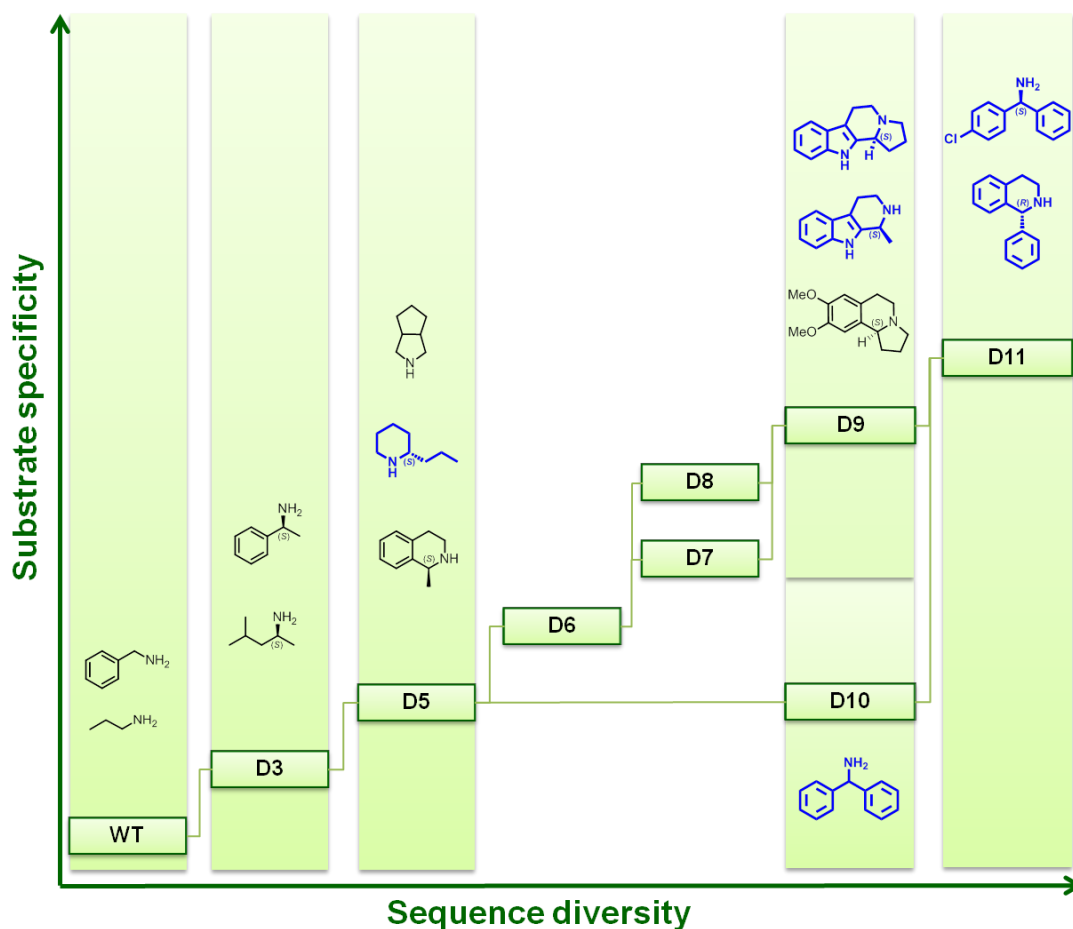


**Figure 5. Synthesis of the drug molecules Levocetirizine (**13**) and Solifenacin (**14**).** a) Deracemisation of ( $\pm$ )-**16** with MAO-N D11 provided (*R*)-**16**, a key chiral building block in the synthesis of the pharmaceutical Levocetirizine (**13**). The completion of the synthesis was carried out according to a literature procedure [14]. b) MAO-N D11 mediated deracemisation of ( $\pm$ )-**18** provided (*S*)-**18** (98% e.e.) which was used in the synthesis of Solifenacin (**14**). Interestingly, MAO-N D11 showed a preference for the oxidation of (*R*)-enantiomer. c) The crystal structure of the MAO-N D11 variant with (*S*)-**16** and (*R*)-**18** docked into the active site.

## Discussion

Biocatalysis is increasingly being viewed as a sustainable, green and cost-effective technology for the manufacture of a diverse range of chemical products including

pharmaceuticals, agrochemicals, fine chemicals and biofuels. Modern tools for enzyme discovery, combined with the development of increasingly sophisticated techniques for protein engineering, have greatly expanded the range of different enzymes that possess suitable properties for biocatalytic applications.[36,37] In the examples presented here, we have used a combination of directed evolution, rational design and high-throughput screening methods to develop a ‘toolbox’ of MAO-N variants which display complementary substrate specificity and which are able to mediate the synthesis of enantiomerically pure chiral amines with diverse structural architectures (Figure 6). Interestingly, in the case of MAO-N, it has been possible to derive all of the variants D3-D11 from the original wild-type sequence by systematic introduction of point mutations in and around the active site. Remarkably, all variants display a high degree of selectivity and hence broad substrate coverage has been achieved without compromising the optical purity of the amine products. The broad applicability of this technology has been demonstrated by synthesis of the APIs Levocetirizine and Solifenacin as well as a number of important classes of biologically active alkaloid natural products including the pyrrolidines, piperidines, isoquinolines and beta-carbolines. The application of the MAO-N variants is not limited to the deracemisation of chiral amines as demonstrated by previous studies from our group regarding the desymmetrisation of prochiral amines[38] and the development of a MAO-N mediated asymmetric oxidative Pictet-Spengler reaction described in the current study. This later process in particular highlights the potential for future applications of the MAO-N variants in the design of novel synthetic strategies to access target structures.



**Figure 6. The development of a ‘toolbox’ of MAO-N variants with broad substrate scope.** A combination of directed evolution and rational design has led to the development of a panel of MAO-N variants which display complementary activity and are able to mediate the deracemisation of primary, secondary and tertiary amines with broad structural features. Substrates highlighted in blue represent previously unreported structural classes which are oxidised by MAO-N variants.

An increasingly important challenge associated with biocatalysis remains the commercialisation of enzymes to facilitate their use by the wider synthetic community. Research groups often lack the facilities or the expertise for protein expression and application of enzymes in organic synthesis is often met with a degree of scepticism. In order to make our technology broadly accessible, the MAO-N variants generated in our laboratory have recently been made commercially available.[39] These enzymes have great potential to become the catalyst of choice in synthetic laboratories for the generation of imines and iminium ions from amines, a transformation which is often challenging using traditional chemical reagents.

This point is perfectly highlighted by the recent application of MAO-N in an industrial manufacturing process developed by Codexis and Merck for the

desymmetrisation of a prochiral amine to produce a key intermediate in the synthesis of the Hepatitis C drug Boceprevir.[40] With the ever increasing demand for enhanced efficiency and ‘green technologies’ in the pharmaceutical and fine chemical industries, we anticipate that this methodology will find widespread application both in industrial and academic settings.

## Methods

### Representative example of MAO-N D11C mediated deracemisation procedure (Preparative scale)

In a 500 mL screw cap bottle, (*rac*)-**18** (500 mg, 2.41 mmol) and BH<sub>3</sub>-NH<sub>3</sub> (328 mg, 9.66 mmol, 4 eq.) were dissolved in KPO<sub>4</sub>-buffer (185 mL, 1 M, pH = 7.8). The pH of the solution was adjusted to 7.8 by addition of HCl. Cell pellet from *E. coli* cultures (12.5 g) containing MAO-N D11C was added to the solution and the bottle was placed in a shaking incubator (250 rpm) at 37 °C. After 48 h, aqueous NaOH (2 mL, 10 M) and *tert*-butyl methyl ether (200 mL) were added and the resulting mixture was vigorously stirred. After filtration through a Celite<sup>®</sup> pad, the two layers were separated and the aqueous phase was extracted with *tert*-butyl methyl ether (2 × 50 mL). The combined organics were dried over MgSO<sub>4</sub> and concentrated *in vacuo* to give (*S*)-**18** as a yellowish solid (450 mg, 90% yield, 98% e.e.).

## Acknowledgments

This work was generously supported by a Marie Curie ITN (Biotrains FP7-ITN-238531). The authors would like to thank Dr. James Raftery for solving the crystal structure of compound **16** and Almac Group LTD for supplying (*R*)-3-quinuclidinol.

## Author contributions

D.G., A.P.G., M.P., S.C.W., I.R. and N.J.T. conceived the project. N.J.T. supervised the project. D.G. and M.P. performed the chemical synthesis and biotransformations. S.C.W. and I.R. constructed the mutants and performed screening experiments. D.G., A.P.G., M.P., S.C.W. and N.J.T. analysed the data. A.F. and G.G. crystallised the protein. S.C.W. performed the modelling studies. D.G., A.P.G. and N.J.T. co-wrote the paper.

**Supplementary information** is available free of charge under...

## References

- [1] Cassiano, N. M. Alkaloids: Properties, Applications and Pharmacological Effects. (Nova Science Pub. Inc., New York, 2010)
- [2] Harvey, A. L. Natural products in drug discovery. *Drug Discovery Today* **13**, 894-901 (2008).
- [3] Newman, D. J. & Cragg, G. M. Natural products as sources of new drugs over the 30 years from 1981 to 2010. *J. Nat. Prod.* **75**, 311-335 (2012).
- [4] Herbert, R. B. The biosynthesis of secondary metabolites. Second edn, (Chapman and Hall, London, 1989).
- [5] Woodward, R. B. et al. The total synthesis of strychnine. *J. Am. Chem. Soc.* **76**, 4749-4751 (1954)
- [6] Hong, C. Y., Kado, N. & Overman, L. E. Asymmetric synthesis of either enantiomers of opium alkaloids and morphinans. Total synthesis of (-)-dihydrocodeinone and (+)-dihydrocodeinone and (-)-morphine and (+)-morphine. *J. Am. Chem. Soc.* **115**, 11028-11029 (1993)
- [7] Stork, G. et al. The first stereoselective total synthesis of quinine. *J. Am. Chem. Soc.* **123**, 3239-3242 (2001)
- [8] Kim, J. & Movassaghi, M. Biogenetically inspired syntheses of alkaloid natural products. *Chem. Soc. Rev.* **38**, 3035-3050 (2009).
- [9] Mergott, D. J., Zuend, S. J. & Jacobsen, E. N. Catalytic asymmetric total synthesis of (+)-yohimbine. *Org. Lett.* **10**, 745-748 (2008).
- [10] Breuer, M. et al. Industrial methods for the production of optically active intermediates. *Angew. Chem. Int. Ed.* **43**, 788-824 (2004).
- [11] Alexeeva, M., Enright, A., Dawson, M. J., Mahmoudian, M. & Turner, N. J. Deracemization of alpha-methylbenzylamine using an enzyme obtained by in vitro evolution. *Angew. Chem. Int. Ed.* **41**, 3177-3180 (2002).
- [12] Carr, R. et al. Directed evolution of an amine oxidase possessing both broad substrate specificity and high enantioselectivity. *Angew. Chem. Int. Ed.* **42**, 4807-4810 (2003).
- [13] Dunsmore, C. J., Carr, R., Fleming, T. & Turner, N. J. A chemo-enzymatic route to enantiomerically pure cyclic tertiary amines. *J. Am. Chem. Soc.* **128**, 2224-2225 (2006).
- [14] Badgujar, S. K. H., Sharma V, Patel D, Khan M. A process for the synthesis of Levocetirizine. WO2009/057133A2 (2007).
- [15] Dave, M. G.; Pandey, B.; Kothari, H. M.; Patel, P. R. Process for preparing

- chemically and chirally pure Solifenacin base and its salts. WO/2009/087664 (2009)
- [16] Langeron, M. & Fleury, M.-B. Bioinspired oxidation catalysts. *Science*, **339**, 43-44 (2013).
- [17] Lee, S. T., Green, B. T., Welch, K. D., Pfister, J. A. & Panter, K. E. Stereoselective potencies and relative toxicities of coniine enantiomers. *Chem. Res. Toxicol.* **21**, 2061-2064 (2008).
- [18] Garnier, E. C. & Liebeskind, L. S. Organometallic enantiomeric scaffolding: General access to 2-substituted oxa- and azabicyclo 3.2.1 octenes via a bronsted acid catalyzed 5+2 cycloaddition reaction. *J. Am. Chem. Soc.* **130**, 7449-7458 (2008).
- [19] Beng, T. K. & Gawley, R. E. Highly enantioselective catalytic dynamic resolution of N-Boc-2-lithiopiperidine: synthesis of (R)-(+)-N-Boc-pipecolic acid, (S)-(-)-coniine, (S)-(+)-pelletierine, (+)-beta-conhydrine, and (S)-(-)-ropivacaine and formal synthesis of (-)-lasubine II and (+)-cermizine C. *J. Am. Chem. Soc.* **132**, 12216-12217 (2010).
- [20] Idowu, T.O., Iwalewa, E. O., Aderogba, M.A., Akinpelu, B.A. & Ogundaini, A.O. Antinociceptive, anti-inflammatory and antioxidant activities of Eleagnine: an alkaloid isolated from *Chrysophyllum albidum* seed cotyledons. *J. Biol. Sci.* **6**, 1029-1034 (2006).
- [21] Li, C. & Xiao, J. Asymmetric hydrogenation of cyclic imines with an ionic Cp\*Rh(III) catalyst. *J. Am. Chem. Soc.* **130**, 13208-13209 (2008).
- [22] da Silva, W. A. et al. Novel supramolecular palladium catalyst for the asymmetric reduction of imines in aqueous media. *Org. Lett.* **11**, 3238-3241 (2009).
- [23] Callaway, J. C. Various alkaloid profiles in decoctions of *Banisteriopsis caapi*. *J. Psychoact. Drugs* **37**, 151-155 (2005).
- [24] Rowles, I., Malone, K. J., Etchells, L. L., Willies, S. C. & Turner, N. J. Directed evolution of the enzyme Monoamine Oxidase (MAO-N): highly efficient chemo-enzymatic deracemisation of the alkaloid (+/-)-Crispine A. *ChemCatChem* **4**, 1259-1261 (2012).
- [25] Kam, T. S. & Sim, K. M. Alkaloids from *Kopsia griffithii*. *Phytochemistry* **47**, 145-147 (1998).
- [26] Allin, S. M., Gaskell, S. N., Elsegood, M. R. J. & Martin, W. P. A new asymmetric synthesis of the natural enantiomer of the indolizidino [8,7-b]indole alkaloid (+)-harmicine. *Tetrahedron Lett.* **48**, 5669-5671 (2007).
- [27] Raheem, I. T., Thiara, P. S., Peterson, E. A. & Jacobsen, E. N. Enantioselective pictet-spengler-type cyclizations of hydroxylactams: H-bond donor catalysis by anion binding. *J. Am. Chem. Soc.* **129**, 13404-13405 (2007).
- [28] King, F. D. Novel synthesis of (+/-)-harmacine and (+/-)-1,2,3,4,6,7,12,12b-octahydroindole 2,3-a quinolizine. *J. Heterocycl. Chem.* **44**, 1459-1463 (2007).

- [29] Cami-Kobeci, G., Slatford, P. A., Whittlesey, M. K. & Williams, J. M. J. N-alkylation of phenethylamine and tryptamine. *Bioorg. Med. Chem. Lett.* **15**, 535-537 (2005).
- [30] Atkin, K. E. et al. The Structure of Monoamine Oxidase from *Aspergillus niger* Provides a Molecular Context for Improvements in Activity Obtained by Directed Evolution. *J. Mol. Biol.* **384**, 1218-1231 (2008).
- [31] Clemo, G. R., Gardner, C. & Raper, R. The optical rotatory powers of some 4-substituted benzhydrylamines. *J. Chem. Soc.*, 1958-1960 (1939).
- [32] Hermanns, N., Dahmen, S., Bolm, C. & Bräse, S. Asymmetric, catalytic phenyl transfer to imines: Highly enantioselective synthesis of diarylmethylamines. *Angew. Chem. Int. Ed.* **41**, 3692-3694 (2002).
- [33] Thanh Binh, N., Wang, Q., & Gueritte, F. Chiral phosphoric acid catalyzed enantioselective transfer hydrogenation of ortho-hydroxybenzophenone N-H ketimines and applications. *Chem. Eur. J.* **17**, 9576-9580 (2011).
- [34] Chapple, C. R. et al. Randomized, double-blind placebo- and tolterodine-controlled trial of the once-daily antimuscarinic agent solifenacin in patients with symptomatic overactive bladder. *Bju Int.* **93**, 303-310 (2004).
- [35] Wang, S., Onaran, M. B. & Seto, C. T. Enantioselective synthesis of 1-aryltetrahydroisoquinolines. *Org. Lett.* **12**, 2690-2693 (2010).
- [36] Turner, N. J. Directed evolution drives the next generation of biocatalysts. *Nat. Chem. Biol.* **5**, 568-574 (2009)
- [37] Bornscheuer, U. T. et al. Engineering the third wave of biocatalysis. *Nature* **485**, 185-194 (2012).
- [38] Kohler, V. et al. Enantioselective biocatalytic oxidative desymmetrization of substituted pyrrolidines. *Angew. Chem. Int. Ed.* **49**, 2182-2184 (2010).
- [39] MAO Screening Kits, <http://www.discovery-bc.co.uk/monoamineoxidase.php> (2013).
- [40] Li, T. et al. Efficient, Chemoenzymatic process for manufacture of the Boceprevir bicyclic 3.1.0 proline intermediate based on amine oxidase-catalyzed desymmetrization. *J. Am. Chem. Soc.* **134**, 6467-6472 (2012).

# **Engineering an Enantioselective Amine Oxidase for the Synthesis of Alkaloid Natural Products and Pharmaceutical Building Blocks**

D.Ghislieri, A. P. Green, M. Pontini, S. C. Willies, I. Rowles, A. Frank, G. Grogan  
and N. J. Turner\*

**Supplementary information**



## General Experimental Information and Materials

Competent cells (BL21 (DE3)) were purchased from Invitrogen and transformed according to the manufacturer's protocol. The empty vector (pET-16b) originates from Novagen. Cell lysis for the liquid phase assay was performed by sonication using a Soniprep 150 (MSE UK Ltd.) and lysozyme from chicken egg white from Sigma. Starting materials were purchased from Acros and Sigma-Aldrich and used as received. 1-Phenyltetrahydroisoquinoline was obtained by reduction of the corresponding lactam with NaBH<sub>4</sub>/I<sub>2</sub> instead of LiAlH<sub>4</sub> according to Amat *et al.* [1] Solvents were analytical or HPLC grade or were purchased dried over molecular sieves where necessary. Column chromatography was performed on silica gel (Sigma-Aldrich, 220-440 mesh). <sup>1</sup>H and <sup>13</sup>C NMR spectra were recorded on a Bruker Avance 400 (400.1 MHz or 399.9 MHz for <sup>1</sup>H and 100.6 MHz for <sup>13</sup>C) without additional internal standard. Chemical shifts are reported in δ values (ppm) and are calibrated against residual solvent signal. The following abbreviations were used to define the multiplicities: s, singlet; d, doublet; t, triplet; q, quartet; m, multiplet; b, broad.

HPLC analysis was performed on an Agilent system equipped with a G1379A degasser, G1312A binary pump, a G1329 autosampler unit, a G1315B diode array detector and a G1316A temperature controlled column compartment; column and conditions are indicated separately. GC analysis was performed on Agilent 6850 GCs equipped with a Gerstel Multipurposesampler MPS2L and the column indicated separately

## Mutagenesis (under the strict supervision of SCW)

The D10 library was generated by incorporating NNS codons at positions 429&430 in MAO-N D5 mutant. Mutagenic PCR was performed using the Stratagene QuikChange® site directed mutagenesis kit, as per the manufacturer's instructions with the mutagenic primers shown in Table S1. Template DNA was removed by DpnI digestion, to remove parental DNA, before transformation of 1 μL DNA into XL-1 Blue *E. coli*. After transformation the cells were plated onto 14 cm agar plates containing 100 μg/mL of ampicillin and incubated at 37 °C overnight. Library quality was assessed by sequencing of 10 random samples and was shown to contain a high level of mutant incorporation. The remaining cells were harvested from the plate and the plasmid DNA isolated to provide the DNA library.

D11 mutants were generated by incorporating the W430G mutation into the D9A-D mutants previously identified.[2] Mutagenic PCR was performed using the Stratagene QuikChange® site directed mutagenesis kit, as per the manufacturer's instructions with the mutagenic primers shown in Table S1. Template DNA was removed by DpnI digestion, to remove parental DNA, before transformation of 1 µL DNA into XL-1 Blue *E. coli*. Each mutation was confirmed by DNA sequencing.

Primer name	Sequence (5'-3')
D10 for	ggatgagtttgcaagggcNNSNNSttcttcttaggcctggg
D10 rev	cccaggcctagagaagaaSNNSNNGcccttcgcaaactcatcc
D11 for	ggatgagtttgcaagggcGGCttcttcttaggcctggg
D11 rev	cccaggcctagagaagaaGCCgcccttcgcaaactcatcc

**Table S1.** List of mutagenic PCR primers used. The NNS codon (N = ACTG and S = CG, that gives access to all 20 amino acid residues minimising the frequency of stop codons) was used for the substitutions and are shown in upper case.

### Library Screening

The saturation mutagenesis libraries were screened using a solid phase assay. *E. coli* BL21 (DE3) cells were transformed with 1 µL of the MAO-N library and spread directly onto nitrocellulose membranes placed on top of LB ampicillin agar plates and incubated overnight at 37 °C. After overnight incubation, the membranes were removed from the agar plate and frozen in liquid nitrogen for 45 seconds to partially lyse the cells on the membrane. The membranes were allowed to warm back up to room temperature and the colonies thaw out. To reduce background activity the membranes were first incubated on top of a filter paper pre-soaked in 0.1 mg/mL solution of HRP, in a Petri dish for 30 minutes. The membrane was then transferred to another filter paper soaked in the reagent mix described below. The reaction was incubated at room temperature until colour was observed within some of the colonies. A reagent mix for solid phase assay comprised of the following: 19.5 mL 0.1 M potassium phosphate buffer pH 7.7, 1 DAB tablet (Sigma), 10 mM substrate, 500 µL of HRP (1 mg/mL stock solution). The amine and DAB tablet were solubilised in the buffer solution before the HRP enzyme was added.

## Biotransformations

### Preparation of Biocatalyst

MAO-N (wild-type monoamine oxidase from *Aspergillus niger* with the amino acid substitutions shown in Table S3) was transformed into BL21 (DE3) *E. coli* (Novagen) as the manufacturer's instructions.

```
      10      20      30      40      50      60
MTSRDGYQWT PETGLTQGVV SLGVISPPTN IEDTDKDGW DVIVIGGGYC GLTATRDLTV

      70      80      90     100     110     120
AGFKTLLEEA RDRIGGRSWS SNIDGYPYEM GGTWVHWHQS HVWREITRYK MHNALSPSFN

      130     140     150     160     170     180
FSRQVNHQQL RTNPTTSTYM THEAEDELLR SALHKFTNVD GTNGRTVLPF PHDMFYVPEF

      190     200     210     220     230     240
RKYDEMSYSE RIDQIRDELS LNERSSLEAF ILLCSGGTLE NSSFGFLHW WAMSGYTYQG

      250     260     270     280     290     300
CMDCLISYKF KDGQSAFARR FWEEAAGTGR LGYVFGCPVR SVVNERDAAR VTARDGREFA

      310     320     330     340     350     360
AKRLVCTIPL NVLSTIQFSP ALSTERISAM QAGHVNMTCK VHAEVDNKDM RSWTGIAYPF

      370     380     390     400     410     420
NKLCYAIGDG TTPAGNTHLV CFGTDANHIQ PDEDVRETLK AVGQLAPGTF GVKRLVFHNW

      430     440     450     460     470     480
VKDEFKAGAW FFSRPGMVSE CLQGLREKHR GVVFANSWA LGWRSFIDGA IEEGTRAARV

      490
VLEELGTKRE VKARL
```

MAO-N variant	Phe 210	Leu 213	Met 242	Ile 246	Asn 336	Thr 384	Asp 385	Trp 430
D3	-	-	-	Met	Ser	-	-	-
D5	-	-	-	Met	Ser	Asn	Ser	-
D9	Leu	Thr	Gln	Thr	Ser	Asn	Ser	-
D10	-	-	-	-	Ser	Asn	Ser	Gly
D11A	Met	Cys	Val	Thr	Ser	Asn	Ser	Gly
D11B	Leu	Thr	Val	Thr	Ser	Asn	Ser	Gly
D11C	Leu	Thr	Gln	Thr	Ser	Asn	Ser	Gly
D11D	Met	Cys	Gln	Thr	Ser	Asn	Ser	Gly

**Table S3.** MAO-N variants and mutations respect to wild-type MAO-N (residues shown on top).

A single colony was used to inoculate a pre-culture (5 mL) which was grown in LB

with ampicillin (100 mg/L) at 37 °C and 250 rpm until an OD<sub>600</sub> between 0.6-1.0 was reached. 2 L Erlenmeyer flasks containing 600 mL LB with ampicillin (100 mg/L) were inoculated with 5 mL of pre-culture and incubated at 37 °C and 250 rpm for 24 hours. The cells were harvested by centrifugation at 8000 rpm and 4 °C for 20 min. The cell pellet was stored at -20°C until needed. Typically 4 g of cells were obtained from a 600 mL culture.

### **MAO-N purification**

5 g of frozen cell paste were thawed on ice and resuspended in 25 mL of phosphate buffer (100 mM K-Pi, pH 7.7; containing 1 mg/mL of lysozyme from chicken egg white) and incubated at 30 °C for 30 min. The suspension was cooled to 4 °C and cells were lysed by ultrasonication (30 s pulse, 30 s pause; 20 cycles). Cell debris was removed by centrifugation (20000 rpm, 40 min). Subsequently, the cell-free extracts were filtered through a syringe filter with a 0.22 µm pore size.

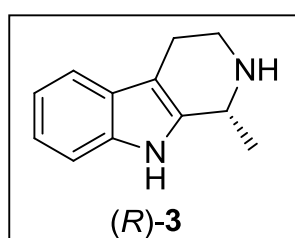
The cell-free extracts, after filtration, were loaded onto a HisTrap Ni-sepharose column (1 mL, *GE Healthcare*) pre-equilibrated with buffer A (100 mM K-Pi, pH 7.7, 300 mM NaCl). The column was loaded in the Äkta explorer system from *GE Healthcare* and the proteins were step-eluted using buffer A (10 mL), buffer A / buffer B (100 mM K-Pi, pH 7.7, 300 mM NaCl, 1 M imidazole)= 80/20 (10 mL) and buffer A / buffer B = 65/35 (10–30 mL); collecting 1 mL fractions. The MAO-N containing fractions (from the 35% buffer B step) were pooled and concentrated using a *Sartorius Vivaspin 6* spin column (30 kDa mass cut-off), the volume was adjusted to 2.5 mL.

The concentrated fractions, eluted at 350 mM imidazole concentration, were desalted using PD-10 Sephadex columns. Per column, 2.5 mL protein sample could be desalted. Each column was pre equilibrated by washing with 25 mL of buffer A. 2.5 mL protein sample was then applied and the flow through was discarded. The desalted protein sample was eluted with 3.5 mL buffer A.

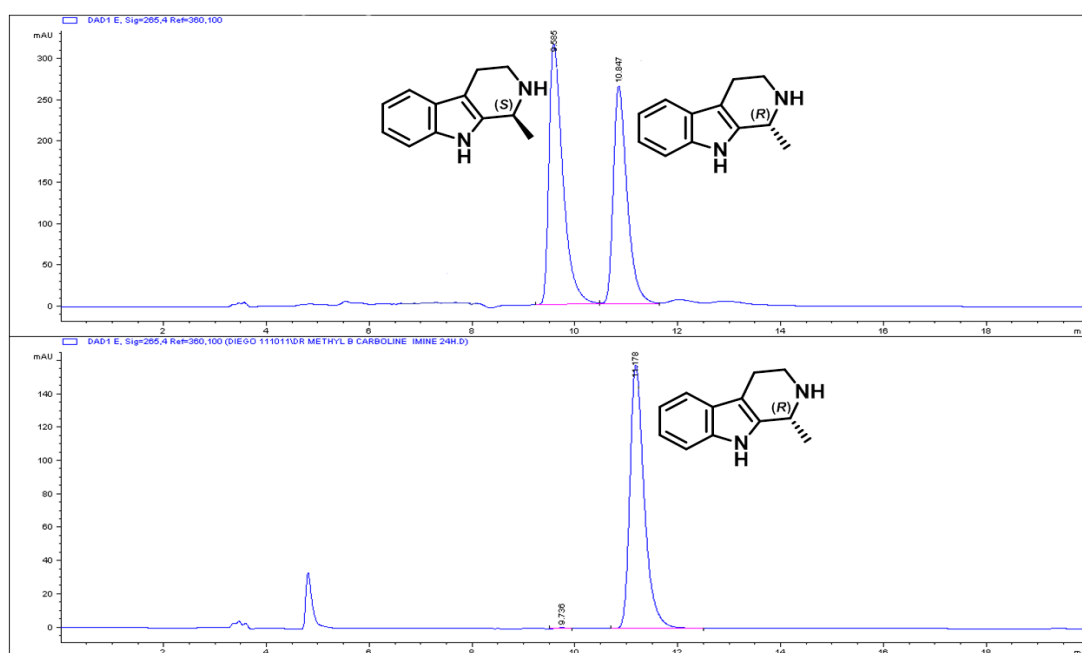
### **MAO-N D5/D9 Deracemisations: analytical procedure**

In a 2 mL Eppendorf tube, the amine (4.5-1.5 µL of 1M solution in DMF) and BH<sub>3</sub>-NH<sub>3</sub> (18-6 µL of 1M solution in KPO<sub>4</sub>-buffer) were added to a solution of cell pellet from *E. coli* cultures (150 mg/mL in 1 M KPO<sub>4</sub>-buffer, pH = 7.8) to obtain a final volume of 300 µL. The tube was placed in a shaking incubator and shaken at 37 °C

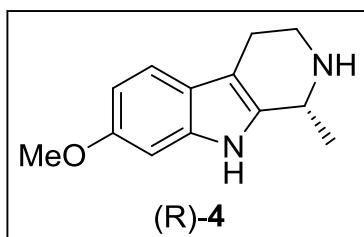
and 250 rpm. In total 5 reactions were set up for each substrate. The reaction was monitored by HPLC or GC taking a reaction and working it up every 3, 6, 24, 48 and 72 hours. HPLC samples were prepared as follows: aqueous NaOH-solution (10  $\mu$ L, 10 M) was added to the reaction mixture in the Eppendorf tube, followed by 1 mL of  $\text{CH}_2\text{Cl}_2$ . After vigorous mixing, by means of a vortex mixer, the sample was centrifuged at 13200 rpm for 1 minute. The organic phase was separated, dried over  $\text{MgSO}_4$  and analyzed by HPLC or GC.



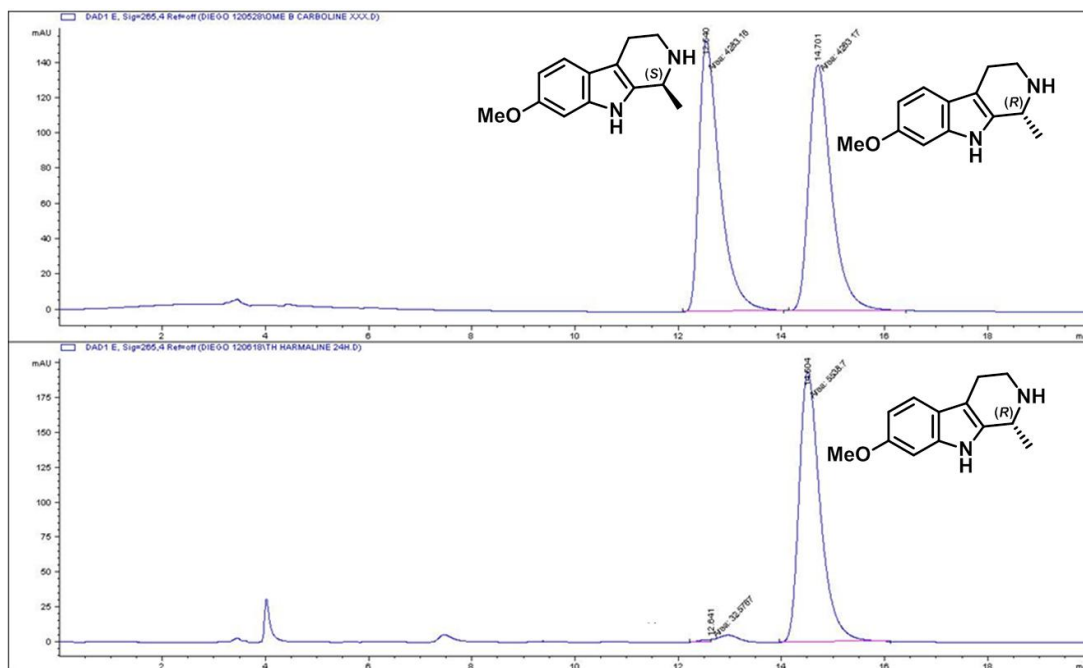
**(R)-Eleagnine (3).** The reaction was set up as described in the general procedure using MAO-N-D9 as biocatalyst. After 24 hours HPLC analysis showed 99% e.e.



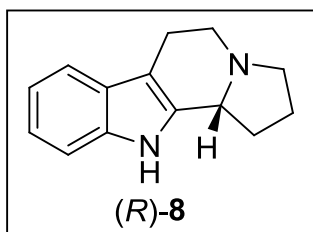
**Figure S3.** Chiral phase HPLC trace of (*rac*)-**3** conversion with MAO-N D9 showing the signals of racemic compound **3** (top) and the deracemisation product (*R*)-**3** (bottom).



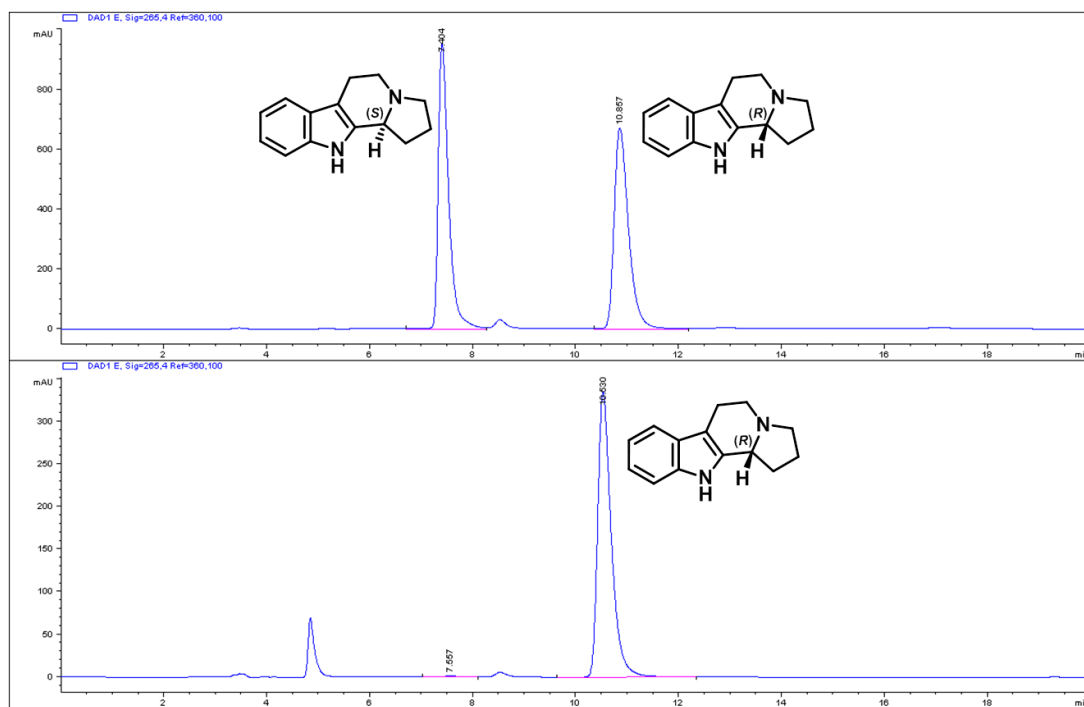
**(R)-Tetrahydroharmaline (4).** The reaction was set up as described in the general procedure using MAO-N D9 as biocatalyst. After 48 hours HPLC analysis showed 99% e.e.



**Figure S4.** Chiral phase HPLC trace of *rac*-4 conversion with MAO-N D9 showing the signals of racemic compound 4 (top) and the deracemisation product (*R*)-4 (bottom).



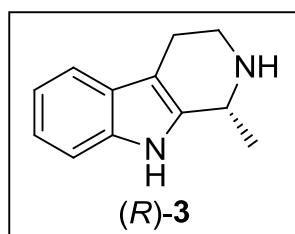
**(R)-Harmicine (8)**. The reaction was set up as described in the general procedure using MAO-N D9 as biocatalyst. After 48 hours HPLC analysis showed 99% e.e.



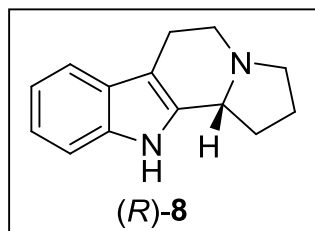
**Figure S5.** Chiral phase HPLC trace of (*rac*)-8 conversion with MAO-N D9 showing the signals of racemic compound 8 (top) and the deracemisation product (*R*)-8 (bottom).

### MAO-N D5/D9 Deracemisations: preparative procedure

In a 250mL screw cap bottle (for **1**) or a 500 mL screw cap bottle (for **3** and **4**), the racemic amine (1 eq) and  $\text{BH}_3\text{-NH}_3$  (4 eq) were dissolved in  $\text{KPO}_4$ -buffer (1 M, pH = 7.8). The pH of the solution was adjusted to 7.8 by addition of HCl. Cell pellet from *E. coli* cultures containing MAO-N D9 or D5 was added to the solution. The bottle was placed in a shaking incubator and shaken at 37 °C and 250 rpm. When HPLC or GC analysis showed the good conversion reached and the amount of imine < 2% (usually after 48-72 hours), aqueous NaOH (2 mL, 10 M) and  $\text{CH}_2\text{Cl}_2$  (200 mL) were added to work up the reaction. The mixture was transferred in Falcon tubes, the layers were separated by centrifugation (4000 rpm, 5 min.) and the aqueous phase was extracted with  $\text{CH}_2\text{Cl}_2$  ( $2 \times 100$  mL). The combined organic phases were dried over  $\text{MgSO}_4$  and concentrated under vacuum.



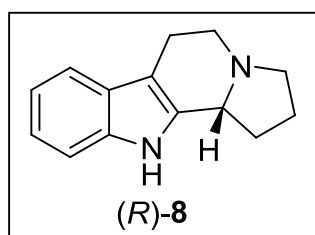
**(R)-Eleagnine (3).** The reaction was set up as described in the general procedure using (*rac*)-**3** (465 mg, 2.5 mmol),  $\text{BH}_3\text{-NH}_3$  (330 mg, 10 mmol),  $\text{KPO}_4$ -buffer (165 ml, 1 M, pH = 7.8) and MAO-N D9 cell pellet (5 g) as biocatalyst. After 40 hours HPLC analysis showed full conversion and the reaction was worked up to give (*R*)-**3** (432 mg, 99% e.e., 93% yield).



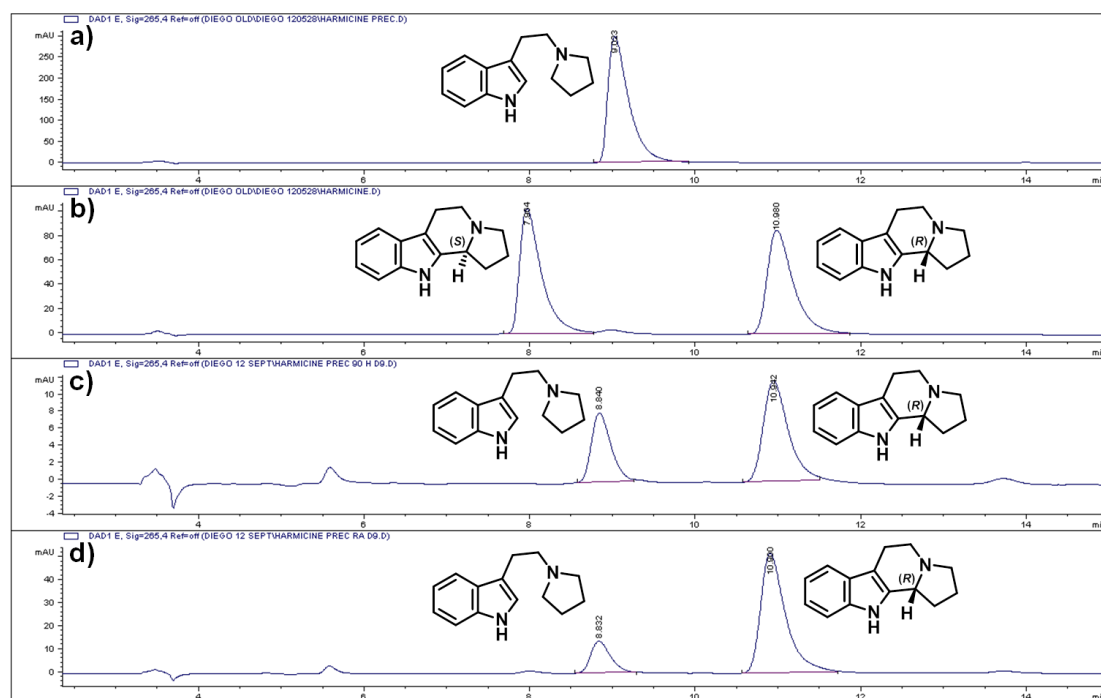
**(R)-Harmicine (8).** The reaction was set up as described in the general procedure using (*rac*)-**8** (530 mg, 2.5 mmol),  $\text{BH}_3\text{-NH}_3$  (330 mg, 10 mmol),  $\text{KPO}_4$ -buffer (165 ml, 1 M, pH = 7.8) and MAO-N D9 cell pellet (5 g) as biocatalyst. After 48 hours HPLC analysis showed full conversion and the reaction was worked up to give (*R*)-**8** (504 mg, 99% e.e., 95% yield).



## Biocatalytic synthesis of (*R*)-Harmicine using MAO-N D9

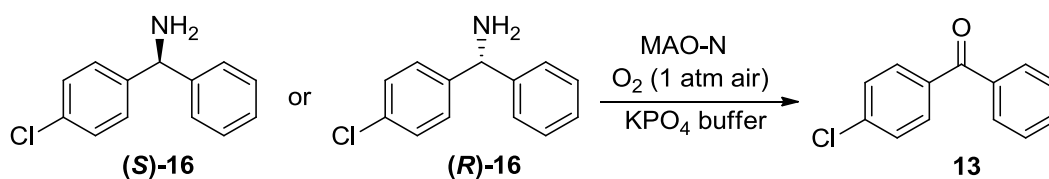


In a 2 mL Eppendorf tube, 3-(2-(pyrrolidin-1-yl)ethyl)-1H-indole **9** (1.5  $\mu$ L of 1M solution in DMF) was added of a solution of purified MAO-N D9 (300  $\mu$ L, 6.25 mg/mL in 1 M  $\text{KPO}_4$ -buffer, pH = 7.8). The tube was placed in a shaking incubator and shaken at 37  $^\circ\text{C}$  and 250 rpm. In total 5 reactions were set up. The reaction was monitored by HPLC taking a reaction and working it up every 24, 48, 72 and 96 hours. When the reaction reached good conversion (usually after 96 hours)  $\text{BH}_3\text{-NH}_3$  (6  $\mu$ L of 1M solution in  $\text{KPO}_4$ -buffer, pH = 7.8) was added and the biotransformation was left for additional 6 hours in the shaking incubator at 37  $^\circ\text{C}$ . HPLC samples were prepared as follows: aqueous NaOH-solution (10  $\mu$ L, 10 M) was added to the reaction mixture in the Eppendorf tube, followed by 1 mL of  $\text{CH}_2\text{Cl}_2$ . After vigorous mixing, by means of a vortex mixer, the sample was centrifuged at 13200 rpm for 1 minute. The organic phase was separated, dried over  $\text{MgSO}_4$  and analyzed by HPLC.



**Figure S6.** Chiral phase HPLC trace of (*rac*)-**8** conversion with MAO-N D9 showing the signals of: **a)** (*rac*)-Harmicine **8**. **b)** Starting material **9**. **c)** Biotransformation after 96 hours. **d)** Biotransformation after the addition of  $\text{BH}_3\text{-NH}_3$ .

### MAO-N oxidations: General procedure



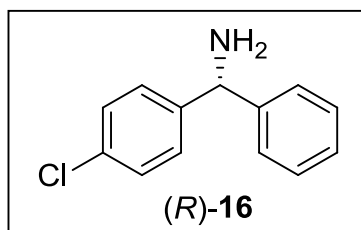
In a 50 mL Falcon tube, the (*S*)-**16** or (*R*)-**16** (0.05 mmol) was dissolved in KPO<sub>4</sub>-buffer (5 mL, 1 M, pH = 7.8). If necessary, the pH of the solution was adjusted to 7.8 by addition of HCl. The solution was added to cell pellet from *E. coli* cultures (500 mg) containing MAO-N D11. The tube was placed in a shaking incubator and shaken at 37 °C and 250 rpm. The reaction was monitored by chiral HPLC. HPLC samples were prepared as follows: aqueous NaOH-solution (20 μL, 10 M) was added to a 250 μL sample of the reaction mixture in an Eppendorf tube, followed by 1 mL of *tert*-butyl methyl ether. After vigorous mixing by means of a vortex mixer the sample was centrifuged at 13200 rpm for 1 minute. The organic phase was separated, dried over MgSO<sub>4</sub> and analyzed by HPLC.

### MAO-N-D11 Deracemisations: Analytical procedure

In a 50 mL Falcon tube, the amine (0.05 mmol) and BH<sub>3</sub>-NH<sub>3</sub> (0.2 mmol, 4 eq.) were dissolved in KPO<sub>4</sub>-buffer (5 mL, 1 M, pH = 7.8). If necessary, the pH of the solution was adjusted to 7.8 by addition of HCl. The solution was added to cell pellet from *E. coli* cultures (500 mg) containing MAO-N D11C. The tube was placed in a shaking incubator and shaken at 37 °C and 250 rpm. The reaction was monitored by HPLC and work up was performed when the e.e. reached > 97 % and the amount of imine was < 3%. HPLC samples were prepared as follows: aqueous NaOH-solution (20 μL, 10 M) was added to a 250 μL sample of the reaction mixture in an Eppendorf tube, followed by 1 mL of *tert*-butyl methyl ether. After vigorous mixing by means of a vortex mixer the sample was centrifuged at 13200 rpm for 1 minute. The organic phase was separated, dried with MgSO<sub>4</sub> and analyzed by HPLC. Work up was performed in the following way, aqueous NaOH-solution (200 μL, 10 M) and *tert*-butyl methyl ether (10 mL) were added. The organic phase was separated, dried over MgSO<sub>4</sub> and analyzed by HPLC.

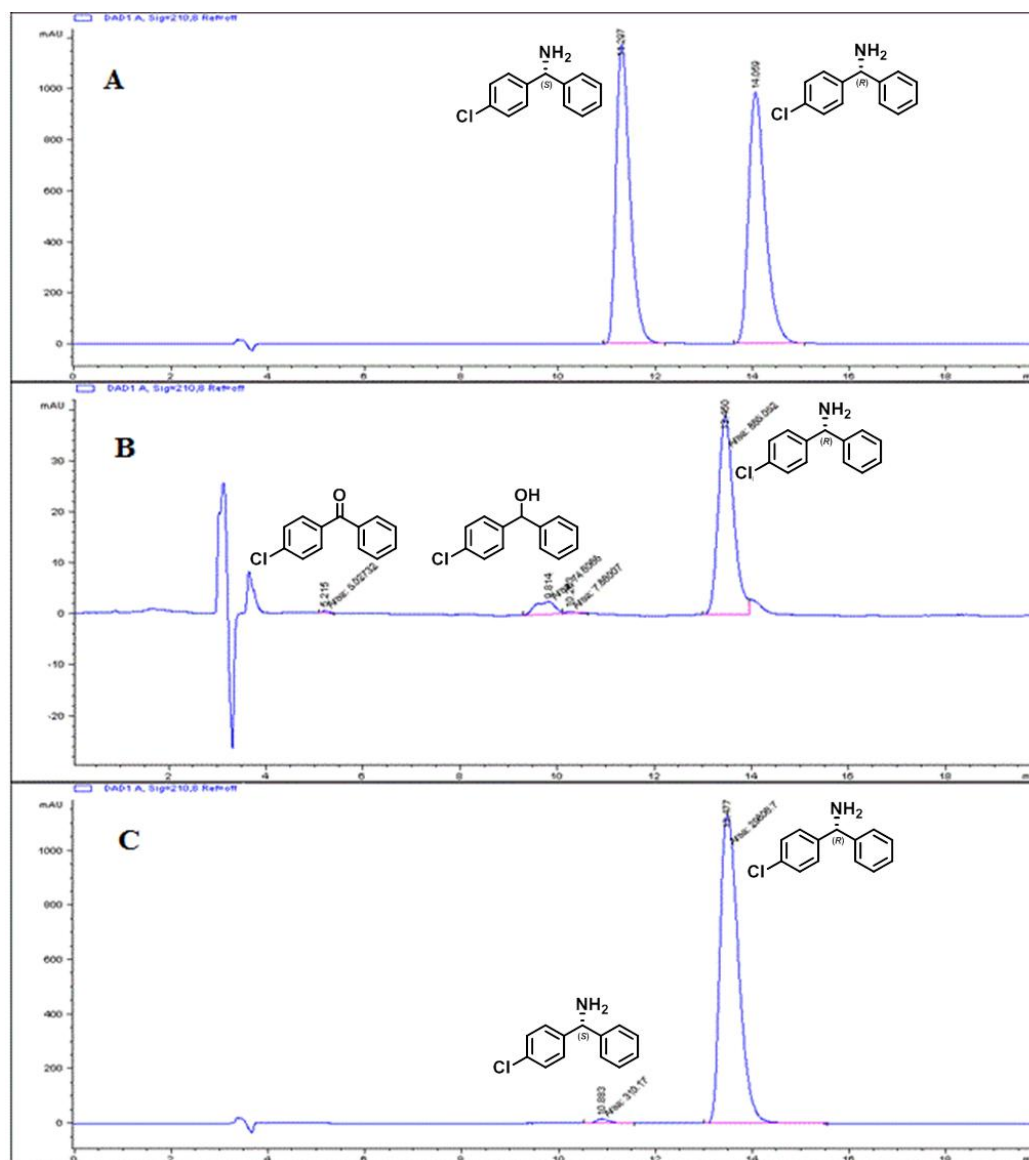
## MAO-N-D11C Deracemisations: Preparative procedure

### (*R*)-4-Chlorobenzhydrylamine (**16**)



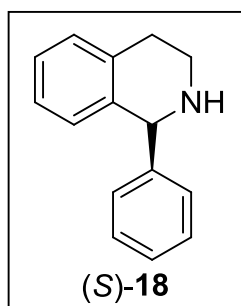
In a 500 mL screw cap bottle, (*rac*)-**16** (500 mg, 2.30 mmol) and  $\text{NH}_3\text{BH}_3$  (315 mg, 9.21 mmol, 4 eq.) were dissolved in  $\text{KPO}_4$ -buffer (175 mL, 1 M, pH = 7.8). The pH of the solution was adjusted to 7.8 by addition of HCl. Cell pellet from *E. coli* cultures (5 g)

containing MAO-N D11C was added to the solution. The bottle was placed in a shaking incubator and shaken at 37 °C and 250 rpm. When HPLC analysis showed the conversion reached > 97 % (usually after 48 hours), aqueous NaOH (2 mL, 10 M) and *tert*-butyl methyl ether (200 mL) were added to work up the reaction. The reaction mixture was vigorously mixed and the enzyme was removed by filtration through a Celite pad. The two layers were separated, 1 M HCl was added to the organic layer till pH=1 and the two phases were separated. The aqueous phase was washed twice with *tert*-butyl methyl ether (2 x 50 mL), then 10 M NaOH was added till pH 10-11 and the aqueous phase was extracted with *tert*-butyl methyl ether (3 x 50 mL). The combined organic phases were dried over  $\text{MgSO}_4$  and concentrated under vacuum to give (*R*)-**16** as a colourless oil (225 mg, 45% yield, 97% e.e.).

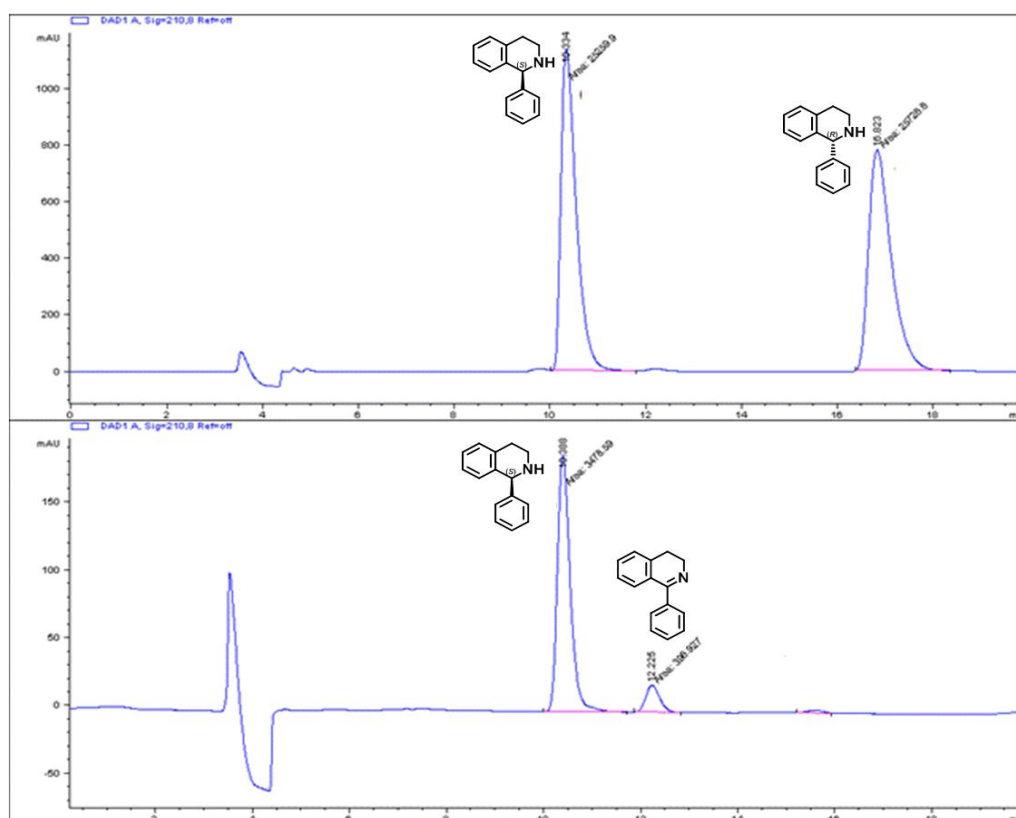


**Figure S7.** Chiral phase HPLC trace of (*rac*)-**16** conversion with MAO-N D11. **A)** (*rac*)-**16**. **B)** Deracemisation of (*rac*)-**16** after 48 hours. **C)** Deracemisation of (*rac*)-**16** after work-up to give (*R*)-**16**.

## 1-Phenyltetrahydroisoquinoline (**18**)



In a 500 mL screw cap bottle, (*rac*)-**18** (500 mg, 2.41 mmol) and  $\text{BH}_3\text{-NH}_3$  (328 mg, 9.66 mmol, 4 eq.) were dissolved in  $\text{KPO}_4$ -buffer (185 mL, 1 M, pH = 7.8). The pH of the solution was adjusted to 7.8 by addition of HCl. Cell pellet from *E. coli* cultures (12.5 g) containing MAO-N D11C was added to the solution. The bottle was placed in a shaking incubator and shaken at 37 °C and 250 rpm. When HPLC analysis showed the conversion reached > 97 % and the amount of imine < 3% (usually after 72 hours), aqueous NaOH (2 mL, 10 M) and *tert*-butyl methyl ether (200 mL) were added to work up the reaction. The reaction mixture was vigorously mixed and the enzyme was removed by filtration through a Celite pad. The two layers were separated and the aqueous phase was extracted with *tert*-butyl methyl ether (2 × 50 mL). The combined organic phases were dried with  $\text{MgSO}_4$  and concentrated under vacuum to give (*S*)-**18** as a yellowish solid (450 mg, 90% yield, 98% e.e.).



**Figure S8.** Chiral phase HPLC trace of (*rac*)-**18** conversion with MAO-N D11. (*rac*)-**18** (top) and deracemisation of (*rac*)-**18** after 72 hours to give (*R*)-**18** (bottom).

## Biotransformation using MAO-N D11: reaction conditions optimization

### (*rac*)-4-Chlorobenzhydrylamine (16)

Substrate (mM)	Enzyme (mg/mL)	BH <sub>3</sub> -NH <sub>3</sub> (eq.)	Co-solvent (%)	Temp. (°C)	Time (h)	Impurity (%) <sup>a</sup>	e.e. (%)
6.5	150	0	0	30	2	>50	100 ( <i>R</i> )
6.5	150	0	0	37	1	>50	100 ( <i>R</i> )
6.5	150	0	5 (DMSO)	30	5	>50	100 ( <i>R</i> )
6.5	150	0	10 (DMSO)	30	6	>50	100 ( <i>R</i> )
6.5	150	0	20 (DMSO)	30	10	30	55 ( <i>R</i> )
13	150	0	10 (MeOH)	30	24	40	80 ( <i>R</i> )
13	150	0	20 (MeOH)	30	48	0	0
13	150	0	0	30	3	>50	100 ( <i>R</i> )
26	150	0	0	30	7	>50	100 ( <i>R</i> )
13	150	6	0	37	20	10	94 ( <i>R</i> )
13	150	4	0	37	8	11	98 ( <i>R</i> )
13	75	4	0	37	20	14	98 ( <i>R</i> )
13	30	4	0	37	40	12	98 ( <i>R</i> )

**Table S4.** Biotransformation of (*rac*)-**16** using different substrate and enzyme concentration, co-solvents, temperature and amount of reducing agent. All the reactions were performed in the following conditions: enzyme MAO-N-D11C, buffer concentration 1 M pH7.7, reaction volume 200  $\mu$ L in a 2 mL Eppendorf, air, shaking at 250 rpm. All e.e. conversions were determined *via* HPLC analysis. <sup>a</sup>Impurity is the total amount of ketone and alcohol by-product observed during the reaction.

As shown in Table S.4, the most important parameter to increase the reaction ratio was the temperature; an increase from 30 °C to 37 °C doubled the reaction ratio. A problem that was found during the biotransformation which could affect the reaction ratio and the selectivity was the substrate solubility (not completely in solution). In order to improve the substrate solubility we added a water-soluble co-solvent (methanol, DMSO) in different concentrations (5% to 20%). Unfortunately both solvents seem to inhibit the enzyme because the reaction ratio decreased quite dramatically (using 20% of methanol there is no activity at all).

The amount of reducing agent (BH<sub>3</sub>-NH<sub>3</sub>) was another important parameter. In order to decrease the amount of by-products (ketone and alcohol), we tried to change the amount of ammonia-borane complex by using 6 equivalents instead of 4. This variation only gave a 1% decrease of alcohol but, at the same time, a worse reaction ratio and e.e. After the optimization of these three important parameters (temperature, co-solvent and reducing agent) the next step was to decrease the

enzyme concentration and increase the substrate concentration in order to achieve a biotransformation that could be transferred into an industrial process.

At the beginning, all deracemisation reactions were carried out with a 6.5 mM substrate concentration and an enzyme concentration of 150 mg/mL. This means that it was necessary to use huge amounts of enzyme and buffer to deracemise only a few grams of substrate. Increasing the substrate concentration from 6.5 to 13 mM gave a higher reaction rate (50% faster to oxidise the same amount of substrate). Even higher concentrations (26 mM) were also tried but, due to the low substrate solubility, without improvements. After the optimization of this parameter we tried to decrease the amount of enzyme. Starting from a concentration of 150 mg/mL, we tried 75 mg/mL and 30 mg/mL. As expected the reaction ratio decreased but it was still reasonably acceptable, so we decided to use an enzyme concentration of 30 mg/mL of whole cells for this deracemisation.

**(rac)-1-phenyl-1,2,3,4-tetrahydroisoquinoline (18)**

Starting from the optimized conditions for the deracemisation of 4-Chlorobenzhydrylamine, we changed some parameters (temperature, pH, buffer and co-solvent) in order to improve the substrate solubility and increase the reaction rate.

Buffer	Co-solvent	Temp. (°C)	pH	Time (h)	Conversion (%)	e.e. (%)
Phosphate	-	20	7.8	4	26	38 ( <i>S</i> )
Phosphate	-	30	7.8	4	29	42 ( <i>S</i> )
Phosphate	-	37	7.8	4	41	72 ( <i>S</i> )
Phosphate	-	42	7.8	4	42	74 ( <i>S</i> )
Phosphate	-	50	7.8	4	40	69 ( <i>S</i> )
Phosphate	-	37	7.8	5	47	90 ( <i>S</i> )
MOPS	-	37	7.8	5	49	95 ( <i>S</i> )
MES	-	37	7.8	5	49	95 ( <i>S</i> )
HEPES	-	37	7.8	5	43	80 ( <i>S</i> )
TRIS	-	37	7.8	5	44	81 ( <i>S</i> )
Phosphate	-	37	6.5	5	40	68 ( <i>S</i> )
Phosphate	-	37	7.0	5	44	78 ( <i>S</i> )
Phosphate	-	37	7.5	5	48	92 ( <i>S</i> )
Phosphate	-	37	8.0	5	48	93 ( <i>S</i> )
Phosphate	-	37	9.0	5	45	83 ( <i>S</i> )
Phosphate	-	37	10.0	5	33	45 ( <i>S</i> )
Phosphate	Hexane	37	7.8	24	47	85 ( <i>S</i> )
Phosphate	Toluene	37	7.8	24	46	89 ( <i>S</i> )
Phosphate	DCM	37	7.8	24	40	69 ( <i>S</i> )
Phosphate	MTBE	37	7.8	24	37	46 ( <i>S</i> )
Phosphate	AcOEt	37	7.8	24	32	45 ( <i>S</i> )

**Table S5.** Biotransformation of (*rac*)-**18** using different temperature, pH, buffer and co-solvent. All the reactions were performed in the following conditions: enzyme MAO-N-D11C 150 mg/mL, buffer concentration 1 M pH7.7, reaction volume 200  $\mu$ L in a 2 mL Eppendorf, air, shaking at 250 rpm. All e.e. conversions were determined *via* HPLC analysis.

As shown in Table S.5, a range of different temperatures was tried and, after 4 hours, the reaction rate was the same at 37 °C to 50 °C. Measurements at 1 and 2 hours showed that the conversion at 42 °C and 50 °C was higher than at 37 °C. This suggests that the enzyme was not stable at those temperatures, so we decided to carry out the biotransformations at 37 °C.

Different buffers were tested, and MOPS and MES showed slightly faster reaction



rates than the phosphate buffer. But due to the higher price of the morpholino-sulfonic buffers we continued to use the phosphate buffer (when scaling up the biotransformation this will become an important factor).

Biotransformations carried out at different pH had shown that the enzyme tolerates a broad pH range, and indeed between 7.0 and 9.0 the enzyme is working without a big difference in reaction rate.

The use of an immiscible co-solvent (50% in volume) led to a significant decrease in reaction rate without an implementation of enantiomeric excess yield.

### **Experiments to establish the absolute configuration**

#### **Coniine (1), Eleagnine (3), Harmicine (8) and Leptaflorin (4)**

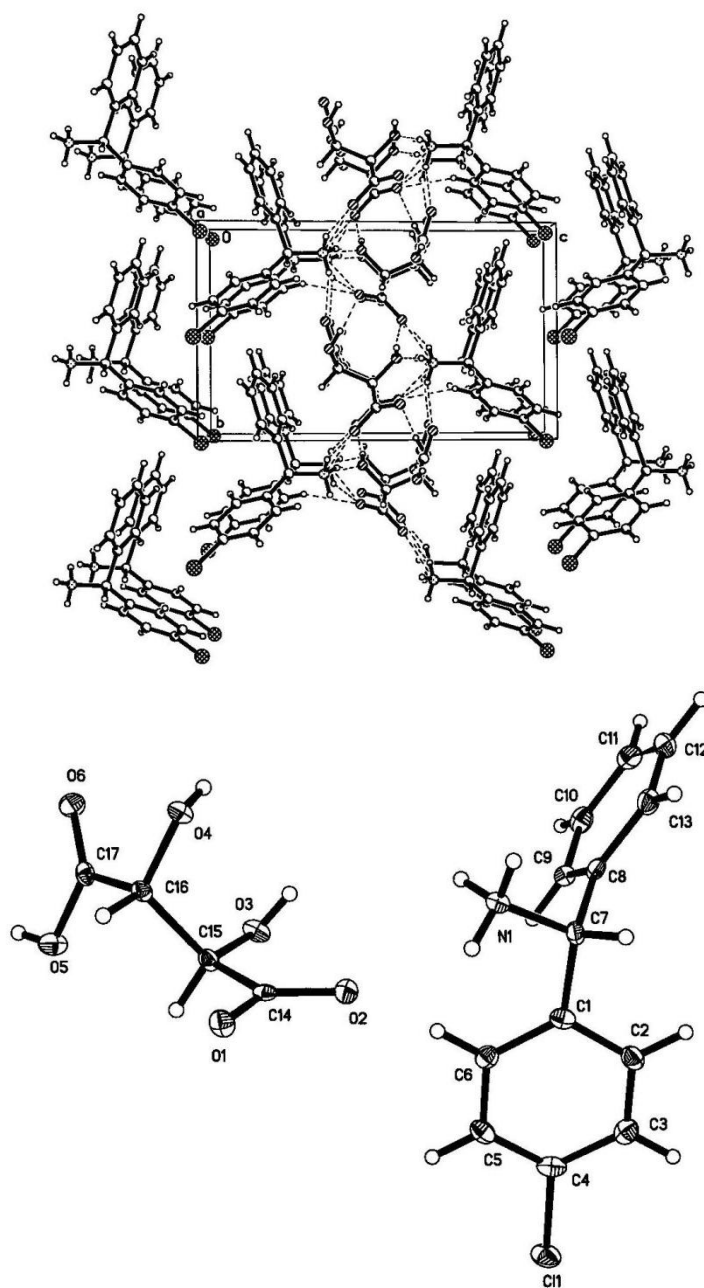
The absolute configurations of the products Coniine (1), Eleagnine (3) and Harmicine (8) were assigned by comparison of their optical rotation with the literature (see below). The absolute configuration of Leptaflorin (4) was assigned by analogy and by comparison of its HPLC retention times with the literature.[11]

Observed value for (*R*)-Coniine **1**:  $[\alpha]_{\text{D}}^{20}$ : -7.0 ° (c = 0.50, CHCl<sub>3</sub>), (*R*)-Eleagnine **3**:  $[\alpha]_{\text{D}}^{20}$ : +60.3 ° (c = 1.0, EtOH), (*R*)-Harmicine **8**:  $[\alpha]_{\text{D}}^{20}$ : +116.7 ° (c = 1.0, CHCl<sub>3</sub>).

Literature values for (*R*)-Coniine **1**:  $[\alpha]_{\text{D}}^{24}$ : -7.9 ° (c = 0.52, CHCl<sub>3</sub>) [12], (*S*)-Eleagnine **3**:  $[\alpha]_{\text{D}}^{25}$ : -62.1 ° (c = 1.36, EtOH) [13], (*R*)-Harmicine **8**:  $[\alpha]_{\text{D}}$ : +119.0° (c = 0.09, CHCl<sub>3</sub>) [14]

#### **(*R*)-4-Chlorobenzhydrylamine (16)**

Following the procedure reported by Clemo *et al.* [15], a standard sample of (*R*)-**16** was prepared by diastereoisomeric crystallization with L-(+)-tartaric acid. (*rac*)-**16** (1 g) was dissolved in ethanol (7 mL), L-(+)-tartaric acid (700 mg) was added and the mixture was heated until complete dissolution. Water (3 mL) was added to the clear solution and the mixture was allowed to crystallize at r.t. The crystals were filtered off and washed with a cold 1:1 Ethanol-Water mixture (2 mL). A further crystallization under the same conditions was necessary to achieve 99% e.e. Single crystal analysis of the salt confirmed the absolute conformation of the (*R*)-**16** (Figure S9).



**Figure S9.** (*R*)-4-Chlorobenzhydramine tartaric salt crystal structure.

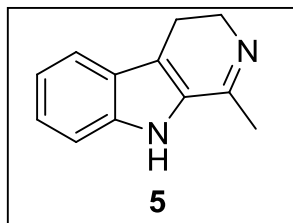
**(*S*)-1-Phenyltetrahydroisoquinoline (18)**

A standard sample of (*S*)-**18** was prepared by diastereoisomeric crystallization with D-(-)-tartaric acid. (*rac*)-**18** (1 g) and D-(-)-tartaric acid (670 mg) were suspended in methanol (10 mL), the mixture was heated until complete dissolution and allowed to crystallize at r.t. The crystals were filtered off and washed with methanol (2 mL). A further crystallization under the same conditions was necessary to achieve 99% e.e. The absolute configuration of **18** was determined to be (*S*) by comparing its specific optical rotation to the value reported in literature.[16]

Observed value for (*S*)-**18**:  $[\alpha]_{\text{D}}^{20}$ : +33.9 ° (c = 1.0, CH<sub>2</sub>Cl<sub>2</sub>).

Literature value for (*S*)-**18**:  $[\alpha]_{\text{D}}^{22}$ : +36.1 ° (c = 0.74, CH<sub>2</sub>Cl<sub>2</sub>).

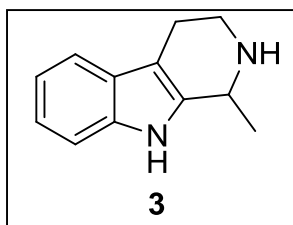
### Chemical Synthesis



**1-Methyl-4,9-dihydro-3H-β-carboline (5)**: To a stirred and cooled (0 °C) solution of tryptamine (1.0 g, 6.24 mmol) in CH<sub>2</sub>Cl<sub>2</sub> (20 mL) and triethylamine (2 mL) was added a solution of acetyl chloride (488 μL, 6.86 mmol). The resulting mixture was stirred at room temperature for 1 hour, washed with water and dried over MgSO<sub>4</sub>. The solvents were removed under vacuum and the resulting amide was reacted directly without purification with POCl<sub>3</sub> (1.75 mL, 18.7 mmol) in a 9:1 mixture of toluene/acetonitrile (20 mL). The reaction mixture was allowed to reflux for 4 hours, then cooled and poured onto ice. The resulting solution was brought to pH 10 with aqueous 40% NaOH and MeOH (5 mL) was added. The resulting mixture was filtered and the filtrate was extracted twice with toluene (2 x 100 mL), dried over MgSO<sub>4</sub> and concentrated under vacuum. Purification on silica gel (Et<sub>2</sub>O) afforded **5** (1.0 g, 87% yield) as yellowish solid. Analytical data matches with the literature. [22]

<sup>1</sup>H NMR, 400 MHz, CDCl<sub>3</sub> δ: 8.21 (bs, 1H, NH), 7.60 (d, *J* = 8.1 Hz, 1H, ArH), 7.40 (d, *J* = 8.2 Hz, 1H, ArH), 7.28 (t, *J* = 7.5 Hz, 1H, ArH), 7.16 (t, *J* = 7.5 Hz, 1H, ArH), 3.87 (t, *J* = 8.4 Hz, 2H, -CH<sub>2</sub>CH<sub>2</sub>N), 2.87 (t, *J* = 8.8 Hz, 2H, -CH<sub>2</sub>CH<sub>2</sub>N), 2.37 (s, 3H, -CH<sub>3</sub>).

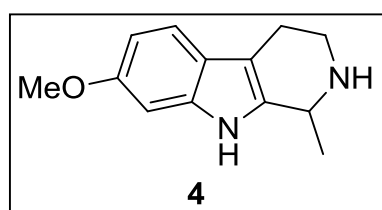
<sup>13</sup>C NMR, 100 MHz, CDCl<sub>3</sub> δ: 138.1 (ArC), 136.8 (ArC), 129.1 (ArC), 125.5 (ArC), 124.5 (ArC), 120.3 (ArC), 120.1 (ArC), 116.6 (ArC), 112.1 (ArC), 48.1 (-CH<sub>2</sub>CH<sub>2</sub>N), 22.0 (-CH<sub>3</sub>), 19.4 (-CH<sub>2</sub>CH<sub>2</sub>N).



**Eleagnine (3)**: A solution of **5** (500 mg, 2.71 mmol) in MeOH (20 mL) was cooled at 0 °C and NaBH<sub>4</sub> (103 mg, 2.71 mmol) added. The resulting mixture was stirred at room temperature for 1 hour. After concentration under vacuum the residue was added of 5% NaOH, extracted with CH<sub>2</sub>Cl<sub>2</sub> (2 x 20 mL) and dried over MgSO<sub>4</sub>. The organic phases were concentrated under vacuum to give **3** (466 mg, 93% yield) obtained as a yellowish solid. Analytical data matches with the literature. [17]

$^1\text{H}$  NMR, 400 MHz,  $\text{CDCl}_3$   $\delta$ : 8.24 (bs, 1H, NH), 7.50 (d,  $J = 7.3$  Hz, 1H, ArH), 7.29 (d,  $J = 8.3$  Hz, 1H, ArH), 7.21-7.06 (m, 2H, ArH), 4.17 (q,  $J = 6.5$  Hz, 1H,  $-\text{CHCH}_3$ ), 3.37 (dt,  $J = 13.2, 4.5$  Hz 1H,  $-\text{CH}_2\text{CHHN}$ ), 3.05 (ddd,  $J = 14.0, 8.8, 5.2$ , 1H,  $-\text{CH}_2\text{CHHN}$ ), 2.83-2.66 (m, 2H,  $-\text{CH}_2\text{CH}_2\text{N}$ ), 1.45 (d,  $J = 6.7$  Hz, 3H,  $-\text{CHCH}_3$ ).

$^{13}\text{C}$  NMR, 100 MHz,  $\text{CDCl}_3$   $\delta$ : 137.0 (ArC), 135.6 (ArC), 127.5 (ArC), 121.6 (ArC), 119.4 (ArC), 118.1 (ArC), 110.8 (ArC), 108.5 (ArC), 48.2 ( $\text{CHCH}_3$ ), 42.8 ( $-\text{CH}_2\text{CH}_2\text{N}$ ), 22.7 ( $-\text{CH}_3$ ), 20.7 ( $-\text{CH}_2\text{CH}_2\text{N}$ ).



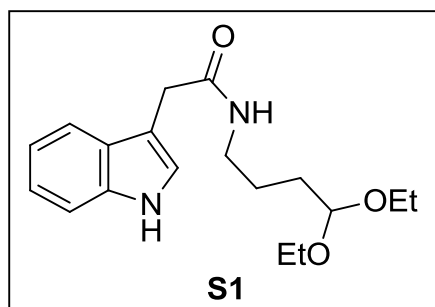
**Leptaflorin (4)**: Under nitrogen atmosphere, to a solution of **13** (100 mg, 0.47 mmol) in MeOH (5 mL) at  $0^\circ\text{C}$  was added  $\text{NaBH}_4$  (18 mg, 0.47 mmol).

The solution was stirred for 1 hour at room temperature. Water (20 mL) and  $\text{CH}_2\text{Cl}_2$  (25 mL) were added, the two phases separated and the aqueous phase extract with  $\text{CH}_2\text{Cl}_2$  (25 mL). The combined organic phases were dried over  $\text{MgSO}_4$  and concentrated under vacuum to give **4** (89 mg, 89% yield) as a white solid. Analytical data matches with the literature. [11]

$^1\text{H}$  NMR, 400 MHz,  $\text{CD}_3\text{OD}$   $\delta$ : 7.21 (d,  $J = 8.6$  Hz, 1H, ArH), 6.81 (d,  $J = 2.0$  Hz, 1H, ArH), 6.64-6.59 (m, 1H, ArH), 4.04 (q,  $J = 6.6$  Hz, 1H,  $-\text{CHCH}_3$ ), 3.76 (s, 3H,  $\text{CH}_3\text{O}-$ ), 3.27-3.19 (m, 1H,  $-\text{CH}_2\text{CHHN}$ ), 2.90 (ddd,  $J = 13.6, 9.6, 4.8$  Hz 1H,  $-\text{CH}_2\text{CHHN}$ ), 2.76-2.65 (m, 1H,  $-\text{CHHCH}_2\text{N}$ ), 2.64-2.55 (m, 1H,  $-\text{CHHCH}_2\text{N}$ ), 1.41 (d,  $J = 6.7$  Hz, 3H,  $-\text{CHCH}_3$ ).

$^{13}\text{C}$  NMR, 100 MHz,  $\text{CD}_3\text{OD}$   $\delta$ : 157.3 ( $\text{ArCOCH}_3$ ), 138.4 (ArC), 136.6 (ArC), 123.2 (ArC), 119.1 (ArC), 109.3 (ArC), 108.0 (ArC), 95.8 (ArC), 56.0 ( $\text{CH}_3\text{O}-$ ), 49.5 ( $\text{CHCH}_3$ ), 43.6 ( $-\text{CH}_2\text{CH}_2\text{N}$ ), 22.9 ( $-\text{CH}_3$ ), 20.3 ( $-\text{CH}_2\text{CH}_2\text{N}$ ).

### Synthesis Harmicine (8) [18]

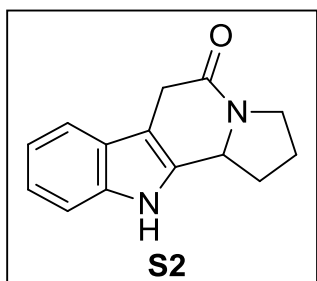


**N - (4,4 - diethoxybutyl) - 2 - (3 - indolyl) - acetamide (S1)**: Under nitrogen atmosphere, DCC (4.1 g, 20 mmol) was added to a solution of 3-indolylacetic acid (3.5 g, 20 mmol) and HOSu (2.3 g, 20 mmol) in EtOAc (150 mL). The mixture was stirred for 6 hours, then 4,4-

diethoxybutan-1-amine (3.4 mL, 0.02 mol., 90% purity) was added and the mixture stirred overnight.  $\text{Et}_2\text{O}$  (150 mL) was added and the precipitated DCU collected by

filtration and washed with Et<sub>2</sub>O (50 mL). The combined filtrate was washed with 2 *N* NaOH (50 mL), H<sub>2</sub>O (50 mL), dried over MgSO<sub>4</sub> and concentrated under vacuum to give **S1** as a viscous orange oil (5.92 g, 93% yield), which was used without further purification. Analytical data matches with the literature.[18]

<sup>1</sup>H NMR 400 MHz, CDCl<sub>3</sub> δ: 8.32 (bs, 1H, ArNH), 7.56 (d, *J* = 7.9 Hz, 1H, ArH), 7.41 (dt, *J* = 8.2, 0.8 Hz, 1H, ArH), 7.25 – 7.19 (m, 1H, ArH), 7.18 – 7.11 (m, 2H, ArH), 5.78 (bt, *J* = 6.0 Hz, 1H, NH), 4.37 (t, *J* = 5.2 Hz, 1H, -CH(OCH<sub>2</sub>CH<sub>3</sub>)<sub>2</sub>), 3.73 (s, 2H, CH<sub>2</sub>CO), 3.55 (dq, *J* = 9.3, 7.1 Hz, 2H, -CH(OCHHCH<sub>3</sub>)<sub>2</sub>), 3.38 (dq, *J* = 9.4, 7.1 Hz, 2H, -CH(OCHHCH<sub>3</sub>)<sub>2</sub>), 3.19 (q, *J* = 6.7 Hz, 2H, -CH<sub>2</sub>NH), 1.53 – 1.39 (m, 4H, -CH<sub>2</sub>CH<sub>2</sub>-), 1.13 (t, *J* = 7.1 Hz, 6H, -CH(OCH<sub>2</sub>CH<sub>3</sub>)<sub>2</sub>).

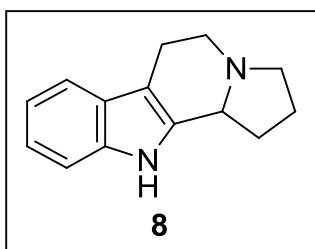


(±) **2,3,11,11b-tetrahydro-1*H*-indolizino[8,7-*b*]indol-6-one (S2)**: Under nitrogen atmosphere, BF<sub>3</sub>-Et<sub>2</sub>O (900 μL, 7 mmol) was added to a stirred solution of **S1** (2.15 g, 7 mmol) in CH<sub>2</sub>Cl<sub>2</sub> (80 mL). After 2 hours, H<sub>2</sub>O (5 mL) was added and the mixture stirred for an additional 5 min. Et<sub>2</sub>O (100 mL) was added and the solid collected, washed with

H<sub>2</sub>O (10 mL) and Et<sub>2</sub>O (20 mL). The organic layer from the filtrate was separated, dried over MgSO<sub>4</sub> and concentrated under vacuum to give a solid. The crude solid was purified by silica column chromatography to give **S2** as a pale yellow solid (1.27 g, 83% yield). Analytical data matches with the literature.[18]

<sup>1</sup>H NMR 400 MHz, DMSO δ: 11.19 (bs, 1H, ArNH), 7.43 (d, *J* = 7.8 Hz, 1H, ArH), 7.36 (d, *J* = 8.1 Hz, 1H, ArH), 7.10 (td, *J* = 7.1, 1.1 Hz, 1H, ArH), 6.98 (td, *J* = 7.5, 1.0 Hz, 1H, ArH), 4.77-4.68 (m, 1H, -CHN), 3.65 (dt, *J* = 11.7, 8.8 Hz, 1H, -CHHN), 3.55 (dd, *J* = 20.0, 4.5 Hz, 1H, CHHCO), 3.50 (dd, *J* = 20.0, 2.9 Hz, 1H, CHHCO), 3.36 (ddd, *J* = 11.9, 9.7, 2.4 Hz, 1H, -CHHN), 2.57-2.48 (m, 1H, -CHCHHCH<sub>2</sub>-), 2.10-1.87 (m, 2H, -CHCHHCHH-), 1.59 (qd, *J* = 11.6, 7.7 Hz, 1H, -CHCH<sub>2</sub>CHH-).

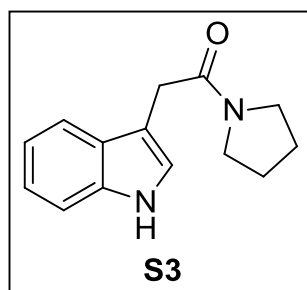
<sup>13</sup>C NMR, 100 MHz, DMSO δ: 166.5 (CO), 136.7 (ArC), 131.9 (ArC), 125.4 (ArC), 121.2 (ArC), 118.7 (ArC), 118.0 (ArC), 111.2 (ArC), 104.0 (ArC), 56.0 (-CHN), 44.2 (-CH<sub>2</sub>N), 31.3 (-CHCH<sub>2</sub>CH<sub>2</sub>-), 29.9 (-CH<sub>2</sub>CO), 22.1 (-CHCH<sub>2</sub>CH<sub>2</sub>-).



**Harmicine (8):** Under nitrogen atmosphere, concentrated  $\text{H}_2\text{SO}_4$  (80  $\mu\text{L}$ , 3.3 mmol) was dropwise added to a solution of  $\text{LiAlH}_4$  (3.5 mL of a 1 M solution in THF, 3.5 mmol) in dry THF (10 mL) at 0 °C. After stirring at 0 °C for 15 min, **S2** (500 mg, 2.2 mmol) was added in one portion and the reaction heated under reflux for 1 h. The reaction mixture was then cooled to 0 °C, 2 N NaOH (3 mL) in THF (20 mL) was carefully added and the reaction mixture stirred for 15 min.  $\text{CH}_2\text{Cl}_2$  (100 mL) was then added and the solid was collected and washed with  $\text{CH}_2\text{Cl}_2$  (2 x 50 mL). The combined organic fractions were dried over  $\text{MgSO}_4$ , concentrated under vacuum and the residue purified by silica column chromatography to give the solid product **8** (380 mg, 81% yield). Analytical data matches with the literature.[18]

$^1\text{H}$  NMR 400 MHz,  $\text{CDCl}_3$   $\delta$ : 7.78 (bs, 1H, ArNH), 7.51-7.46 (m,  $J = 7.8$  Hz, 1H, ArH), 7.34-7.30 (m, 1H, ArH), 7.17-7.07 (m, 2H, ArH), 4.25 (m, 1H, -CHN), 3.34 (ddd,  $J = 12.8, 5.4, 2.1$  Hz, 1H, -CHHCH<sub>2</sub>N-), 3.09 (ddd,  $J = 12.8, 10.7, 4.7$  Hz, 1H, -CHHCH<sub>2</sub>N-), 3.02-2.85 (m, 3H, -CH<sub>2</sub>NCHH-), 2.70-2.63 (m, 1H, -CH<sub>2</sub>NCHH-), 2.36-2.25 (m, 1H, -CHCHHCH<sub>2</sub>-), 1.98-1.80 (m, 3H, -CHCHHCH<sub>2</sub>-).

$^{13}\text{C}$  NMR, 100 MHz, DMSO  $\delta$ : 136.4 (ArC), 129.2 (ArC), 125.6 (ArC), 121.7 (ArC), 118.9 (ArC), 118.1 (ArC), 111.3 (ArC), 105.0 (ArC), 58.7 (-CHN), 50.1 (-CH<sub>2</sub>N), 45.6 (-CH<sub>2</sub>N), 29.1 (-CHCH<sub>2</sub>CH<sub>2</sub>-), 22.0 (-CHCH<sub>2</sub>CH<sub>2</sub>-), 16.4 (-CH<sub>2</sub>CH<sub>2</sub>N-).

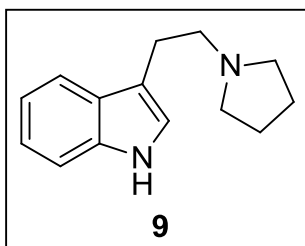


**2-(1H-indol-3-yl)-1-(pyrrolidin-1-yl)ethanone (S3):** Under nitrogen atmosphere to a solution of indole-3-acetic acid (500 mg, 2.85 mmol) in a mixture 1:1  $\text{CH}_2\text{Cl}_2/\text{THF}$  (10 mL) was added DIC (510  $\mu\text{L}$ , 3.28 mmol). The mixture was stirred for 1 hour at r.t., then pyrrolidine (309  $\mu\text{L}$ , 3.71 mmol) was added and the mixture was stirred for other 3

hours at r.t. Water (20 mL) was added and the mixture extracted with  $\text{CH}_2\text{Cl}_2$  (2 x 30 mL), the combined organic phases were dried over  $\text{MgSO}_4$ , concentrated under vacuum and the residue purified by silica column chromatography to give **S3** (650 mg, 97% yield). Analytical data matches with the literature.[19]

$^1\text{H}$  NMR 400 MHz,  $\text{CDCl}_3$   $\delta$ : 8.35 (bs, 1H, NH), 7.66 (d,  $J = 7.8$  Hz, 1H, ArH), 7.35 (d,  $J = 8.0$  Hz, 1H, ArH), 7.23-7.15 (m, 1H, ArH), 7.15-7.08 (m, 2H, ArH), 3.78 (s,

2H, -CH<sub>2</sub>CO), 3.59-3.39 (m, 4H, -CH<sub>2</sub>CH<sub>2</sub>N-), 1.97-1.74 (m, 4H, -CH<sub>2</sub>CH<sub>2</sub>N-).

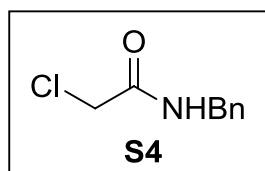


**3-(2-(pyrrolidin-1-yl)ethyl)-1H-indole (9):** Under nitrogen atmosphere to a solution of **S3** (500 mg, 2.19 mmol) in anhydrous THF (10 mL) was slowly added LiAlH<sub>4</sub> (2.62 mL of a 1 M solution in THF, 2.62 mmol) and the reaction was heated at reflux for 4 hours. The reaction mixture was then cooled to 0 °C, water (100 μL), 3 M NaOH (100 μL) and water (300 μL) were carefully added and the reaction mixture stirred for 10 min. The solid formed was filtered off and then washed with THF. The filtered was concentrated under vacuum to give **9** as a brownish solid (474 mg, 96% yield). Analytical data matches with the literature.[20]

<sup>1</sup>H NMR 400 MHz, CDCl<sub>3</sub> δ: 8.92 (bs, 1H), 7.63 (d, *J* = 7.7, 1H, Ar*H*), 7.32 (d, *J* = 8.0, 1H, Ar*H*), 7.25-7.19 (m, 1H, Ar*H*), 7.19-7.13 (m, 1H, Ar*H*), 6.96 (s, 1H, Ar*H*), 3.07 (dt, *J* = 13.0, 8.7, 2H, -CH<sub>2</sub>CH<sub>2</sub>N-), 2.96-2.85 (m, 2H, -CH<sub>2</sub>CH<sub>2</sub>N-), 2.77-2.66 (m, 4H, -NCH<sub>2</sub>CH<sub>2</sub>-), 1.95-1.83 (m, 4H, -NCH<sub>2</sub>CH<sub>2</sub>-).

<sup>13</sup>C NMR, 100 MHz, CDCl<sub>3</sub> δ: 136.4 (ArC), 127.5 (ArC), 121.8 (ArC), 121.8 (ArC), 119.0 (ArC), 118.8 (ArC), 114.1 (ArC), 111.3 (ArC), 57.4 (-CH<sub>2</sub>CH<sub>2</sub>N-), 54.3 (-CH<sub>2</sub>CH<sub>2</sub>N-), 25.1 (-CH<sub>2</sub>CH<sub>2</sub>N-), 23.6 (-CH<sub>2</sub>CH<sub>2</sub>N-).

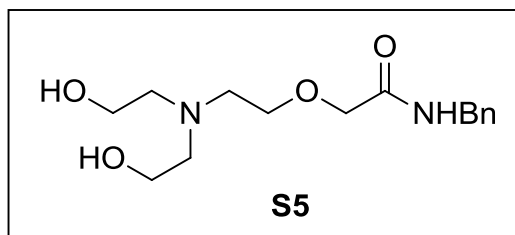
### Synthesis Levocetirizine 13 [21]



**N-benzyl-2-chloroacetamide (S4)** Under nitrogen atmosphere, a solution of benzylamine (34.5 mL, 301.40 mmol, 2.4 eq.) in CH<sub>2</sub>Cl<sub>2</sub> (100 mL) was cooled to 0 °C and chloroacetylchloride (10 mL, 125.64 mmol, 1 eq.) was added dropwise over 1 hour. The mixture was stirred for an additional hour at r.t. after which the solid was filtered off and washed with CH<sub>2</sub>Cl<sub>2</sub> (15 mL). The organic phase was washed with 0.5 M HCl (2 x 15 mL), dried over MgSO<sub>4</sub> and concentrated under vacuum to give **S4** as a white solid. (20.7 g, 90% yield). Analytical data matches with the literature.[21]

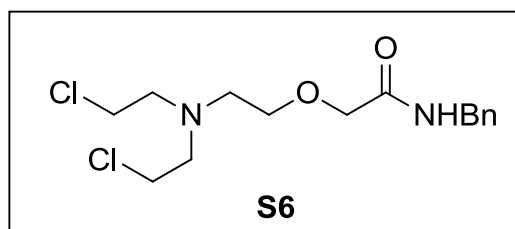
<sup>1</sup>H NMR, 400 MHz, CDCl<sub>3</sub> δ ppm: 7.32 (m, 5H, Ar*H*), 7.04 (bs, 1H, NH), 4.49 (d, *J* = 5.8, 2H, -CH<sub>2</sub>Ph), 4.08 (s, 2H, ClCH<sub>2</sub>CO).

<sup>13</sup>C NMR, 100 MHz, CDCl<sub>3</sub> δ ppm: 166.0 (CON), 137.3 (ArC), 128.8 (ArC), 127.8 (ArC), 127.5 (ArC), 43.8 (ClCH<sub>2</sub>CO), 42.6 (-CH<sub>2</sub>Ph).



**N - benzyl - 2 - (2 -(bis(2-hydroxyethyl) amino)ethoxy) acetamide (S5):** Under nitrogen atmosphere, a suspension of NaOH (2.18 g, 54.6 mmol, 1 eq.) in triethanolamine (36 mL, 272.2 mmol, 5

eq.) was heated at 100 °C for 1 hour. A solution of compound **S4** (10 g, 45.6 mmol, 1 eq.) in toluene (20 mL) was added to the reaction mixture and stirred for 4 hours at 100 °C. The solution was then cooled at room temperature and 6 M HCl was added till pH 1-2. The two phases were separated and the aqueous phase was basified till pH 12. The product was extracted with CH<sub>2</sub>Cl<sub>2</sub> (3 x 50 mL) and the solvent was dried over MgSO<sub>4</sub> and then removed under vacuum to give 13.1 g of crude product **S5** which was used without further purification.



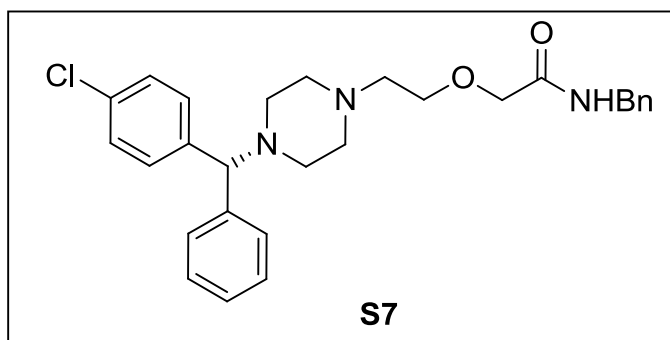
**N - benzyl - 2- (2 - (bis (2-chloroethyl)amino)ethoxy) acetamide (S6)** Under nitrogen atmosphere, a solution of compound **S5** (5 g, 16.87 mmol, 1 eq.) and DIPEA (8.08 mL, 47.23

mmol, 2.8 eq.) in CH<sub>2</sub>Cl<sub>2</sub> (50 mL) was cooled to 0 °C. Mesyl chloride (3.13 mL, 40.49 mmol, 2.4 eq.) was added dropwise keeping the temperature below 10 °C. The mixture was stirred overnight at r.t. Water (30 mL) was added, the two phases were separated and the organic phase was concentrated under vacuum. The crude solid was purified by silica column chromatography to give **S6** as a yellowish oil (4.7 g, 69% yield over 2 steps). Analytical data matches with the literature.[21]

<sup>1</sup>H NMR, 400 MHz, CDCl<sub>3</sub> δ ppm: 7.28 (m, 5H, ArH), 4.45 (d, *J* = 6.0 Hz, 2H, -CH<sub>2</sub>Ph), 3.98 (s, 2H, -OCH<sub>2</sub>CO), 3.50 (t, *J* = 5.2 Hz, 2H, -NCH<sub>2</sub>CH<sub>2</sub>O-), 3.39 (t, *J* = 6.8 Hz, 4H, -NCH<sub>2</sub>CH<sub>2</sub>Cl), 2.80 (t, *J* = 6.8 Hz, 4H, -NCH<sub>2</sub>CH<sub>2</sub>Cl), 2.73 (t, *J* = 5.2 Hz, 2H, -NCH<sub>2</sub>CH<sub>2</sub>O-).

<sup>13</sup>C NMR, 100 MHz, CDCl<sub>3</sub> δ ppm: 169.7 (CON), 138.2 (ArC), 128.7 (ArC), 127.8 (ArC), 127.5 (ArC), 70.5 (CH<sub>2</sub>O), 70.4 (CH<sub>2</sub>O), 56.9 ((CH<sub>2</sub>)<sub>2</sub>N), 54.1 (CH<sub>2</sub>N), 42.8 (-CH<sub>2</sub>Ph), 41.8 (ClCH<sub>2</sub>).



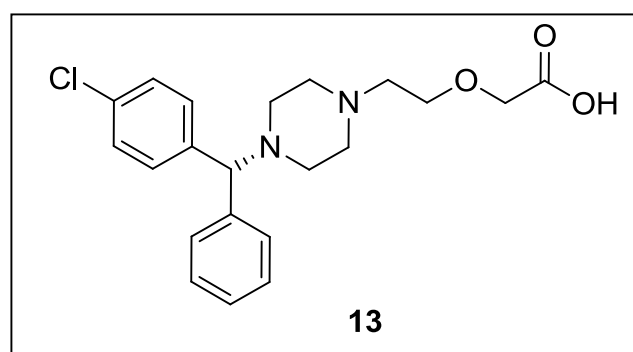


**Levocetirizine N - Benzyl amide (S7):** Under nitrogen atmosphere, a solution of compound **S6** (368 mg, 1.10 mmol, 1.2 eq.), (*R*)-**16** (200 mg, 0.92 mmol, 1 eq.) and DIPEA (392  $\mu$ L, 2.30 mmol,

2.5 eq.) was heated at 130  $^{\circ}$ C. After 4 hours the mixture was cooled to r.t. and ethyl acetate (15 mL) and brine (15 mL) were added, the two phases were separated and the organic phase was dried over  $\text{MgSO}_4$  and concentrated under vacuum. The crude solid was purified by silica column chromatography to give **S7** as a yellowish oil (329 mg, 75% yield). Analytical data matches with the literature.[21]

$^1\text{H}$  NMR, 400 MHz,  $\text{CDCl}_3$   $\delta$  ppm: 7.88 (bs, 1H, *NHBn*), 7.16 (m, 14H, *ArH*), 4.41 (d,  $J = 6.0$  Hz, 2H,  $-\text{CH}_2\text{Ph}$ ), 3.95 (s, 2H,  $-\text{OCH}_2\text{CO}$ ), 3.91 (s, 1H, *CHN*), 3.52 (t,  $J = 5.1$  Hz, 2H,  $-\text{NCH}_2\text{CH}_2\text{O}-$ ), 2.44 (t,  $J = 5.1$  Hz, 2H,  $-\text{NCH}_2\text{CH}_2\text{O}-$ ), 2.37 and 2.12 (2 x bs, 2 x 4H,  $-\text{N}(\text{CH}_2\text{CH}_2)_2\text{N}-$ ).

$^{13}\text{C}$  NMR, 100 MHz,  $\text{CDCl}_3$   $\delta$  ppm: 170.6 (*CON*), 142.0 (*ArC*), 141.3 (*ArC*), 138.4 (*ArC*), 132.6 (*ArC*), 129.1 (*ArC*), 128.7 (*ArC*), 128.7 (*ArC*), 128.6 (*ArC*), 127.8 (*ArC*), 127.5 (*ArC*), 127.4 (*ArC*), 127.2 (*ArC*), 75.2 (*CHN*), 70.6 ( $\text{CH}_2\text{O}$ ), 69.2 ( $\text{CH}_2\text{O}$ ), 57.6 ( $\text{CH}_2\text{N}$ ), 53.7 ( $(\text{CH}_2)_2\text{N}$ ), 51.5 ( $(\text{CH}_2)_2\text{N}$ ), 42.6 ( $-\text{CH}_2\text{Ph}$ ).



**Levocetirizine (13):** To a solution of  $\text{H}_2\text{SO}_4$  (500  $\mu$ L) in methanol (2 mL) was added **S7** (250 mg, 0.52 mmol). The mixture was stirred at reflux for 16 hours. After cooling to r.t., 10 M NaOH was added till pH 10-

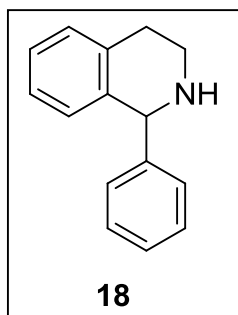
12 and the mixture was stirred for a further 2 hours. 1 M HCl was then added till pH 4.5 and it was extracted with  $\text{CH}_2\text{Cl}_2$  (3 x 25 mL). The organic phases were dried over  $\text{MgSO}_4$  and concentrated under vacuum yielding **13** as a white solid (140 mg, 70% yield). Analytical data matches with the literature.[21]

$^1\text{H}$  NMR, 400 MHz,  $\text{CDCl}_3$   $\delta$  ppm: 11.48 (bs, 1H,  $-\text{COOH}$ ), 7.37-7.21 (m, 9H, *ArH*),

4.30 (s, 1H, -CHN-), 4.03 (s, 2H, -OCH<sub>2</sub>CO), 3.81 (t, J = 5.1 Hz, 2H, -NCH<sub>2</sub>CH<sub>2</sub>O-), 3.40-2.50 (m, 10H, -NCH<sub>2</sub>-).

<sup>13</sup>C NMR, 100 MHz, CDCl<sub>3</sub> δ ppm: 175.9 (COOH), 141.1 (ArC), 140.7 (ArC), 132.8 (ArC), 129.0 (ArC), 128.9 (ArC), 127.6 (ArC), 74.3 (CHN), 70.0 (CH<sub>2</sub>O), 65.6 (CH<sub>2</sub>O), 56.3 (CH<sub>2</sub>N), 52.6 ((CH<sub>2</sub>)<sub>2</sub>N), 48.8 ((CH<sub>2</sub>)<sub>2</sub>N).

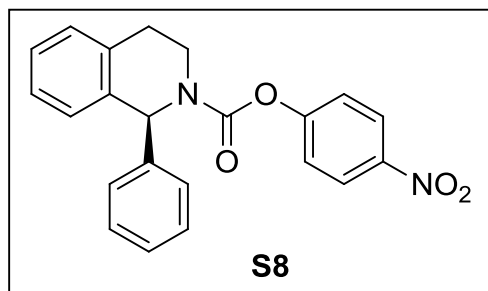
### Synthesis of Solifenacin **14** [16]



**1-phenyl-1,2,3,4-tetrahydroisoquinoline (18):** Under nitrogen atmosphere, to a suspension of NaBH<sub>4</sub> (1.06 g, 28.01 mmol) in anhydrous THF was cooled at 0 °C and a solution of iodine (2.84 g, 11.20 mmol) in THF was slowly added. After 30 minutes, a solution of 1-phenyl-1,2-dihydroisoquinolin-3(4H)-one (2.5 g, 11.20 mmol) in THF was added to the solution. The resulting mixture was heated at reflux for 16 h. Then the mixture was cooled at 0 °C and MeOH (4 mL) was slowly added, and the stirring was continued at room temperature for 10 min. The mixture was concentrated, and the resulting solid was digested with 2M NaOH (30 min). The resulting suspension was extracted with CH<sub>2</sub>Cl<sub>2</sub>, the combined organic extracts were dried over MgSO<sub>4</sub> and concentrated under vacuum. The residue was purified by silica column chromatography to give **18** (1.90 g, 9.07 mmol) as a white solid. Analytical data matches with the literature.[16]

<sup>1</sup>H NMR, 400 MHz, CDCl<sub>3</sub> δ ppm: 7.45 – 7.30 (m, 5H, ArH), 7.22 (dd, J = 7.7, 3.8 Hz, 2H, ArH), 7.15 – 7.06 (m, 1H, ArH), 6.84 (d, J = 7.8 Hz, 1H, ArH), 5.17 (s, 1H-CHNH), 3.34 (dt, J = 15.8, 7.1 Hz, 1H, -CH<sub>2</sub>CHHNH), 3.21 – 3.05 (m, 2H, -CHHCHHNH), 2.96 – 2.83 (m, 1H, -CHHCH<sub>2</sub>NH), 2.03 (s, 1H, NH).

<sup>13</sup>C NMR, 100 MHz, CDCl<sub>3</sub> δ ppm: 145.0 (ArC), 138.4 (ArC), 135.5 (ArC), 129.1 (ArC), 129.1 (ArC), 128.5 (ArC), 128.2 (ArC), 127.4 (ArC), 126.3 (ArC), 125.7 (ArC), 62.2 (CHNH), 42.4 (CH<sub>2</sub>CH<sub>2</sub>NH), 29.9 (CH<sub>2</sub>CH<sub>2</sub>NH).

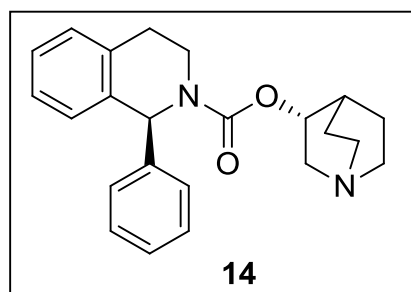


**(S) - 4 - nitrophenyl - 1 - phenyl - 3,4 - dihydroisoquinoline - 2(1H) - carboxylate (S8):** Under nitrogen atmosphere, a solution of (S)-**18** (300 mg, 1.43 mmol, 1 eq.) and triethylamine (225 μL, 1.61 mmol, 1.15 eq.)

in THF (20 mL) was cooled to 0 °C. A solution of *p*-nitrophenyl chloroformate (161 mg, 0.80 mmol) in THF (10 mL) was added dropwise maintaining the internal temperature below 5 °C. The solution was then slowly warmed to 25 °C, and stirred at this temperature for 2 hours. During this time, a precipitate of triethylammonium chloride formed in the solution. The solution was filtered, and the solvent was evaporated under vacuum to give the crude product. The crude solid was purified by silica column chromatography to give **S8** as a white solid (480 mg, 90% yield). Analytical data matches with the literature.[16] This product exists as a mixture of rotamers in CDCl<sub>3</sub>.

<sup>1</sup>H NMR, 400 MHz, CDCl<sub>3</sub> δ ppm: 8.17 (d, *J* = 8.9 Hz, 2H, *ArH*), 7.24-7.14 (m, 10H, *ArH*), 7.01 (d, *J* = 7.6 Hz, 1H, *ArH*), 6.46 and 6.42 (2 x s, 1H, -*CHN*-), 4.15-4.11 (m, 1H, -CH<sub>2</sub>*CHHN*), 3.43-3.31 (m, 1H, -CH<sub>2</sub>*CHHN*), 3.07-3.00 (m, 1H, -*CHHCH*<sub>2</sub>N), 2.84-2.78 (m, 1H, -*CHHCH*<sub>2</sub>N).

<sup>13</sup>C NMR, 100 MHz, CDCl<sub>3</sub> δ ppm: 156.3 (CO), (152.6, 152.3, 144.9, 142.0, 141.8, 134.7, 134.4, 129.1, 128.9, 128.6, 128.5, 128.2, 127.9, 127.4, 126.5, 125.1, 122.4, *ArC*), (58.8, 58.2, *CHNH*), (39.1, 38.8, CH<sub>2</sub>CH<sub>2</sub>NH), (28.7, 28.2, CH<sub>2</sub>CH<sub>2</sub>NH).



**Solifenacin (14)**: Under nitrogen atmosphere, to a solution of (*R*)-quinuclidin-3-ol (550 mg, 4.32 mmol) in DMF (25 mL) was added NaH (220 mg, 5.52 mmol, 60% dispersion in mineral oil). A white suspension formed, and a solution of compound **S8** (900 mg, 2.40 mmol) in DMF (5

mL) was added dropwise to the above mixture at r.t. The mixture was heated to reflux at 110 °C. After 4 hours, the reaction mixture was cooled to r.t., added to toluene (50 mL) and washed with water (3 x 20 mL). The organic layer was dried over MgSO<sub>4</sub>, and concentrated under vacuum. The crude solid was purified by silica column chromatography to give **14** as a colourless oil (615 mg, 70% yield). Analytical data matches with the literature.[16] This product exists as a mixture of rotamers in CDCl<sub>3</sub>.

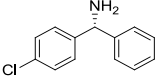
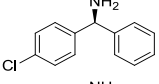
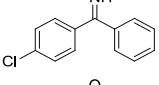
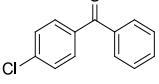
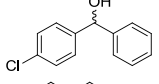
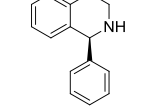
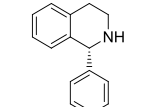
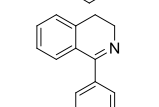
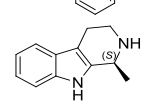
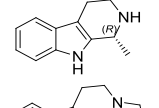
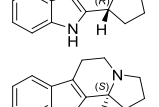
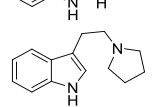

<sup>1</sup>H NMR, 400 MHz, CDCl<sub>3</sub> δ ppm: 7.21-6.96 (m, 8H, *ArH*), 6.98 (t, *J* = 6.2 Hz, 1H, *ArH*), 6.37 and 6.14 (2 x s, 1H, -*CHN*-), 4.77-4.67 (m, 1H, -*CHO*), 4.10-3.75 (m, 1H, -CH<sub>2</sub>*CHHN*), 3.35-3.10 (m, 2H, -*CHHCHHN*), 2.95-2.60 (m, 7H, -*CHHCH*<sub>2</sub>N and

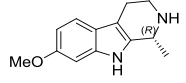
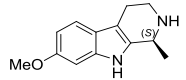
(CH<sub>2</sub>)<sub>3</sub>N), 2.06-1.93 (m, 1H, -CH), 1.82-1.26 (m, 4H, 2 x -CH<sub>2</sub>).

<sup>13</sup>C NMR, 100 MHz, CDCl<sub>3</sub> δ ppm: 155.0, 142.7, 135.3, 134.9, 128.9, 128.3, 127.7, 127.4, 127.0, 126.2, 71.9, 58.3, 57.4, 55.9, 47.4, 46.4, 38.4, 28.5, 25.4, 24.3, 19.5.

### HPLC columns, conditions and retention times

HPLC analysis was performed on an Agilent 1200 Series using chiral columns. Measurements were carried under isocratic conditions. \*Retention times varied to a small extent. The identity of compounds was confirmed by comparison with independently synthesized samples whenever necessary.

Compound	Column	Eluent	Temp (°C)	Wavelength (nm)	Retention Time* (min)
	Chiralcel OD-H	Hexane:iPrOH 90:10	40	220	13.3
	Chiralcel OD-H	Hexane:iPrOH 90:10	40	220	10.2
	Chiralcel OD-H	Hexane:iPrOH 90:10	40	220	7.2
	Chiralcel OD-H	Hexane:iPrOH 90:10	40	220	5.2
	Chiralcel OD-H	Hexane:iPrOH 90:10	40	220	9.6 9.9
	Chiralcel OD-H	Hexane:iPrOH 97:3	40	220	10.4
	Chiralcel OD-H	Hexane:iPrOH 97:3	40	220	15.6
	Chiralcel OD-H	Hexane:iPrOH 97:3	40	220	12.2
	Chiralcel IC	Hexane:iPrOH 90:10	25	265	9.6
	Chiralcel IC	Hexane:iPrOH 90:10	25	265	10.8
	Chiralcel IC	Hexane:iPrOH 90:10	25	265	10.8
	Chiralcel IC	Hexane:iPrOH 90:10	25	265	7.4
	Chiralcel IC	Hexane:iPrOH 90:10	25	265	9.0

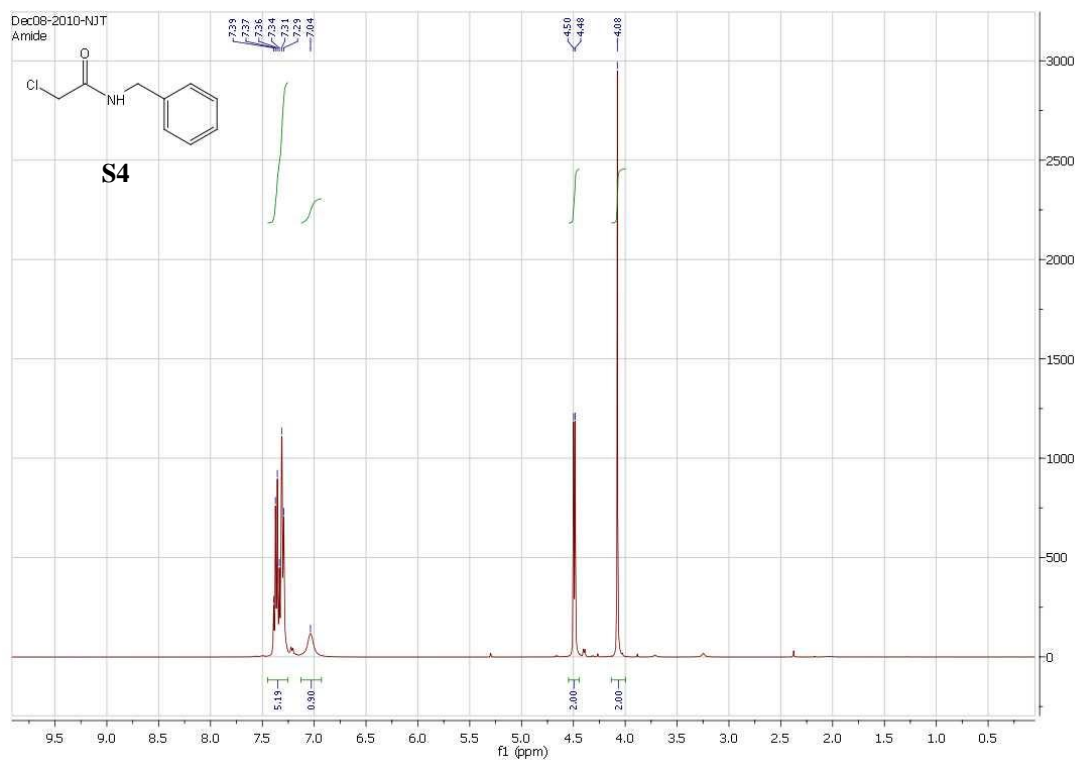
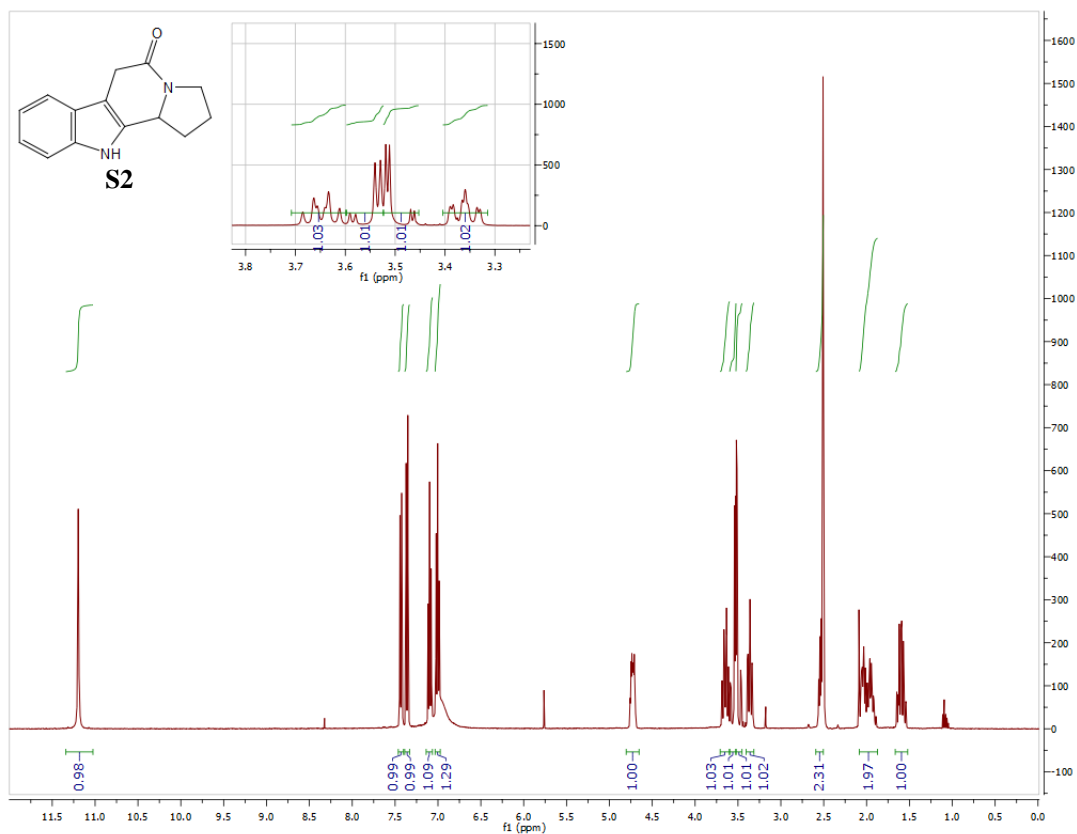
	Chiralcel IC	Hexane:iPrOH 80:20	25	265	14.7
	Chiralcel IC	Hexane:iPrOH 80:20	25	265	12.6

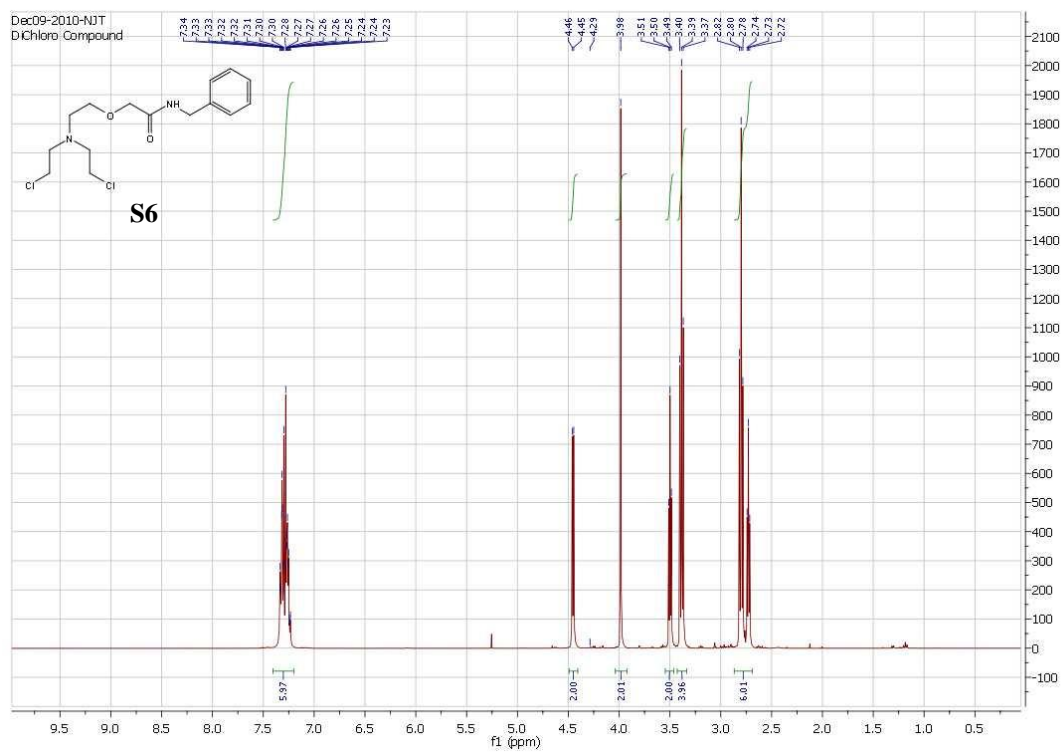
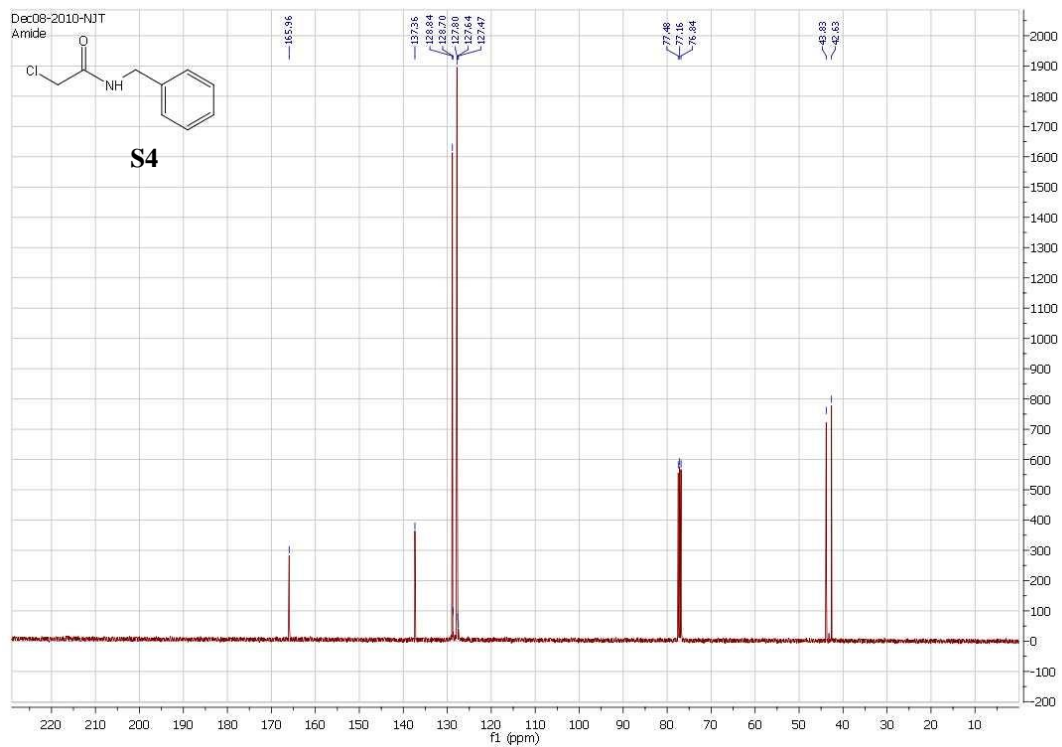
### GC columns, conditions and retention times

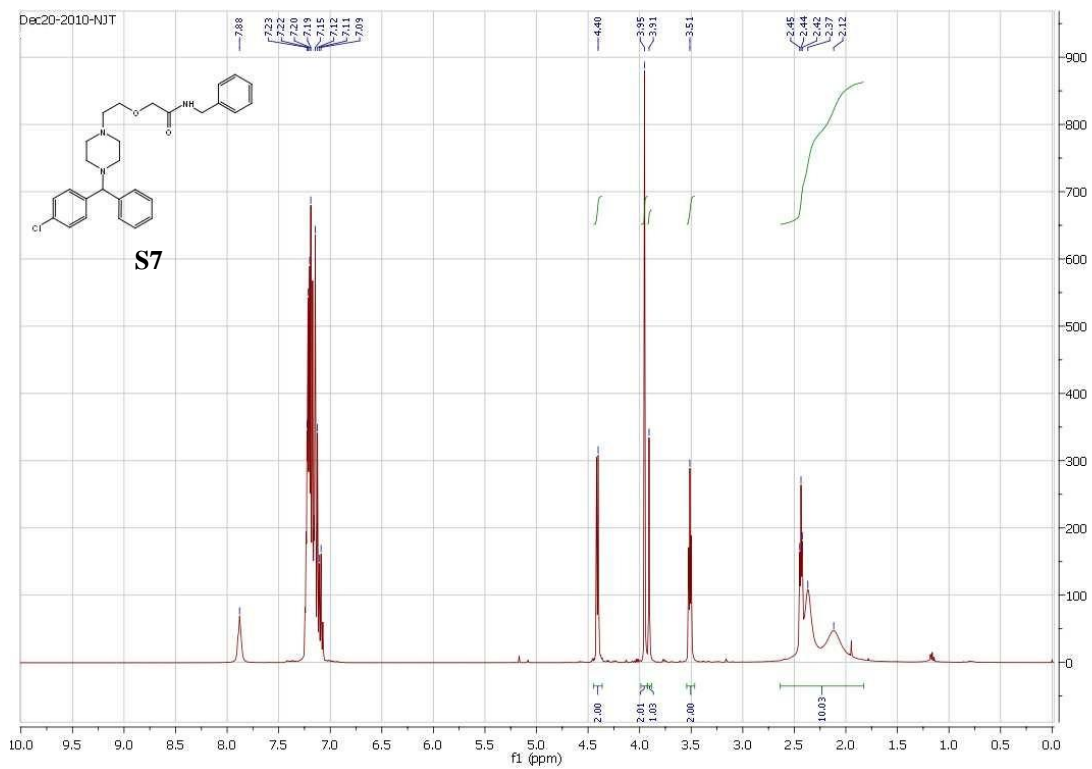
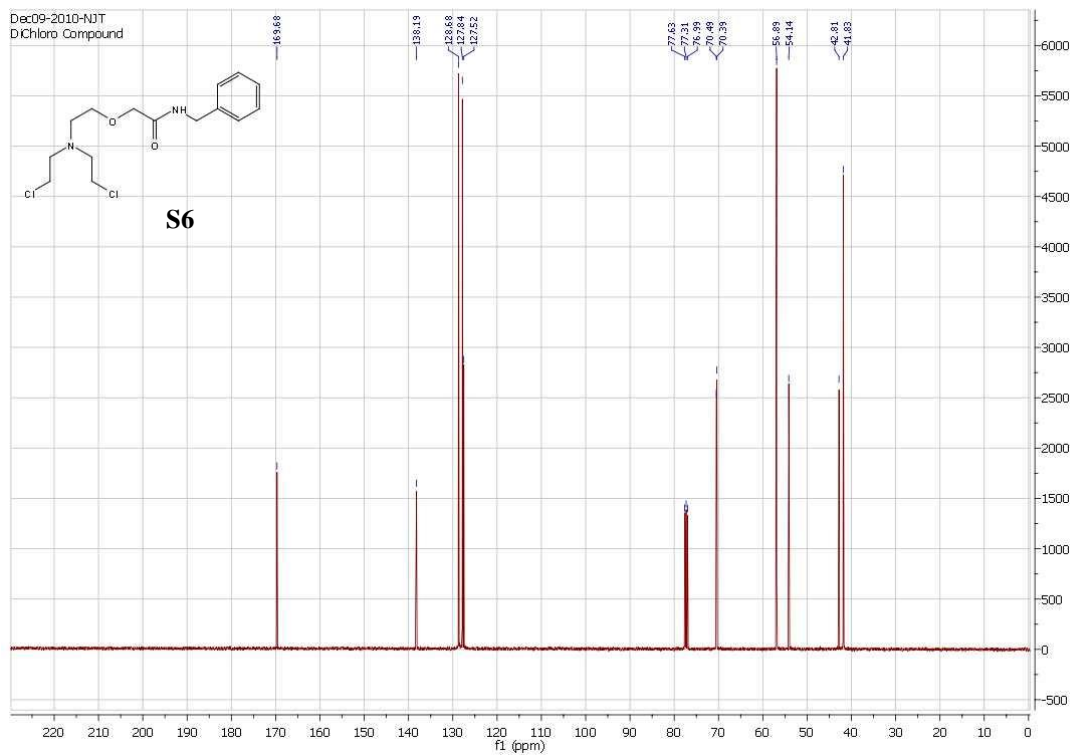
GC-FID analysis was performed on Agilent 6850 GCs equipped with a Gerstel Multipurposesampler MPS2L. Measurements were carried out using Varian Chirasil-Dex CB column 25 m × 0.25 mm × 0.26 μm at a constant flow of He (0.7 mL/min), injector temperature 200 °C, detector temperature (FID) 200 °C, oven temperature 50 °C to 150 °C with slope 10 °C/min, 150 to 200 with slope 5 °C/min.

For GC analysis compound **1** was acetylated using acetic anhydride and triethylamine. Retention times: (*R*)-**1**: 14.47 (*S*)-**1**: 14.59

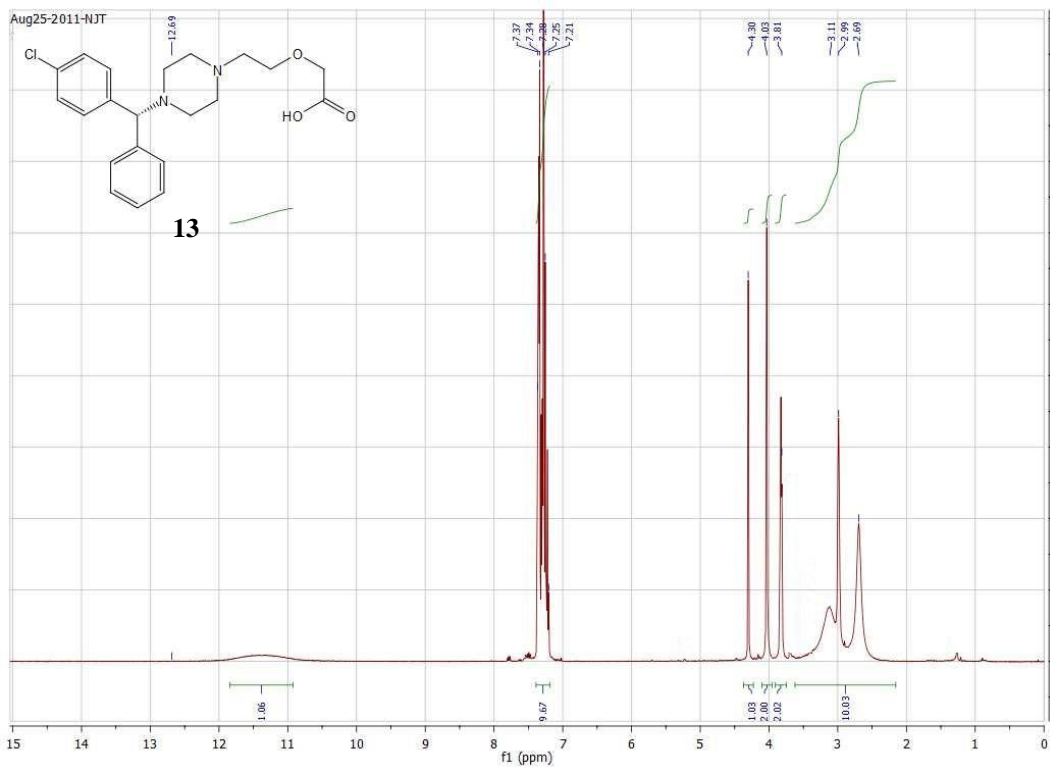
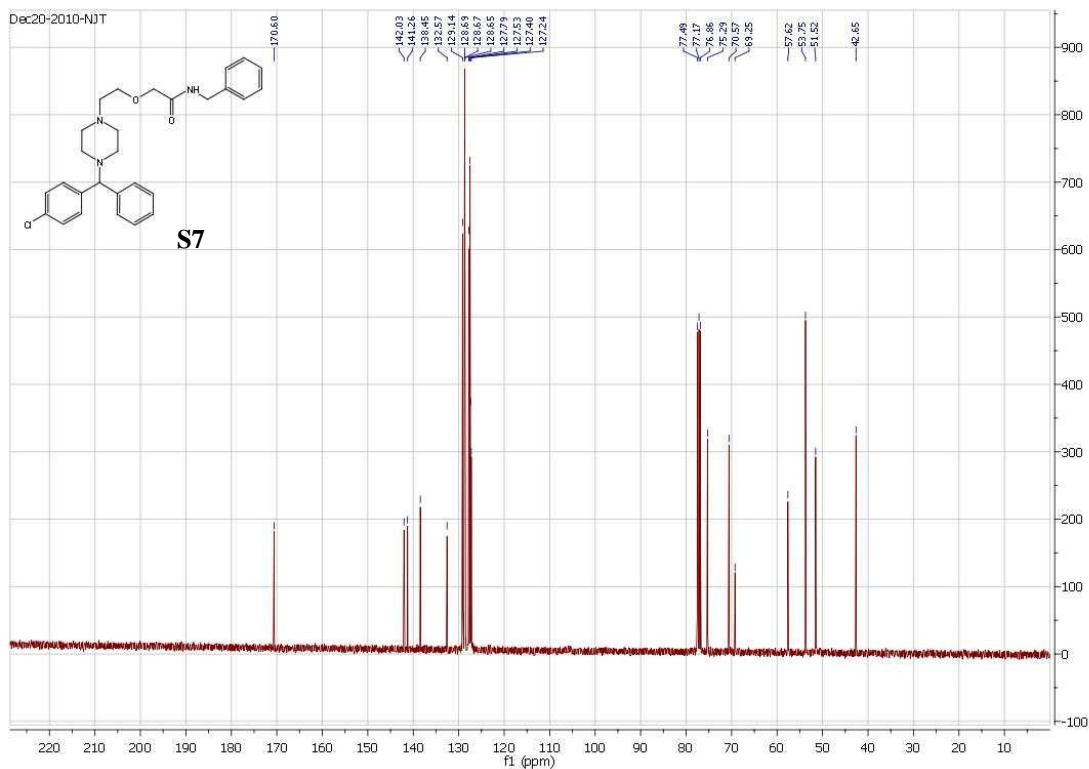
# NMR

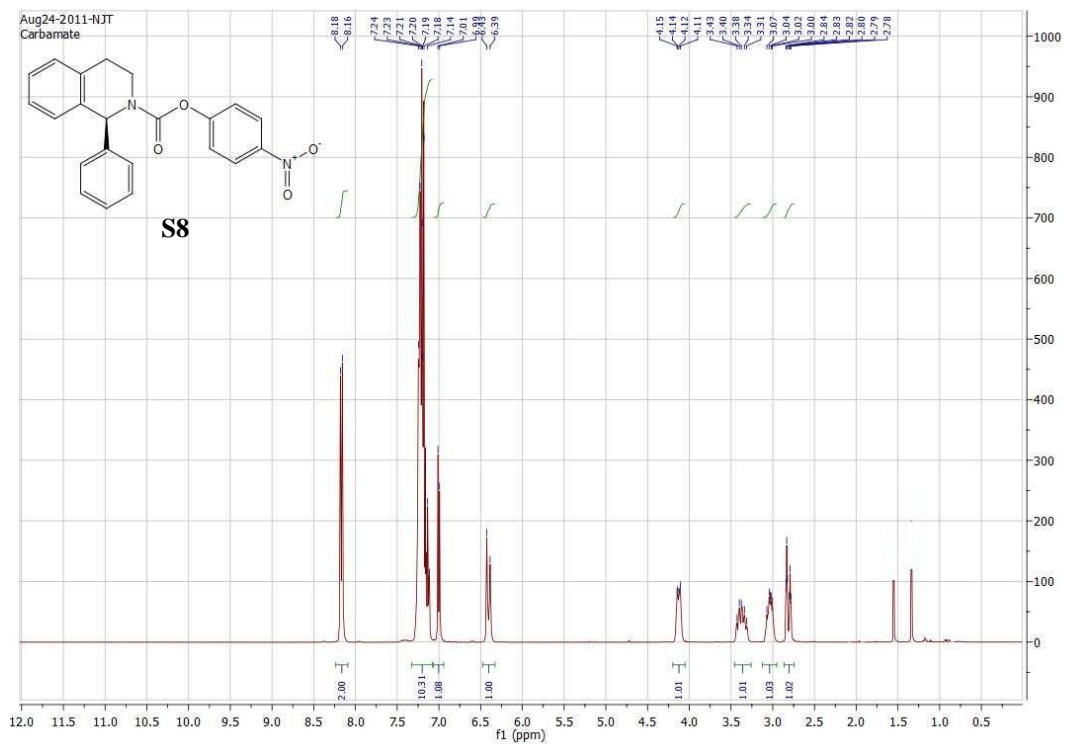
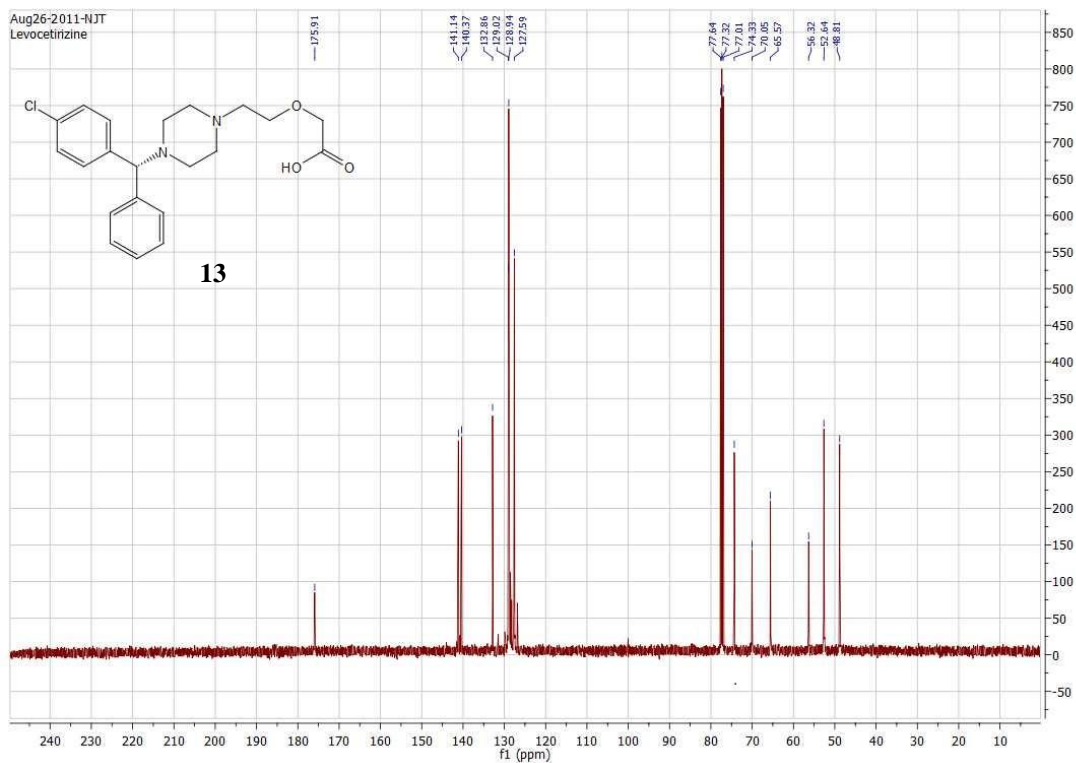


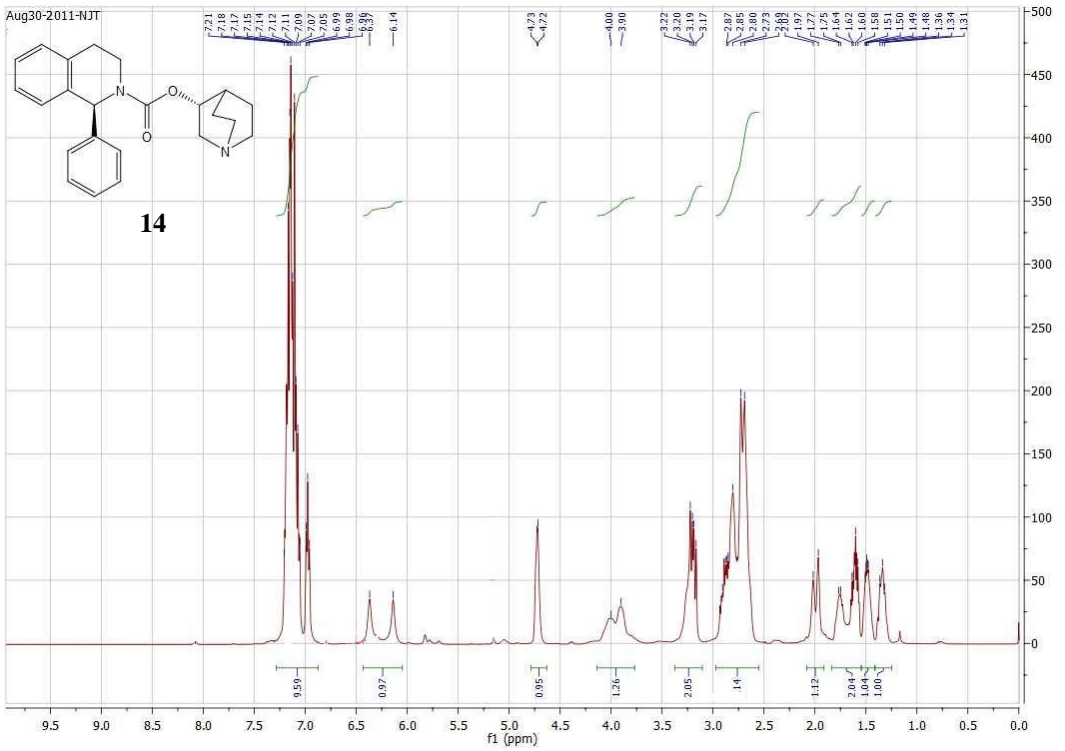
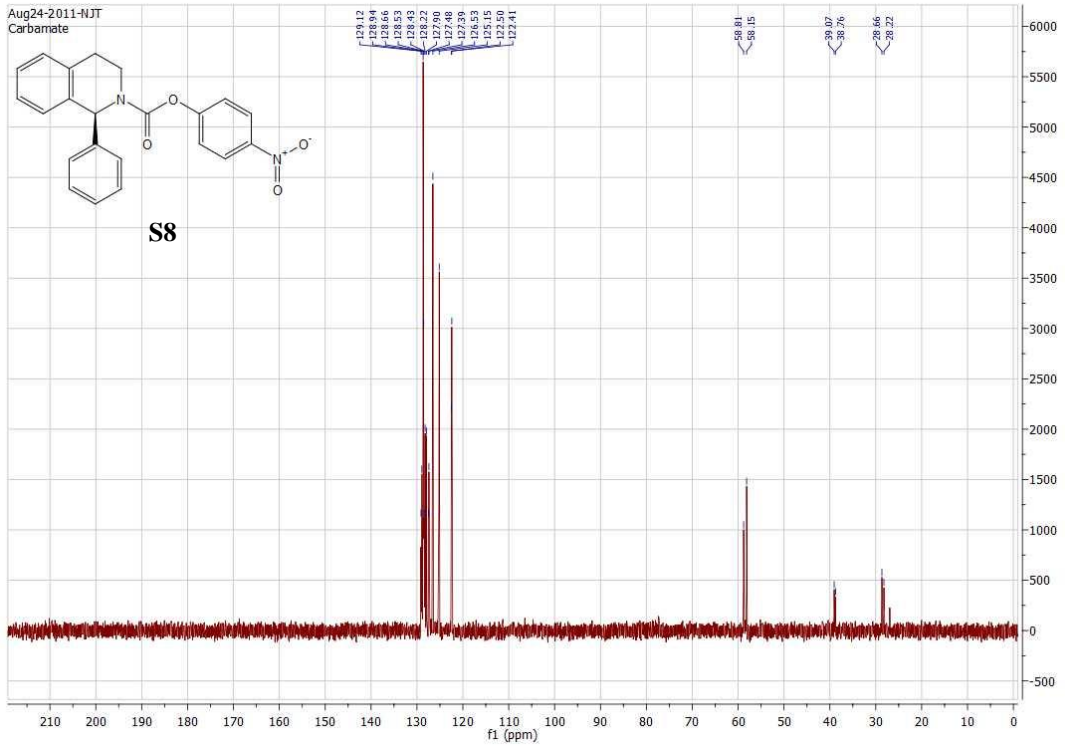


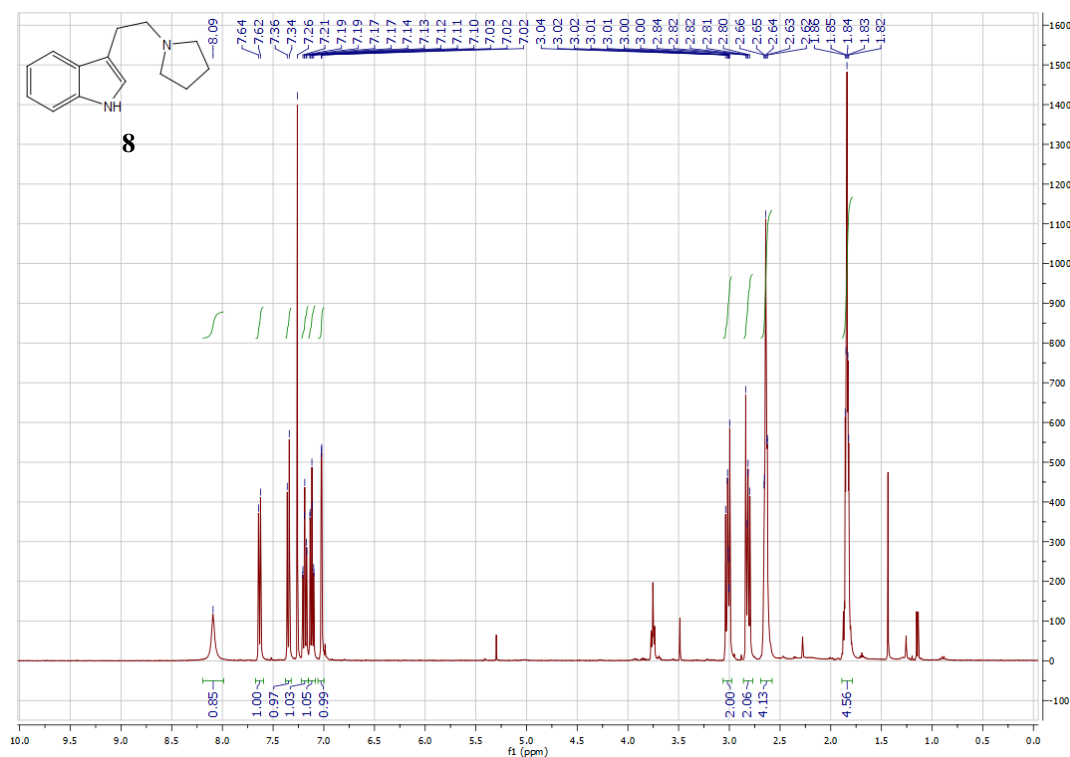
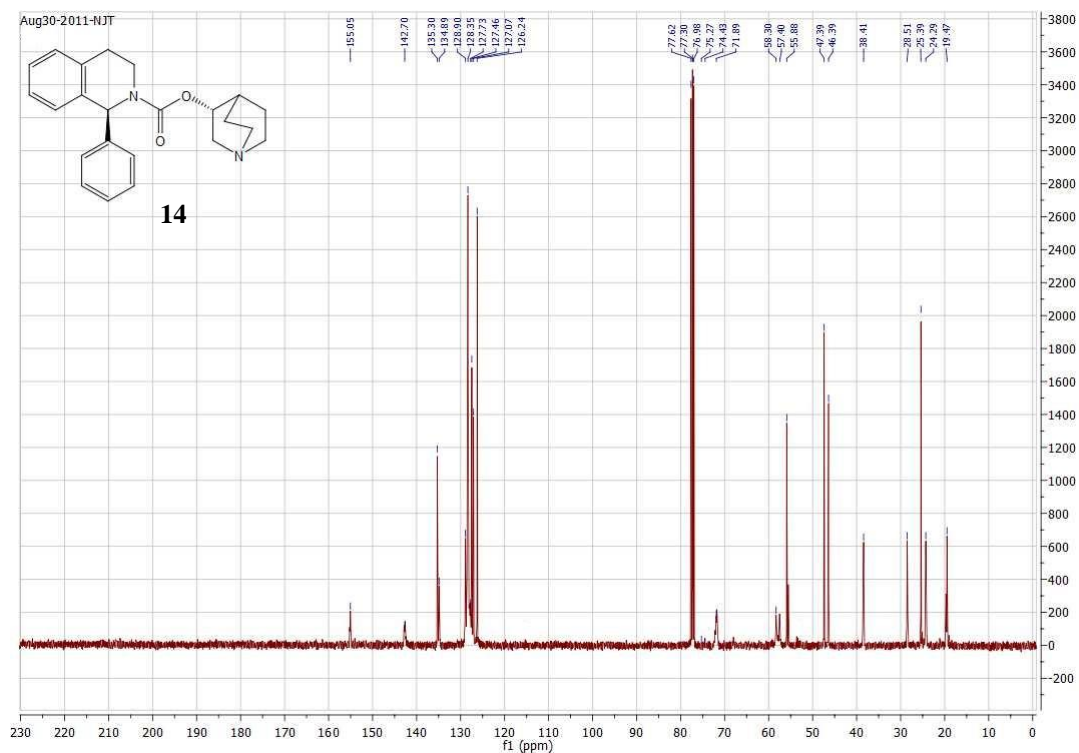












## References

- [1] Naito, R. *et al.* Synthesis and antimuscarinic properties of quinuclidin-3-yl 1,2,3,4-tetrahydroisoquinoline-2-carboxylate derivatives as novel muscarinic receptor antagonists. *J. Med. Chem.* **48**, 6597-6606 (2005).
- [2] Rowles, I., Malone, K. J., Etchells, L. L., Willies, S. C. & Turner, N. J. Directed evolution of the enzyme monoamine oxidase (MAO-N): highly efficient

- chemo-enzymatic deracemisation of the alkaloid (+/-)-Crispine A. *Chemcatchem* **4**, 1259-1261 (2012).
- [3] Atkin, K. E., Reiss, R., Turner, N. J., Brzozowski, A. M. & Grogan, G. Cloning, expression, purification, crystallization and preliminary X-ray diffraction analysis of variants of monoamine oxidase from *Aspergillus niger*. *Acta Crystallogr., Sect. F: Struct. Biol. Cryst. Commun.* **64**, 182-185 (2008).
- [4] Atkin, K. E. *et al.* The Structure of Monoamine Oxidase from *Aspergillus niger* Provides a Molecular Context for Improvements in Activity Obtained by Directed Evolution. *J. Mol. Biol.* **384**, 1218-1231 (2008).
- [5] Winter, G. Xia2: an expert system for macromolecular crystallography data reduction. *J. Appl. Crystallogr.* **43**, 186-190 (2010).
- [6] McCoy, A. J. *et al.* Phaser crystallographic software. *J. Appl. Crystallogr.* **40**, 658-674 (2007).
- [7] Emsley, P. & Cowtan, K. Coot: model-building tools for molecular graphics. *Acta Crystallogr., Sect. D: Biol. Cryst.* **60**, 2126-2132 (2004).
- [8] Murshudov, G. N., Vagin, A. A. & Dodson, E. J. Refinement of macromolecular structures by the maximum-likelihood method. *Acta Crystallogr., Sect. D: Biol. Cryst.* **53**, 240-255 (1997).
- [9] Laskowski, R. A., MacArthur, M. W., Moss, D. S. & Thornton, J. M. Procheck - A program to check the stereochemical quality of protein structures. *J. Appl. Crystallogr.* **26**, 283-291 (1993).
- [10] Carr, R. *et al.* Directed evolution of an amine oxidase possessing both broad substrate specificity and high enantioselectivity. *Angew. Chem. Int. Ed.* **42**, 4807-4810 (2003).
- [11] Schonenberger, B. & Bossi, A. Fragmentation of optically-active (1-phenylethyl)urea and (1-naphthylethyl)urea in refluxing alcohols – easy preparation of optically-active amines of high optical purity. *Helv. Chim. Acta* **69**, 1486-1497 (1986).
- [12] Enders, D. & Tiebes, J. A new asymmetric synthesis of both enantiomers of coniine by 1,2-addition of RLi/YbCl<sub>3</sub> to aldehyde and SAMP hydrazones *Liebigs Ann. Chem.*, 173-177 (1993).
- [13] Wu, J. S. *et al.* Asymmetric transfer hydrogenation of imines and iminiums catalyzed by a water-soluble catalyst in water. *Chem. Commun.*, 1766-1768 (2006).
- [14] Kam, T. S. & Sim, K. M. Alkaloids from *Kopsia griffithii*. *Phytochemistry* **47**, 145-147, (1998).
- [15] Clemons, G. R., Gardner, C. & Raper, R. The optical rotatory powers of some 4-substituted benzhydrylamines. *J. Chem. Soc. (Resumed)*, 1958-1960 (1939).
- [16] Wang, S., Onaran, M. B. & Seto, C. T. Enantioselective Synthesis of 1-

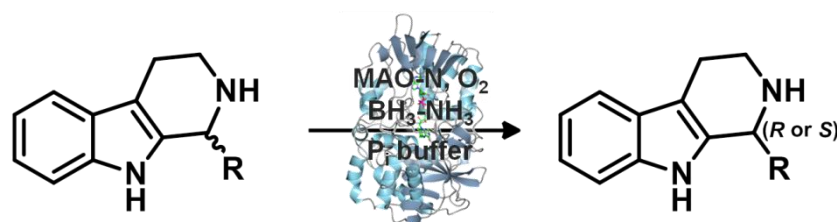
- Aryltetrahydroisoquinolines. *Org. Lett.* **12**, 2690-2693 (2010).
- [17] Ivanov, I., Nikolova, S. & Statkova-Abeghe, S. Simple method for the synthesis of 1-substituted beta-carboline derivatives from tryptamine and carboxylic acids in polyphosphoric acid. *Heterocycles* **65**, 2483-2492 (2005).
- [18] King, F. D. Novel synthesis of ( $\pm$ )-harmaline and (+/-)-1,2,3,4,6,7,12,12b-octahydroindole 2,3-a quinolizine. *J. Heterocycl. Chem.* **44**, 1459-1463 (2007).
- [19] Pfeiffer, M. J. and Hanna, S. B. Aminolysis of activated esters of indole acetic acid in acetonitrile. *J. Org. Chem.* **58**, 735-740 (1993).
- [20] Cami-Kobeci, G. et al. *Bioorg. Med. Chem. Lett.* **15**, 535-537 (2005).
- [21] Badgular, S. K. H., Sharma, V., Patel, D., Khan, M. A process for the synthesis of Levocetirizine. *WO2009/057133A2* (2007).
- [22] Da Silva W. A. et al. Novel supramolecular palladium catalyst for the asymmetric reduction of imines in aqueous media *Org. Lett.* **15**, 3238-3241 (2009)

# MAO-N CATALYSED DERACEMISATION OF TETRAHYDRO- $\beta$ -CARBOLINES

---

*Adv. Synth. Catal.*, Manuscript prepared for submission

D. Ghislieri, A.P. Green, S. C. Willies, N. J. Turner\*



Tetrahydro- $\beta$ -carbolines (THBCs) are bioactive alkaloids commonly found in nature and representative examples include yohimbine, eleagnine and komeroidine. A chemo-enzymatic deracemisation system was applied which allows to obtain single enantiomer of THBCs from the racemate in high yield and excellent optical purity ( $ee >97\%$ ) *via* enantioselective oxidation by a monoamine oxidase (MAO) and concomitant reduction by ammonia-borane. The switch in enantioselectivity was also explored relating the results of extensive substrate screening to docking simulations.

In this paper D.G. conceived the project, performed the chemical synthesis and biotransformations, analysed the data, co-wrote the paper and wrote the supplementary info.

# MAO-N catalysed deracemisation of tetrahydro- $\beta$ -carbolines

D. Ghislieri, A.P. Green, S. C. Willies, N. J. Turner\*

School of Chemistry, University of Manchester, Manchester Institute of Biotechnology, 131 Princess Street, Manchester, M1 7DN, UK.

*Nicholas.Turner@manchester.ac.uk*

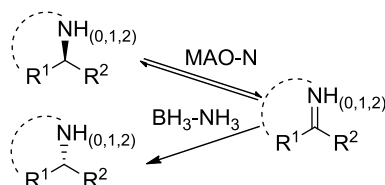
## Abstract

Tetrahydro- $\beta$ -carbolines (THBCs) are bioactive alkaloids widely spread in nature; representative examples include yohimbine, eleagnine and strychnine. Herein we assess the generality of this methodology by investigating the activity of the D11, D10 and D9 variants of MAO-N towards a series of 1-substituted THBCs. Interestingly, a switch in enantioselectivity is observed as the nature of the C1 substituent is varied. These results provide a previously unreported insight into the factors which influence the selectivity of MAO-N variants, and offer a platform for future directed evolution projects aimed towards the significant challenge of engineering enantio-complementary amine oxidase enzymes.

The tetrahydro- $\beta$ -carboline (THBC) ring system is an important structural motif found in a large number of bioactive, alkaloid natural products. Important examples include the antihypertensive drug reserpine, the stimulant yohimbine, the neurotoxin strychnine and the analgesic eleagnine. The complex molecular architectures and the wealth of biological activities associated with the THBCs have attracted significant attention from the synthetic community, and numerous pioneering studies describing the total synthesis of these structures have been reported.[1] The development of methods for the asymmetric synthesis of THBCs represents an important synthetic challenge. Although a number of approaches have been described previously, including the use of chiral auxiliaries,[2] transition metal catalysts,[3] organocatalysts[4] and more recently biocatalysts,[5] the development of broadly applicable, alternative strategies remains of great interest.

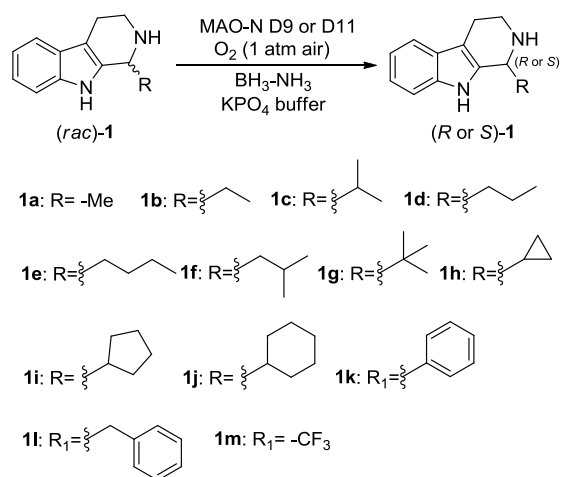


We have previously described a chemoenzymatic method for the deracemisation of chiral amines to the optically pure product in a single step.[6] Variants of monoamine oxidase from *Aspergillus niger* (MAO-N) have been developed in our laboratory which catalyse the enantioselective oxidation of a chiral amines with broad structural features. When coupled with a non-selective chemical reducing agent, these engineered enzymes have been shown to mediate the deracemisation of chiral primary, secondary[7] and tertiary amines[8] (Scheme 1).



**Scheme 1.** Generic deracemisation process

We have recently described the application of the D9 variant of MAO-N in the deracemisation of Eleagnine, Leptaflorin and Harmicine, three alkaloids natural products belonging to the  $\beta$ -carboline subclass.[9] In trying to increase the substrate scope of this mutant we screened with a liquid assay method different classes of substrates which could be oxidised and potentially deracemised by MAO-Ns (see SI). In particular, the new D11 mutant showed a good activity toward different 1-substituted tetrahydro- $\beta$ -carbolines. Therefore, a panel of aliphatic and aromatic 1-substituted racemic tetrahydro- $\beta$ -carbolines was synthesized from tryptamine hydrochloride and the corresponding aldehyde via a Pictet-Spengler reaction as a previously reported method.[5b] The racemic amines have been subjected to deracemisation using two MAO-N variants (D9-D11). The biotransformations were carried on at 15 mM concentration using 4 equivalents of  $\text{BH}_3\text{-NH}_3$  as reducing agent in 1 M phosphate buffer (pH: 7.8).



Entry	Time (h)	MAO-N D9	MAO-N D11
		e.e. (%)	e.e. (%)
<b>1a</b>	24	>99 ( <i>R</i> )	99 ( <i>R</i> )
<b>1b</b>	84	36 ( <i>R</i> )	25 ( <i>R</i> )
<b>1c</b>	72	40 ( <i>S</i> )	33 ( <i>S</i> )
<b>1d</b>	48	99 ( <i>S</i> )	>99 ( <i>S</i> )
<b>1e</b>	48	96 ( <i>S</i> )	99 ( <i>S</i> )
<b>1f</b>	48	58 ( <i>S</i> )	>99 ( <i>S</i> )
<b>1g</b>	48	62 ( <i>S</i> )	96 ( <i>S</i> )
<b>1h</b>	48	86 ( <i>S</i> )	35 ( <i>S</i> )
<b>1i</b>	48	85 ( <i>S</i> )	96 ( <i>S</i> )
<b>1j</b>	48	80 ( <i>S</i> )	97 ( <i>S</i> )
<b>1k</b>	72	30 ( <i>S</i> )	92 ( <i>S</i> )
<b>1l</b>	48	-	-
<b>1m</b>	48	-	-

**Table 1.** Results of whole-cell catalyzed oxidation reactions. Biotransformation conditions: substrate: 15 mM,  $\text{BH}_3\text{-NH}_3$ : 60 mM, wet cells: 200 mg / mL, 1 M  $\text{KPO}_4$  buffer, 37°C, 250 rpm, pH = 7.8. Reactions were carried out on a 4.5  $\mu\text{mol}$  scale. Enantiomeric excess were determined by chiral HPLC.

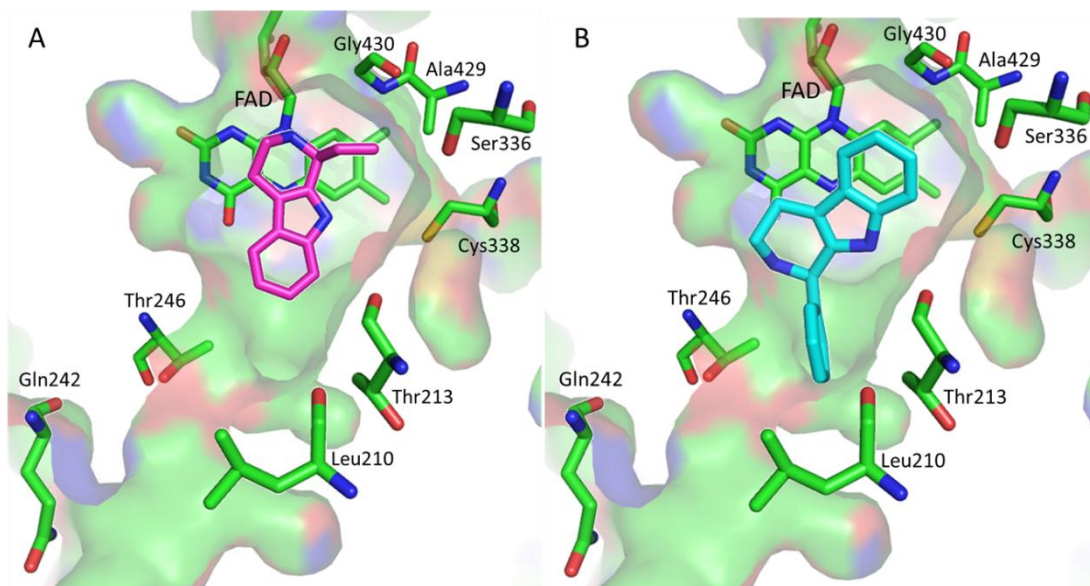
The MAO-N variants have shown good activity and, in most of the cases, excellent enantioselectivity in the deracemisation process. As shown in Table 1, in the case of MAO-N D9 and D11 replacing the methyl group with the bulkier ethyl and *iso*-propyl substituents the deracemisation necessitated longer reaction times (>72 h) and the enantioselectivity decreased significantly. Moving to more lipophilic substituents (Entry **1d-k**), we detected an increase in enantioselectivity as well as reaction rate. Particularly interesting is to highlight that the D9 mutant showed higher activity

toward less hindered substrates, while the D11 variant was faster in the deracemisation of bulkier substrates. An explanation could be given by the different structures of the two variants, where in the MAO-N D11 mutant a glycine replaced a histidine residue allowing the binding of bigger substrates.

To demonstrate the applicability of these MAO-N mutants in preparative scale, biotransformations were scaled-up and the enantiopure products isolated in good yields (>85%) and enantiomeric excess (>98%) showing robustness of the enzyme as well as the method.

Unfortunately, neither of the MAO-N variants displayed activity toward benzyl and -CF<sub>3</sub> substituted THBCs.

Experiments to detect the absolute configuration of the amines showed the enzyme to be (*S*)-selective for **1a-b** and (*R*)-selective for **1c-k** highlighting a switch in enantioselectivity, which is maintained in both variants. In an attempt to better understand the molecular basis behind this change in enantioselectivity we decided to look at the different binding mode of the substrates in the active site. We docked both enantiomers of **1a-k** in the active site of the MAO-N D11 mutant.[9] Consistent with the experimental results, this study highlighted that the MAO-N (*S*)-selectivity decreases in relationship with the increase of the substrate size due to the clash of the substituent (Fig 1a). The docking results for the (*R*)-enantiomer appeared to suggest that the THBC does not position itself far enough into the active site to reach a productive conformation, due to steric clashes in the region of Ala429. Upon closer inspection it appears that a large *R*-group is necessary to ‘push’ the tetrahydro-β-carboline ring into the active conformation (Fig 1b). In this way the activity with (*S*)-enantiomers of tetrahydro-β-carbolines decreases as the *R*-group increases in size, whereas the activity with (*R*)-enantiomers increases as the *R*-group becomes more bulky leading to the observed inversion of stereoselectivity with larger substituents.



**Figure 1.** Docking of A, (*S*)-**1b** and B, (*R*)-**1k**, in active site of MAO-N D11. A, Enlargement of ethyl substituent causes steric clashes in the active site causing. B, a large substituent is required to fill the active site channel to promote catalysis of the *R*-enantiomer

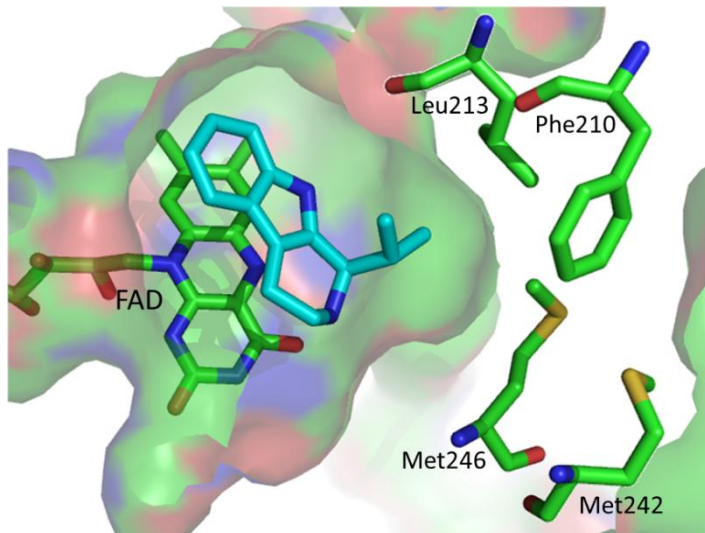
Experiments with MAO-N D10 variant to test this theory have shown that the enantio-specificity switch occurs at substituents as small as the ethyl group (**1b**), with D10 showing relatively good selectivity towards the (*R*)-enantiomer, whereas both D9 and D11, showed poor enantioselectivity with a preference for the (*S*)-enantiomer. In addition the selectivity of D10 with slightly larger substituents such as *iso*-propyl (**1c**) shows high (*R*)-enantioselectivity (94% e.e.) whereas the other mutants were (*R*)-selective but only with low e.e.'s (33-40%).

Entry	Time (h)	MAO-N D10 e.e. (%)	MAO-N D11 e.e. (%)
<b>1a</b>	24	96 ( <i>R</i> )	99 ( <i>R</i> )
<b>1b</b>	48	49 ( <i>S</i> )	12 ( <i>R</i> )
<b>1c</b>	48	94 ( <i>S</i> )	22 ( <i>S</i> )
<b>1d</b>	48	99 ( <i>S</i> )	>99 ( <i>S</i> )

**Table 2.** Results of whole-cell catalyzed oxidation reactions. Biotransformation conditions: substrate: 15 mM, BH<sub>3</sub>-NH<sub>3</sub>: 60 mM, wet cells: 200 mg / mL, 1 M KPO<sub>4</sub> buffer, 37°C, 250 rpm, pH = 7.8. Reactions were carried out on a 4.5 μmol scale. Enantiomeric excess were determined by chiral HPLC.

Modeling of **1c** into D10 and D11 shows the substrate is positioned closer to the FAD, where the THBC-N2 – FAD-N5 distance in D11 is 3.90 Å whereas in D10 this

is now significantly shorter at 3.56 Å, This shows that the residues in the active site channel (Figure 2) have an important effect upon the enantioselectivity of THBC's, and further engineering of these and other residues in the channel could serve to further optimize the selectivity of MAO-N towards these substrates.



**Figure 2.** Modelling of **1c** in the active site of MAO-N D10, showing interaction of *iso*-propyl substituent with residues in the active site channel.

In conclusion, after the previously reported synthesis of (*R*)-eleagnine **1a**, we have increased the scope of chemo-enzymatic deracemisations by a combination of monoamine oxidase from *Aspergillus niger* and a non-selective reducing agent to different 1-substituted tetrahydro- $\beta$ -carboline. Interestingly, a switch in enantioselectivity is observed as the nature of the C1 substituent is varied. The results of extensive substrate screening and docking simulations provide a previously unreported insight into the factors which influence the selectivity of MAO-N variants, and offer a platform for future directed evolution projects aimed towards the significant challenge of engineering enantio-complementary amine oxidase enzymes.

## Experimental Section

### MAO-N preparative deracemisation: General procedure.

In a 50 mL Falcon tube, the hydrochloric salt (0.4 mmol) and  $\text{BH}_3\text{-NH}_3$  (1.6 mmol) were dissolved in  $\text{KPO}_4$ -buffer (25 mL, 1 M, pH = 7.8). The pH of the solution was adjusted to 7.8 by addition of NaOH. Cell pellet from *E. coli* cultures (4 g) containing MAO-N D11 was added to the solution. The tube was placed in a shaking incubator and shaken at 37 °C and 250 rpm. When HPLC analysis showed the good

conversion reached and the amount of imine < 2%, aqueous NaOH (200  $\mu$ L, 10 M) and CH<sub>2</sub>Cl<sub>2</sub> (25 mL) were added to work up the reaction and layers were separated by centrifugation (4000 rpm, 5 min.) and the aqueous phase was extracted again with CH<sub>2</sub>Cl<sub>2</sub> (20 mL). The combined organic phases were dried over MgSO<sub>4</sub> and concentrated under vacuum.

## References

- [1] a) Woodward, R. B. *J. Am. Chem. Soc.* **1954**, *76*, 4749-4751 b) Mergott, D. J., Zuend, S. J., Jacobsen, E. N. *Org. Lett.* **2008**, *10*, 745-748.
- [2] a) Gremmen, C.; Willemse, B.; Wanner, M. J.; Koomen, G. J. *Org. Lett.* **2000**, *2*, 1955; b) Chen, X. C.; Zhu, J. P. *Angew. Chem., Int. Ed.* **2007**, *46*, 3962
- [3] a) C. Li, J. Xiao, *J. Am. Chem. Soc.* **2008**, *130*, 13208-13209; b) P. Roszkowski, K. Wojtasiewicz, A. Leniewski, J. K. Maurin, T. Lis, Z. Czarnocki, *J. Mol. Cat. A: Chem.* **2005**, *232*, 143-149; c) J. S. Wu, F. Wang, Y. P. Ma, X. C. Cui, L. F. Cun, J. Zhu, J. G. Deng, B. L. Yu, *Chem. Commun.* **2006**, 1766-1768.
- [4] a) Taylor, M. S.; Jacobsen, E. N. *J. Am. Chem. Soc.* **2004**, *126*, 10558; b) Seayad, J.; Seayad, A. M.; List, B. *J. Am. Chem. Soc.* **2006**, *126*, 1086.
- [5] a) M. Espinoza-Moraga, T. Petta, M. Vasquez-Vasquez, V. Felipe Laurie, L. A. B. Moraes, L. Silva Santos, *Tetrahedron:Asymmetry* **2010**, *21*, 1988-1992; b) P. Bernhardt, A. R. Usera, S. E. O'Connor, *Tetrahedron Lett.* **2010**, *51*, 4400-4402; c) F. Leipold, D. Ghislieri, N. J. Turner, *submitted*.
- [6] M. Alexeeva, A. Enright, M. J. Dawson, M. Mahmoudian, N. J. Turner, *Angew. Chem. Int. Ed.* **2002**, *41*, 3177-3180.
- [7] R. Carr, M. Alexeeva, A. Enright, T. S. C. Eve, M. J. Dawson, N. J. Turner, *Angew. Chem. Int. Ed.* **2003**, *42*, 4807-4810.
- [8] C. J. Dunsmore, R. Carr, T. Fleming, N. J. Turner, *J. Am. Chem. Soc.* **2006**, *128*, 2224-2225.
- [9] D. Ghislieri, A. P. Green, M. Pontini, S. C. Willies, I. Rowles, A. Frank, G. Grogan, N. J. Turner, *submitted*

# **MAO-N catalysed deracemisation of tetrahydro- $\beta$ -carbolines**

D. Ghislieri, A. P. Green, S. C. Willies and N. J. Turner\*

**Supplementary information**

## General Information

Competent cells (BL21 (DE3)) were purchased from Invitrogen and transformed according to the manufacturer's protocol. The empty vector (pET-16b) originates from Novagen.

Starting materials were purchased from Acros and Sigma-Aldrich and used as received. Solvents were analytical or HPLC grade or were purchased dried over molecular sieves where necessary. Column chromatography was performed on silica gel (Sigma-Aldrich, 220-440 mesh).  $^1\text{H}$  and  $^{13}\text{C}$  NMR spectra were recorded on a Bruker Avance 400 (400.1 MHz or 399.9 MHz for  $^1\text{H}$  and 100.6 MHz for  $^{13}\text{C}$ ) without additional internal standard. Chemical shifts are reported in  $\delta$  values (ppm) and are calibrated against residual solvent signal. The following abbreviations were used to define the multiplicities: s, singlet; d, doublet; t, triplet; q, quartet; m, multiplet; b, broad.

HPLC analysis was performed on an Agilent system equipped with a G1379A degasser, G1312A binary pump, a G1329 autosampler unit, a G1315B diode array detector and a G1316A temperature controlled column compartment; column and conditions are indicated separately.

## Biotransformations

### Preparation of Biocatalyst

MAO-N (wild-type monoamine oxidase from *Aspergillus niger* with the amino acid substitutions shown in Table S1) was transformed into *E. coli* (C43) as the manufacturer's instructions.

MAO-N variant	F210	L213	M242	I246	W430
D9	L	T	Q	T	H
D10	-	-	-	M	G
D11	L	T	Q	T	G

**Table S1.** MAO-N variants and mutations respect to MAO-N WT; residues shown on top.

**Cultivation in LB medium without induction.** A single colony was used to inoculate a pre-culture (5 mL) which was grown in LB with ampicillin (100 mg/L) at 37 °C and 250 rpm until an  $\text{OD}_{600}$  between 0.6-1.0 was reached. 2 L Erlenmeyer flasks containing 600 mL LB with ampicillin (100  $\mu\text{g/L}$ ) were inoculated with 5 mL of pre-



culture and incubated at 37 °C and 250 rpm for 24 hours. The cells were harvested by centrifugation at 8000 rpm and 4 °C for 20 min. The cell pellet was stored at -20°C until needed. Typically 4 g of cells were obtained from a 600 mL culture.

**Cultivation under auto-inducing conditions.** A single colony was used to inoculate a pre-culture (5 mL) which was grown in LB with ampicillin (100 mg/L) at 37 °C and 250 rpm until an OD<sub>600</sub> between 0.6-1.0 was reached. 2 L Erlenmeyer flasks containing autoinduction medium (600 mL, 4ZY-LAC-SUC; containing 100 µg/mL ampicillin) were inoculated with 5 mL of pre-culture and incubated at 25 °C and 150 rpm for 72 hours. The cells were harvested by centrifugation at 8000 rpm and 4 °C for 20 min. The cell pellet was stored at -20°C until needed. Typically 20 g of cells were obtained from a 600 mL culture.

Media and media components:

LB medium: 10 g/L tryptone, 5 g/L yeast extract, 10 g/L NaCl

4ZY-LAC-SUC: 20 mL/L 50x LAC, 50 mL/L 20x NPSC, 1 mL/L 1000x trace element solution, 2 mL/L 500x MgSO<sub>4</sub> stock, 50 mL/L 20x SUC stock, 410 mL/L 8x ZY, 470 mL/L H<sub>2</sub>O dest.

50x LAC: 25% w/v glycerol, 2.5% w/v glucose, 10% w/v α-lactose monohydrate

20x NPSC: 1 M NH<sub>4</sub>Cl, 0.1 M Na<sub>2</sub>SO<sub>4</sub>, 0.5 M KH<sub>2</sub>PO<sub>4</sub>, 0.5 M Na<sub>2</sub>HPO<sub>4</sub>.

1000x trace element solution: 50 mM FeCl<sub>3</sub>, 20 mM CaCl<sub>2</sub>, 10 mM MnCl<sub>2</sub>, 10 mM ZnSO<sub>4</sub>, 2 mM CoCl<sub>2</sub>, 2 mM CuCl<sub>2</sub>, 2 mM NiCl<sub>2</sub>, 2 mM Na<sub>2</sub>MoO<sub>4</sub>, 2 mM Na<sub>2</sub>SeO<sub>3</sub>, 2 mM H<sub>3</sub>BO<sub>4</sub>

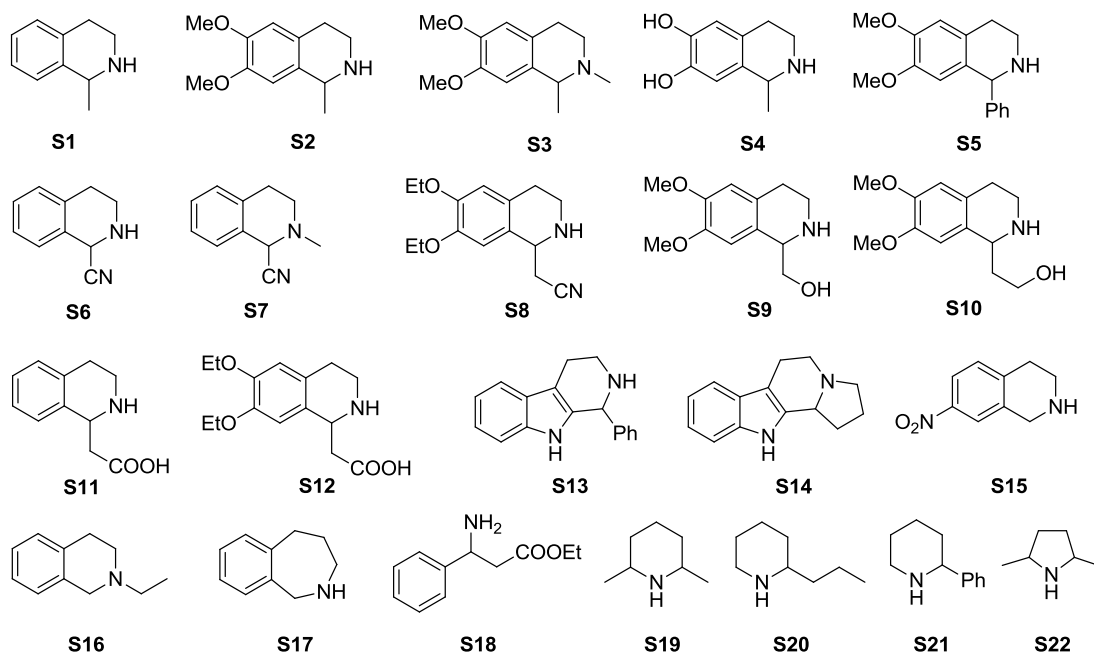
500x MgSO<sub>4</sub> stock: 1 M MgSO<sub>4</sub>

20x SUC: 0.5 M sodium succinate

8x ZY: 80 g/L tryptone, 40 g/L yeast extract

## Liquid phase screening

A broad range of different substrates which could potentially be oxidised by MAO-N was chosen for the liquid phase screen (Figure S1).



**Figure S1.** Substrates tested with the liquid assay screening

All the compounds, with the exception of achiral **S15**, **S16** and **S17**, were analysed as racemic mixtures. From previous experiments it was known that (*rac*)-**S1** can be oxidised by all the mutants and for this reason it was chosen as standard. All the  $V_{max}$  results were normalized toward this standard substrate. All the screenings have been carried out in triplicate and an *E. coli* empty vector was used as blank.

Chromatogenic solutions for kinetic determination:

### 1) Substrate mix:

1 M stock solutions of **S1-S22** were prepared in DMF

### 2) Colourimetric mix:

2 mg Horseradish Peroxidase

60  $\mu$ L 1 M aminoantipyrine in water

200  $\mu$ L 1M tribromohydroxybenzoic acid in DMSO

adjust volume to 10 mL with 100 mM phosphate buffer pH 7.8

2  $\mu$ L of solution 1 was mixed with 50  $\mu$ L of solution 2 and 98  $\mu$ L 100 mM phosphate buffer (pH 7.8) directly in the 96 well plates. To the preformed mixture, 50 $\mu$ L of

MAO-N in 100 mM phosphate buffer (pH 7.8) was added resulting in a final volume of 200  $\mu$ L. Dye formation was followed at  $\lambda=510$  nm and 37°C for 1 hour.

The average results are shown in Table S2.

Substrates	D5	D9	D10	D11
<b>S1</b> <sup>(a)</sup>	100	100	100	100
<b>S2</b>	-	31	-	-
<b>S3</b>	-	-	-	-
<b>S4</b> <sup>(b)</sup>	No result	No result	No result	No result
<b>S5</b>	-	-	6	69
<b>S6</b>	-	-	-	-
<b>S7</b>	-	-	-	-
<b>S8</b>	-	-	-	-
<b>S9</b>	-	-	-	-
<b>S10</b>	-	-	-	-
<b>S11</b>	-	-	-	-
<b>S12</b>	-	-	-	-
<b>S13</b>	-	4	10	48
<b>S14</b>	n.a. <sup>(c)</sup>	87	n.a.	75
<b>S15</b>	27	46	-	5
<b>S16</b>	23	62	9	52
<b>S17</b>	-	-	-	-
<b>S18</b>	-	-	-	-
<b>S19</b>	-	-	-	-
<b>S20</b>	4	19	-	-
<b>S21</b>	3	11	-	1
<b>S22</b>	-	-	-	-

**Table S2.** Relative activity of the MAO-N variants towards the substrates. <sup>(a)</sup>**S1** is the standard (activity 100). <sup>(b)</sup>Substrate **S4** interacted with the dye preventing analysis. <sup>(c)</sup>not analysed.

Trying to find positive hits for a new deracemisation process, we started to screen different 1-methyltetrahydroisoquinolines (**S2-S5**). The alkaloid natural product salsolidine (**S2**) showed high activity only with the D9 variant. Substrate **S3** did not show any oxidation, probably the hindrance of the tertiary amine can cause some

steric effects and FAD might not be able to be attacked by the substrate. Substrate **S4**, which contains two phenolic –OH groups, was not compatible with the dye which turned immediately to a black colour. To avoid this, the phenolic groups, were protected together as “acetonide” and protected **S4** was subjected to oxidation with the D9 mutant; HPLC analysis showed a fairly good activity (results not shown).

As expected, substrate **S5**, directly related to 1-phenyl tetrahydroisoquinoline, was oxidised by D10 and D11 mutants.

Changing to other classes of substrates such as the amino nitriles **S6-S8**, the amino alcohols **S9-S10** and the amino acids **S11-S12**, we did not observe any activity.

Compounds containing a tetrahydro- $\beta$ -carboline skeleton as **S13-S14** have also been tested and the new D11 mutant showed a good activity; therefore, a number of substrates belonging to the tetrahydro- $\beta$ -carbolines have been synthesised and subjected to oxidation/deracemisation.

The substrates **S15-S16** were oxidized by all the MAO-N variants; but of course these substrates could not be used for a deracemisation, but they could be considered as potential building blocks for other chiral substrates.

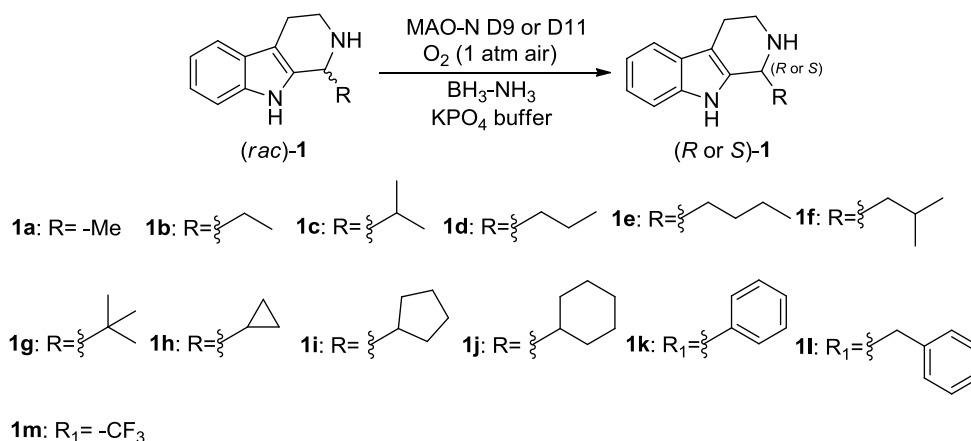
Substrate **S17** had no activity, probably because of the seven membered ring which is too big to be fit in the active site. The same holds for the beta amino ester **S18** that did not show any activity with all the mutants tested.

In the case of the piperidines **S19-S21**, different results were found. Probably compound **S19** is not lipophilic enough to reach the active site, while **S20-S21** showed a good activity towards D5 and, especially, D9. The pyrrolidine **S22** followed the same trend as **S19** being probably not lipophilic enough to be oxidised.

#### **MAO-N D9/D11 deracemisations: analytical procedure**

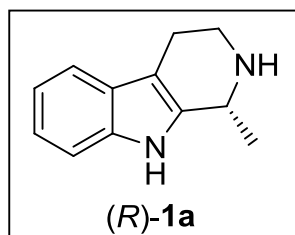
In a 2 mL Eppendorf tube, the amine (4.5  $\mu$ L of 1M solution in DMF) and  $\text{BH}_3\text{-NH}_3$  (18  $\mu$ L of 1M solution in  $\text{KPO}_4$ -buffer) were added to a solution of cell pellet from *E. coli* MAO-N D9/D11 cultures (150 mg/mL in 1 M  $\text{KPO}_4$ -buffer, pH = 7.8) to obtain a final volume of 300  $\mu$ L. The tube was placed in a shaking incubator and shaken at 37 °C and 250 rpm. In total 5 reactions were set up for each substrate. The reaction was monitored by HPLC taking a reaction and working it up every 3, 6, 24, 48 and 72 hours. HPLC samples were prepared as follows: aqueous NaOH-solution (10  $\mu$ L, 10 M) was added to the reaction mixture in the Eppendorf tube, followed by 1 mL of  $\text{CH}_2\text{Cl}_2$ . After vigorous mixing, by means of a vortex mixer, the sample was

centrifuged at 13200 rpm for 1 minute. The organic phase was separated, dried over MgSO<sub>4</sub> and analysed by HPLC.

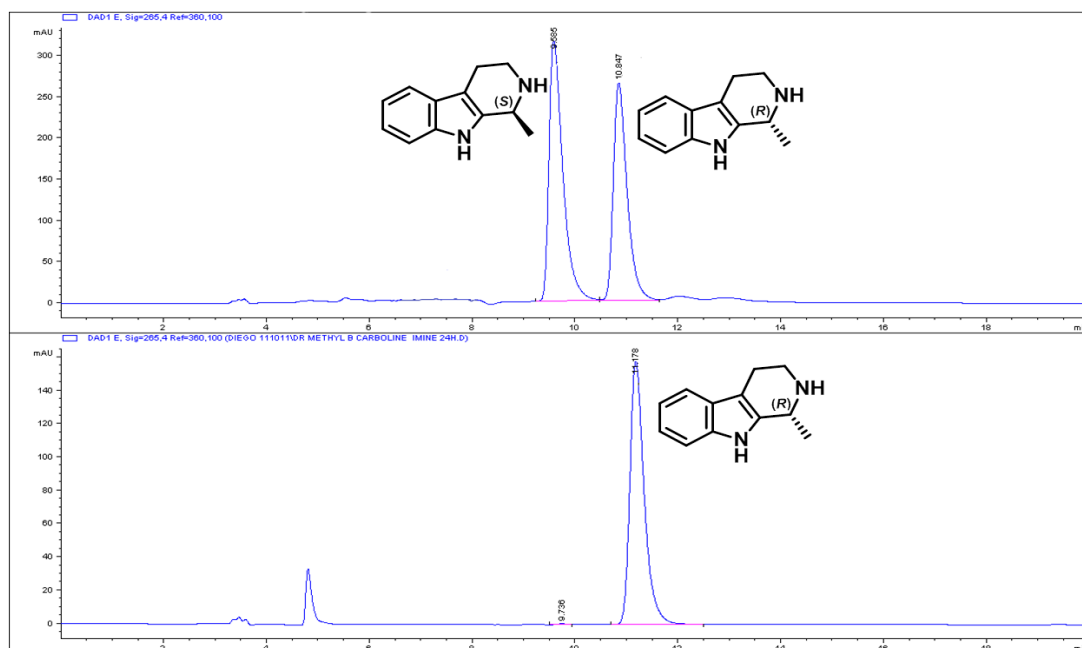


Entry	Time	MAO-N	MAO-N	MAO-N
		D9	D10	D11
		e.e.	e.e.	e.e.
		(%)	(%)	(%)
<b>1a</b>	24	>99 ( <i>R</i> )	99 ( <i>R</i> )	99 ( <i>R</i> )
<b>1b</b>	48		49 ( <i>S</i> )	12 ( <i>R</i> )
<b>1b</b>	84	36 ( <i>R</i> )		25 ( <i>R</i> )
<b>1c</b>	48		94 ( <i>S</i> )	22 ( <i>S</i> )
<b>1c</b>	72	40 ( <i>S</i> )		33 ( <i>S</i> )
<b>1d</b>	48	99 ( <i>S</i> )	98 ( <i>S</i> )	>99 ( <i>S</i> )
<b>1e</b>	48	96 ( <i>S</i> )		99 ( <i>S</i> )
<b>1f</b>	48	58 ( <i>S</i> )		>99 ( <i>S</i> )
<b>1g</b>	48	62 ( <i>S</i> )		96 ( <i>S</i> )
<b>1h</b>	48	86 ( <i>S</i> )	30 ( <i>S</i> )	35 ( <i>S</i> )
<b>1i</b>	48	85 ( <i>S</i> )		96 ( <i>S</i> )
<b>1j</b>	48	80 ( <i>S</i> )	91 ( <i>S</i> )	97 ( <i>S</i> )
<b>1k</b>	72	30 ( <i>S</i> )		92 ( <i>S</i> )
<b>1l</b>	48	-		-
<b>1m</b>	48	-		-

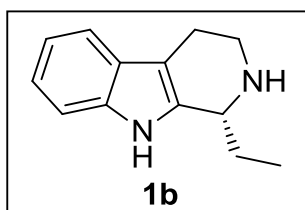
**Table S3.** Results of whole-cell catalyzed oxidation reactions. Biotransformation conditions: substrate: 15 mM, BH<sub>3</sub>-NH<sub>3</sub>: 60 mM, wet cells: 200 mg / mL, 1 M KPO<sub>4</sub> buffer, 37°C, 250 rpm, pH = 7.8. Reactions were carried out on a 4.5 μmol scale.



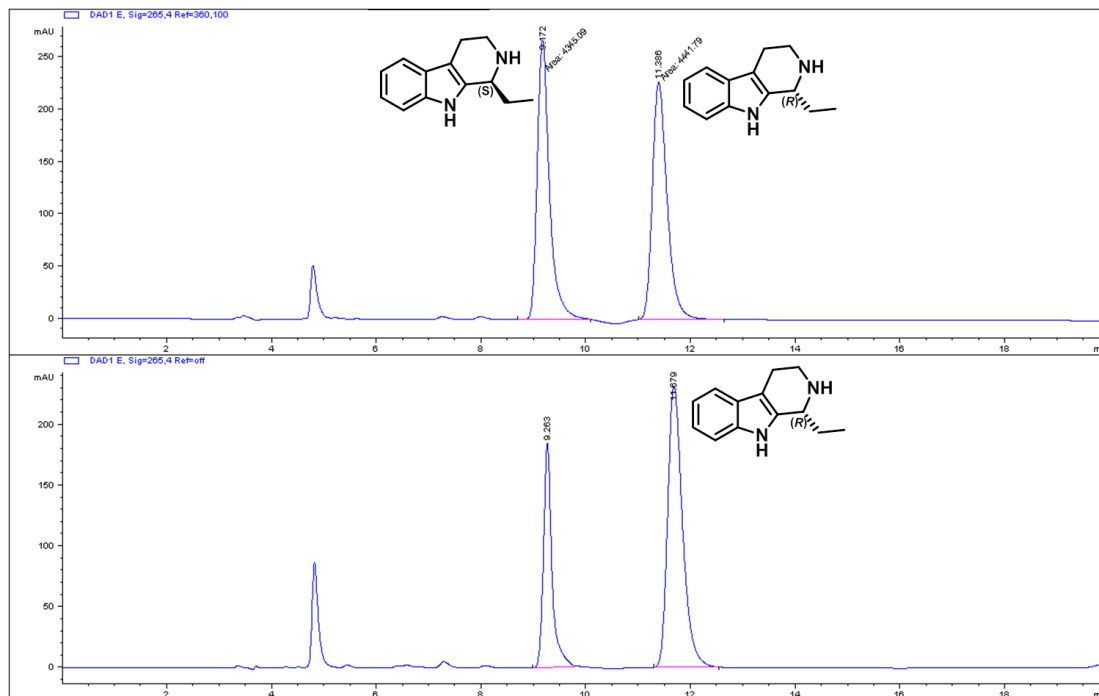
**(R)-1-methyl-2,3,4,9-tetrahydro-1H-pyrido[3,4-b]indole (1a).** The reaction was set up as described in the general procedure using MAO-N D9 as biocatalyst. After 24 hours HPLC analysis showed 99% e.e.



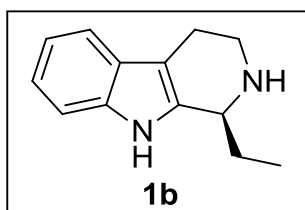
**Figure S2.** Chiral phase HPLC trace of (*rac*)-**1a** conversion with MAO-N D9 showing the signals of racemic compound **1a** (top) and the deracemisation product (*R*)-**1a** (bottom).



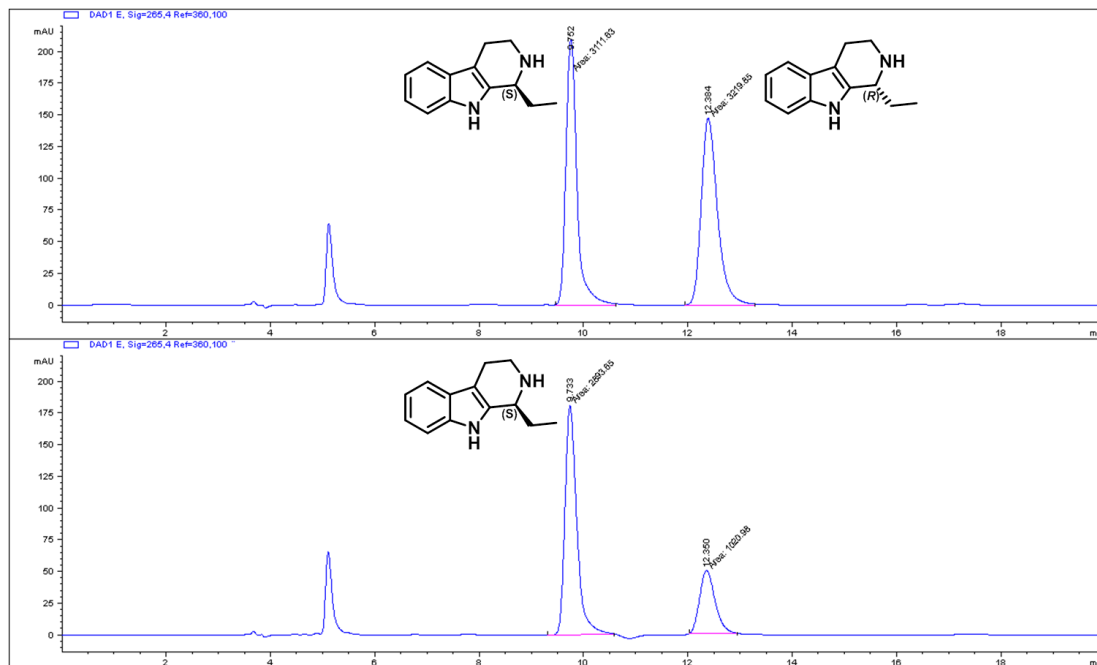
**(R) – 1-ethyl-2,3,4,9-tetrahydro-1H-pyrido[3,4-b]indole (1b).** The reaction was set up as described in the general procedure using MAO-N D9 as biocatalyst. After 72 hours HPLC analysis showed 36% e.e.



**Figure S3.** Chiral phase HPLC trace of *(rac)*-**1b** conversion with MAO-N D9 showing the signals of racemic compound **1b** (top) and the deracemisation product *(R)*-**1b** (bottom)

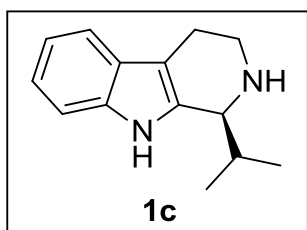


(*S*) – 1-ethyl-2,3,4,9-tetrahydro-1H-pyrido[3,4-b]indole (**1b**). The reaction was set up as described in the general procedure using MAO-N D10 as biocatalyst. After 48 hours HPLC analysis showed 49% e.e.

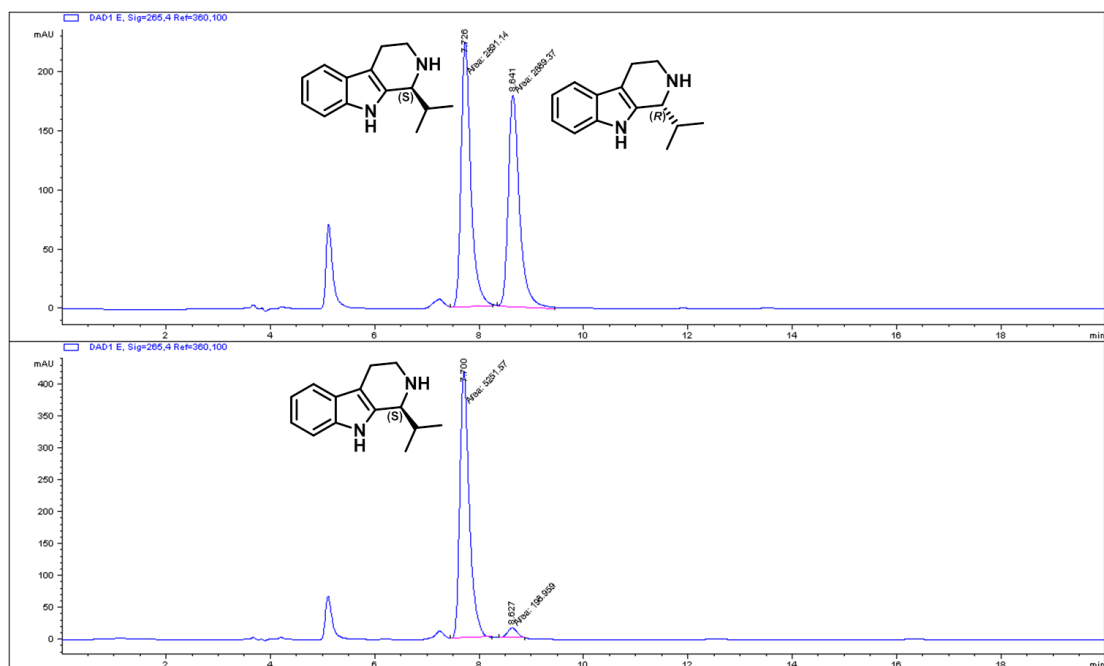


**Figure S4.** Chiral phase HPLC trace of (*rac*)-**1b** conversion with MAO-N D9 showing the signals of racemic compound **1b** (top) and the deracemisation product (*S*)-**1b** (bottom)

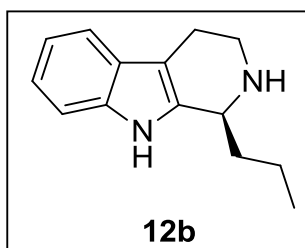




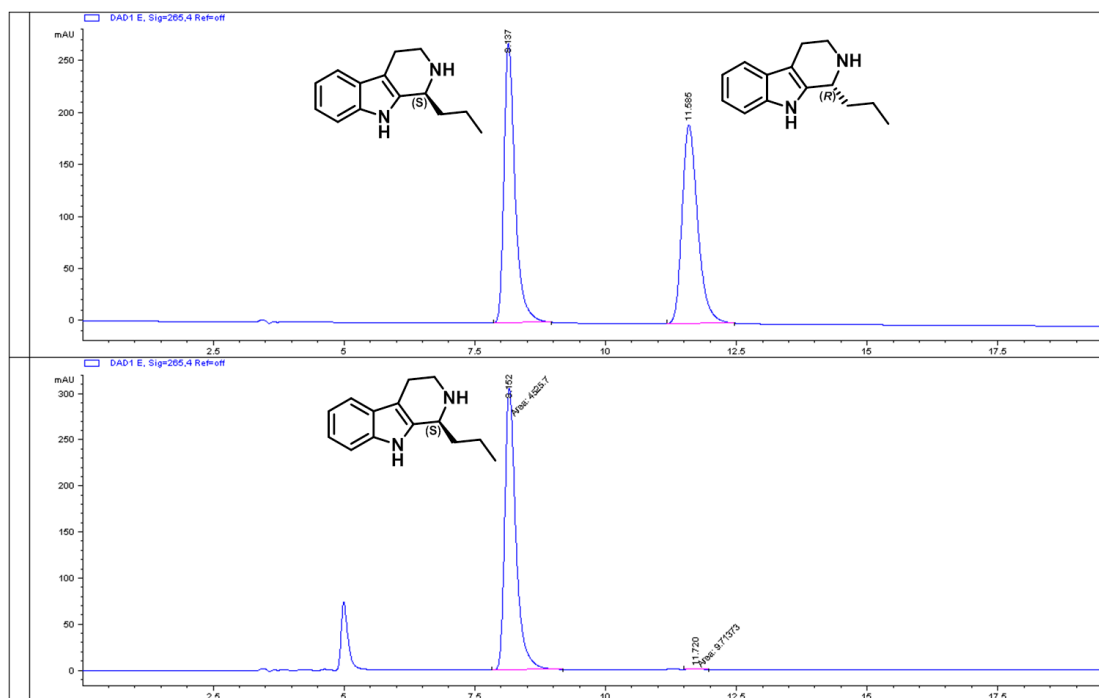
**(S) – 1 – isopropyl - 2,3,4,9 – tetrahydro - 1H-pyrido[3,4-b]indole (1c).** The reaction was set up as described in the general procedure using MAO-N D10 as biocatalyst. After 48 hours HPLC analysis showed 40% e.e.



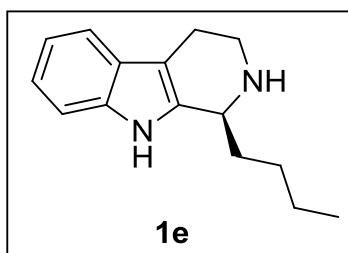
**Figure S5.** Chiral phase HPLC trace of *(rac)*-**1c** conversion with MAO-N D9 showing the signals of racemic compound **1c** (top) and the deracemisation product *(S)*-**1c** (bottom).



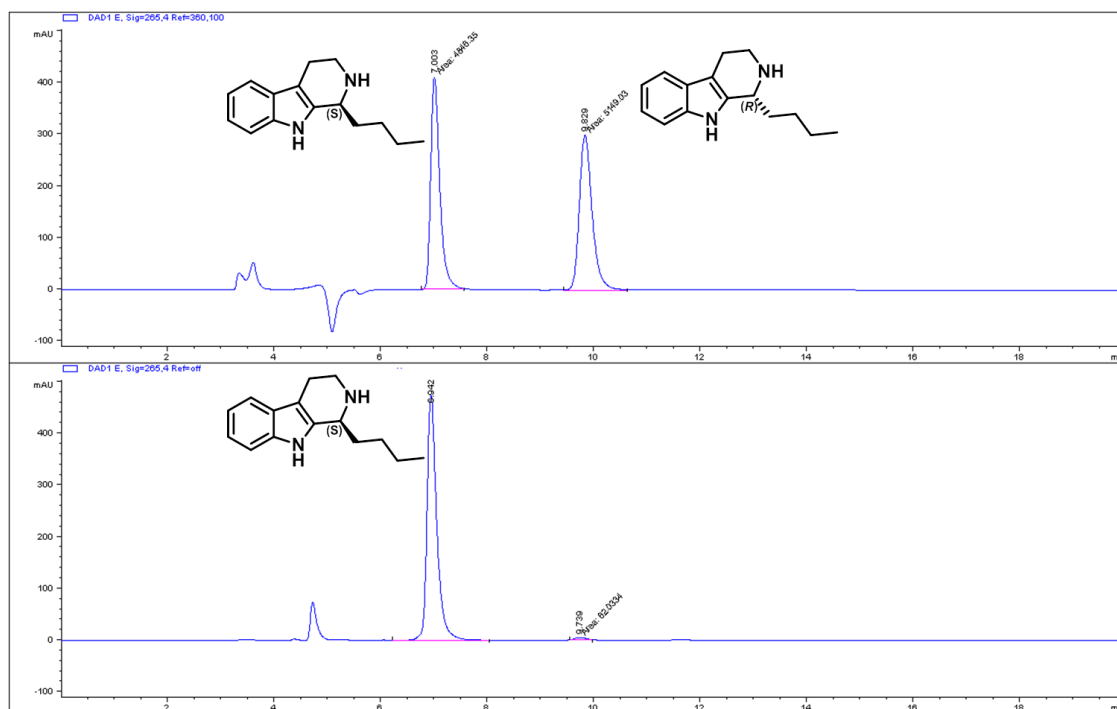
**(S) – 1-propyl-2,3,4,9-tetrahydro-1H-pyrido[3,4-b]indole (1d).** The reaction was set up as described in the general procedure using MAO-N D11 as biocatalyst. After 48 hours HPLC analysis showed >99% e.e.



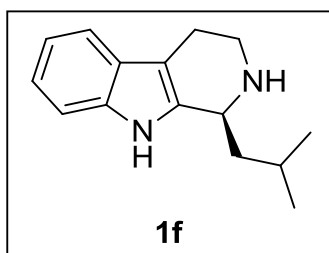
**Figure S6.** Chiral phase HPLC trace of (*rac*)-**1d** conversion with MAO-N D11 showing the signals of racemic compound **1d** (top) and the deracemisation product (*R*)-**1d** (bottom).



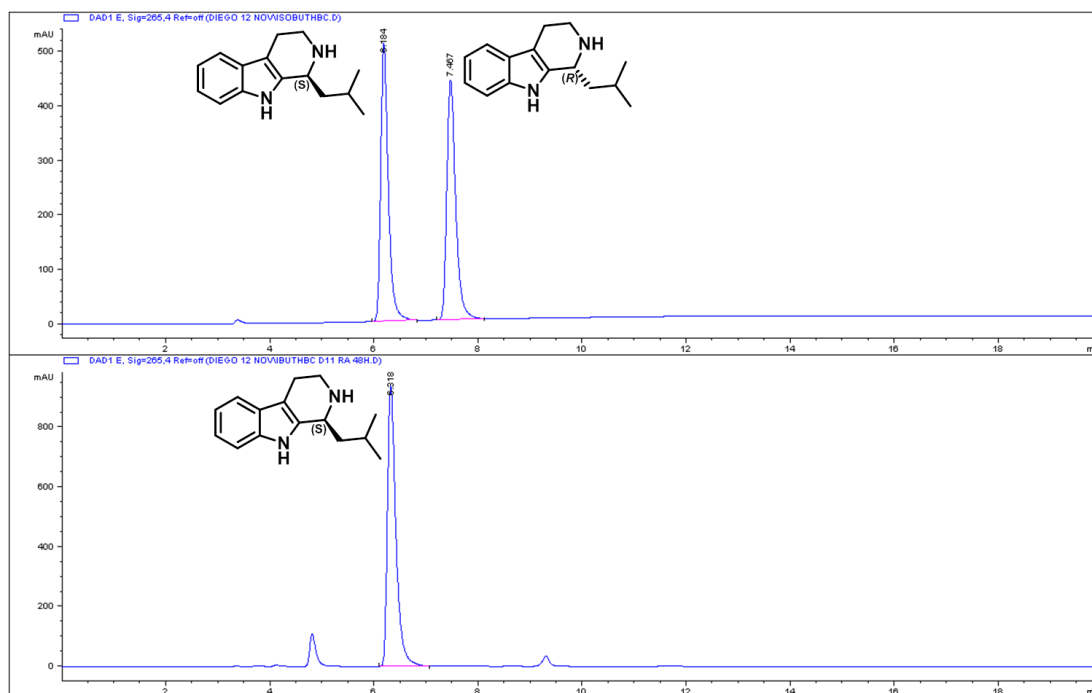
**(S) – 1 – butyl - 2,3,4,9 – tetrahydro - 1H-pyrido[3,4-b]indole (1e).** The reaction was set up as described in the general procedure using MAO-N D11 as biocatalyst. After 48 hours HPLC analysis showed 99% e.e.



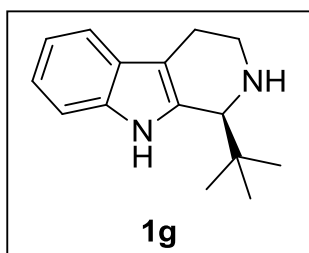
**Figure S7.** Chiral phase HPLC trace of (*rac*)-**1e** conversion with MAO-N D11 showing the signals of racemic compound **1e** (top) and the deracemisation product (*R*)-**1e** (bottom).



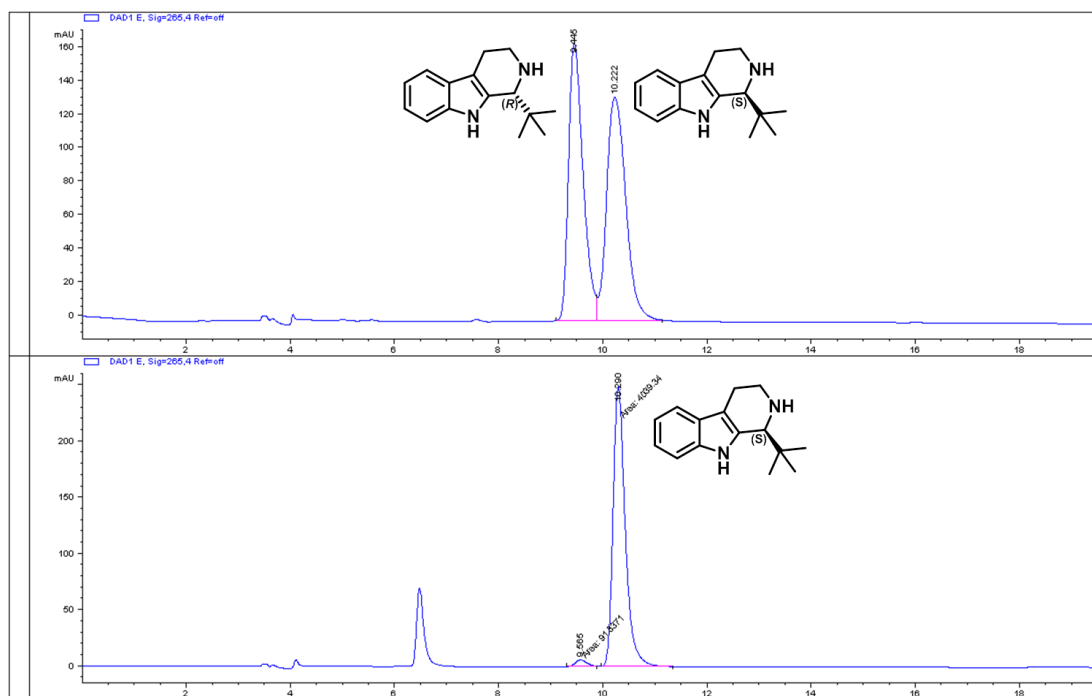
**(S) – 1 - isobutyl - 2,3,4,9 - tetrahydro- 1H-pyrido[3,4-b]indole (1f).** The reaction was set up as described in the general procedure using MAO-N D11 as biocatalyst. After 48 hours HPLC analysis showed >99% e.e.



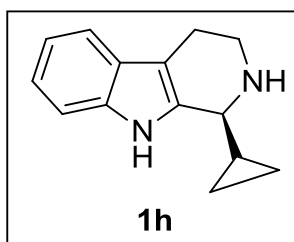
**Figure S8.** Chiral phase HPLC trace of (*rac*)-**1f** conversion with MAO-N D11 showing the signals of racemic compound **1f** (top) and the deracemisation product (*R*)-**1f** (bottom).



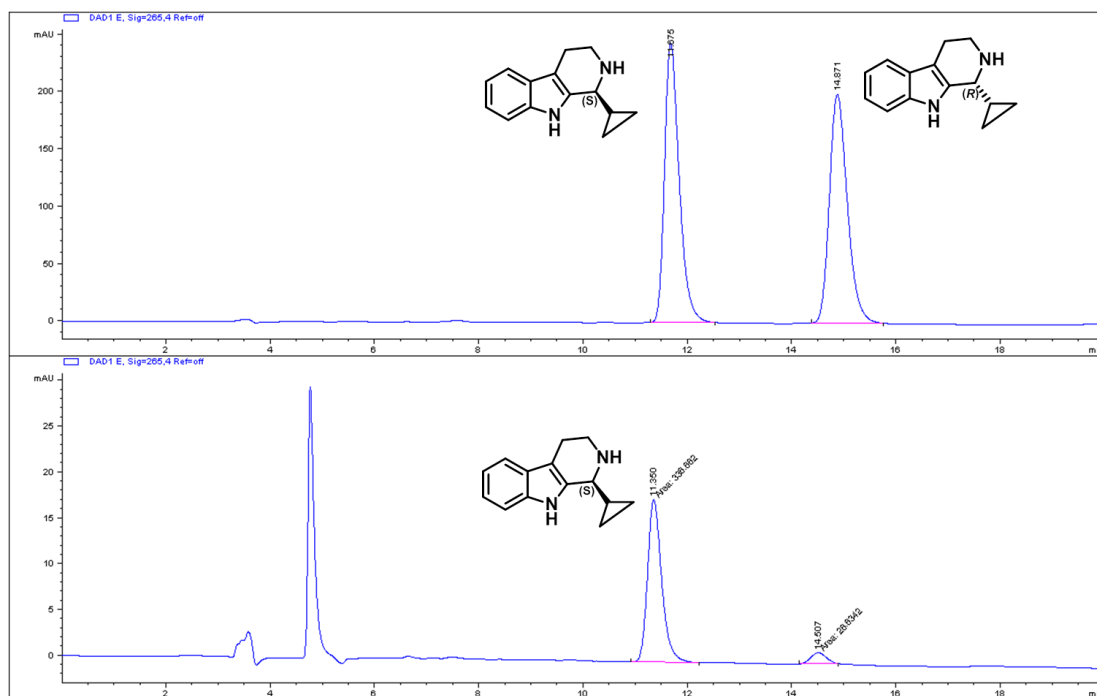
**(S) – 1 – tertbutyl - 2,3,4,9 – tetrahydro -1H-pyrido[3,4-b]indole (1g).** The reaction was set up as described in the general procedure using MAO-N D11 as biocatalyst. After 48 hours HPLC analysis showed 96% e.e.



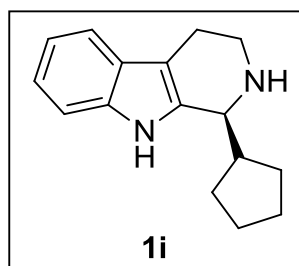
**Figure S9.** Chiral phase HPLC trace of (*rac*)-**1g** conversion with MAO-N D11 showing the signals of racemic compound **1g** (top) and the deracemisation product (*R*)-**1g** (bottom).



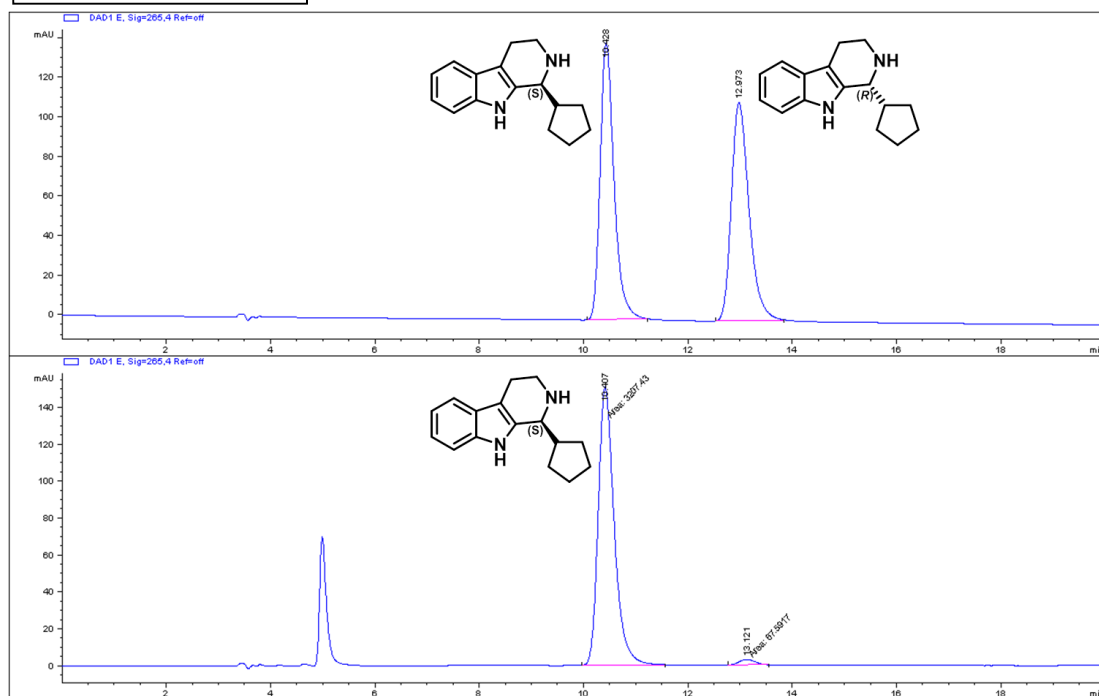
(*S*) – 1 – ciclopropyl - 2,3,4,9 -tetrahydro-1H-pyrido[3,4-b]indole (**1h**). The reaction was set up as described in the general procedure using MAO-N D9 as biocatalyst. After 48 hours HPLC analysis showed 86% e.e.



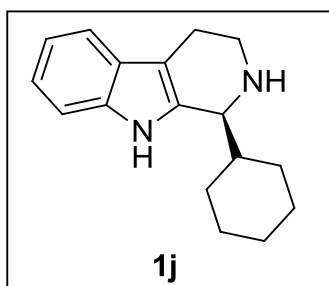
**Figure S10.** Chiral phase HPLC trace of (*rac*)-**1h** conversion with MAO-N D11 showing the signals of racemic compound **1h** (top) and the deracemisation product (*R*)-**1h** (bottom).



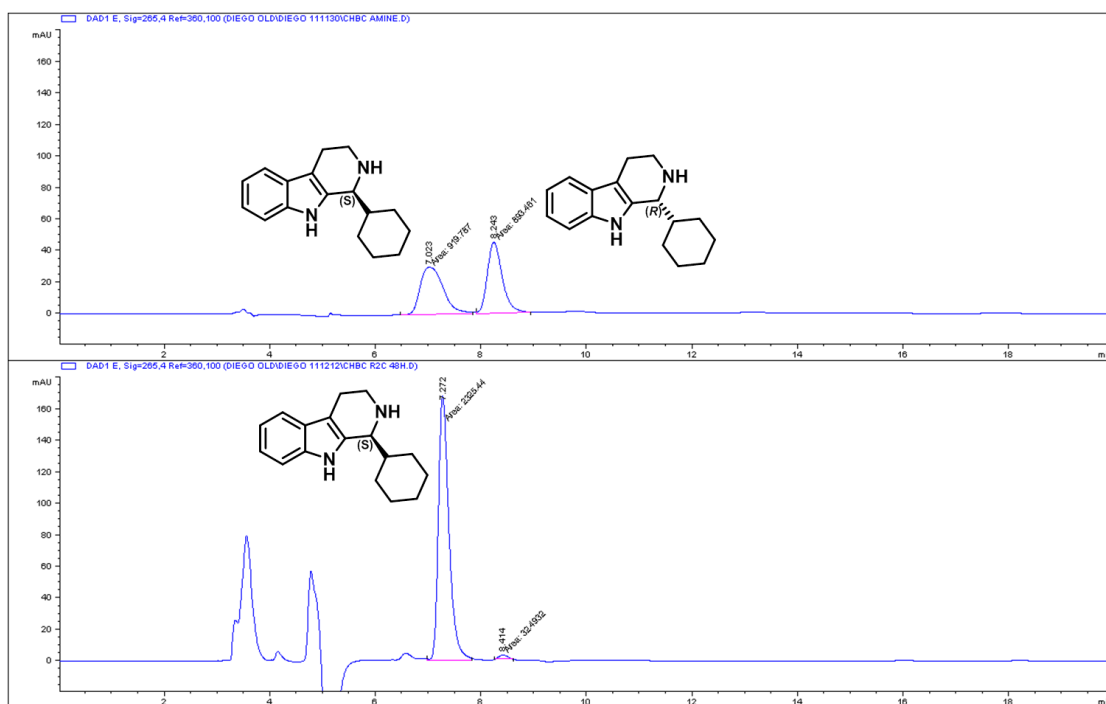
**(S) – 1 – cyclopentyl - 2,3,4,9 -tetrahydro-1H-pyrido[3,4-b]indole (1i).** The reaction was set up as described in the general procedure using MAO-N D11 as biocatalyst. After 48 hours HPLC analysis showed 96% e.e.



**Figure S11.** Chiral phase HPLC trace of (*rac*)-**1i** conversion with MAO-N D11 showing the signals of racemic compound **1i** (top) and the deracemisation product (*R*)-**1i** (bottom).

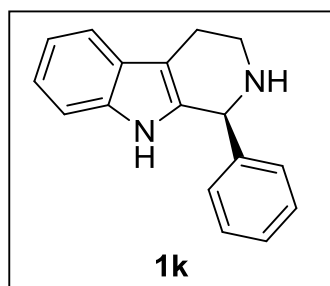


**(S) - 1 - ciclohexyl -2,3,4,9- tetrahydro-1H-pyrido[3,4-b]indole (1j).** The reaction was set up as described in the general procedure using MAO-N D11 as biocatalyst. After 48 hours HPLC analysis showed 97% e.e.

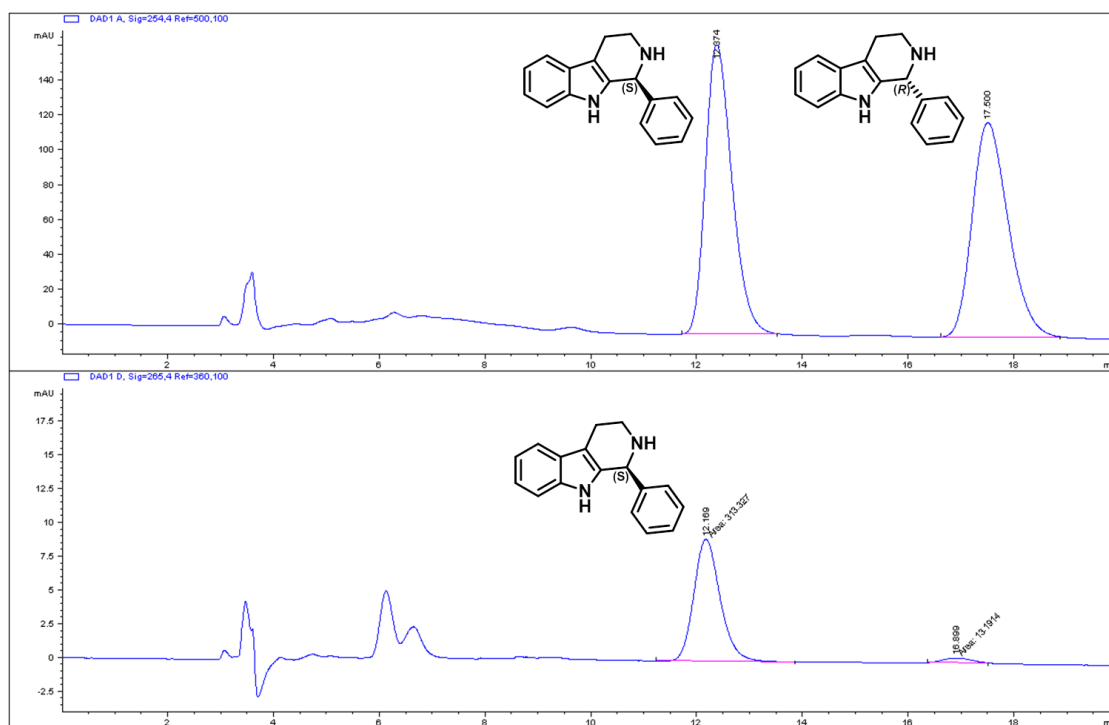


**Figure S12.** Chiral phase HPLC trace of (*rac*)-**1j** conversion with MAO-N D11 showing the signals of racemic compound **1j** (top) and the deracemisation product (*R*)-**1j** (bottom).





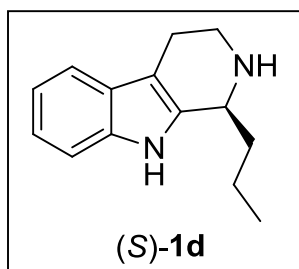
**(S) - 1 - phenyl - 2,3,4,9 – tetrahydro - 1H -pyrido[3,4-b]indole (1k).** The reaction was set up as described in the general procedure using MAO-N D11 as biocatalyst. After 72 hours HPLC analysis showed 92% e.e.



**Figure S13.** Chiral phase HPLC trace of (*rac*)-**1k** conversion with MAO-N D11 showing the signals of racemic compound **1k** (top) and the deracemisation product (*R*)-**1k** (bottom).

### MAO-N D11 deracemisations: preparative procedure

In a 50 mL Falcon tube, the hydrochloric salt (0.4 mmol) and  $\text{BH}_3\text{-NH}_3$  (1.6 mmol) were dissolved in  $\text{KPO}_4$ -buffer (25 mL, 1 M, pH = 7.8). The pH of the solution was adjusted to 7.8 by addition of NaOH. Cell pellet from *E. coli* cultures (4 g) containing MAO-N D11 was added to the solution. The tube was placed in a shaking incubator and shaken at 37 °C and 250 rpm. When HPLC analysis showed the good conversion reached and the amount of imine < 2% (usually after 48 hours), aqueous NaOH (200  $\mu\text{L}$ , 10 M) and  $\text{CH}_2\text{Cl}_2$  (30 mL) were added to work up the reaction and layers were separated by centrifugation (4000 rpm, 5 min.) and the aqueous phase was extracted again with  $\text{CH}_2\text{Cl}_2$  (20 mL). The combined organic phases were dried over  $\text{MgSO}_4$  and concentrated under vacuum.

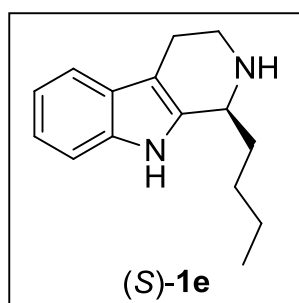


**(S)-Komaroidine (1d).** The reaction was set up as described in the general procedure using (*rac*)-**1d**HCl (100 mg, 0.4 mmol),  $\text{BH}_3\text{-NH}_3$  (56 mg, 1.6 mmol) and MAO-N D11 (4 g) as biocatalyst. After 48 hours HPLC analysis showed full conversion and the reaction was worked up to give (*S*)-**1d** (80 mg, 99% e.e., 93% yield). Characterisation data were in good agreement with literature values.[2]

$[\alpha]_{\text{D}}^{20}$ :  $-72.6^\circ$  ( $c = 1.0$ , EtOH)

$^1\text{H}$  NMR (400 MHz, MeOD)  $\delta$ : 7.31 (t,  $J = 0.8$  Hz, 1H, ArH), 7.29 (t,  $J = 1.2$  Hz, 1H, ArH), 7.14 (ddd,  $J = 7.6, 7.6, 1.2$  Hz, 1H, ArH), 7.08 (ddd,  $J = 7.6, 7.6, 0.8$  Hz, 1H, ArH), 4.07 (ddd,  $J = 6.4, 4.0, 2.0$  Hz, 1H, -CHNH), 3.35 (dt,  $J = 13.0, 4.0$  Hz, 1H, - $\text{CH}_2\text{CHHN}$ ), 3.02 (ddd,  $J = 13.0, 8.0, 5.6$  Hz, 1H, - $\text{CH}_2\text{CHHN}$ ), 2.74 (m, 2H, - $\text{CH}_2\text{CH}_2\text{N}$ ), 1.80–1.88 (m, 1H, - $\text{CHHCH}_2\text{CH}_3$ ), 1.62–1.71 (m, 1H, - $\text{CHHCH}_2\text{CH}_3$ ), 1.46–1.60 (m, 2H, - $\text{CH}_2\text{CH}_2\text{CH}_3$ ), 0.99 (t,  $J = 7.2$  Hz, 3H, - $\text{CH}_2\text{CH}_2\text{CH}_3$ ).

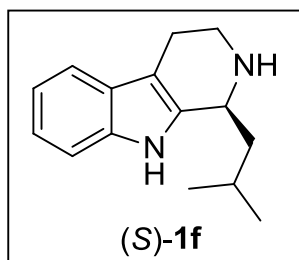
$^{13}\text{C}$  NMR (100 MHz, MeOD)  $\delta$ : 136.3 (ArC), 135.6 (ArC), 127.6 (ArC), 121.4 (ArC), 119.4 (ArC), 118.1 (ArC), 110.6 (ArC), 108.9 (ArC), 52.5 (CHNH), 46.3 (CH<sub>2</sub>NH), 37.2 (CHCH<sub>2</sub>), 22.7 (CH<sub>2</sub>CH<sub>2</sub>), 19.2 (CH<sub>2</sub>CH<sub>2</sub>), 14.2 (CH<sub>3</sub>).



**(S) - 1 - butyl-2,3,4,9-tetrahydro-1H-pyrido[3,4-b]indole (1e).** The reaction was set up as described in the general procedure using (*rac*)-**1e**HCl (106 mg, 0.4 mmol),  $\text{BH}_3\text{-NH}_3$  (56 mg, 1.6 mmol) and MAO-N D11 (4 g) as biocatalyst. After 48 hours HPLC analysis showed full conversion and the reaction was worked up to give (*S*)-**1e** (78 mg, 99% e.e., 85% yield). Characterization data were in good agreement with literature values.[3]

$[\alpha]_{\text{D}}^{20}$ :  $-79.3^\circ$  ( $c = 1.0$ , EtOH).

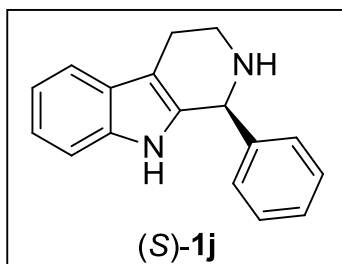
$^1\text{H}$  NMR (400 MHz,  $\text{CDCl}_3$ )  $\delta$ : 7.77 (bs, 1H, ArNH), 7.48 (d,  $J = 7.8$  Hz, 1H, ArH), 7.31 (dd,  $J = 8.0, 0.9$  Hz, 1H, ArH), 7.15 (dt,  $J = 7.9, 1.1$  Hz, 1H, ArH), 7.09 (dt,  $J = 7.9, 1.0$  Hz, 1H, ArH), 4.10-4.02 (m, 1H, -CHNH), 3.40-3.30 (m, 1H, - $\text{CH}_2\text{CHHN}$ ), 3.03 (ddd,  $J = 13.8, 8.4, 5.2$  Hz, 1H, - $\text{CH}_2\text{CHHN}$ ), 2.75-2.68 (m, 2H, - $\text{CH}_2\text{CH}_2\text{N}$ ), 1.91-1.83 (m, 1H, - $\text{CHHCH}_2\text{CH}_2\text{CH}_3$ ), 1.70-1.34 (m, 5H, - $\text{CHHCH}_2\text{CH}_2\text{CH}_3$ ), 0.94 (t,  $J = 7.3$  Hz, 1H, - $\text{CH}_2\text{CH}_2\text{CH}_2\text{CH}_3$ ).



**(S)-1-isobutyl-2,3,4,9-tetrahydro-1H-pyrido[3,4-b]indole (1f).** The reaction was set up as described in the general procedure using (*rac*)-**1f**HCl (106 mg, 0.4 mmol), BH<sub>3</sub>-NH<sub>3</sub> (56 mg, 1.6 mmol) and MAO-N D11 (4 g) as biocatalyst. After 48 hours HPLC analysis showed full conversion and the reaction was worked up to give (*S*)-**1f** (80 mg, 99% e.e., 88% yield). Characterisation data were in good agreement with literature values.[3]

$[\alpha]_D^{20}$ : -81.0 ° (c = 1.0, MeOH)

<sup>1</sup>H NMR (400 MHz, CDCl<sub>3</sub>) δ: 8.11 (s, 1H, ArNH), 7.53 (d, *J* = 7.5 Hz, 1H, ArH), 7.31 (dd, *J* = 7.9 Hz, 1H, ArH), 7.21 – 7.11 (m, 2H, ArH), 4.16 (dd, *J* = 7.7, 6.1 Hz, 1H, -CHNH), 3.40 (dt, *J* = 12.8, 4.7 Hz, 1H, -CH<sub>2</sub>CHHN), 3.15–3.00 (m, 1H, -CH<sub>2</sub>CHHN), 2.85 – 2.70 (m, 2H, -CH<sub>2</sub>CH<sub>2</sub>N), 2.09 – 1.95 (m, 1H, -CHHCH(CH<sub>3</sub>)<sub>2</sub>), 1.73–1.60 (m, 2H, -CHHCH(CH<sub>3</sub>)<sub>2</sub>) 1.02 (d, *J* = 6.0 Hz, 3H, -CHH<sub>2</sub>CH(CH<sub>3</sub>)<sub>2</sub>), 0.99 (d, *J* = 6.0 Hz, 3H, -CHH<sub>2</sub>CH(CH<sub>3</sub>)<sub>2</sub>).



**(S) – 1 – phenyl - 2,3,4,9 – tetrahydro -1H-pyrido[3,4-b]indole (1j).** The reaction was set up as described in the general procedure using (*rac*)-**1j**HCl (113 mg, 0.4 mmol), BH<sub>3</sub>-NH<sub>3</sub> (56 mg, 1.6 mmol) and MAO-N D11 (4 g) as biocatalyst. After 48 hours HPLC analysis showed full conversion and the reaction was worked up to give (*S*)-**1j** (90 mg, 90% e.e., 91% yield). Characterisation data were in good agreement with literature values.[3]

$[\alpha]_D^{20}$ : -4.5 ° (c = 1.0, Acetone)

<sup>1</sup>H NMR (400 MHz, CDCl<sub>3</sub>) δ: 7.66 (s, 1H, ArNH), 7.58 (dd, *J* = 6.5, 2.3 Hz, 1H, ArH), 7.42 – 7.30 (m, 5H, ArH), 7.24 (dd, *J* = 6.8, 2.3 Hz, 1H, ArH), 7.20 – 7.11 (m, 2H, ArH), 5.20 (s, 1H, -CHNH), 3.44 – 3.33 (m, 1H, -CH<sub>2</sub>CHHN), 3.23 – 3.08 (m, 1H, -CH<sub>2</sub>CHHN), 3.03 – 2.91 (m, 1H, -CHHCH<sub>2</sub>N), 2.91 – 2.79 (m, 1H, -CHHCH<sub>2</sub>N).

### Experiments to establish the absolute configuration

The configuration of products (*R*)-**1a**, (*R*)-**1b**, (*S*)-**1c**, (*S*)-**1g**, (*S*)-**1k** and (*S*)-**1j** was determinate by comparison with literature HPLC retention time.[1] The absolute configuration of (*S*)-**1h** and (*S*)-**1i** were assigned by analogy with the other

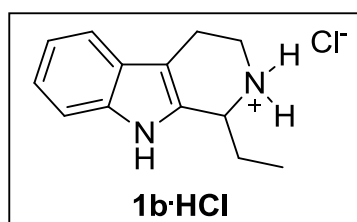
compounds.

The configuration of the products (*S*)-**1d**, (*S*)-**1e**, (*S*)-**1f** and (*S*)-**1j** was assigned by comparison of their optical rotation values with the literature.

Observed value for (*S*)-**1d**:  $[\alpha]_{\text{D}}^{20}$ : -72.6° (c = 1.0, EtOH),[2] (*S*)-**1e**:  $[\alpha]_{\text{D}}^{20}$ : -79.3° (c = 1.0, EtOH),[3] (*S*)-**1f**:  $[\alpha]_{\text{D}}^{20}$ : -81.0° (c = 1.0, MeOH).[3] (*S*)-**1f**:  $[\alpha]_{\text{D}}^{20}$ : -4.5° (c = 1.0, Acetone) [4]

### General procedure for the preparation of starting chloride salts **1b-m**. [5]

In an Eppendorf tube, tryptamine hydrochloride (0.5 M) and the required aldehyde (0.5 M) were added to aqueous maleic acid buffer (10 mM, pH 2.0, total volume 2 mL) and the solution was stirred overnight at 60 °C. Either during the reaction or upon standing, the tetrahydro-β-carboline hydrochloride salts precipitated and could be filtered and washed with water (2 mL) to afford analytically pure products.

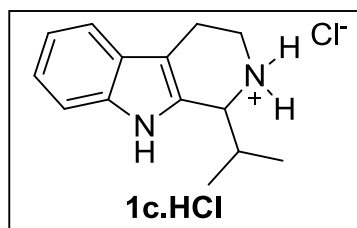


**1 - ethyl - 2,3,4,9-tetrahydro-1H-pyrido[3,4-b]indol-2-ium chloride (1b·HCl).** Tryptamine hydrochloride (197 mg, 1 mmol) and propionaldehyde (72 μL, 1 mmol) were added to aqueous maleic acid buffer (10 mM, pH 2.0, total volume 2 mL). The suspension was

filtered to give **1b·HCl** (179 mg, 76% yield). Characterisation data were in good agreement with literature values.[5]

$^1\text{H}$  NMR, 400 MHz,  $\text{CD}_3\text{OD}$   $\delta$ : 7.50 (dt,  $J = 8.0, 0.8$ , 1H, ArH), 7.38 (dt,  $J = 8.2, 0.8$ , 1H, ArH), 7.17 (ddd,  $J = 8.2, 7.1, 1.1$ , 1H, ArH), 7.07 (ddd,  $J = 8.0, 7.1, 1.0$ , 1H, ArH), 4.66 (m, 1H, -CHNH<sub>2</sub>), 3.76 (ddd,  $J = 12.5, 5.4, 3.9$ , 1H, -CH<sub>2</sub>CHHNH<sub>2</sub>), 3.46 (ddd,  $J = 12.6, 9.3, 5.8$ , 1H, -CH<sub>2</sub>CHHNH<sub>2</sub>), 3.19-3.02 (m, 2H, -CH<sub>2</sub>CH<sub>2</sub>NH<sub>2</sub>), 2.35 (dq,  $J = 15.2, 7.6, 4.3$ , 1H, -CHHCH<sub>3</sub>), 2.01 (dq,  $J = 15.2, 8.8, 7.2$ , 1H, -CHHCH<sub>3</sub>), 1.21 (t,  $J = 7.5$ , 3H, -CH<sub>2</sub>CH<sub>3</sub>).

$^{13}\text{C}$  NMR, 100 MHz,  $\text{CD}_3\text{OD}$   $\delta$ : 138.4 (ArC), 130.1 (ArC), 127.4 (ArC), 123.5 (ArC), 120.6 (ArC), 119.1 (ArC), 112.4 (ArC), 107.3 (ArC), 56.2 (CHNH), 43.1 (CH<sub>2</sub>NH), 26.3 (CH<sub>2</sub>CH<sub>2</sub>), 19.5 (CH<sub>2</sub>CH<sub>2</sub>), 9.9 (CH<sub>3</sub>).

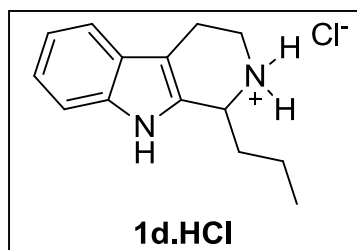


**1 - isopropyl - 2,3,4,9 - tetrahydro - 1H - pyrido[3,4-b]indol - 2 - ium chloride (1c.HCl).** Tryptamine hydrochloride (197 mg, 1 mmol) and isobutyraldehyde (91  $\mu$ L, 1 mmol) were added to aqueous maleic acid buffer (10 mM, pH 2.0, total volume 2 mL). The

suspension was filtered to give **1c.HCl** (197 mg, 79% yield). Characterisation data were in good agreement with literature values.[5]

$^1\text{H}$  NMR, 400 MHz,  $\text{CD}_3\text{OD}$   $\delta$ : 7.50 (d,  $J = 7.9$ , 1H, ArH), 7.39 (d,  $J = 8.1$ , 1H, ArH), 7.18 (t,  $J = 7.6$ , 1H, ArH), 7.08 (t,  $J = 7.5$ , 1H, ArH), 4.69 (m, 1H, -CHNH<sub>2</sub>), 3.77 (ddd,  $J = 12.4, 5.3, 3.1$ , 1H, -CH<sub>2</sub>CHHNH<sub>2</sub>), 3.47 (ddd,  $J = 12.5, 10.1, 5.7$ , 1H, -CH<sub>2</sub>CHHNH<sub>2</sub>), 3.20-3.01 (m, 2H, -CH<sub>2</sub>CH<sub>2</sub>NH<sub>2</sub>), 2.73-2.60 (m, 1H, -CH(CH<sub>3</sub>)<sub>2</sub>), 1.28 (d,  $J = 7.1$ , 3H, -CH(CH<sub>3</sub>)<sub>2</sub>), 0.99 (d,  $J = 7.1$ , 3H, -CH(CH<sub>3</sub>)<sub>2</sub>).

$^{13}\text{C}$  NMR, 100 MHz,  $\text{CD}_3\text{OD}$   $\delta$ : 138.4 (ArC), 129.3 (ArC), 127.4 (ArC), 123.6 (ArC), 120.6 (ArC), 119.1 (ArC), 112.4 (ArC), 108.5 (ArC), 60.5 (CHNH), 43.9 (CH<sub>2</sub>NH), 31.1 (CHCH), 19.2 (CH<sub>2</sub>CH<sub>2</sub>), 16.4 (CH<sub>3</sub>)<sub>2</sub>.

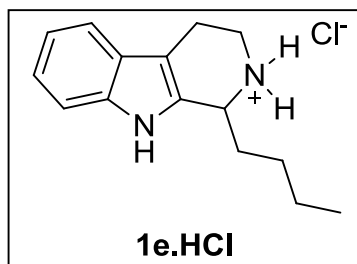


**1 - propyl - 2,3,4,9 - tetrahydro - 1H-pyrido[3,4-b]indol - 2 - ium chloride (1d.HCl).** Tryptamine hydrochloride (197 mg, 1 mmol) and butyraldehyde (90  $\mu$ L, 1 mmol) were added to aqueous maleic acid buffer (10 mM, pH 2.0, total volume 2 mL). The

suspension was filtered to give **1d.HCl** (187 mg, 75% yield).

$^1\text{H}$  NMR (400 MHz, MeOD)  $\delta$  7.49 (d,  $J = 7.8$  Hz, 1H, ArH), 7.38 (d,  $J = 8.1$  Hz, 1H, ArH), 7.17 (t,  $J = 7.6$  Hz, 1H, ArH), 7.07 (t,  $J = 7.4$  Hz, 1H, ArH), 4.70 (dd,  $J = 5.4, 3.5$  Hz, 1H, -CHNH<sub>2</sub>), 3.81 – 3.70 (m, 1H, -CH<sub>2</sub>CHHNH<sub>2</sub>), 3.45 (ddd,  $J = 12.6, 9.3, 5.8$  Hz, 1H, -CH<sub>2</sub>CHHNH<sub>2</sub>), 3.20 – 2.98 (m, 2H, -CH<sub>2</sub>CH<sub>2</sub>NH<sub>2</sub>), 2.34 – 2.19 (m, 1H, -CHHCH<sub>2</sub>CH<sub>3</sub>), 2.01 – 1.87 (m, 1H, -CHHCH<sub>2</sub>CH<sub>3</sub>), 1.71 – 1.55 (m, 2H, -CH<sub>2</sub>CH<sub>2</sub>CH<sub>3</sub>), 1.12 (t,  $J = 7.3$  Hz, 3H, -CH<sub>2</sub>CH<sub>2</sub>CH<sub>3</sub>).

$^{13}\text{C}$  NMR (100 MHz, MeOD)  $\delta$ : 138.3 (ArC), 130.3 (ArC), 127.4 (ArC), 123.5 (ArC), 120.6 (ArC), 119.1 (ArC), 112.3 (ArC), 107.1 (ArC), 54.9 (CHNH), 43.1 (CH<sub>2</sub>NH), 35.4(CHCH<sub>2</sub>), 28.7 (CH<sub>2</sub>CH<sub>2</sub>), 19.5 (CH<sub>2</sub>CH<sub>2</sub>), 14.2 (CH<sub>3</sub>).

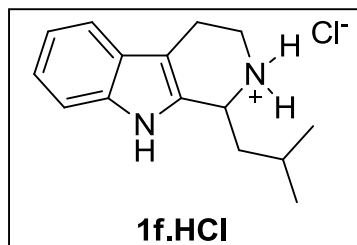


**1 - butyl-2,3,4,9-tetrahydro-1H-pyrido[3,4-b]indol - 2- ium chloride (1e.HCl).** Tryptamine hydrochloride (197 mg, 1 mmol) and valeraldehyde (106  $\mu$ L, 1 mmol) were added to aqueous maleic acid buffer (10 mM, pH 2.0, total volume 2 mL). The suspension was

filtered to give **1e.HCl** (218 mg, 83% yield). Characterisation data were in good agreement with literature values.[5]

$^1\text{H}$  NMR (400 MHz, MeOD)  $\delta$  7.49 (d,  $J = 7.9$  Hz, 1H, ArH), 7.38 (d,  $J = 8.1$  Hz, 1H, ArH), 7.23 – 7.13 (m, 1H, ArH), 7.07 (td,  $J = 7.6, 1.0$  Hz, 1H, ArH), 4.76 – 4.61 (m, 1H,  $-\text{CHNH}_2$ ), 3.74 (ddd,  $J = 12.5, 5.4, 3.8$  Hz, 1H,  $-\text{CH}_2\text{CHHNH}_2$ ), 3.54 – 3.36 (m, 1H,  $-\text{CH}_2\text{CHHNH}_2$ ), 3.21 – 2.94 (m, 2H,  $-\text{CH}_2\text{CH}_2\text{NH}_2$ ), 2.39 – 2.22 (m, 1H,  $-\text{CHHCH}_2\text{CH}_2\text{CH}_3$ ), 1.96 (ddd,  $J = 15.4, 8.8, 7.2$  Hz, 1H,  $-\text{CHHCH}_2\text{CH}_2\text{CH}_3$ ), 1.66 – 1.42 (m, 4H,  $-\text{CH}_2\text{CH}_2\text{CH}_2\text{CH}_3$ ), 1.04 (t,  $J = 7.2$  Hz, 3H,  $-\text{CH}_2\text{CH}_2\text{CH}_2\text{CH}_3$ ).

$^{13}\text{C}$  NMR (100 MHz, MeOD)  $\delta$ : 138.3 (ArC), 130.3 (ArC), 127.4 (ArC), 123.5 (ArC), 120.6 (ArC), 119.1 (ArC), 112.4 (ArC), 107.2 (ArC), 55.1 (CHNH), 43.2 (CH<sub>2</sub>NH), 33.1 (CHCH<sub>2</sub>), 28.3 (CHCH<sub>2</sub>), 23.6 (CHCH<sub>2</sub>), 19.5 (CHCH<sub>2</sub>), 14.2 (CH<sub>3</sub>).



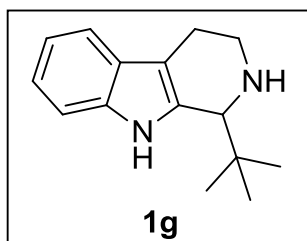
**1 - isobutyl - 2,3,4,9 - tetrahydro - 1H - pyrido[3,4-b]indol - 2-ium chloride (1f.HCl).** Tryptamine hydrochloride (197 mg, 1 mmol) and isovaleraldehyde (108  $\mu$ L, 1 mmol) were added to aqueous maleic acid buffer (10 mM, pH 2.0, total volume 2 mL). The

suspension was filtered to give **1f.HCl** (225 mg, 86% yield). Characterisation data were in good agreement with literature values.[5]

$^1\text{H}$  NMR (400 MHz, MeOD)  $\delta$  7.49 (d,  $J = 7.9$  Hz, 1H, ArH), 7.38 (d,  $J = 8.1$  Hz, 1H, ArH), 7.16 (ddd,  $J = 8.0, 7.1, 1.1$ , 1H, ArH), 7.06 (ddd,  $J = 8.2, 7.1, 1.0$ , 1H, ArH), 4.83 – 4.73 (m, 1H,  $-\text{CHNH}_2$ ), 3.74 (ddd,  $J = 12.5, 5.3, 3.8$  Hz, 1H,  $-\text{CH}_2\text{CHHNH}_2$ ), 3.46 (ddd,  $J = 12.6, 9.4, 5.9$  Hz, 1H,  $-\text{CH}_2\text{CHHNH}_2$ ), 3.20 – 2.98 (m, 2H,  $-\text{CH}_2\text{CH}_2\text{NH}_2$ ), 2.10 (ddd,  $J = 14.0, 10.2, 3.8$  Hz, 1H,  $-\text{CHHCH}(\text{CH}_3)_2$ ), 2.05 – 1.93 (m, 1H,  $-\text{CHHCH}(\text{CH}_3)_2$ ), 1.87 (ddd,  $J = 14.1, 10.3, 3.8$  Hz, 1H,  $-\text{CH}_2\text{CH}(\text{CH}_3)_2$ ), 1.16 (d,  $J = 6.3$  Hz, 3H,  $-\text{CH}_2\text{CH}(\text{CH}_3)_2$ ), 1.11 (d,  $J = 6.4$  Hz, 3H,  $-\text{CH}_2\text{CH}(\text{CH}_3)_2$ ).

$^{13}\text{C}$  NMR (100 MHz, MeOD)  $\delta$ : 138.3 (ArC), 130.5 (ArC), 127.5 (ArC), 123.4

(ArC), 120.6 (ArC), 119.0 (ArC), 112.4 (ArC), 107.1 (ArC), 53.0 (CHNH), 43.1(CH<sub>2</sub>NH), 42.6 (CH<sub>2</sub>CH), 25.2 (CH<sub>2</sub>CH), 23.9 (CH<sub>3</sub>), 21.6 (CH<sub>3</sub>), 19.5 (CH<sub>2</sub>CH<sub>2</sub>).

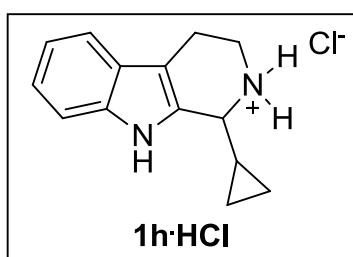


**1 - (tert - butyl) - 2,3,4,9 - tetrahydro - 1H - pyrido[3,4-b]indole (1g).** Tryptamine hydrochloride (197 mg, 1 mmol) and pivalaldehyde (109  $\mu$ L, 1 mmol) were added to aqueous maleic acid buffer (10 mM, pH 2.0, total volume 2 mL). The solution was basified with NaOH (10  $\mu$ L, 10

M) and extracted with CH<sub>2</sub>Cl<sub>2</sub> (2 x 10 ml). The combined organic phases were dried over MgSO<sub>4</sub> and concentrated under vacuum. The crude solid was purified by silica column chromatography to give **1g** (166 mg, 63% yield). Characterisation data were in good agreement with literature values.[1]

<sup>1</sup>H NMR (400 MHz, CDCl<sub>3</sub>)  $\delta$  7.84 (s, 1H, ArNH), 7.50 (d,  $J$  = 7.7 Hz, 1H, ArH), 7.33 (d,  $J$  = 8.0 Hz, 1H, ArH), 7.19 – 7.13 (m, 1H, ArH), 7.13 – 7.07 (m, 1H, ArH), 3.89 (d,  $J$  = 1.7 Hz, 1H, CHNH), 3.40 (dt,  $J$  = 12.2, 4.0 Hz, 1H, -CH<sub>2</sub>CHHNH<sub>2</sub>), 2.97 – 2.86 (m, 1H, -CH<sub>2</sub>CHHNH<sub>2</sub>), 2.74 (ddd,  $J$  = 7.9, 4.3, 2.1 Hz, 2H, -CH<sub>2</sub>CH<sub>2</sub>NH<sub>2</sub>), 1.13 (s, 9H, C(CH<sub>3</sub>)<sub>3</sub>).

<sup>13</sup>C NMR (100 MHz, CDCl<sub>3</sub>)  $\delta$ : 136.0 (ArC), 134.6 (ArC), 127.5 (ArC), 122.0 (ArC), 119.7 (ArC), 118.3 (ArC), 112.2 (ArC), 111.0 (ArC), 62.8 (CHNH), 43.9 (CH<sub>2</sub>NH), 36.2 (C), 27.8 (CH<sub>3</sub>), 23.3 (CH<sub>2</sub>CH<sub>2</sub>).



**1 - cyclopropyl - 2,3,4,9 - tetrahydro - 1H - pyrido[3,4-b]indol-2-ium chloride (1h·HCl).**

Tryptamine hydrochloride (197 mg, 1 mmol) and cyclopropanecarboxaldehyde (75  $\mu$ L, 1 mmol) were added to aqueous maleic acid buffer (10 mM, pH 2.0,

total volume 2 mL). The suspension was filtered to give **1h·HCl** (203 mg, 82% yield).

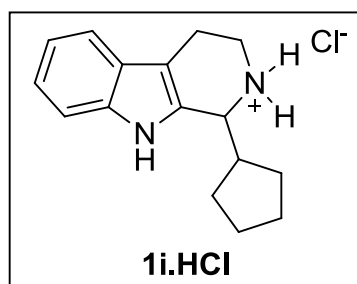
HRMS for C<sub>14</sub>H<sub>17</sub>N<sub>2</sub> [M+H]<sup>+</sup>:  $m/z$  theoretical 213.1386, found 213.1382

UV analysis: 230 nm, 280 nm

<sup>1</sup>H NMR (400 MHz, MeOD)  $\delta$  7.49 (d,  $J$  = 7.9 Hz, 1H, ArH), 7.41 (d,  $J$  = 8.2 Hz, 1H, ArH), 7.16 (ddd,  $J$  = 8.2, 7.2, 1.1 Hz, 1H, ArH), 7.06 (ddd,  $J$  = 8.0, 7.2, 1.0 Hz, 1H, ArH), 3.92 (d,  $J$  = 10.1 Hz, 1H, CHNH<sub>2</sub>), 3.75 (ddd,  $J$  = 12.6, 5.5, 4.2 Hz, 1H, -

CH<sub>2</sub>CHHNH<sub>2</sub>), 3.44 (ddd, *J* = 12.6, 9.1, 5.7 Hz, 1H, -CH<sub>2</sub>CHHNH<sub>2</sub>), 3.24 – 2.98 (m, 2H, -CH<sub>2</sub>CH<sub>2</sub>NH<sub>2</sub>), 1.33 – 1.21 (m, 1H, -CHCH<sub>2</sub>CH<sub>2</sub>-), 1.04 (tdd, *J* = 8.6, 6.2, 4.7 Hz, 1H, -CHCHHCH<sub>2</sub>-), 0.92 – 0.78 (m, 2H, -CHCHHCHH-), 0.71 tdd, *J* = 9.7, 6.3, 4.7 Hz, 1H, -CHCHHCH<sub>2</sub>-).

<sup>13</sup>C NMR (100 MHz, MeOD) δ: 138.5 (ArC), 130.0 (ArC), 127.4 (ArC), 123.5 (ArC), 120.6 (ArC), 119.1 (ArC), 112.5 (ArC), 107.0 (ArC), 60.2 (CHNH), 42.9 (CH<sub>2</sub>NH), 19.6 (CH<sub>2</sub>CH<sub>2</sub>NH), 13.7 (CHCH), 5.2 (CH<sub>2</sub>CH<sub>2</sub>), 3.4 (CH<sub>2</sub>CH<sub>2</sub>).



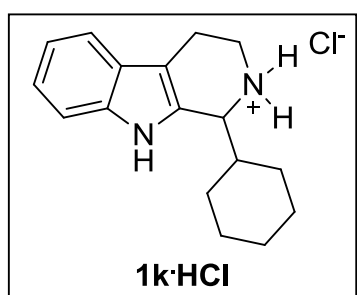
**1 – cyclopentyl - 2,3,4,9 – tetrahydro-1H-pyrido[3,4-b]indol – 2 - ium chloride (1i·HCl).** Tryptamine hydrochloride (197 mg, 1 mmol) and cyclopentanecarboxaldehyde (107 μL, 1 mmol) were added to aqueous maleic acid buffer (10 mM, pH 2.0, total volume 2 mL). The suspension was filtered to give **1i·HCl** (234 mg, 85% yield).

HRMS for C<sub>16</sub>H<sub>21</sub>N<sub>2</sub> [M+H]<sup>+</sup>: *m/z* theoretical 241.1699, found 241.1707

UV analysis: 226 nm, 280 nm

<sup>1</sup>H NMR (400 MHz, MeOD) δ 7.50 (d, *J* = 7.9 Hz, 1H, ArH), 7.41 (d, *J* = 8.2 Hz, 1H, ArH), 7.17 (t, *J* = 7.2 Hz, 1H, ArH), 7.08 (t, *J* = 7.2 Hz, 1H, ArH), 4.66 (d, *J* = 7.3 Hz, 1H, CHNH<sub>2</sub>), 3.74 (dt, *J* = 12.2, 5.4 Hz, 1H, -CH<sub>2</sub>CHHNH<sub>2</sub>), 3.55 – 3.42 (m, 1H, -CH<sub>2</sub>CHHNH<sub>2</sub>), 3.21 – 3.01 (m, 2H, -CH<sub>2</sub>CH<sub>2</sub>NH<sub>2</sub>), 2.72 – 2.49 (m, 1H, -CH(CH<sub>2</sub>)<sub>4</sub>), 2.17 – 2.02 (m, 1H, -CpH), 1.94 (dt, *J* = 12.3, 7.6 Hz, 1H, -CpH), 1.89 – 1.60 (m, 5H, -CpH), 1.47 (dt, *J* = 12.4, 8.9 Hz, 1H, -CpH).

<sup>13</sup>C NMR (101 MHz, MeOD) δ: 138.4 (ArC), 130.0 (ArC), 127.3 (ArC), 123.6 (ArC), 120.6 (ArC), 119.0 (ArC), 112.5 (ArC), 107.5 (ArC), 58.4 (CHNH), 43.7 (CHCH), 42.6 (CH<sub>2</sub>NH), 30.4 (CH<sub>2</sub>CH), 29.6 (CH<sub>2</sub>CH), 26.5 (CH<sub>2</sub>CH<sub>2</sub>), 26.0 (CH<sub>2</sub>CH<sub>2</sub>), 19.5 (CH<sub>2</sub>CH<sub>2</sub>NH).



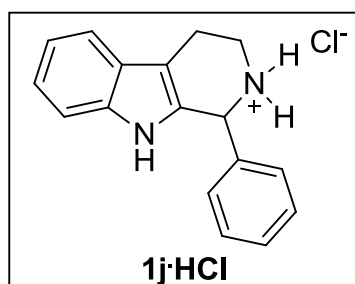
**1 – cyclohexyl - 2,3,4,9 – tetrahydro-1H-pyrido[3,4-b]indol-2-ium chloride (1k·HCl).** Tryptamine hydrochloride (197 mg, 1 mmol) and cyclopentanecarboxaldehyde (121 μL, 1 mmol) were added to aqueous maleic acid buffer (10 mM, pH 2.0,



total volume 2 mL). The suspension was filtered to give **1k**HCl (255 mg, 88% yield). Characterisation data were in good agreement with literature values.[5]

<sup>1</sup>H NMR, 400 MHz, CD<sub>3</sub>OD δ: 7.49 (dt, *J* = 7.9, 0.8, 1H, Ar*H*), 7.39 (dt, *J* = 8.1, 0.8, 1H, Ar*H*), 7.17 (ddd, *J* = 8.2, 8.0, 0.8, 1H, Ar*H*), 7.07 (ddd, *J* = 8.0, 7.2, 1.2, 1H, Ar*H*), 4.66 (m, 1H, CHNH<sub>2</sub>), 3.75 (ddd, *J* = 12.5, 5.4, 3.5, 1H, -CH<sub>2</sub>CHHNH<sub>2</sub>), 3.46 (ddd, *J* = 12.5, 9.7, 5.7, 1H, -CH<sub>2</sub>CHHNH<sub>2</sub>), 3.19-3.01 (m, 2H, -CH<sub>2</sub>CH<sub>2</sub>NH<sub>2</sub>), 2.37-2.25 (m, 1H, -CH(CH<sub>2</sub>)<sub>5</sub>), 2.01-1.74 (m, 4H, -C*xH*), 1.57-1.14 (m, 6H, -C*xH*).

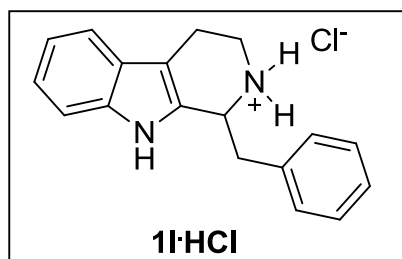
<sup>13</sup>C NMR, 100 MHz, CD<sub>3</sub>OD δ: 138.4 (ArC), 129.0 (ArC), 127.4 (ArC), 123.5 (ArC), 120.6 (ArC), 119.0(ArC), 112.3 (ArC), 108.0 (ArC), 60.0 (CHNH), 43.8 (CH<sub>2</sub>NH), 41.0 (CHCH), 30.8 (CH<sub>2</sub>), 27.8 (CH<sub>2</sub>), 27.5 (CH<sub>2</sub>), 27.1 (CH<sub>2</sub>), 19.4 (CH<sub>2</sub>CH<sub>2</sub>).



**1 – phenyl - 2,3,4,9 - tetrahydro - 1H - pyrido[3,4 - b]indol - 2 - ium chloride (1j)HCl**. Tryptamine hydrochloride (197 mg, 1 mmol) and benzaldehyde (101 μL, 1 mmol) were added to aqueous maleic acid buffer (10 mM, pH 2.0, total volume 2 mL). The suspension was filtered to give **1j**HCl (232 mg, 82%

yield). Characterisation data were in good agreement with literature values.[5]

<sup>1</sup>H NMR, 400 MHz, CD<sub>3</sub>OD δ: 7.58 (d, *J* = 7.8 Hz, 1H, Ar*H*), 7.56 – 7.50 (m, 3H, Ar*H*), 7.49 – 7.43 (m, 2H, Ar*H*), 7.32 (dt, *J* = 8.2, 0.9 Hz, 1H, Ar*H*), 7.21 – 7.15 (m, 1H, Ar*H*), 7.14 – 7.08 (m, 1H, Ar*H*), 5.94 (s, 1H, CHNH<sub>2</sub>), 3.66 (dt, *J* = 12.5, 5.5 Hz, 1H, -CH<sub>2</sub>CHHNH<sub>2</sub>), 3.56 (ddd, *J* = 21.7, 13.6, 9.7 Hz, 1H, -CH<sub>2</sub>CHHNH<sub>2</sub>), 3.32 – 3.12 (m, 2H, -CH<sub>2</sub>CH<sub>2</sub>NH<sub>2</sub>).



**1 - (benzyl) - 2,3,4,9 – tetrahydro-1H-pyrido[3,4- b]indol-2-ium chloride (1l)HCl**. Tryptamine hydrochloride (197 mg, 1 mmol) and phenylacetaldehyde (119 μL, 1 mmol) were added

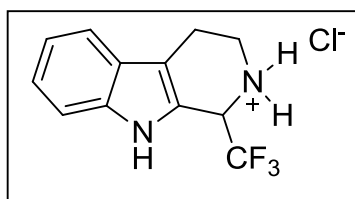
to aqueous maleic acid buffer (10 mM, pH 2.0, total volume 2 mL). The suspension was filtered to give **1l**HCl (238 mg, 80% yield).

Characterisation data were in good agreement with literature values.[5]

<sup>1</sup>H NMR, 400 MHz, CD<sub>3</sub>OD δ: 7.55–7.37 (m, 7H, Ar*H*), 7.21 (ddd, *J* = 8.2, 7.0, 1.1 Hz, 1H, Ar*H*), 7.11 (dd, *J* = 8.1, 7.0, 1.0 Hz, 1H, Ar*H*), 5.08–5.01 (m, 1H, CHNH<sub>2</sub>),

3.78–3.72 (m, 1H,  $-\text{CH}_2\text{CHHNH}_2$ ), 3.60 (ddd,  $J = 12.5, 5.3, 3.6$  Hz, 1H,  $-\text{CH}_2\text{CHHNH}_2$ ), 3.35 (ddd,  $J = 12.6, 9.6, 5.7$  Hz, 1H,  $-\text{CHHCH}_2\text{NH}_2$ ), 3.20–2.99 (3H, m,  $-\text{CHHCH}_2\text{NH}_2$  and  $\text{CH}_2\text{Ph}$ ).

$^{13}\text{C}$  NMR, 100 MHz,  $\text{CD}_3\text{OD}$   $\delta$ : 136.6 (ArC), 135.8 (ArC), 130.0 (ArC), 129.7 (ArC), 127.6 (ArC), 126.2 (ArC), 122.3 (ArC), 119.5 (ArC), 118.5 (ArC), 111.8 (ArC), 106.6 (ArC), 54.1 (CHNH), 41.8 ( $\text{CH}_2\text{NH}$ ), 37.7 ( $\text{CH}_2\text{Ph}$ ), 18.4 ( $\text{CH}_2\text{CH}_2$ ).



**1 - (trifluoromethyl) - 2,3,4,9 - tetrahydro - 1H - pyrido[3,4-b] indol-2-ium chloride (1j·HCl).**

Tryptamine hydrochloride (197 mg, 1 mmol) and trifluoroacetaldehyde (90  $\mu\text{L}$ , 1 mmol) were added to

aqueous maleic acid buffer (10 mM, pH 2.0, total volume 2 mL). The suspension was filtered to give **1j**·HCl (236 mg, 86% yield).

HRMS for  $\text{C}_{12}\text{H}_{12}\text{N}_2\text{F}_3$   $[\text{M}+\text{H}]^+$ :  $m/z$  calcd 241.0947, found 241.0942

UV analysis: 226 nm, 272 nm

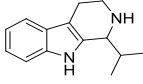
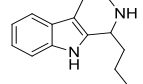
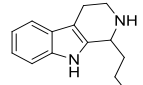
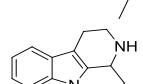
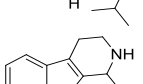
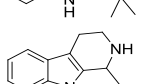
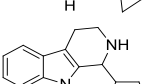
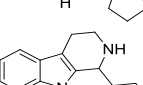
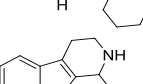
$^1\text{H}$  NMR, 400 MHz,  $\text{CD}_3\text{OD}$   $\delta$ : 7.45 (d,  $J = 7.9$  Hz, 1H, ArH), 7.36 (d,  $J = 8.1$  Hz, 1H, ArH), 7.12 (td,  $J = 7.5, 1.0$  Hz, 1H, ArH), 7.01 (td,  $J = 7.6, 0.9$  Hz, 1H, ArH), 4.56 (q,  $J = 8.0$  Hz, 1H, CHNH<sub>2</sub>), 3.26 – 3.14 (m, 1H,  $-\text{CH}_2\text{CHHNH}_2$ ), 3.09 (dt,  $J = 12.7, 4.9$  Hz, 1H,  $-\text{CH}_2\text{CHHNH}_2$ ), 2.80 – 2.64 (m, 2H,  $-\text{CH}_2\text{CH}_2\text{NH}_2$ ).

$^{13}\text{C}$  NMR, 100 MHz,  $\text{CD}_3\text{OD}$   $\delta$ : 138.2 (ArC), 128.5 (ArC), 127.8 (ArC), 126.1 (ArC), 123.2 (ArC), 120.0 (ArC), 119.1 ( $\text{CF}_3$ ), 112.6 (ArC), 112.3 (ArC), 54.5 (q,  $J = 30.2$  Hz) (CHNH), 41.6 ( $\text{CH}_2\text{NH}$ ), 22.4 ( $\text{CH}_2\text{CH}_2$ ).

**HPLC columns, conditions and retention times**

HPLC analysis was performed on an Agilent 1200 Series using chiral columns. Measurements were carried under isocratic conditions. \*Retention times varied to a small extent. The identity of compounds was confirmed by comparison with independently synthesized samples whenever necessary.

Compound	Column	Eluent	Temp (°C)	Wavelength (nm)	Retention Time* (min)
	Chiralcel IC	Hexane:iPrOH:DEA	25	265	10.8 (R)
	IC	90:10:0.1			9.6 (S)
	Chiralcel IC	Hexane:iPrOH:DEA	25	265	11.4 (R)
	IC	90:10:0.1			9.2 (S)

	Chiralcel IC	Hexane:iPrOH:DEA 90:10:0.1	25	265	8.0 ( <i>R</i> ) 7.2 ( <i>S</i> )
	Chiralcel IC	Hexane:iPrOH:DEA 90:10:0.1	25	265	11.6 ( <i>R</i> ) 8.1 ( <i>S</i> )
	Chiralcel IC	Hexane:iPrOH:DEA 90:10:0.1	25	265	9.8 ( <i>R</i> ) 7.0 ( <i>S</i> )
	Chiralcel IC	Hexane:iPrOH:DEA 90:10:0.1	25	265	7.4 ( <i>R</i> ) 6.1 ( <i>S</i> )
	Chiralcel IC	Hexane:iPrOH:DEA 97:3:0.1	25	265	9.4 ( <i>R</i> ) 10.2 ( <i>S</i> )
	Chiralcel IC	Hexane:iPrOH:DEA 90:10:0.1	25	265	14.8 ( <i>R</i> ) 11.6 ( <i>S</i> )
	Chiralcel IC	Hexane:iPrOH:DEA 90:10:0.1	25	265	13.1 ( <i>R</i> ) 10.4 ( <i>S</i> )
	Chiralcel IC	Hexane:iPrOH:DEA 90:10:0.1	25	265	8.4 ( <i>R</i> ) 7.2 ( <i>S</i> )
	Chiralcel OD-H	Hexane:iPrOH:DEA 90:10:0.1	25	265	17.5 ( <i>R</i> ) 10.1 ( <i>S</i> )

## References

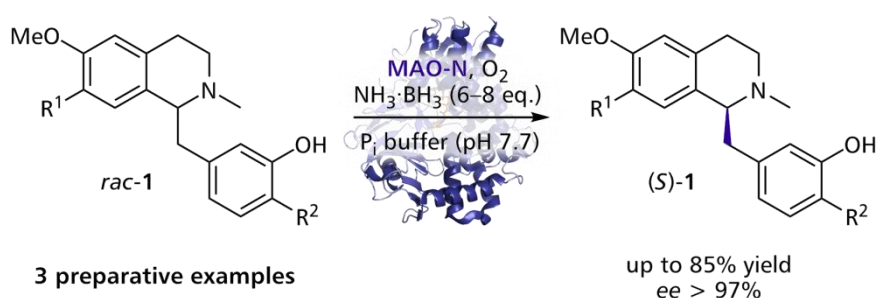
- [1] C. Li, J. Xiao, *J. Am. Chem. Soc.* **2008**, *130*, 13208-13209
- [2] P. Roszkowski, K. Wojtasiewicz, A. Leniewski, J. K. Maurin, T. Lis, Z. Czarnocki, *J. Mol. Cat. A: Chem.* **2005**, *232*, 143-149
- [3] M. Nakagawa, T. Kawate, T. Kakikawa, H. Yamada, T. Matsui, T. Hino, *Tetrahedron* **1993**, *49*, 1739-1748
- [4] M. J. Wanner, R. N. S. van der Haas, K. R. de Cuba, J. H. van Maarseveen, H. Hiemstra *Angew. Chem. Int. Ed.* **2007**, *46*, 7485-7487
- [5] P. Bernhardt, A. R. Usera, S. E. O'Connor, *Tetrahedron Lett.* **2010**, *51*, 4400-4402

# DERACEMISATION OF BENZYLISOQUINOLINE ALKALOIDS EMPLOYING MONOAMINE OXIDASE VARIANTS

---

Manuscript prepared for submission

J. H. Schrittwieser, B. Groenendaal, S. C. Willies, D. Ghislieri,  
I. Rowles, V. Resch, J. H. Sattler, E. M. Fischereeder,  
B. Grischek W. D. Lienhart, N. J. Turner, W. Kroutil\*



Benzylisoquinoline alkaloids represent a class of natural products with diverse pharmacological properties. A chemo-enzymatic deracemisation system was applied which allows to obtain the (*S*)-enantiomer of benzylisoquinolines from the racemate in high yield and excellent optical purity (e.e. >97%) *via* enantioselective oxidation by a monoamine oxidase (MAO) and concomitant reduction by ammonia-borane. For the transformation of these bulky substrates novel variants of MAO possessing a widened active site were required. The applicability of the deracemisation system was demonstrated on preparative scale (150 mg) for three different benzylisoquinoline alkaloids (natural as well as non-natural), including the hypotensive and anti-spasmodic agent (*S*)-reticuline.

In this project D.G. provided the MAO-N D11 mutant, supervised the substrate liquid phase screening and analysed the data

# Deracemisation of Benzyloquinoline Alkaloids Employing Monoamine Oxidase Variants

Joerg H. Schrittwieser,<sup>†</sup> Bas Groenendaal,<sup>‡</sup> Simon C. Willies,<sup>‡</sup> Diego Ghislieri,<sup>‡</sup> Ian Rowles,<sup>‡</sup> Verena Resch,<sup>†</sup> Johann H. Sattler,<sup>†</sup> Eva-Maria Fischereeder,<sup>†</sup> Barbara Grischek,<sup>†</sup> Wolf-Dieter Lienhart,<sup>†</sup> Nicholas J. Turner,<sup>‡</sup> Wolfgang Kroutil<sup>\*,†</sup>

<sup>†</sup> Department of Chemistry, Organic & Bioorganic Chemistry, University of Graz  
Heinrichstrasse 28, 8010 Graz (Austria)

<sup>‡</sup> School of Chemistry, University of Manchester, Manchester Interdisciplinary  
Biocentre, 131 Princess Street, Manchester, M1 7DN (UK)

\* wolfgang.kroutil@uni-graz.at

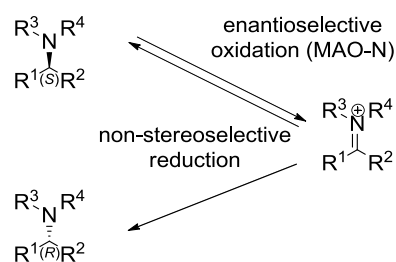
## Abstract

Benzyloquinoline alkaloids are a class of natural products with multifarious pharmacological properties. A chemo-enzymatic deracemisation system was applied to obtain the (*S*)-enantiomer of benzyloquinolines from the racemate in high yield and excellent optical purity (e.e. >97%) *via* enantioselective oxidation by a monoamine oxidase (MAO) and concomitant reduction by ammonia-borane. For the transformation of these bulky substrates, novel variants of MAO featuring a widened active-site pocket and unprecedented (*R*)-enantioselectivity were employed. The applicability of the deracemisation system was demonstrated on preparative scale (150 mg) for three different benzyloquinoline alkaloids (natural as well as non-natural), including the hypotensive and anti-spasmodic agent (*S*)-reticuline.

Benzylisoquinolines are a class of alkaloids produced by higher plants, such as those belonging to the *Papaveraceae* and *Berberidaceae* families.[1] They represent biosynthetic intermediates *en route* to, amongst others, the benzophenanthridine, protopine, and morphinan alkaloids, and as such do usually not accumulate in substantial amounts in the plant tissue.[2] However, benzylisoquinolines show diverse and potent biological effects ranging from sedative, antispasmodic and hypotensive properties to anti-cancer and anti-HIV activity.[3] Many different strategies for the asymmetric synthesis of these natural products have been developed, but a large number of steps and harsh reaction conditions are often required, resulting in limited overall yields and enantiomeric excess.[4] Furthermore, the majority of the established syntheses still rely on chiral auxiliaries in the asymmetric key step,[5] and out of the few catalytic procedures that have been reported, only asymmetric hydrogenation[6] and transfer hydrogenation[7] have proven to be of general use.[8]

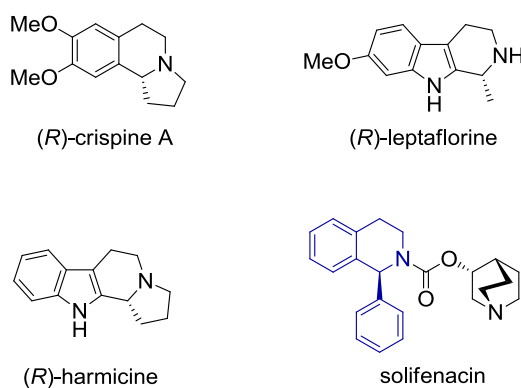
In Nature, benzylisoquinolines are produced in optically pure form by highly stereoselective enzymes.[2] Using these biocatalysts in synthetic organic chemistry can open up novel routes to enantiomerically pure alkaloids, often with favorable yields and enantioselectivities. For instance, the broad applicability of norcoclaurine synthase (NCS) for the preparation of (*S*)-benzyl-isoquinolines by stereoselective Pictet-Spengler cyclisation has recently been demonstrated,[9] and berberine bridge enzyme (BBE) has been used to access (*R*)-benzylisoquinolines *via* oxidative kinetic resolution of the racemate.[10] Herein, we describe deracemisation using engineered variants of monoamine oxidase from *Aspergillus niger* as a novel biocatalytic entry to benzylisoquinolines, which offers high yields and excellent enantioselectivity.

The one-pot combination of enantioselective oxidases with chemical reducing agents has been shown to allow the deracemisation of amino acids, keto acids, alcohols, and amines *via* a “cyclic” oxidation/reduction cascade (Scheme 1).[11]



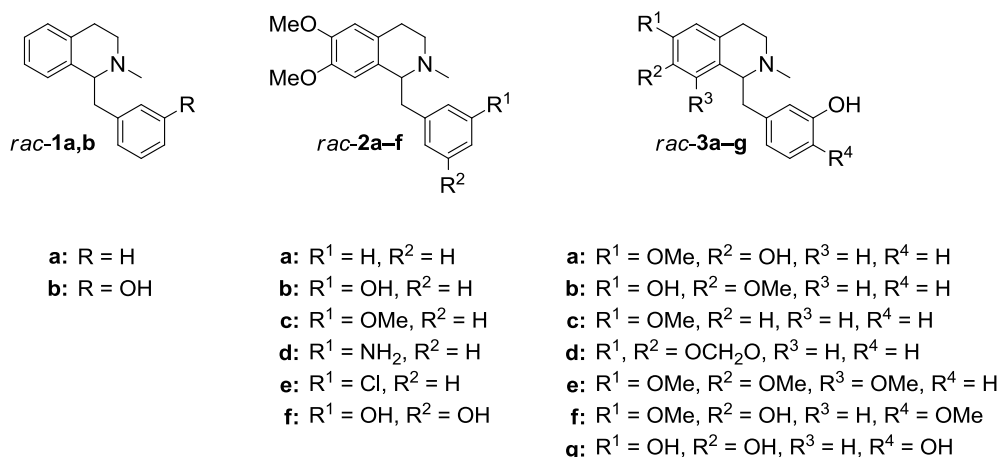
**Scheme 1.** Deracemisation of amines *via* a “cyclic” oxidation/reduction cascade.

Monoamine oxidase from *Aspergillus niger* (MAO-N) has been engineered for the deracemisation of selected amines, and variants optimized for the conversion of  $\alpha$ -chiral primary,[12] secondary,[13] and tertiary [14] amines have been reported. The fifth-generation variant MAO-N D5 has proven suitable for deracemisation of the naturally occurring tetrahydro-isoquinoline alkaloid (*R*)-crispine A (Scheme 2).[15]



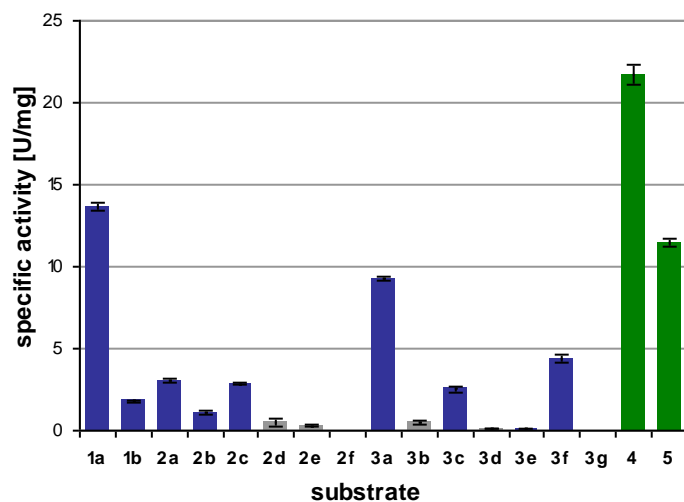
**Scheme 2.** Examples of alkaloids that have been obtained in optically pure form using MAO-catalyzed deracemisation.

Efforts to extend the scope of MAO-N to more bulky substrates have recently led to the development of variants with a more spacious active-site pocket (called D9 and D11), which show increased activity on crispine A,[16] and which have also been used in the chemo-enzymatic asymmetric synthesis of indole alkaloids (*e.g.*, leptaflorin and harmicine) and the acetylcholine receptor antagonist Solifenacin (Scheme 2).[17] Notably, the deracemisation of 1-phenyltetrahydro-isoquinoline with MAO-N D11 (carried out *en route* to Solifenacin) gave the (*S*)-enantiomer in 98% *ee*, representing the first example of (*R*)-enantiopreference observed with MAO-N. This stereochemical switch prompted us to investigate the activity and enantioselectivity of MAO-N variants for benzylisoquinolines, as a structurally related class of alkaloids. Thus, we screened MAO-N D5, D9 and D11 against a panel of 15 racemic 1-benzyl-1,2,3,4-tetrahydroisoquinolines using a previously reported[12a] colorimetric assay on hydrogen peroxide formation. The substrates (Scheme 3) can be classified into three groups according to their substitution pattern: Compounds **1a** and **1b** lack any substituents on the isoquinoline ring, and are thus the sterically least demanding substrates. Compounds **2a–f** share 6,7-dimethoxy substitution on the isoquinoline ring as the common structural feature, but carry different functionalities on the benzyl moiety. Compounds **3a–g** vary in the substitution on both the isoquinoline and the benzyl ring system, although they all have a 3'-hydroxy group.



**Scheme 3.** Substrates used for activity screening of MAO-N variants.

While MAO-N D5 was inactive on all substrates except for the positive controls (*rac*)-crispine A and (*rac*)-1-phenylethylamine (Supporting Figure S1), variant D9 converted five of the tested compounds, although at very low rates (Supporting Figure S2).[18] Variant D11 showed fair activity on eight benzyloquinolines, and the rate of oxidation measured for the smallest substrate, **1a**, even superseded the one for crispine A (Figure 1).



**Figure 1.** Results of substrate screening with MAO-N variant D11. Activity (criterion: mean > 5 standard deviations) was found for substrates **1a**, **1b**, **2a–c**, **3a**, **3c**, and **3f** (blue) as well as the positive controls (*rac*)-1-phenylethylamine **4** and (*rac*)-crispine A **5** (both green). Error ranges represent standard deviations of triplicate experiments.

Encouraged by these results, we went on to investigate the enantioselectivity of MAO-N D11 in benzyloquinoline oxidation. As shown in Table 1, six out of the



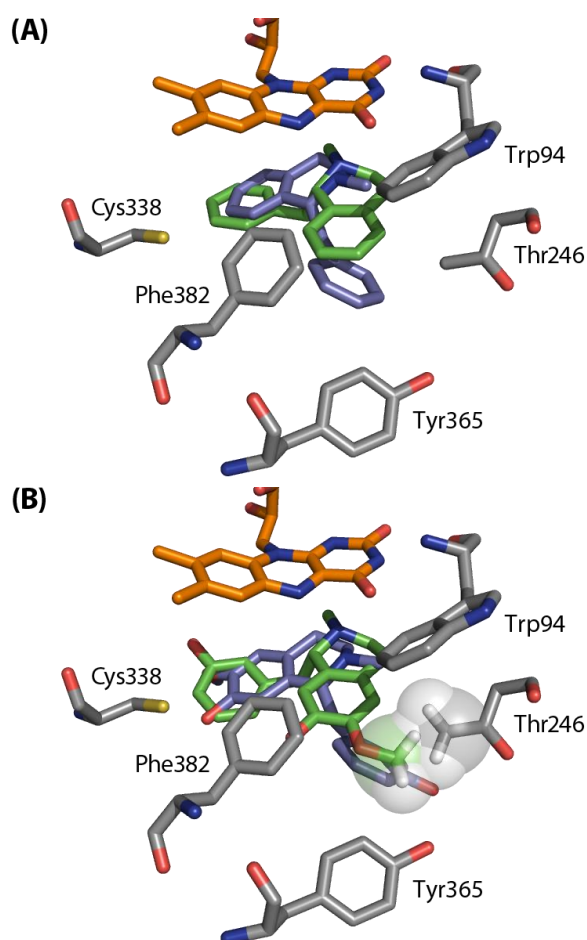
eight accepted substrates were oxidized with very high preference for the (*R*)-enantiomer, while **1a** and **1b** were converted with low selectivity.

substrate	conversion [%]	e.e. [%] <sup>a</sup>	<i>E</i> <sup>b</sup>
<b>1a</b>	39.3 <sup>c</sup>	36 ( <i>S</i> )	4.9
<b>1b</b>	26.2 <sup>d</sup>	24 ( <i>S</i> )	6.5
<b>2a</b>	9.1 <sup>d</sup>	10 ( <i>S</i> )	> 200
<b>2b</b>	1.9 <sup>d</sup>	2 ( <i>S</i> )	> 200
<b>2c</b>	6.1 <sup>d</sup>	7 ( <i>S</i> )	> 200
<b>3a</b>	28.7 <sup>d</sup>	40 ( <i>S</i> )	> 200
<b>3c</b>	15.2 <sup>d</sup>	18 ( <i>S</i> )	> 200
<b>3f</b>	26.0 <sup>d</sup>	35 ( <i>S</i> )	> 200

**Table 1.** Results of whole-cell catalyzed oxidation reactions. <sup>a</sup> Determined by HPLC analysis on a chiral stationary phase. <sup>b</sup> Determined from conversion (*c*) and substrate e.e. (e.e.<sub>s</sub>) according to the equation:  $E = \ln[(1-c) \cdot (1 - \text{e.e.}_s)] / \ln[(1-c) \cdot (1 + \text{e.e.}_s)] \cdot [19]^c$ . <sup>c</sup> Determined by GC analysis. <sup>d</sup> Determined by HPLC analysis using an internal standard. For experimental procedure, see Supporting Information.

To elucidate this dramatic difference in enantioselectivity, docking simulations on the MAO-N D11 variant were carried out with substrates **1a** and **3a** (for details, see Supporting Information).

Consistent with the experimental results, both enantiomers of **1a** were docked in conformations that allow productive interaction with the FAD prosthetic group (*i.e.*, the lone pair of N2 of the isoquinoline ring pointing towards C4a of the flavin, and the hydrogen atom at C1 positioned close to N5 of FAD; see Figure 2, A). In contrast, only the (*R*)-enantiomer of **3a** was successfully docked into the D11 structure, with the substituents on the isoquinoline ring tightly accommodated in a large pocket created by the Trp430Gly mutation (Figure 2, B). When docking of (*S*)-**3a** is forced in a position analogous to (*S*)-**1a**, the 6-methoxy and 7-hydroxy substituents produce steric clashes with the side chains of Thr246 and Phe382, respectively, which seem to prevent (*S*)-**3a** from binding in a productive conformation.

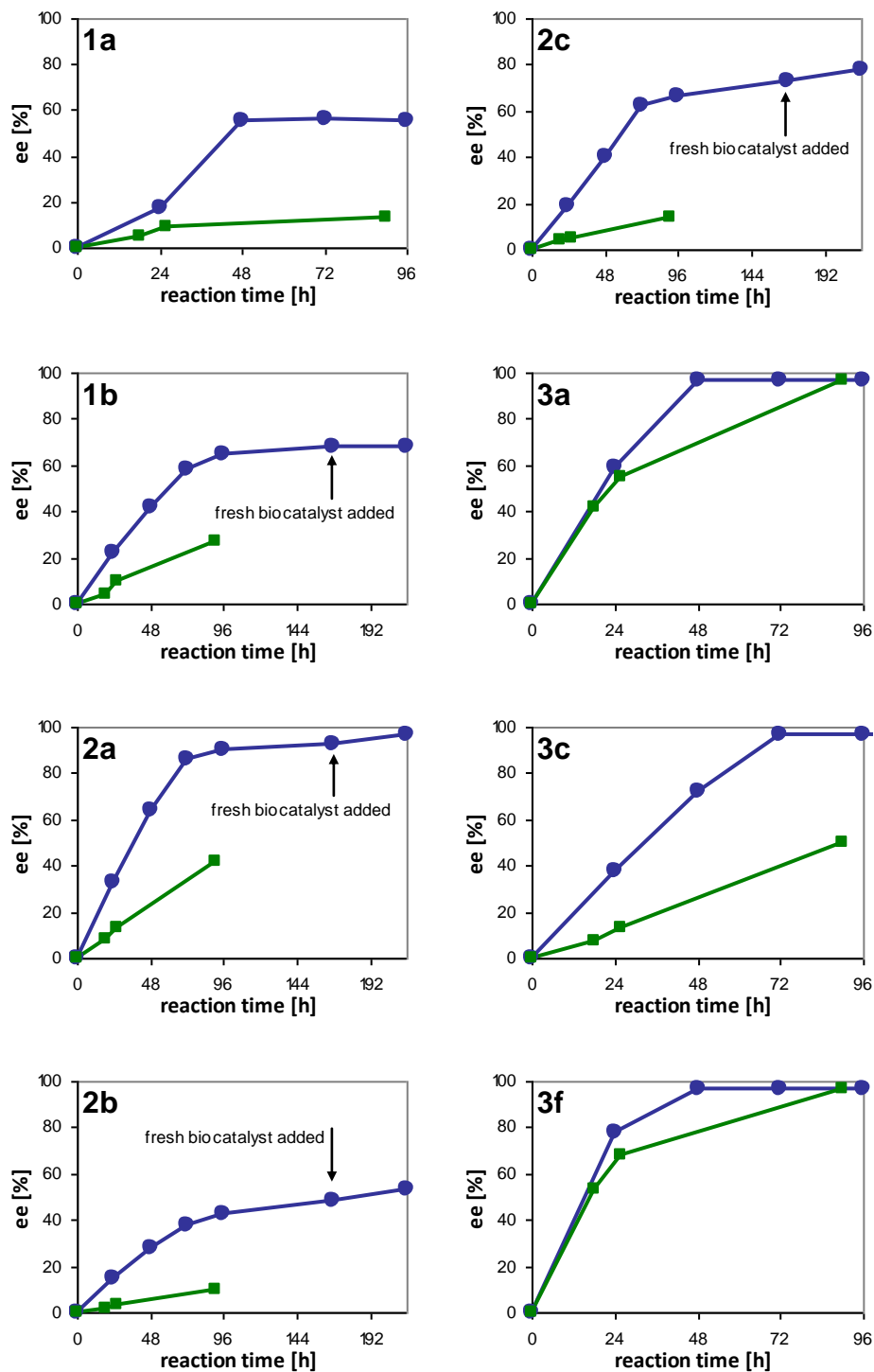


**Figure 2.** Docked structures of (A) (*R*)-**1a** (blue) and (*S*)-**1a** (green), and (B) (*R*)-**3a** (blue) and (*S*)-**3a** (green, forced docking) in the active site of MAO-N D11. Active-site residues are shown in gray and the FAD cofactor is shown in orange. The steric clash between the methoxy group of (*S*)-**3a** and the side chain of Thr246 is illustrated using space-filling models. The images were generated using the PyMol v. 0.99 software.

After collecting information on substrate scope and enantioselectivity of the MAO-N-catalyzed oxidation of benzyloquinolines, we sought to establish the preparative value of this transformation. However, while the high enantioselectivity with six substrates was promising, the conversions attained after 24 h of reaction time seemed rather disappointing. The low expression level of MAO-N (below 0.5 mg of protein per g of wet cell weight) was identified as the main source of this limitation, and hence we decided to test alternative expression hosts and cultivation conditions in order to optimize protein production and thus the specific activity of the cells. The key to success in this regard was the use of *E. coli* C43(DE3) as expression host[20] in combination with cultivation under auto-inducing conditions (for details on the optimization study, see Supporting Information).[21] These modifications resulted in

a more than 3-fold improvement in the specific activity of the whole cell biocatalyst compared to the previously reported expression protocol, along with a ~5-fold increase in cell yield (Supplementary Tables S4 and S5). Furthermore, it was found that lyophilized cells could be used instead of wet cells with no loss of specific activity (corrected for the weight loss caused by the lyophilisation), and we chose to use lyophilized cells prepared by the auto-induction protocol for all further experiments.

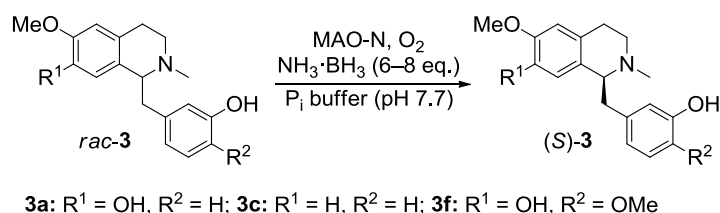
Time studies of deracemisation reactions were carried out for all substrates to evaluate the stability of the biocatalyst under the process conditions (37 °C, 10% v/v DMSO, 40 mM BH<sub>3</sub>-NH<sub>3</sub>; for details see Supporting Information) and also to confirm the enantioselectivity values determined from the oxidation experiments. A first set of experiments using 30 mg/mL cell mass revealed a good long-term performance of the system (as indicated by the linear increase in substrate enantiomeric excess over a period of 90 h; Figure 3), but complete deracemisation was only achieved for two substrates (**3a** and **3f**). The study was therefore repeated employing 100 mg/mL of lyophilized cells. Under these conditions, borane was quickly depleted in the samples where oxidation took place with low enantioselectivity, and had to be supplemented as the reaction proceeded. Using the higher amount of MAO-expressing cells, four substrates (**2a**, **3a**, **3c**, **3f**) could be deracemised to enantiomeric purity (e.e. >97% by HPLC) within 2–9 days. In two cases (**1a**, **1b**) the enantiomeric excess leveled out at a lower value (55% and 68%, respectively), and two substances (**2b**, **2c**) were still turned over too slowly to reach equilibrium within 9 days of reaction time (Figure 3). Enantioselectivity values *E* of 3.4 and 5.3 were determined from the final enantiomeric excess reached in the deracemisation reactions for substrates **1a** and **1b**, respectively.[22] These values are in good agreement with those calculated from the substrate enantiomeric excess and conversion obtained in the oxidation reactions.



**Figure 2.** Time studies of deracemisation reactions employing 30 mg/mL (green squares) or 100 mg/mL (blue circles) lyophilized whole cells. Mind the different time scales for **1a**, **3a**, **3c** and **3f** vs. **1b** and **2a–c**.

Finally, we scaled three deracemisation reactions to a preparative batch size, converting 0.5 mmol (142–165 mg) of the racemic benzyliisoquinoline substrates.[23] The deracemised alkaloids were recovered in high yields and enantiomerically pure

form after column chromatography (Table 2), which clearly demonstrates the synthetic potential of the investigated transformation. In particular, the deracemisation of reticuline **3f**, in combination with the previously reported preparation of the racemate,[10c] establishes an asymmetric total synthesis of this sedative,[3g] hypotensive, [3f] and anti-spasmodic [3e] natural product in 9 linear steps and an overall yield of 13%.



substrate	reaction time	yield	e.e.
	[h]	[%] <sup>a</sup>	[%] <sup>b</sup>
<b>3a</b>	48	77	>97 ( <i>S</i> )
<b>3c</b>	72	85	>97 ( <i>S</i> )
<b>3f</b>	48	80	>97 ( <i>S</i> )

**Table 2.** Results of preparative-scale deracemisation reactions employing MAO-N variant D11 and BH<sub>3</sub>-NH<sub>3</sub>. <sup>a</sup>Isolated yield after column chromatography. <sup>b</sup>Determined by HPLC analysis.

In summary, the scope of chemo-enzymatic deracemisation by a combination of monoamine oxidase from *Aspergillus niger* and ammonia-borane has been extended to (*S*)-benzylisoquinolines, thereby establishing a novel biocatalytic entry to these alkaloids. After the single example of 1-phenyl-1,2,3,4-tetrahydroisoquinoline, the benzylisoquinolines have been identified as an entire class of substrates that are oxidized by MAO-N D11 with (*R*)-enantiopreference. Insights into the structural determinants of enantioselectivity have been gained by relating the results of extensive substrate screening to *in silico* docking simulations. Optimization of the MAO expression level also turned out to be crucial for achieving a satisfactory specific activity of the whole-cell biocatalyst, and thus for enabling reactions on a preparative scale.

#### Acknowledgments:

This study was financed by the Austrian Science Fund (FWF Project P20903-N17

and P22115-N17). The authors would like to thank Dr. Niels van Oosterwijk (University of Groningen) for providing *E. coli* C43(DE3) and Bernd Werner (University of Graz) for acquiring NMR spectra. Financial support by the European Commission (Marie Curie Networks for Initial Training fellowship, project "BIOTRAINS"FP7-PEOPLE-ITN-2008-238531; THEME KBBE-2009-3-3-02, project: AmBioCas, Grant agreement no.: 245144), by the COST Action CM0701 "Cascade Chemoenzymatic Processes – New Synergies Between Chemistry and Biochemistry", by NAWI Graz and by OeFG is gratefully acknowledged.

**Supporting Information Available:** Detailed experimental information, analytical methods, protein expression and purification procedures, <sup>1</sup>H- and <sup>13</sup>C-NMR spectra, MS spectra, HRMS results, and chiral-phase HPLC chromatograms of new compounds. This material is available free of charge via the Internet at <http://pubs.acs.org>.

## References

- [1] (a) Bentley, K. W. *The Isoquinoline Alkaloids*; Harwood Academic Publishers: Amsterdam, 1998. (b) Shamma, M. *The Isoquinoline Alkaloids. Chemistry and Pharmacology*; Academic Press: New York/London, 1972.
- [2] Facchini, P. J. *Annu. Rev. Plant Physiol. Plant Mol. Biol.* **2001**, *52*, 29–66.
- [3] (a) Liu, C.-P.; Tsai, W.-J.; Shen, C.-C.; Lin, Y.-L.; Liao, J.-F.; Chen, C.-F.; Kuo, Y.-C. *Eur. J. Pharmacol.* **2006**, *531*, 270–279. (b) Cui, W.; Iwasa, K.; Tokuda, H.; Kashiwada, A.; Mitani, Y.; Hasegawa, T.; Nishiyama, Y.; Moriyasu, M.; Nishino, H.; Hanaoka, M.; Mukai, C.; Takeda, K. *Phytochemistry* **2006**, *67*, 70–79. (c) Kashiwada, Y.; Aoshima, A.; Ikeshiro, Y.; Chen, Y.-P.; Furukawa, H.; Itoigawa, M.; Fujioka, T.; Mihashi, K.; Cosentino, L. M.; Morris-Natschke, S. L.; Lee, K.-H. *Bioorg. Med. Chem.* **2005**, *13*, 443–448. (d) Liu, J. K.; Couldwell, W. T. *Neurocrit. Care* **2005**, *2*, 124–132. (e) Jow, G.-M.; Wu, Y.-C.; Guh, J.-H.; Teng, C.-M. *Life Sci.* **2004**, *75*, 549–557. (f) Dias, K. L. G.; da Silva Dias, C.; Barbosa-Filho, J. M.; Almeida, R. N.; de Azevedo Correia, N.; Medeiros, I. A. *Planta Med.* **2004**, *70*, 328–333. (g) Morais, L. C. S. L.; Barbosa-Filho, J. M.; Almeida, R. N. *J. Ethnopharmacol.* **1998**, *62*, 57–61. (h) Chuliá, S.; Ivorra, M. D.; Lugnier, C.; Vila, E.; Noguera, M. A.; D'Ocon, P. *Br. J. Pharmacol.* **1994**, *113*, 1377–1385. (i) Martin, M. L.; Diaz, M. T.; Montero, M. J.; Prieto, P.; Roman, L. S.; Cortes, D. *Planta Med.* **1993**, *59*, 63–67.
- [4] Chrzanowska, M.; Rozwadowska, M. D. *Chem. Rev.* **2004**, *104*, 3341–3370.

- [5] For examples, see: (a) Zein, A. L.; Dakhil, O. O.; Dawe, L. N.; Georghiou, P. E. *Tetrahedron Lett.* **2010**, *51*, 177–180. (b) Wang, Y.-C.; Georghiou, P. E. *Org. Lett.* **2002**, *4*, 2675–2678. (c) Watanabe, A.; Kunitomo, J.-I. *Heterocycles* **1998**, *48*, 1623–1630. (d) Yamazaki, N.; Suzuki, H.; Aoyagi, S.; Kibayashi, C. *Tetrahedron Lett.* **1996**, *37*, 6161–6164. (e) Meyers, A. I. *Tetrahedron* **1992**, *48*, 2589–2612.
- [6] Imuro, A.; Yamaji, K.; Kandula, S.; Nagano, T.; Kita, Y.; Mashima, K. *Angew. Chem. Int. Ed.* **2013**, *in press*. (b) Yan, P.-C.; Xie, J.-H.; Hou, G.-H.; Wang, L.-X.; Zhou, Q.-L. *Adv. Synth. Catal.* **2009**, *351*, 3243–3250. (c) Lu, S.-M.; Wang, Y.-Q.; Han, X.-W.; Zhou, Y.-G. *Angew. Chem. Int. Ed.* **2006**, *45*, 2260–2263. (d) Morimoto, T.; Suzuki, N.; Achiwa, K. *Heterocycles* **1996**, *43*, 2557–2560. (e) Kitamura, M.; Hsiao, Y.; Ohta, M.; Tsukamoto, M.; Ohta, T.; Takaya, H.; Noyori, R. *J. Org. Chem.* **1994**, *59*, 297–310. (f) Noyori, R.; Ohta, M.; Hsiao, Y.; Kitamura, M.; Ohta, T.; Takaya, H. *J. Am. Chem. Soc.* **1986**, *108*, 7117–7119.
- [7] Uematsu, N.; Fujii, A.; Hashiguchi, S.; Ikariya, T.; Noyori, R. *J. Am. Chem. Soc.* **1996**, *118*, 4916–4917.
- [8] For recent asymmetric total syntheses of benzylisoquinolines employing asymmetric transfer hydrogenation, see: (a) Pyo, M. K.; Lee, D.-H.; Kim, D.-H.; Lee, J.-H.; Moon, J.-C.; Chang, K. C.; Yun-Choi, H. S. *Bioorg. Med. Chem. Lett.* **2008**, *18*, 4110–4114. (b) Werner, F.; Blank, N.; Opatz, T. *Eur. J. Org. Chem.* **2007**, 3911–3915. (c) Mujahidin, D.; Doye, S. *Eur. J. Org. Chem.* **2005**, 2689–2693. (d) Meuzelaar, G. J.; Van Vliet, M. C. A.; Maat, L.; Sheldon, R. A. *Eur. J. Org. Chem.* **1999**, 2315–2321.
- [9] (a) Pesnot, T.; Gershater, M. C.; Ward, J. M.; Hailes, H. C. *Adv. Synth. Catal.* **2012**, *354*, 2997–3008. (b) Ruff, B. M.; Bräse, S.; O'Connor, S. E. *Tetrahedron Lett.* **2012**, *53*, 1071–1074. (c) Bonamore, A.; Rovardi, I.; Gasparrini, F.; Baiocco, P.; Barba, M.; Molinaro, C.; Botta, B.; Boffi, A.; Macone, A. *Green Chem.* **2010**, *12*, 1623–1627.
- [10] (a) Schrittwieser, J. H.; Resch, V.; Sattler, J. H.; Lienhart, W.-D.; Durchschein, K.; Winkler, A.; Gruber, K.; Macheroux, P.; Kroutil, W. *Angew. Chem. Int. Ed.* **2011**, *50*, 1068–1071. (b) Resch, V.; Schrittwieser, J. H.; Wallner, S.; Macheroux, P.; Kroutil, W. *Adv. Synth. Catal.* **2011**, *353*, 2377–2383. (c) Schrittwieser, J. H.; Resch, V.; Wallner, S.; Lienhart, W.-D.; Sattler, J. H.; Resch, J.; Macheroux, P.; Kroutil, W. *J. Org. Chem.* **2011**, *76*, 6703–6714. (d) Resch, V.; Lechner, H.; Schrittwieser, J. H.; Wallner, S.; Gruber, K.; Macheroux, P.; Kroutil, W. *Chem. Eur. J.* **2012**, *18*, 13173–13179.
- [11] For reviews, see: (a) Turner N. J. *Chem. Rev.* **2011**, *111*, 4073–4087. (b) Schrittwieser, J. H.; Sattler, J.; Resch, V.; Mutti, F. G.; Kroutil, W. *Curr. Opin. Chem. Biol.* **2011**, *15*, 249–256. (c) Turner, N. J. *Curr. Opin. Chem. Biol.* **2010**, *14*, 115–121. (d) Matsuda, T.; Yamanaka, R.; Nakamura, K. *Tetrahedron: Asymm.* **2009**, *20*, 513–557.

- [12] (a) Carr, R.; Alexeeva, M.; Enright, A.; Eve, T. S. C.; Dawson, M. J.; Turner, N. J. *Angew. Chem. Int. Ed.* **2003**, *42*, 4807–4810. (b) Alexeeva, M.; Enright, A.; Dawson, M. J.; Mahmoudian, M.; Turner, N. J. *Angew. Chem. Int. Ed.* **2002**, *41*, 3177–3180.
- [13] Carr, R.; Alexeeva, M.; Dawson, M. J.; Gotor-Fernández, V.; Humphrey, C.; Turner, N. J. *ChemBioChem* **2005**, *6*, 637–639.
- [14] Dunsmore, C. J.; Carr, R.; Fleming, T.; Turner, N. J. *J. Am. Chem. Soc.* **2006**, *128*, 2224–2225.
- [15] Bailey, K. R.; Ellis, A. J.; Reiss, R.; Snape, T. J.; Turner, N. J. *Chem. Commun.* **2007**, 3640–3642.
- [16] Rowles, I.; Malone, K. J.; Etchells, L. L.; Willies, S. C.; Turner, N. J. *ChemCatChem* **2012**, *4*, 1259–1261.
- [17] Ghislieri, D.; Green, A. P.; Pontini, M.; Willies, S. C.; Rowles, I.; Frank, A.; Grogan G.; Turner N. J., *submitted*
- [18] Interestingly, in the samples using **2f** and **3g** as substrates, the decrease in absorbance measured was slower than in the negative controls. Thus, these substances apparently have an anti-oxidative effect and interfere with the colorimetric assay.
- [19] Chen, C.-S.; Fujimoto, Y.; Girdaukas, G.; Sih, C. J. *J. Am. Chem. Soc.* **1982**, *104*, 7294–7299.
- [20] *E. coli* C43(DE3) has been reported to be more suitable for expression of genes with rare codons: (a) Sørensen, H. P.; Sperling-Petersen, H. U.; Mortensen, K. K. *J. Chromatogr. B* **2003**, *786*, 207–214. In addition, the C43(DE3) strain has been found to be advantageous when toxic proteins are to be expressed: (b) Dumon-Seignovert, L.; Cariot, G.; Vuillard, L. *Protein Expression Purif.* **2004**, *37*, 203–206. (c) Miroux, B.; Walker, J. E. *J. Mol. Biol.* **1996**, *260*, 289–298.
- [21] (a) Deacon, S. E.; McPherson, M. J. *ChemBioChem* **2011**, *12*, 593–601. (b) Studier; F. W. *Protein Expression Purif.* **2005**, *41*, 207–234.
- [22] In “cyclic deracemization” systems, the enantioselectivity *E* can be calculated from the final *ee* using the formula  $E = (1 + ee)/(1 - ee)$ . See: Kroutil, W.; Faber, K. *Tetrahedron: Asymm.* **1998**, *9*, 2901–2913.
- [23] *Representative procedure:* In an Erlenmeyer flask (250 mL), lyophilized cells of *E. coli* C43(DE3) [pET16b–MAO-N(D11)] from auto-induction cultures (5.0 g) were resuspended in phosphate buffer (45 mL; 100 mM K-P<sub>i</sub>, pH 7.7). BH<sub>3</sub>-NH<sub>3</sub> (62 mg, 2 mmol) and a solution of substrate **3a** (150 mg, 0.5 mmol) in DMSO (5 mL) were added and the mixture was shaken at 37 °C and 150 rpm. After 24 h, further BH<sub>3</sub>-NH<sub>3</sub> (31 mg, 1 mmol) was added and shaking continued. After 48 h, a sample (250 µL) was taken, extracted with EtOAc and analyzed for substrate *ee*. HPLC analysis indicated complete deracemization, and the reaction mixture was aliquoted



into Falcon tubes (50 mL) and centrifuged (4000 rpm, 45 min, rt) to remove the cell mass. The supernatant was extracted with EtOAc (3 × 20 mL), whereby phase separation was accelerated by centrifugation; the cell pellets were suspended in EtOAc, centrifuged again (4000 rpm, 10 min, rt) and the EtOAc phase was combined with the extracts. The combined organic phases were dried over Na<sub>2</sub>SO<sub>4</sub> and the solvent was evaporated under reduced pressure to give 0.511 g of a yellowish liquid. Column chromatography (silica; CH<sub>2</sub>Cl<sub>2</sub>/MeOH/NH<sub>3</sub>(aq) = 96/3/1) afforded 115 mg (77%) of (*S*)-**3a**, which was spectroscopically identical to the racemic material.

# **Deracemisation of Benzyloisoquinoline Alkaloids Employing Monoamine Oxidase Variants**

Joerg H. Schrittwieser, Bas Groenendaal, Simon C. Willies, Diego Ghislieri, Ian Rowles, Verena Resch, Johann H. Sattler, Eva-Maria Fischereder, Barbara Grischek, Wolf-Dieter Lienhart, Nicholas J. Turner, Wolfgang Kroutil\*

**Supplementary information**

## General Methods

$^1\text{H}$  and  $^{13}\text{C}$  NMR spectra were recorded using a 300 MHz instrument. Chemical shifts are given in parts per million (ppm) relative to TMS ( $\delta = 0$  ppm) and coupling constants ( $J$ ) are reported in Hertz (Hz). Melting points were determined on a Gallenkamp MPD350 apparatus in open capillary tubes and are uncorrected. Thin layer chromatography was carried out on silica gel 60 F<sub>254</sub> plates and compounds were visualized either by spraying with Mo reagent [ $(\text{NH}_4)_6\text{Mo}_7\text{O}_{24} \cdot 4\text{H}_2\text{O}$  (100 gL<sup>-1</sup>),  $\text{Ce}(\text{SO}_4)_2 \cdot 4\text{H}_2\text{O}$  (4 gL<sup>-1</sup>) in  $\text{H}_2\text{SO}_4$  (10%)] or by UV. Unit resolution GC-MS analyses were performed using electron impact (EI) ionisation at 70 eV and quadrupole mass selection. High resolution MS analyses were performed using electron impact (EI) ionisation at 70 eV and TOF mass selection. Optical rotation values  $[\alpha]_{\text{D}}^{20}$  were measured at 589 nm (Na line) on a Perkin-Elmer Polarimeter 341 using a cuvette of 1 dm path length.

Unless otherwise noted, reagents and organic solvents were obtained from commercial sources and used without further purification. Toluene, methanol and acetonitrile used for anhydrous reactions were dried over appropriate molecular sieves (4Å for toluene, 3Å for MeOH and MeCN) for at least 48 hours. THF used for anhydrous reactions was distilled from potassium/benzophenone directly before use. For anhydrous reactions, flasks were oven-dried and flushed with dry argon just before use. Standard syringe techniques were applied to transfer dry solvents and reagents in an inert atmosphere of dry argon.

Catalase (Lot.: 81H7146; from bovine liver), lysozyme from chicken egg white (cat. L6876, from chicken egg white, min. 40,000 U/mg protein), and horseradish peroxidase (cat. P6782, type VI-A, 250–330 U/mg solid) were purchased from *Sigma-Aldrich*. Pyrogallol red (cat. 207540050) was obtained from *Acros*.

### Purification of MAO-N.

Protein purification was performed on an ÄKTA-explorer 900 system (*GE Healthcare*) at 10 °C according to the following protocol: 5 g of cell pellet prepared as described above were resuspended in 25 mL of phosphate buffer A (100 mM K-P<sub>i</sub>, pH 7.7, 300 mM NaCl) containing 1 mg/mL of lysozyme and incubated at 30 °C for 30 min. The suspension was cooled to 4 °C and cells were disrupted by ultrasonication (*MSE Soniprep 150*; 30 s pulse, 30 s pause; 15 cycles). The cell debris was removed by centrifugation (20000 rpm, 40 min), the supernatant was

filtered (0.45  $\mu\text{m}$  syringe microfilter) and loaded onto a HisTrap Ni-sepharose column (1 mL, *GE Healthcare*) pre-equilibrated with buffer A (100 mM K-P<sub>i</sub>, pH 7.7, 300 mM NaCl). Proteins were step-eluted using buffer A (10 mL), buffer A/ buffer B (100 mM K-P<sub>i</sub>, pH 7.7, 300 mM NaCl, 1 M imidazole) = 80/20 (10 mL) and buffer A/buffer B = 65/35 (10–30 mL); collecting 1 mL fractions. The MAO-containing fractions (from the 35% buffer B step) were pooled and concentrated using the *Sartorius* Vivaspin 6 system (30 kDa mass cut-off), the volume was adjusted to 2.5 mL and the protein solution was desalted using a PD-10 column (*GE Healthcare*) and MAO reaction buffer (100 mM K-P<sub>i</sub>, pH 7.7) for elution. The protein solution thus prepared was directly used for the activity assay. Protein concentration was determined using the Pierce BCA protein assay (*Thermo Scientific*) preparing all samples (MAO and BSA standard) in triplicate.

### Substrate Screening of MAO-N Variants

Stock solutions of the test substrates (20 mM; final concentration after dilution 1 mM) in DMSO were prepared. For each colorimetric reaction, the substrate stock solution (5  $\mu\text{L}$ ) was mixed with MAO reaction buffer (20  $\mu\text{L}$ ; 100 mM K-P<sub>i</sub>, pH 7.7), pyrogallol red solution (50  $\mu\text{L}$ ; 0.3 mM in MAO reaction buffer), horseradish peroxidase solution (5  $\mu\text{L}$ ; 1 mg/mL in MAO reaction buffer) and purified MAO-N solution (20  $\mu\text{L}$ ; 0.4–1.1 mg/mL) in a 96-well microtiter plate. In addition, reactions with (*rac*)-1-phenylethanol (1 mM) and (*rac*)-crispine A (1 mM) as well as negative controls (lacking substrate and MAO, respectively) were set up. All reactions, including the blanks, were performed in triplicate. Reactions were followed by measuring the absorbance at 550 nm every minute for a period of 4 h using a *Molecular Devices* SpectraMax M2 plate reader. Slopes were determined by applying a linear fit to the linear range of the absorbance curve using the built-in function of the plate reader's *Molecular Devices* Softmax Pro v5.0 software. Slopes were corrected for spontaneous decolorisation of pyrogallol red (rate obtained from the blank samples) and the specific MAO activity was calculated using formula (1) given below.

$$A = \frac{\Delta OD \cdot Y}{\epsilon \cdot L \cdot c_p} \quad (1)$$

where  $A$  [ $\text{U} \cdot \text{mg}^{-1}$ ] ... MAO activity;  $\Delta OD$  [ $\text{min}^{-1}$ ] ... slope of absorbance decrease;  $Y$  ... dilution factor of MAO solution (5 in this case);  $\epsilon$  [ $\text{L} \cdot \text{mmol}^{-1} \cdot \text{cm}^{-1}$ ] ... extinction coefficient of pyrogallol red (30.9 at 550 nm);  $L$  [cm] ... path length of sample (0.31 in this case);  $c_p$  [ $\text{mg} \cdot \text{mL}^{-1}$ ] ... protein concentration of MAO stock solution.

## **Biotransformations**

### Oxidation of benzyloquinolines catalyzed by MAO-N D11.

In Eppendorf vials (2 mL), frozen cells of *E. coli* BL21(DE3) [pET16b MAO-N (D11)] (50 mg) were thawed and resuspended in reaction buffer (450  $\mu$ L; 100 mM K-P<sub>i</sub>, pH 7.7). Substrate (5  $\mu$ mol, final concentration 10 mM) was dissolved in DMSO (50  $\mu$ L; containing 4 mg/mL 2,3-dimethoxy-9-hydroxyberbine as internal standard) and added to the cell suspension. The reaction mixture was shaken at 37 °C and 150 rpm for 24 h. Samples using **1a**, **2a** and **2c** as substrate were basified by addition of 2 M NaOH solution (100  $\mu$ L). Afterwards, all samples were extracted with EtOAc (2  $\times$  500  $\mu$ L) and dried over Na<sub>2</sub>SO<sub>4</sub>. The solvent was evaporated under a stream of air, the sample was re-dissolved in HPLC-grade methanol (700  $\mu$ L) and conversion as well as substrate e.e. were determined by GC-FID and HPLC analysis.

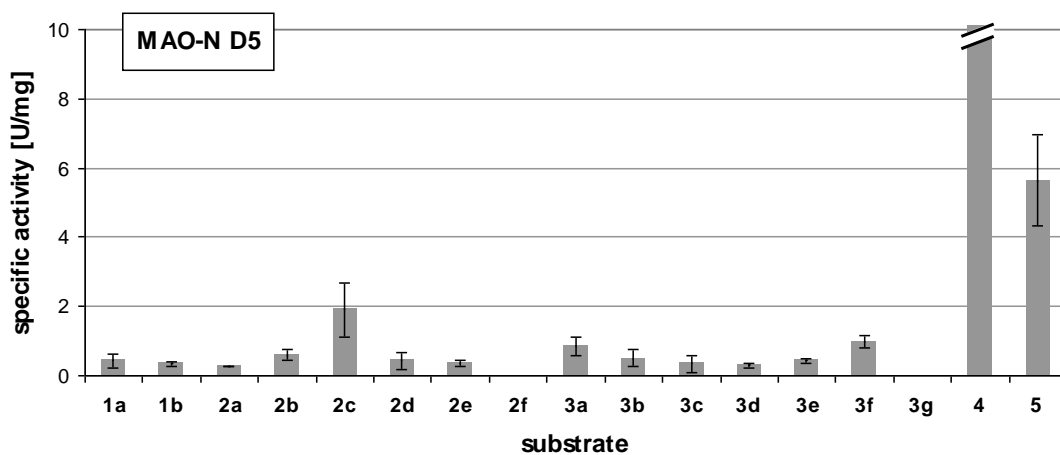
### Deracemisation of benzyloquinolines by MAO-N D11 and BH<sub>3</sub>-NH<sub>3</sub> (time study).

*Using 30 mg/mL lyophilized cells:* In Falcon tubes (15 mL), lyophilized cells of *E. coli* C43(DE3) [pET16b MAO-N (D11)] from auto-induction cultures (75 mg) were resuspended in reaction buffer (2.25 mL; 100 mM K-P<sub>i</sub>, pH 7.7). Borane-ammonia complex (3.1 mg, final concentration 40 mM) and a solution of substrate (25  $\mu$ mol, final concentration 10 mM) in DMSO (250  $\mu$ L) were added to the cell suspension. The reaction mixture was shaken at 37 °C and 150 rpm for 90 h. Samples (500  $\mu$ L) were taken after 18, 26 and 90 h and samples with **1a**, **2a** and **2c** as substrate were basified by addition of 2 M aq. NaOH solution (50  $\mu$ L). Afterwards, all samples were extracted with EtOAc (2  $\times$  500  $\mu$ L) and dried over Na<sub>2</sub>SO<sub>4</sub>. The solvent was evaporated under a stream of air, the sample was re-dissolved in HPLC-grade methanol (700  $\mu$ L) and the substrate *ee* was determined by HPLC analysis.

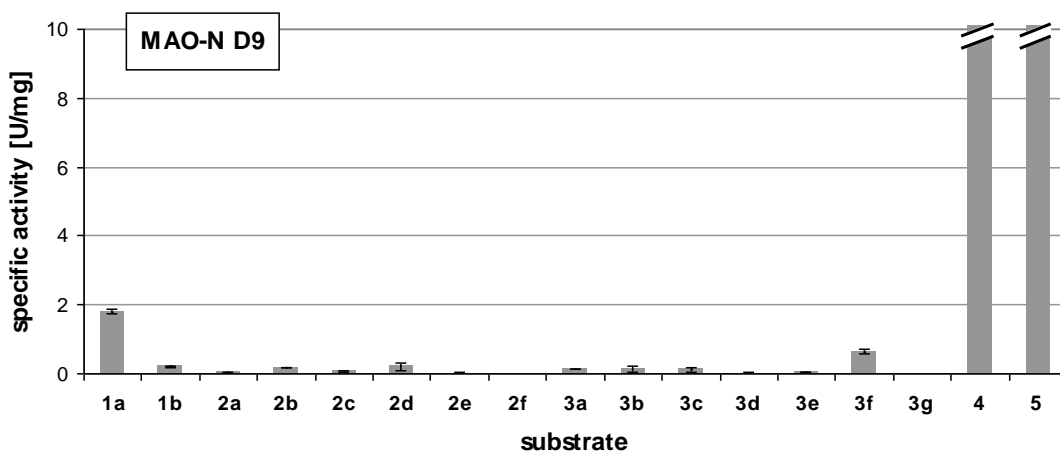
## **Supplementary Data**

### Substrate screening of MAO-N variants

The results obtained with MAO-N variants D5 and D9 in the colorimetric screening employing substrates **1a**, **1b**, **2a–f** and **3a–g** are represented in Figure S1 and Figure S2, respectively.



**Figure S1.** Results of substrate screening with MAO-N variant D5. Activity (criterion: mean > 5 standard deviations) was only found for the positive controls (*rac*)-1-phenylethyl-amine **4** and (*rac*)-crispine A **5**. Error ranges represent standard deviations of triplicate experiments.



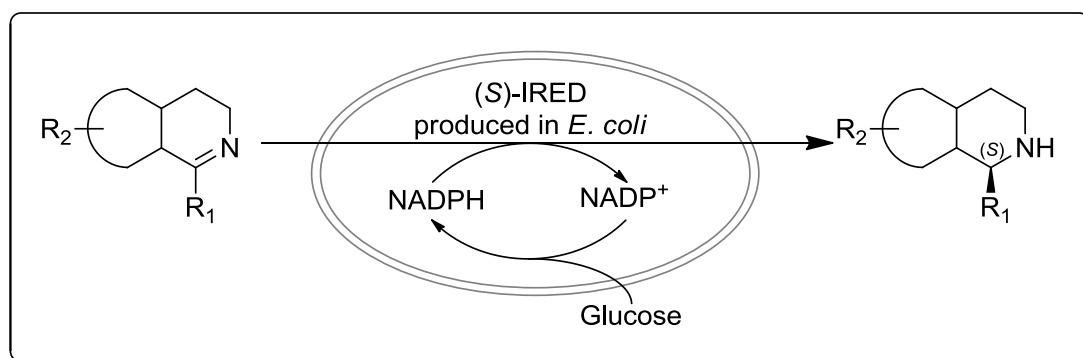
**Figure S2.** Results of substrate screening with MAO-N variant D9. Activity (criterion: mean > 5 standard deviations) was found for substrates **1a**, **1b**, **2b**, **3a**, and **3f** as well as the positive controls (*rac*)-1-phenylethylamine **4** and (*rac*)-crispine A **5**. Error ranges represent standard deviations of triplicate experiments.

# ASYMMETRIC REDUCTION OF CYCLIC IMINES CATALYSED BY A WHOLE CELL BIOCATALYST PRODUCING AN (S)- IMINE REDUCTASE

---

*Angew. Chem. Int. Ed.*, submitted

F. Leipold, D. Ghislieri and N. J. Turner\*



In this study, we show the biocatalytic capability of a whole-cell recombinant *E. coli* system producing an (*S*)-selective imine reductase (IRED) from *Streptomyces* sp. GF3546. This biocatalyst has been used for the enantioselective reduction of a broad range of substrates such as dihydroisoquinolines and dihydro- $\beta$ -carbolines as well as iminium ions.

In this paper D.G. performed the chemical reactions, helped to analyse the data, co-wrote the supplementary information and helped in the writing of the paper.

# Asymmetric reduction of cyclic imines catalyzed by a whole cell biocatalyst expressing an (*S*)-imine reductase

F. Leipold, D. Ghislieri and N. J. Turner\*

School of Chemistry, University of Manchester, Manchester Interdisciplinary Biocentre, 131 Princess Street, Manchester, M1 7DN, United Kingdom

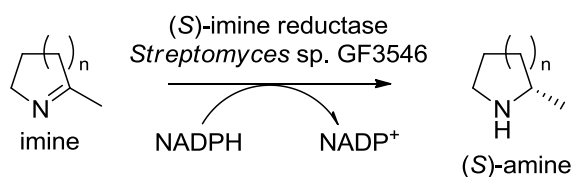
*Nicholas.Turner@manchester.ac.uk*

In view of the importance of chiral amines as building blocks for biologically active pharmaceutical drugs, considerable effort has been devoted to the development of asymmetric catalytic methods for their preparation. Notable advances have been made using both transition metal catalysis and organocatalysis. However, biocatalytic approaches have emerged as being especially important including those based upon transaminases,[1] monoamine oxidases,[2] lipases[3] and recently engineered NADH dependent L-amino acid dehydrogenases[4]. These methods are complementary both in terms of the substrates they use (amine, ketone) and also the amine product that they generate (primary, secondary or tertiary). In some cases these biocatalytic processes have been successfully demonstrated at an industrial scale for the manufacture of recently launched drugs[5]. However, currently there are no general biocatalytic strategies available that are based upon asymmetric reduction of imines as a route to enantiomerically pure amines.

Imine reductases (IREDs) catalyze the reduction of imines to amines utilizing NADH or NADPH as a cofactor (Scheme 1)[6]. IREDs from different *Streptomyces* strains have been shown to reduce 2-methyl-1-pyrroline **1** to the corresponding pyrrolidine **2**[7] and the sequences of two enantiocomplementary imine reductases from *Streptomyces* sp. GF3587 and *Streptomyces* sp. GF3546 have been previously reported[8]. These IREDs have been expressed recombinantly with some initial data reported concerning their properties[8]. The (*R*)-IRED from *Streptomyces* sp. GF3587 was able to convert **1** to **2** (99% e.e.) although it displayed no activity towards related imine substrates[9] whereas the (*S*)-IRED from *Streptomyces* sp. GF3587 showed similarly good activity towards **1** with much lower level activity towards 6-membered ring imines[10]. Other IREDs have also been described, e.g.  $\Delta^1$ -piperidine-2-carboxylate/ $\Delta^1$ -pyrroline-2-carboxylate reductases have been reported in several *Pseudomonas* strains and the enzyme from *P. syringae* has been



expressed recombinantly and was crystallized[11].



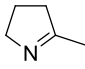
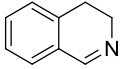
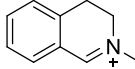
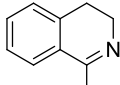
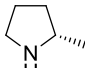
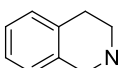
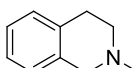
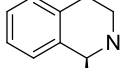
**Scheme 1.** Asymmetric reduction of imines using an imine reductase.

In order to assess more fully the scope for using IREDs in preparative biocatalysis we report here the cloning, over-expression and kinetic characterization of the (*S*)-selective imine reductase, (*S*)-IRED, from *Streptomyces* sp. GF3546. The enzyme has been produced in *E. coli* to yield a whole-cell biocatalyst suitable for preparative biotransformations. Substrate specificity studies reveal that the enzyme is able to reduce both 5- and 6-membered ring imines with high activity and enantioselectivity yielding amines of (*S*)-configuration.

The gene sequence of (*S*)-IRED was initially codon-optimized for expression in *E. coli* (using the OptimumGene<sup>TM</sup> algorithm) with the addition of an N-terminal His<sub>6</sub>-Tag to enable purification by metal ion affinity chromatography. Expression in *E. coli* BL21 (DE3), using a pET-28a (+)-based vector construct containing the (*S*)-IRED gene, yielded active recombinant enzyme suitable for initial activity studies. Biotransformations were carried out using resting *E. coli* cells and glucose was added to regenerate the cofactor. Conversion of 10 mM 2-methyl-pyrroline **1** to 2-methyl-1-pyrrolidine **2** was achieved (82%) after 22h. Subsequently, the (*S*)-IRED was purified to homogeneity by Ni<sup>2+</sup>-affinity chromatography using a HisTrap column (Table S1 & Figure S5) yielding pure protein with a molecular weight of 32 kDa possessing a specific activity of 0.03 U/mg.

The kinetic constants of (*S*)-IRED were determined towards 2-methyl-1-pyrrolidine **1** and a small panel of imines **3** and **7** as well as the iminium ion **5** (Table 1, Figures S6-S9). For the previously reported substrate **1**, the turnover number ( $k_{\text{cat}}$ ) was 0.024 s<sup>-1</sup> with a Michaelis constant  $K_{\text{m}} = 11.82$  mM. Interestingly (*S*)-IRED displayed higher activity and significantly lower  $K_{\text{m}}$  values towards the 6-membered cyclic imines **3**, **5** and **7**. For both the imine **3** and the iminium ion **5** the catalytic efficiency ( $k_{\text{cat}}/K_{\text{m}}$ ) of (*S*)-IRED was >100-fold higher than for 2-methyl-1-pyrroline **1**. Indeed the activity towards **7** is much higher than previously reported[10]. Our data suggest that 6-membered, rather than 5-membered, cyclic imines may represent the natural

substrates for (*S*)-IRED.

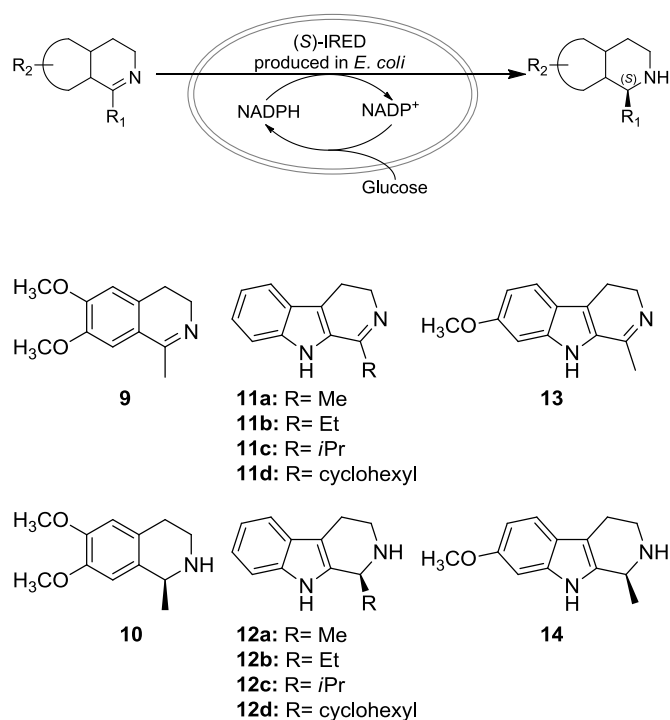
	$K_m$ [mM]	$V_{max}$ [U/mg]	$k_{cat}$ [s <sup>-1</sup> ]	$k_{cat}/K_m$ [s <sup>-1</sup> mM <sup>-1</sup> ]
 <b>1</b>	11.82	0.044	0.024	0.002
 <b>3</b>	0.63	0.807	0.445	0.708
 <b>5</b>	0.68	0.900	0.497	0.734
 <b>7</b>	1.05	0.072	0.040	0.038
 <b>2</b>				
 <b>4</b>				
 <b>6</b>				
 <b>8</b>				

**Table 1.** Kinetic constants determined for (*S*)-imine reductase substrates.

In order to address the challenge of developing a preparative biocatalyst for asymmetric imine reduction, we examined the use of a whole cell system using resting *E. coli* cells expressing (*S*)-IRED, together with the addition of glucose, to enable in situ cofactor recycling. These reactions were carried out at 5 mM substrate concentration and monitored by chiral HPLC to determine both conversion and enantioselectivity of the reduction. Control reactions, in which the *E. coli* cells contained an empty pET-28a (+) plasmid instead of the (*S*)-IRED-containing vector, showed no conversion with any of the substrates. In the light of the high in vitro activity observed for the reduction of 6-membered ring imines (Table 2), we focused on the activity and enantioselectivity of (*S*)-IRED towards substituted dihydroisoquinolines **7** and **9** together with a series of 1-substituted dihydro- $\beta$ -carbolines **11a–d** and **13** (Table 3). The dihydro- $\beta$ -carbolines used in this study were all synthesized according to previously reported methods[12]. In contrast to a recent report,[10] we were able to obtain high levels of conversion using this whole-cell system. All of the substrates tested showed good to excellent conversions after 6h (ranging from 50 to 99%) with excellent levels of enantioselectivity (>98%). Activities towards imines **7** and **9** in vivo were significantly higher than those previously reported in vitro[10] highlighting the advantage of the whole-cell based

approach. To probe the substrate range further we examined a series of dihydro- $\beta$ -carbolines in which both the indole ring and the imine ring were variously substituted. Remarkably, substitutions with bulky aliphatic chains and rings on both the imine (**11a-d**) and the indole ring (**13**) were tolerated with relatively little change in activity. Conversions ranged from 50-99% with e.e. values greater than 98%. In all cases the products obtained (**12a-d** and **14**) were shown to possess (*S*)-configuration by comparison with known standards. (*S*)-configured tetrahydroisoquinolines and tetrahydro- $\beta$ -carbolines are important building blocks for the synthesis of biologically active amines[13, 14].

The data shown in Table 3 may provide insight into the exact role of imine reductases in the synthesis of cyclic secondary and tertiary amines. The biosynthesis of the natural product eleagnine **12a** in pea seedlings from L-tryptophan has been shown to proceed via the imine **11a** which was itself generated *in situ* by internal cyclisation of an amine onto an aldehyde[15]. Conversion of **11a** to **12a** was suggested to be due to a putative imine reductase. In a separate study, it has been shown that the reduction of a series of dihydro- $\beta$ -carbolines can be effected using whole cells of *Saccharomyces bayanus*[16]. This appears to be the only report of an imine reductase activity present in yeast which are well documented to exhibit high ketoreductase and ene reductase activities.



	Conversion (1h)	Conversion (6h)	% e.e. (6h)	Product
<b>3</b>	>99	>99	n/a	<b>4</b>
<b>5</b> <sup>[a]</sup>	60	60	n/a	<b>6</b>
<b>7</b>	99	>99	98	( <i>S</i> )- <b>8</b>
<b>9</b>	48	92	>99	( <i>S</i> )- <b>10</b>
<b>11a</b>	99	>99	>99	( <i>S</i> )- <b>12a</b>
<b>11b</b>	69	>99	>99	( <i>S</i> )- <b>12b</b>
<b>11c</b>	21	69	98	( <i>S</i> )- <b>12c</b>
<b>11d</b>	29	97	>99	( <i>S</i> )- <b>12d</b>
<b>13</b>	29	50	99	( <i>S</i> )- <b>14</b>

**Table 2.** Whole cell biocatalysis with various imine reductase substrates. Conversions after 1 and 6 h as well as enantioselectivities after 6 h are given below. [a] Substrate concentration used for **5** was 2.76 mM

In conclusion we have shown that the (*S*)-imine reductase from *Streptomyces* sp. GF3546 is able to catalyze the highly enantioselective reduction of both 5- and 6-membered imines, including different substituted dihydro- $\beta$ -carboline, highlighting the preference for 6-membered imines as well as the broad substrate scope of this enzyme. In addition, we have demonstrated the enzymatic reduction of an iminium ion for the first time. Reactions using an *E. coli* whole cell biocatalyst supplemented with glucose gave excellent conversions pointing the way towards future applications of these IREDs on a preparative scale. Despite this unexpectedly broad specificity of the wild-type enzyme, there is undoubtedly further scope for engineering these enzymes to enhance their properties.

### Experimental Section

The (*S*)-IRED biocatalyst was produced using *E. coli* BL21 (DE3) bearing a pET-28a (+) plasmid with inserted codon-optimized (*S*)-IRED gene cloned using *Nde*I and *Xho*I restriction sites. Cultivation was carried out in 500 mL LB medium at 37°C and 250 rpm to an OD<sub>600nm</sub> of 0.6-0.8 and recombinant protein expression induced using 0.2 mM IPTG. Cells were harvested after a further cultivation at 20°C and 250 rpm for 18-22 h. Cell disruption was carried out by ultrasonication of a suspension of *E. coli* BL21 (DE3) expressing (*S*)-IRED in sodium phosphate buffer (100 mM, pH 7.0).

(S)-IRED was purified by Ni<sup>2+</sup>-chelating affinity chromatography using a HisTrap column whereby elution was carried out using sodium phosphate buffer (100 mM, pH 7.0) containing 300 mM NaCl and 300 mM imidazole.

Kinetic constants were determined from a liquid-phase spectrophotometric assay by monitoring the decrease of NADPH at 340 nm ( $\epsilon=6.22 \text{ mM}^{-1} \text{ cm}^{-1}$ ) or 370 nm ( $\epsilon=2.216 \text{ mM}^{-1} \text{ cm}^{-1}$ ). Reaction mixtures contained sodium phosphate buffer (100 mM, pH 7.0), NADPH to an absorbance of 0.8-1 at the respective wavelength, 1% (v/v) dimethylsulfoxide and the substrate at the desired concentration. The reaction was started by adding the purified enzyme to the mixture. One unit of (S)-IRED is defined as the amount of protein that oxidizes 1  $\mu\text{mol}$  NADPH per minute.

Biotransformations were carried out at 30°C in sodium phosphate buffer (100 mM, pH 7.0) using resting cells of *E. coli* BL21 (DE3) expressing (S)-IRED at a final OD<sub>600nm</sub> of 30. The reaction mixtures typically contained the 5 mM of the substrate imine, 50 mM of glucose and 2% (v/v) dimethylformamide unless otherwise stated. **1** was used at a final concentration of 10 mM and **5** at 2.76 mM. Samples were typically taken after 0, 1, 3, 6, 18 and 30 h, extracted using dichloromethane and used directly for analysis. Negative control biotransformations were carried out in the same way using cells harboring empty pET-28a (+) vector cultivated and induced like the cells expressing the biocatalyst.

## References

- [1] S. Schätzle, F. Steffen-Munsberg, A. Thontowi, M. Höhne, K. Robins, U. T. Bornscheuer, *Adv. Synth. Catal.* **2011**, 353, 2439-2445.
- [2] a) K. R. Bailey, A. J. Ellis, R. Reiss, T. J. Snape, N. J. Turner, *Chem. Commun.* **2007**, 3640-3642; b) V. Köhler, K. R. Bailey, A. Znabet, J. Raftery, M. Helliwell, N. J. Turner, *Angew. Chem., Int. Ed.* **2010**, 49, 2182-2184.
- [3] F. van Rantwijk, R. A. Sheldon, *Tetrahedron* **2004**, 60, 501-519.
- [4] M. J. Abrahamson, E. Vázquez-Figueroa, N. B. Woodall, J. C. Moore, A. S. Bommarium, *Angew. Chem., Int. Ed.* **2012**, 51, 3969-3972.
- [5] C. K. Savile, J. M. Janey, E. C. Mundorff, J. C. Moore, S. Tam, W. R. Jarvis, J. C. Colbeck, A. Krebber, F. J. Fleitz, J. Brands, P. N. Devine, G. W. Huisman, G. J. Hughes, *Science* **2010**, 329, 305-309.
- [6] M. Taylor, C. Scott, G. Grogan, *Trends Biotechnol.* **2010**, 31, 63-64.
- [7] K. Mitsukura, M. Suzuki, K. Tada, T. Yoshida, T. Nagasawa, *Org. Biomol. Chem.* **2011**, 8, 4533-4535.

- [8] a) T. Nagasawa, T. Yoshida, K. Ishida, H. Yamamoto, N. Kimoto (Daicel Chemical Industries Ltd), EP2330190 (2011); b) T. Nagasawa, T. Yoshida, K. Ishida, H. Yamamoto, N. Kimoto (Daicel Chemical Industries Ltd), EP2330210 (2011).
- [9] K. Mitsukura, M. Suzuki, S. Shinoda, T. Kuramoto, T. Yoshida, T. Nagasawa, *Biosci., Biotechnol., Biochem.* **2011**, 75, 1778-1782.
- [10] K. Mitsukura, T. Kuramoto, T. Yoshida, N. Kimoto, H. Yamamoto, T. Nagasawa, *Appl. Microbiol. Biotechnol.* **2013**, in press.
- [11] M. Goto, H. Muramatsu, H. Mihara, T. Kurihara, N. Esaki, R. Omi, I. Miyahara, K. Hirotsu, *J. Biol. Chem.* **2005**, 280, 40875-40884.
- [12] J. Wu, F. Wang, Y. Ma, X. Cui, L. Cun, J. Zhu, J. Deng, B. Yu, *Chem. Commun.* **2006**, 1766-1768.
- [13] T.O. Idowu, E.O. Iwalewa, M.A. Aderogba, B.A. Akinpelu, A.O. Ogundaini, *J. Biol. Sci.* **2006**, 6, 1029-1034
- [14] J. C. Callaway, *Journal of Psychoactive Drugs* **2005**, 37, 151-155
- [15] R. B. Herbert & J. Mann, *J. Chem. Soc., Perkin Trans.* **1982**, 1, 1523-1525.
- [16] M. Espinoza-Moraga, T. Petta, M. Vasquez-Vasquez, V. F. Laurie, L. A. B. Moraes, L. S. Santos, *Tetrahedron: Asymm.* **2010**, 21, 1988-1992.

**Asymmetric reduction of cyclic  
imines catalyzed by a whole cell  
biocatalyst expressing an (*S*)-imine  
reductase**

F. Leipold, D. Ghislieri and N. J. Turner\*

**Supplementary information**

## General Experimental Information and Materials

### Chemicals

All chemicals were of highest purity and purchased from Sigma-Aldrich (Poole, Dorset, UK), Melford Laboratories (Ipswich, Suffolk, UK), Alfa Aesar (Karlsruhe, Germany) and Acros Organics (Geel, Belgium) unless stated otherwise. HPLC solvents were obtained from Sigma-Aldrich (Poole, Dorset, UK) or ROMIL (Waterbeach, Cambridge, UK) and GC gases from BOC gases (Guildford, UK). 2-methyl-1-pyrroline (**1**), harmaline (**13**) and 3,4-dihydroisoquinoline (**3**) were purchased from Sigma-Aldrich (Poole, Dorset, UK). 2-Methylpyrrolidine (**2**), 1-Methyl-3,4-dihydroisoquinoline hydrochloride (**7**), 1-methyl-6,7-dimethoxy-3,4-dihydroisoquinoline (**9**) and 6,7-dimethoxy-1-methyl-1,2,3,4-tetrahydroisoquinoline hydrochloride (**10**) were sourced from Acros Organics (Geel, Belgium). 1-Methyl-1,2,3,4-tetrahydroisoquinoline (**8**) was obtained from GlaxoSmithKline (Stevenage, UK).

### General analysis and purification procedures

Solvents were of HPLC grade and were purchased dried over molecular sieves where necessary. Column chromatography was performed on silica gel (Fluka (Buchs, Switzerland), 220-440 mesh).  $^1\text{H}$  and  $^{13}\text{C}$  NMR spectra were recorded on a Bruker Avance 400 instrument (400 MHz for  $^1\text{H}$  and 100 MHz for  $^{13}\text{C}$ ) in  $\text{CDCl}_3$  or  $\text{CD}_3\text{OD}$  without additional standard using residual protic solvent as an internal standard. Chemical shifts ( $\delta$ ) are reported in parts per million (ppm) relative to the residual protic solvent signal ( $\text{CHCl}_3$  in  $\text{CDCl}_3$ ,  $^1\text{H} = 7.26$ ;  $\text{CDCl}_3$ ,  $^{13}\text{C} = 77.0$ ;  $\text{CHD}_2\text{OD}$  in  $\text{CD}_3\text{OD}$ ,  $^1\text{H} = 3.31$ ;  $\text{CD}_3\text{OD}$ ,  $^{13}\text{C} = 49.0$ ). Chiral normal phase HPLC was performed on an Agilent system (Santa Clara, CA, USA) equipped with a G1379A degasser, G1312A binary pump, a G1367A well plate autosampler unit, a G1316A temperature controlled column compartment and a G1315C diode array detector. CHIRALPAK<sup>®</sup>IC Analytical (Daicel (Osaka, Japan), 250 mm length, 4.6 mm diameter, 5  $\mu\text{m}$  particle size) and CHIRALCEL<sup>®</sup>OD-H Analytical (Daicel (Osaka, Japan), 250 mm length, 4.6 mm diameter, 5  $\mu\text{m}$  particle size) columns were used. The typical injection volume was 10  $\mu\text{l}$  and chromatograms were monitored at 265 nm. All solvent mixtures are given in (v/v) ratios.

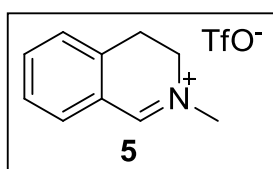
GC analysis was performed on a Agilent 6850 GC (Agilent, Santa Clara, CA, USA)



with a flame ionization detector (FID) equipped with a Gerstel multipurpose autosampler MPS2L and a 30 m Carbowax Amine column with 0.320 mm inner diameter and 0.25  $\mu\text{m}$  film thickness (Agilent, Santa Clara, CA, USA).

### Synthesis of imines and racemic amines

#### Preparation of 2-methyl-3,4-dihydroisoquinolin-2-ium triflate (5)

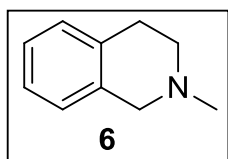


To a solution of 3,4-dihydroisoquinoline (158 mg, 1.20 mmol) in  $\text{CH}_2\text{Cl}_2$  (2 mL), methyl triflate (143  $\mu\text{L}$ , 1.26 mmol) was added and the solution stirred at room temperature for 1.5 hours. After removal of the solvent, pentane (5 mL) was added. The solid was filtrated, washed with pentane (2 mL) and dried to give **5** (306 mg, 86% yield) as a pale yellow solid. Experimental value match the literature data.[6]

$^1\text{H}$  NMR ( $\text{CD}_3\text{OD}$ )  $\delta$ : 9.08 (s, 1H,  $-\text{CHN}$ ), 7.86-7.78 (m, 2H,  $\text{ArH}$ ), 7.60-7.49 (m, 2H,  $\text{ArH}$ ), 4.11 (t,  $J = 8.1$  Hz, 2H,  $-\text{CH}_2\text{CH}_2\text{N}$ ), 3.83 (s, 3H,  $-\text{CH}_3$ ), 3.33 (t,  $J = 8.1$  Hz, 2H,  $-\text{CH}_2\text{CH}_2\text{N}$ ).

$^{13}\text{C}$  NMR ( $\text{CD}_3\text{OD}$ )  $\delta$ : 168.6 ( $\text{CHN}$ ), 139.2 ( $-\text{CF}_3$ ), 137.6 ( $\text{ArC}$ ), 134.7 ( $\text{ArC}$ ), 129.5 ( $\text{ArC}$ ), 126.1 ( $\text{ArC}$ ), 123.4 ( $\text{ArC}$ ), 120.3 ( $\text{ArC}$ ), 51.2 ( $\text{CH}_3$ ), 48.1 ( $\text{CH}_2\text{CH}_2\text{N}$ ), 25.9 ( $\text{CH}_2\text{CH}_2\text{N}$ ).

#### Preparation of standard sample of 2-methyl-1,2,3,4-tetrahydroisoquinoline (6)



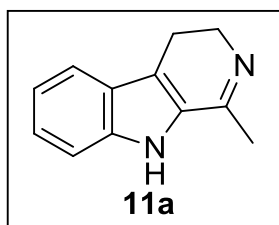
To a solution of iminium ion **5** (100 mg, 0.34 mmol) in MeOH (5 mL) was added  $\text{NaBH}_4$  (13 mg, 0.34 mmol) at  $0^\circ\text{C}$  under nitrogen atmosphere. The solution was stirred for 1 hour at room temperature. Water (20 mL) and  $\text{CH}_2\text{Cl}_2$  (25 mL) were added, the two phases separated and the aqueous phase extracted with  $\text{CH}_2\text{Cl}_2$  (25 mL). The combined organic phases were dried over  $\text{MgSO}_4$  and concentrated under vacuum to give **6** (47 mg, 95% yield) as a white solid. Experimental value match the literature data.[1]

$^1\text{H}$  NMR, 400 MHz,  $\text{CDCl}_3$   $\delta$ : 7.21-7.01 (m, 4H,  $\text{ArH}$ ), 3.63 (s, 2H,  $-\text{CH}_2\text{N}$ ), 2.96 (t,  $J = 6.0$  Hz, 2H,  $-\text{CH}_2\text{CH}_2\text{N}$ ), 2.73 (t,  $J = 6.0$  Hz, 2H,  $-\text{CH}_2\text{CH}_2\text{N}$ ), 2.49 (s, 3H,  $-\text{CH}_3$ ).

$^{13}\text{C}$  NMR, 100 MHz,  $\text{CDCl}_3$   $\delta$ : 134.5, 133.7, 128.7, 126.4, 126.0, 125.6, 57.9, 52.9, 46.0, 29.1 ( $\text{CH}_2\text{CH}_2\text{N}$ ).

### General procedure for the preparation of imines **11a-d**.<sup>[2]</sup>

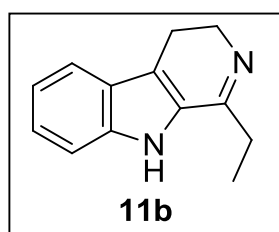
To a stirred and cooled (0 °C) solution of tryptamine (1.0 g, 6.24 mmol) in CH<sub>2</sub>Cl<sub>2</sub> (20 mL) and triethylamine (2 mL) a solution of the required acyl chloride (6.86 mmol) was added. The resulting mixture was stirred at room temperature for 1 hour, washed with water and dried over MgSO<sub>4</sub>. The solvents were removed under vacuum and the resulting amide was reacted directly without purification with POCl<sub>3</sub> (1.75 mL, 18.7 mmol) in a 9:1 mixture of toluene/acetonitrile (20 mL). The reaction mixture was allowed to reflux for 4 hours and subsequently cooled and poured onto ice. The resulting solution was adjusted to pH 10 with aqueous 40% NaOH and MeOH (5 mL) was added. The resulting mixture was filtered and the filtrate was extracted twice with toluene (2 x 100 mL), dried over MgSO<sub>4</sub> and concentrated under vacuum. Purification on silica gel afforded the desired product.



**1-Methyl-4,9-dihydro-3H-β-carboline (11a):** Purification on silica gel (Diethyl ether) afforded **11a** (1.0 g, 87% yield) as yellowish solid. Experimental value match the literature data.<sup>[2]</sup>

<sup>1</sup>H NMR, 400 MHz, CDCl<sub>3</sub> δ: 8.21 (bs, 1H, ArNH), 7.60 (d, *J* = 8.1 Hz, 1H, ArH), 7.40 (d, *J* = 8.2 Hz, 1H, ArH), 7.28 (t, *J* = 7.5 Hz, 1H, ArH), 7.16 (t, *J* = 7.5 Hz, 1H, ArH), 3.87 (t, *J* = 8.4 Hz, 2H, -CH<sub>2</sub>CH<sub>2</sub>N), 2.87 (t, *J* = 8.8 Hz, 2H, -CH<sub>2</sub>CH<sub>2</sub>N), 2.37 (s, 3H, -CH<sub>3</sub>).

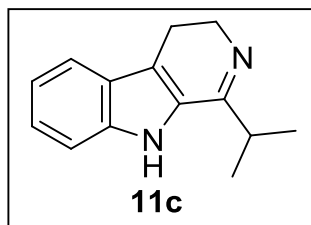
<sup>13</sup>C NMR, 100 MHz, CDCl<sub>3</sub> δ: 158.1 (CN), 136.8 (ArC), 129.1 (ArC), 125.5 (ArC), 124.5 (ArC), 120.3 (ArC), 120.1 (ArC), 116.6 (ArC), 112.1 (ArC), 48.1 (CH<sub>2</sub>CH<sub>2</sub>N), 22.0 (CH<sub>3</sub>), 19.4 (CH<sub>2</sub>CH<sub>2</sub>N).



**1-Ethyl-4,9-dihydro-3H-β-carboline (11b):** Purification on silica gel (Diethyl ether) afforded **11b** (694 mg, 78% yield) as pale yellow solid. Experimental value match the literature data.<sup>[2]</sup>

<sup>1</sup>H NMR, 400 MHz, CDCl<sub>3</sub> δ: 8.96 (bs, 1H, ArNH), 7.53 (d, *J* = 8.0 Hz, 1H, ArH), 7.34 (d, *J* = 8.2 Hz, 1H, ArH), 7.20 (t, *J* = 7.5 Hz, 1H, ArH), 7.08 (t, *J* = 7.5 Hz, 1H, ArH), 3.81 (t, *J* = 8.4 Hz, 2H, -CH<sub>2</sub>CH<sub>2</sub>N), 2.81 (t, *J* = 8.6 Hz, 2H, -CH<sub>2</sub>CH<sub>2</sub>N), 2.67 (q, *J* = 7.2 Hz, 2H, -CH<sub>2</sub>CH<sub>3</sub>), 1.21 (t, *J* = 7.3 Hz, 3H, -CH<sub>2</sub>CH<sub>3</sub>).

$^{13}\text{C}$  NMR, 100 MHz,  $\text{CDCl}_3$   $\delta$ : 162.4 (-CN), 136.9 (ArC), 128.5 (ArC), 125.5 (ArC), 124.7 (ArC), 120.4 (ArC), 120.1 (ArC), 117.2 (ArC), 112.1 (ArC), 47.8 ( $\text{CH}_2\text{CH}_2\text{N}$ ), 28.3 ( $\text{CH}_2\text{CH}_3$ ), 19.4 ( $\text{CH}_2\text{CH}_2\text{N}$ ), 11.0 ( $\text{CH}_3$ ).

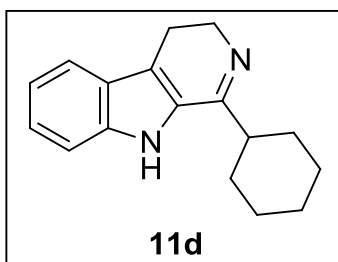


**1 – Isopropyl - 4,9 – dihydro - 3H- $\beta$  - carboline (11c):**

Purification on silica gel (Diethyl ether) afforded **11c** (996 mg, 76% yield) as off-white solid. Experimental value match the literature data.[2]

$^1\text{H}$  NMR, 400 MHz,  $\text{CDCl}_3$   $\delta$ : 8.29 (bs, 1H, ArNH), 7.60 (d,  $J = 8.0$  Hz, 1H, ArH), 7.40 (dt,  $J = 8.3, 0.8$  Hz, 1H, ArH), 7.28 (ddd,  $J = 8.0, 6.8, 0.8$  Hz, 1H, ArH), 7.15 (ddd,  $J = 8.0, 7.1, 1.0$  Hz, 1H, ArH), 3.91-3.84 (m, 2H- $\text{CH}_2\text{CH}_2\text{N}$ ), 3.0 (sept,  $J = 6.8$ , 1H,  $-\text{CH}(\text{CH}_3)_2$ ), 2.88-2.80 (m, 2H,  $-\text{CH}_2\text{CH}_2\text{N}$ ), 1.29 (d,  $J = 6.8$  Hz, 3H,  $-\text{CH}(\text{CH}_3)_2$ ).

$^{13}\text{C}$  NMR, 100 MHz,  $\text{CDCl}_3$   $\delta$ : 165.5(-CN), 136.7 (ArC), 128.2 (ArC), 125.6 (ArC), 124.5 (ArC), 120.3 (ArC), 120.0 (ArC), 117.4 (ArC), 112.0 (ArC), 48.0 ( $\text{CH}_2\text{CH}_2\text{N}$ ), 33.2 ( $\text{CH}(\text{CH}_3)_2$ ), 20.4 ( $\text{CH}(\text{CH}_3)_2$ ), 19.4 ( $\text{CH}_2\text{CH}_2\text{N}$ ).



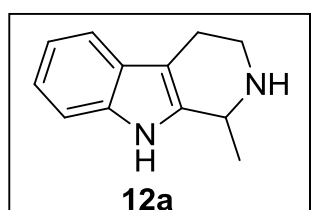
**1 – Cyclohexyl - 4,9 – dihydro - 3H- $\beta$ -carboline (11d):**

Purification on silica gel (Diethyl ether) afforded **11d** (1.33 g, 85% yield) as yellowish solid. Experimental value match the literature data.[2]

$^1\text{H}$  NMR, 400 MHz,  $\text{CDCl}_3$   $\delta$ : 9.46 (bs, 1H), 7.64 (d,  $J = 8.0$  Hz, 1H), 7.44 (d,  $J = 8.2$  Hz, 1H), 7.30 (ddd,  $J = 8.2, 7.0, 1.1$  Hz, 1H), 7.18 (m, 1H), 3.94 (t,  $J = 8.1$  Hz, 2H), 2.90 (t,  $J = 8.3$  Hz, 2H), 2.82 (tt,  $J = 7.8, 2.9$ , 1H), 2.09-2.00 (m, 2H), 1.94-1.83 (m, 2H), 1.80-1.71 (m, 1H), 1.63 (qd,  $J = 12.3, 3.0$  Hz, 2H), 1.48-1.20 (m, 3H).

$^{13}\text{C}$  NMR, 100 MHz,  $\text{CDCl}_3$   $\delta$ : 165.3(-CN), 136.8 (ArC), 128.6 (ArC), 125.6 (ArC), 124.4 (ArC), 120.2 (ArC), 119.9 (ArC), 117.1 (ArC), 112.0 (ArC), 48.1( $\text{CH}_2\text{CH}_2\text{N}$ ), 43.5 ( $-\text{CH}-$ ), 30.9 ( $-\text{CH}_2-$ ), 26.5 ( $-\text{CH}_2-$ ), 26.1 ( $-\text{CH}_2-$ ), 19.5 ( $\text{CH}_2\text{CH}_2\text{N}$ ).

**Preparation of the standard substance 1-methyl-2,3,4,9-tetrahydro-1H-pyrido[3,4-*b*]indole (12a) [3]**



To a solution of **11a** (100 mg, 0.54 mmol) in MeOH (5 mL),  $\text{NaBH}_4$  (20 mg, 0.54 mmol) was added at  $0^\circ\text{C}$  under

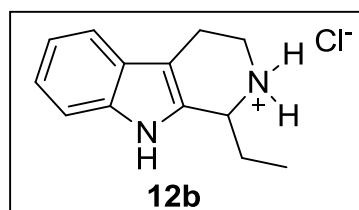
nitrogen atmosphere. The solution was stirred for 1 hour at room temperature. Water (20 mL) and CH<sub>2</sub>Cl<sub>2</sub> (25 mL) were added, the two phases separated and the aqueous phase extracted with CH<sub>2</sub>Cl<sub>2</sub> (25 mL). The combined organic phases were dried over MgSO<sub>4</sub> and concentrated under vacuum to give **12a** (93 mg, 93% yield) as a pale yellow solid.

<sup>1</sup>H NMR, 400 MHz, CDCl<sub>3</sub> δ: 8.24 (bs, 1H, NH), 7.50 (d, *J* = 7.3 Hz, 1H, ArH), 7.29 (d, *J* = 8.3 Hz, 1H, ArH), 7.21-7.06 (m, 2H, ArH), 4.17 (q, *J* = 6.5 Hz, 1H, -CHCH<sub>3</sub>), 3.37 (dt, *J* = 13.2, 4.5 Hz 1H, -CH<sub>2</sub>CHHN), 3.05 (ddd, *J* = 14.0, 8.8, 5.2, 1H, -CH<sub>2</sub>CHHN), 2.83-2.66 (m, 2H, -CH<sub>2</sub>CH<sub>2</sub>N), 1.45 (d, *J* = 6.7 Hz, 3H, -CHCH<sub>3</sub>).

<sup>13</sup>C NMR, 100 MHz, CDCl<sub>3</sub> δ: 137.0 (ArC), 135.6 (ArC), 127.5 (ArC), 121.6 (ArC), 119.4 (ArC), 118.1 (ArC), 110.8 (ArC), 108.5 (ArC), 48.2 (CHCH<sub>3</sub>), 42.8 (-CH<sub>2</sub>CH<sub>2</sub>N), 22.7 (-CH<sub>3</sub>), 20.7 (-CH<sub>2</sub>CH<sub>2</sub>N).

#### General procedure for the preparation of standard substances of chloride salts **12 b-d**.<sup>[4]</sup>

In an Eppendorf tube, tryptamine hydrochloride (0.5 M) and the required aldehyde (0.5 M) were added to aqueous maleic acid buffer (10 mM, pH 2.0, total volume 2 mL) and the solution was stirred overnight at 60°C. Either during the reaction or upon standing, the tetrahydro-β-carboline hydrochloride salts precipitated and could be filtered and washed with water (5 mL) to afford analytically pure products.

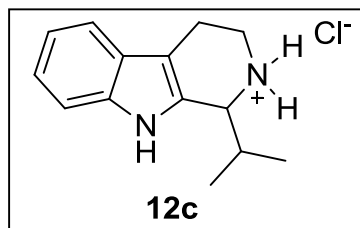


#### **1-Ethyl-2,3,4,9-tetrahydro-1H-pyrido[3,4-b]indol-2-ium chloride (12b)**

Experimental value match the literature data.<sup>[4]</sup>

<sup>1</sup>H NMR, 400 MHz, CD<sub>3</sub>OD δ: 7.50 (dt, *J* = 8.0, 0.8, 1H, ArH), 7.38 (dt, *J* = 8.2, 0.8, 1H, ArH), 7.17 (ddd, *J* = 8.2, 7.1, 1.1, 1H, ArH), 7.07 (ddd, *J* = 8.0, 7.1, 1.0, 1H, ArH), 4.66 (m, 1H, -CHNH<sub>2</sub>), 3.76 (ddd, *J* = 12.5, 5.4, 3.9, 1H, -CH<sub>2</sub>CHHNH<sub>2</sub>), 3.46 (ddd, *J* = 12.6, 9.3, 5.8, 1H, -CH<sub>2</sub>CHHNH<sub>2</sub>), 3.19-3.02 (m, 2H, -CH<sub>2</sub>CH<sub>2</sub>NH<sub>2</sub>), 2.35 (dq, *J* = 15.2, 7.6, 4.3, 1H, -CHHCH<sub>3</sub>), 2.01 (dq, *J* = 15.2, 8.8, 7.2, 1H, -CHHCH<sub>3</sub>), 1.21 (t, *J* = 7.5, 3H, -CH<sub>2</sub>CH<sub>3</sub>).

<sup>13</sup>C NMR, 100 MHz, CD<sub>3</sub>OD δ: 138.4 (ArC), 130.1 (ArC), 127.4 (ArC), 123.5 (ArC), 120.6 (ArC), 119.1 (ArC), 112.4 (ArC), 107.3 (ArC), 56.2 (CHNH), 43.1 (CH<sub>2</sub>NH), 26.3 (CH<sub>2</sub>CH<sub>2</sub>), 19.5 (CH<sub>2</sub>CH<sub>2</sub>), 9.9 (CH<sub>3</sub>).

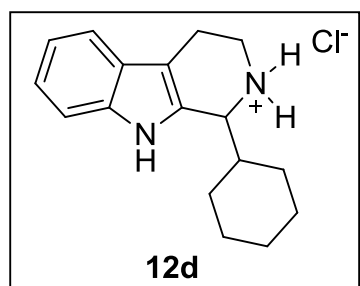


**1 – Isopropyl - 2,3,4,9 – tetrahydro - 1H-pyrido[3,4-b]indol-2-ium chloride (12c)**

Experimental value match the literature data.[2]

$^1\text{H}$  NMR, 400 MHz,  $\text{CD}_3\text{OD}$   $\delta$ : 7.50 (d,  $J = 7.9$ , 1H, ArH), 7.39 (d,  $J = 8.1$ , 1H, ArH), 7.18 (t,  $J = 7.6$ , 1H, ArH), 7.08 (t,  $J = 7.5$ , 1H, ArH), 4.69 (m, 1H, -CHNH<sub>2</sub>), 3.77 (ddd,  $J = 12.4, 5.3, 3.1$ , 1H, -CH<sub>2</sub>CHHNH<sub>2</sub>), 3.47 (ddd,  $J = 12.5, 10.1, 5.7$ , 1H, -CH<sub>2</sub>CHHNH<sub>2</sub>), 3.20-3.01 (m, 2H, -CH<sub>2</sub>CH<sub>2</sub>NH<sub>2</sub>), 2.73-2.60 (m, 1H, -CH(CH<sub>3</sub>)<sub>2</sub>), 1.28 (d,  $J = 7.1$ , 3H, -CH(CH<sub>3</sub>)<sub>2</sub>), 0.99 (d,  $J = 7.1$ , 3H, -CH(CH<sub>3</sub>)<sub>2</sub>).

$^{13}\text{C}$  NMR, 100 MHz,  $\text{CD}_3\text{OD}$   $\delta$ : 138.4 (ArC), 129.3 (ArC), 127.4 (ArC), 123.6 (ArC), 120.6 (ArC), 119.1 (ArC), 112.4 (ArC), 108.5 (ArC), 60.5 (CHNH), 43.9 (CH<sub>2</sub>NH), 31.1 (CHCH), 19.2 (CH<sub>2</sub>CH<sub>2</sub>), 16.4 (CH<sub>3</sub>)<sub>2</sub>.



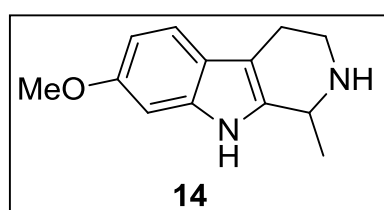
**1 – Cyclohexyl - 2,3,4,9 – tetrahydro-1H-pyrido[3,4-b]indol-2-ium chloride (12d)**

Experimental value match the literature data.[2]

$^1\text{H}$  NMR, 400 MHz,  $\text{CD}_3\text{OD}$   $\delta$ : 7.49 (dt,  $J = 7.9, 0.8$ , 1H, ArH), 7.39 (dt,  $J = 8.1, 0.8$ , 1H, ArH), 7.17 (ddd,  $J = 8.2, 8.0, 0.8$ , 1H, ArH), 7.07 (ddd,  $J = 8.0, 7.2, 1.2$ , 1H, ArH), 4.66 (m, 1H, CHNH<sub>2</sub>), 3.75 (ddd,  $J = 12.5, 5.4, 3.5$ , 1H, -CH<sub>2</sub>CHHNH<sub>2</sub>), 3.46 (ddd,  $J = 12.5, 9.7, 5.7$ , 1H, -CH<sub>2</sub>CHHNH<sub>2</sub>), 3.19-3.01 (m, 2H, -CH<sub>2</sub>CH<sub>2</sub>NH<sub>2</sub>), 2.37-2.25 (m, 1H, -CH(CH<sub>2</sub>)<sub>5</sub>), 2.01-1.74 (m, 4H, -C<sub>x</sub>H), 1.57-1.14 (m, 6H, -C<sub>x</sub>H).

$^{13}\text{C}$  NMR, 100 MHz,  $\text{CD}_3\text{OD}$   $\delta$ : 138.4 (ArC), 129.0 (ArC), 127.4 (ArC), 123.5 (ArC), 120.6 (ArC), 119.0 (ArC), 112.3 (ArC), 108.0 (ArC), 60.0 (CHNH), 43.8 (CH<sub>2</sub>NH), 41.0 (CHCH), 30.8 (CH<sub>2</sub>), 27.8 (CH<sub>2</sub>), 27.5 (CH<sub>2</sub>), 27.1 (CH<sub>2</sub>), 19.4 (CH<sub>2</sub>CH<sub>2</sub>).

**Preparation of the standard substance of 7-methoxy-1-methyl-2,3,4,9-tetrahydro-1H-pyrido[3,4-b]indole (14) [5]**



To a solution of **13** (100 mg 0.47 mmol) in MeOH (5 mL) was added NaBH<sub>4</sub> (18 mg, 0.47 mmol) at 0°C under nitrogen atmosphere. The solution was stirred for 1 hour at room temperature. Water (20 mL) and

CH<sub>2</sub>Cl<sub>2</sub> (25 mL) were added, the two phases separated and the aqueous phase extracted with CH<sub>2</sub>Cl<sub>2</sub> (25 mL). The combined organic phases were dried over MgSO<sub>4</sub> and concentrated under vacuum to give **14** (89 mg, 89% yield) as a white solid. Experimental value match the literature data.[5]

<sup>1</sup>H NMR, 400 MHz, CD<sub>3</sub>OD δ: 7.21 (d, *J* = 8.6 Hz, 1H, Ar*H*), 6.81 (d, *J* = 2.0 Hz, 1H, Ar*H*), 6.64-6.59 (m, 1H, Ar*H*), 4.04 (q, *J* = 6.6 Hz, 1H, -CHCH<sub>3</sub>), 3.76 (s, 3H, CH<sub>3</sub>O-), 3.27-3.19 (m, 1H, -CH<sub>2</sub>CHHN), 2.90 (ddd, *J* = 13.6, 9.6, 4.8 Hz 1H, -CH<sub>2</sub>CHHN), 2.76-2.65 (m, 1H, -CHHCH<sub>2</sub>N), 2.64-2.55 (m, 1H, -CHHCH<sub>2</sub>N), 1.41 (d, *J* = 6.7 Hz, 3H, -CHCH<sub>3</sub>).

<sup>13</sup>C NMR, 100 MHz, CD<sub>3</sub>OD δ: 157.3 (ArCOCH<sub>3</sub>), 138.4 (ArC), 136.6 (ArC), 123.2 (ArC), 119.1 (ArC), 109.3 (ArC), 108.0 (ArC), 95.8 (ArC), 56.0 (CH<sub>3</sub>O-), 49.5 (CHCH<sub>3</sub>), 43.6 (-CH<sub>2</sub>CH<sub>2</sub>N), 22.9 (-CH<sub>3</sub>), 20.3 (-CH<sub>2</sub>CH<sub>2</sub>N).

## Biotransformations

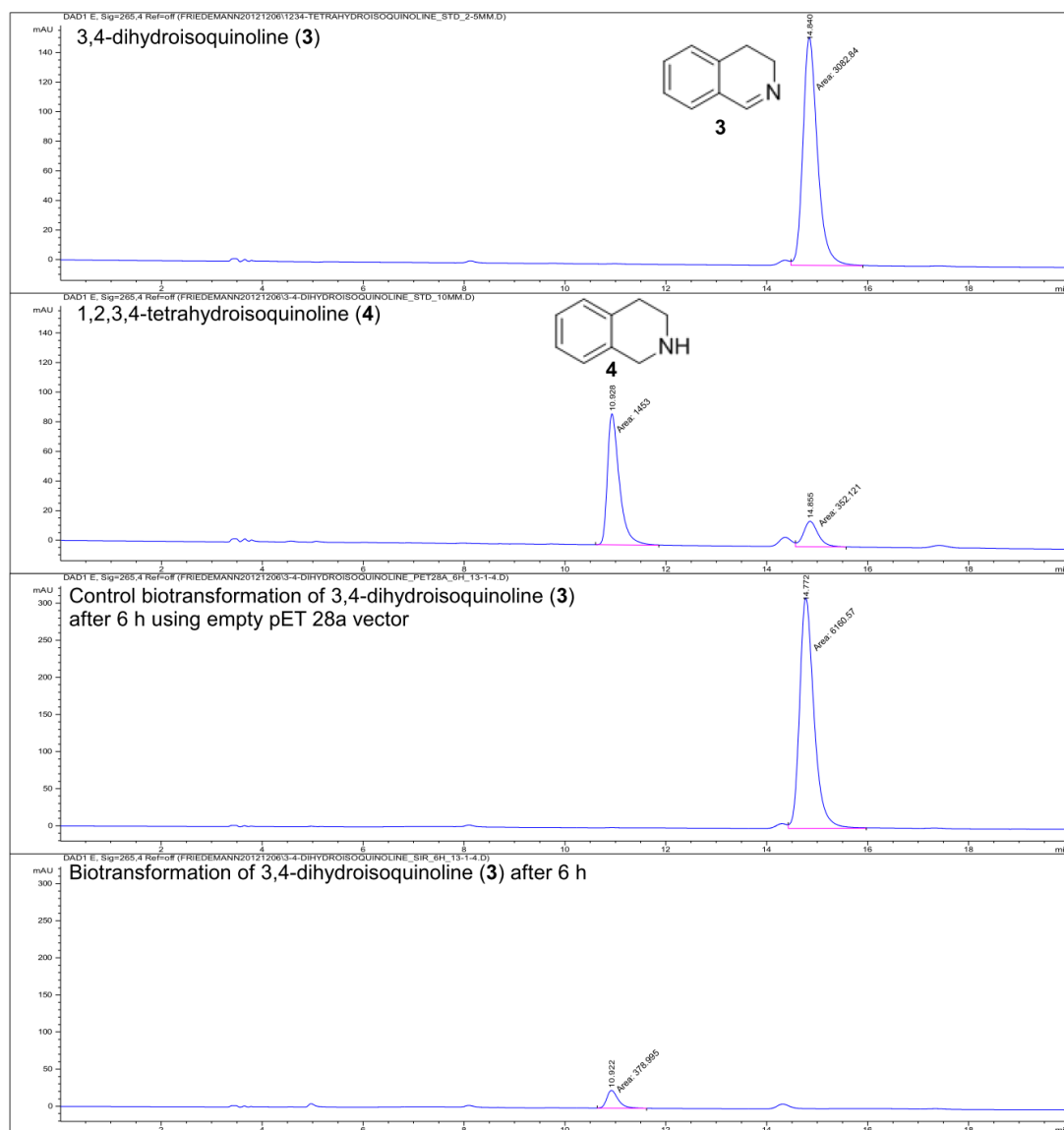
### General procedure of biotransformations

Reactions were performed in 2 mL Eppendorf tubes in a 0.5 mL total reaction volume at 30°C and 250 rpm. *E. coli* cells expressing (*S*)-imine reductase were resuspended in sodium phosphate buffer (100 mM, pH 7.0) to reach a final OD<sub>600nm</sub> of 30. For cofactor regeneration, glucose was added to a final concentration of 50 mM. The substrates were dissolved in DMF and added to the reaction mixture to a final concentration of 5 mM. The final concentration of DMF was 2% (v/v) unless otherwise stated. Contrary to other substrates, 2-methyl-1-pyrroline (**1**) was used at a final concentration of 10 mM and 2-methyl-3,4-dihydroisoquinolin-2-ium triflate (**5**) was used at a final concentration of 2.76 mM. Samples (0.5 mL) were taken after 0, 1, 3, 6, 18 and 30 h, basified using 30 μl 10 M NaOH and extracted using the double sample volume of dichloromethane (1 mL). Conversion and enantioselectivity was determined by normal phase chiral HPLC. For investigating whether the observed conversions might possibly also be caused by the natural metabolism of *E. coli* BL21 (DE3), biotransformations using cells harbouring empty pET-28a(+) vector induced with IPTG in the same way as the cells producing the (*S*)-imine reductase were taken as negative controls.

1 h		3 h		6 h		18 h		30 h	
c	e.e.	c	e.e.	c	e.e.	c	e.e.	c	e.e.

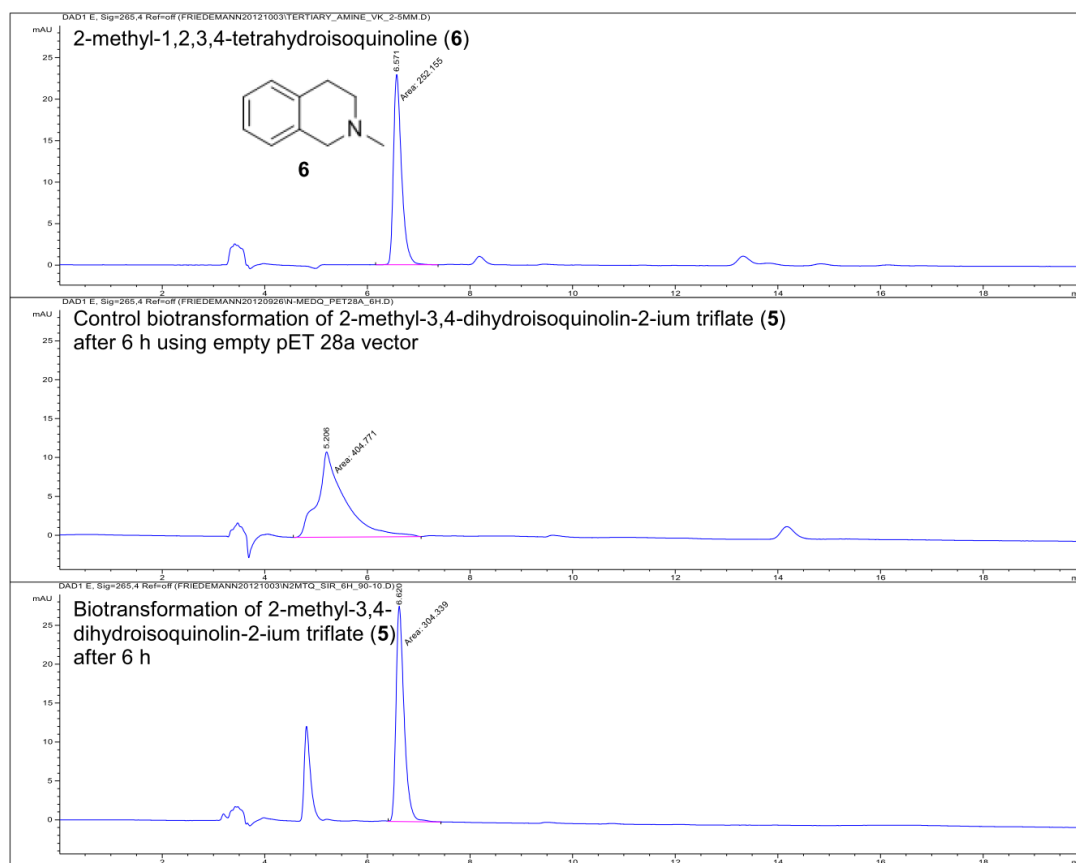
	[%]	[%]	[%]	[%]	[%]	[%]	[%]	[%]	[%]	[%]
<b>3</b>	99.7	n/a	99.8	n/a	99.9	n/a	99.9	n/a	99.8	n/a
<b>5<sup>[a]</sup></b>	60.1	n/a	57.2	n/a	59.6	n/a	61.1	n/a	56.1	n/a
<b>7</b>	98.8	98	99.9	98	99.9	98	99.9	98	99.6	98
<b>9</b>	48.0	100	83.2	100	91.6	100	91.7	100	91.9	100
<b>11a</b>	99.4	100	99.6	100	99.6	100	99.7	100	99.7	>99.5
<b>11b</b>	68.9	>99.5	99.2	>99.5	99.6	>99.5	99.1	>99.5	99.3	>99.5
<b>11c</b>	13.9	100	34.2	100	49.7	98	50.8	98	51.0	100
<b>11d</b>	28.7	>99	82.4	>99.5	97.3	>99.5	98.1	>99.5	98.1	>99.5
<b>13</b>	28.5	100	43.0	100	50.0	100	56.5	100	42.5	100

**Table S8.** Conversions and enantiomeric excesses at different timepoints.[a] Due to the cationic character of the 2-methyl-3,4-dihydroisoquinolin-2-ium ion, a quantitative extraction of the product was not possible using dichloromethane. Therefore, conversions for this substrate were solely calculated from the product concentrations formed and thus might be underestimated.

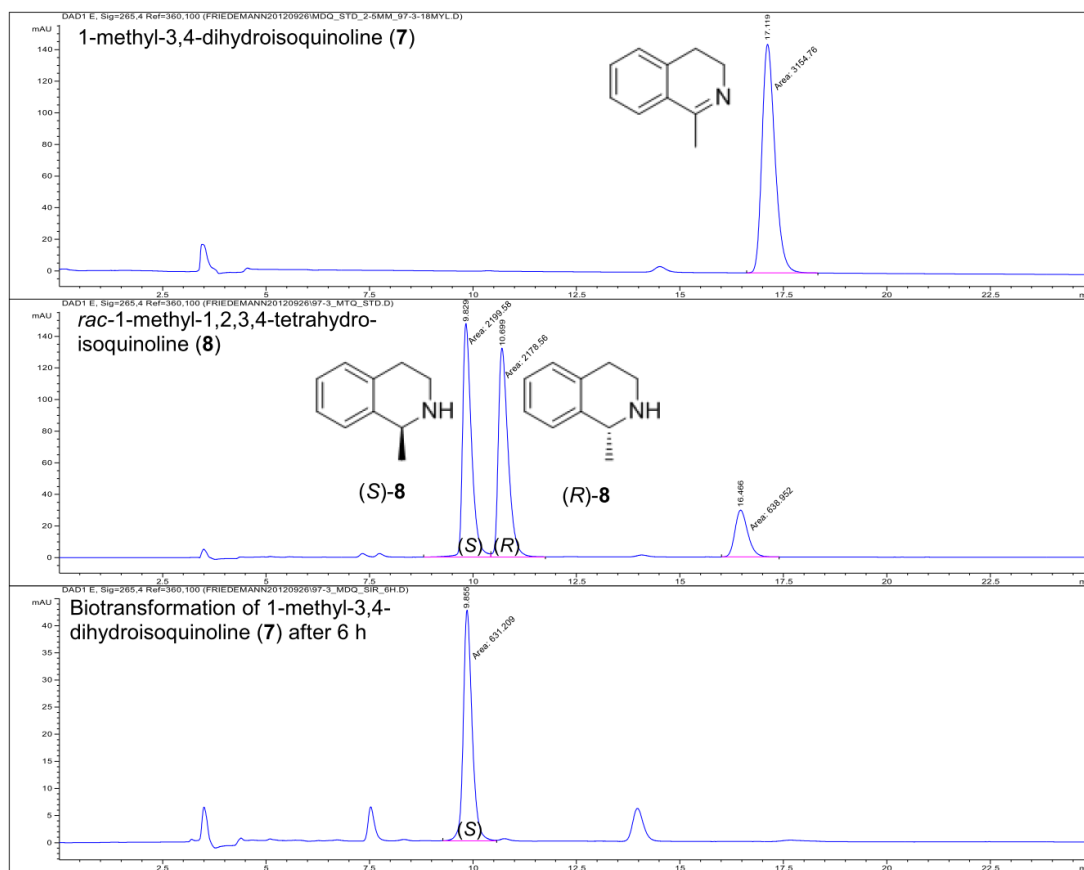


**Figure S17.** HPLC trace (Daicel CHIRALPAK<sup>®</sup> IC 250 mm × 4.6 mm, 5 μm, solvent: hexane/isopropanol/diethylamine = 90/10/0.1, 1 mL/min, 265 nm) of a standard solution showing the signals of **3** (top), **4** (upper middle), empty vector control biotransformation of **3** (lower middle) and of a biotransformation of **3** using (*S*)-imine reductase (bottom). The biotransformation using cells expressing the (*S*)-imine reductase led to full conversion after 6 h.

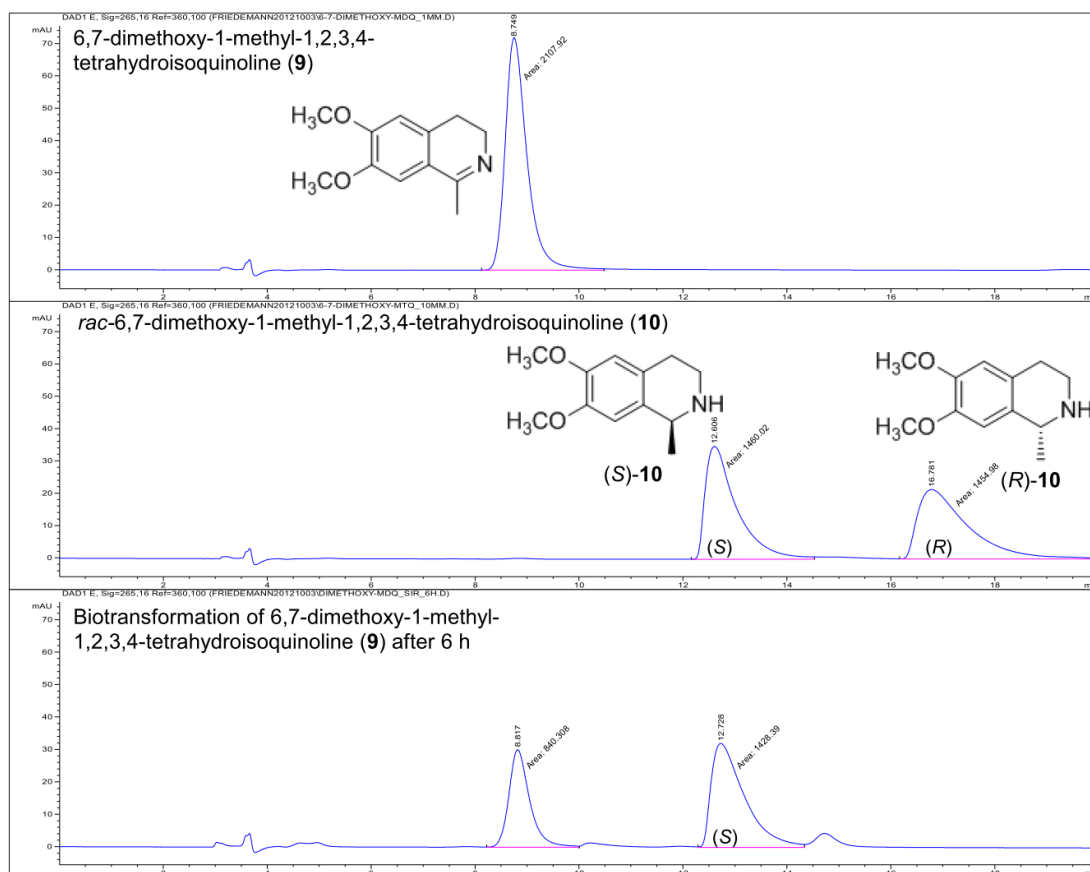




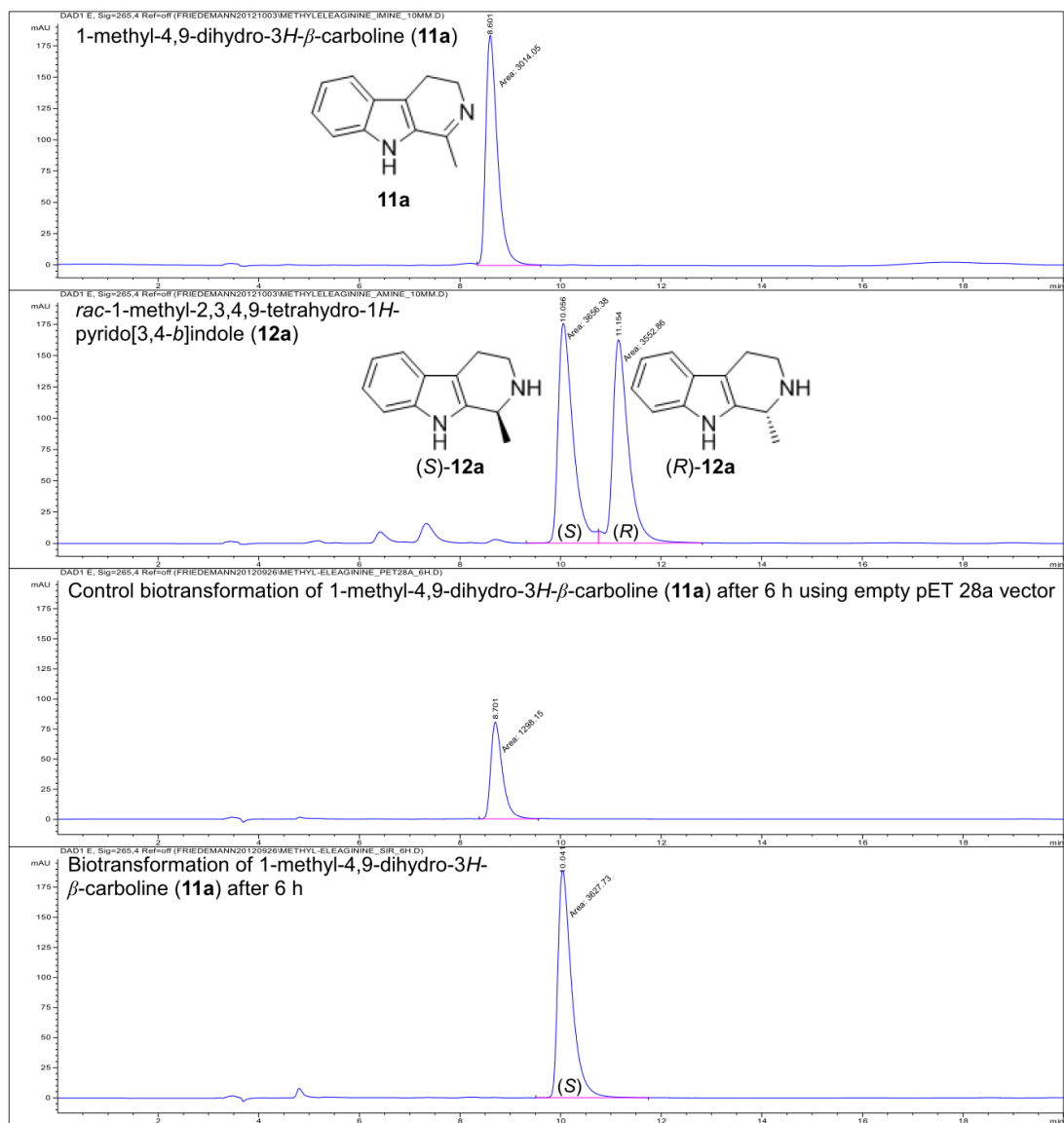
**Figure S17.** Chiral phase HPLC trace (Daicel CHIRALPAK<sup>®</sup> IC 250 mm × 4.6 mm, 5 μm, solvent: hexane/isopropanol/diethylamine = 90/10/0.1, 1 mL/min, 265 nm) of a standard solution showing the signals of **6** (top), empty vector control biotransformation of **5** (middle) and of a biotransformation of **5** using (S)-imine reductase (bottom). The biotransformation using cells expressing the (S)-imine reductase led to a conversion of 60% after 6 h. Due to the cationic character of the 2-methyl-3,4-dihydroisoquinolin-2-ium ion, a quantitative extraction of the product was not possible using dichloromethane. Therefore, conversions for this substrate were solely calculated from the product concentrations formed and thus might be underestimated.



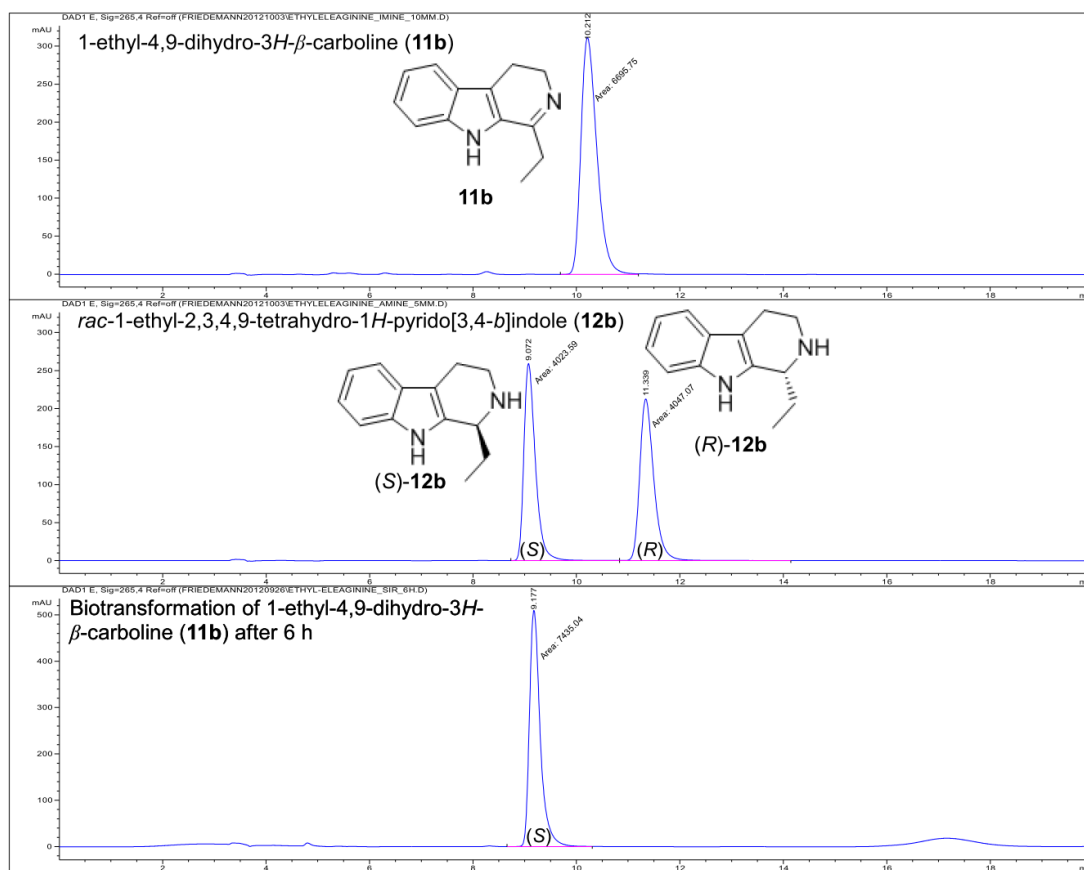
**Figure S18.** Chiral phase HPLC trace (Daicel CHIRALPAK<sup>®</sup> IC 250 mm × 4.6 mm, 5 μm, solvent: hexane/isopropanol/diethylamine = 97/03/0.1, 1 mL/min, 265 nm) of a standard solution of **7** (top), the signals of the two enantiomers of **8** (middle) and of a biotransformation of **7** using (S)-imine reductase (bottom). The biotransformation using cells expressing the (S)-imine reductase led to full conversion after 6 h with 98% e.e.



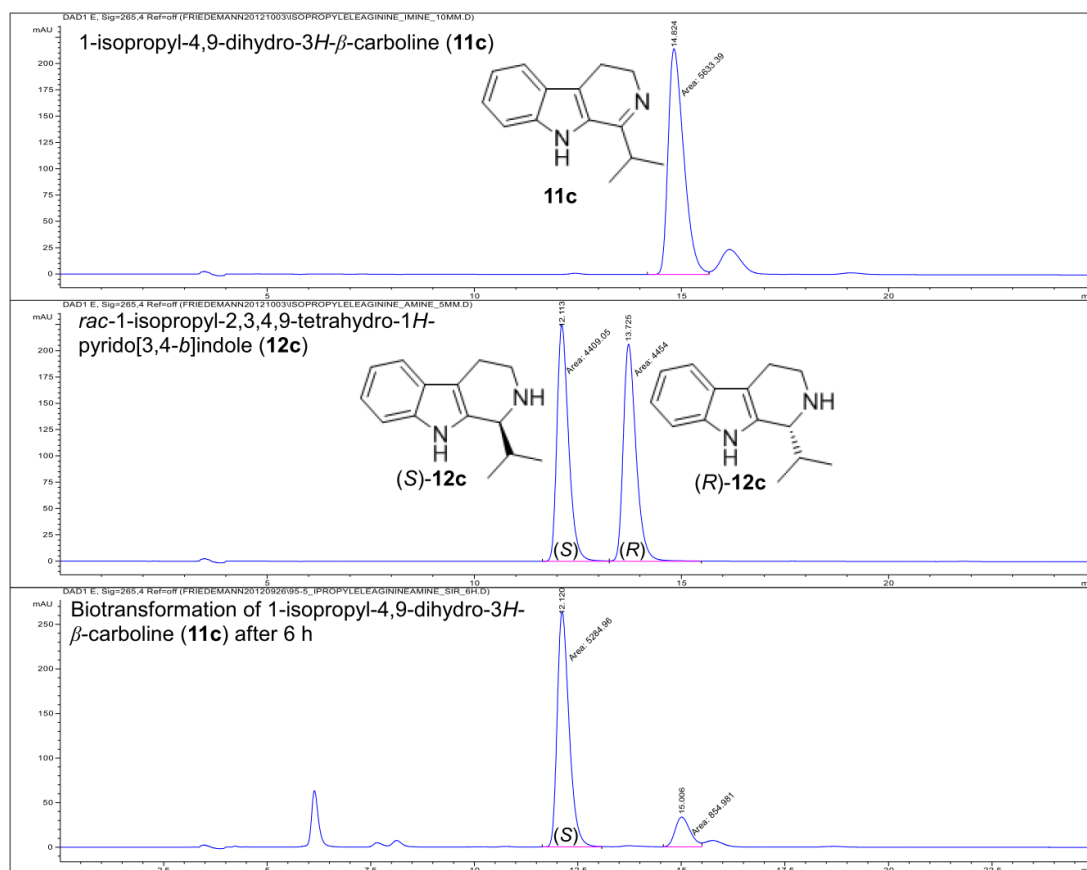
**Figure S19.** Chiral phase HPLC trace (Daicel CHIRALCEL<sup>®</sup> OD-H 250 mm × 4.6 mm, 5 μm, solvent: hexane/isopropanol/diethylamine = 90/10/0.1, 1 mL/min, 265 nm) of a standard solution of **9** (top), the signals of the two enantiomers of **10** (middle) and of a biotransformation of **9** using (*S*)-imine reductase (bottom). The biotransformation using cells expressing the (*S*)-imine reductase led to (*S*)-**10** in enantiopure form with a conversion of 92% after 6 h.



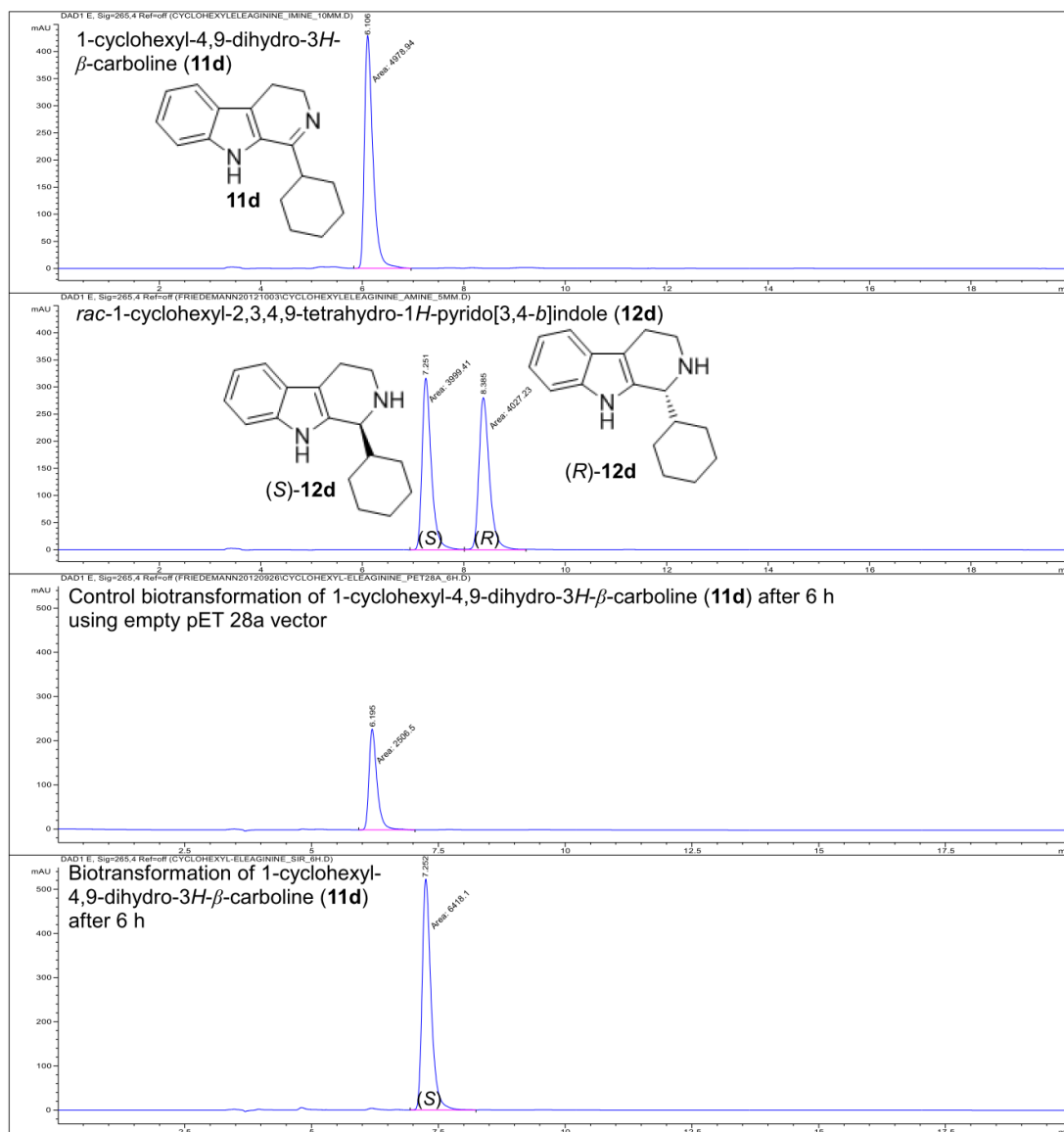
**Figure S20.** Chiral phase HPLC trace (Daicel CHIRALPAK<sup>®</sup> IC 250 mm × 4.6 mm, 5 μm, solvent: hexane/isopropanol/diethylamine = 90/10/0.1, 1 mL/min, 265 nm) of a standard solution of **11a** (top), the signals of the two enantiomers of **12a** (upper middle), an empty vector control biotransformation of **11a** (lower middle) and of a biotransformation of **11a** using (S)-imine reductase (bottom). The biotransformation using cells expressing the (S)-imine reductase fully converted **11a** into the enantiopure (S)-**12a**



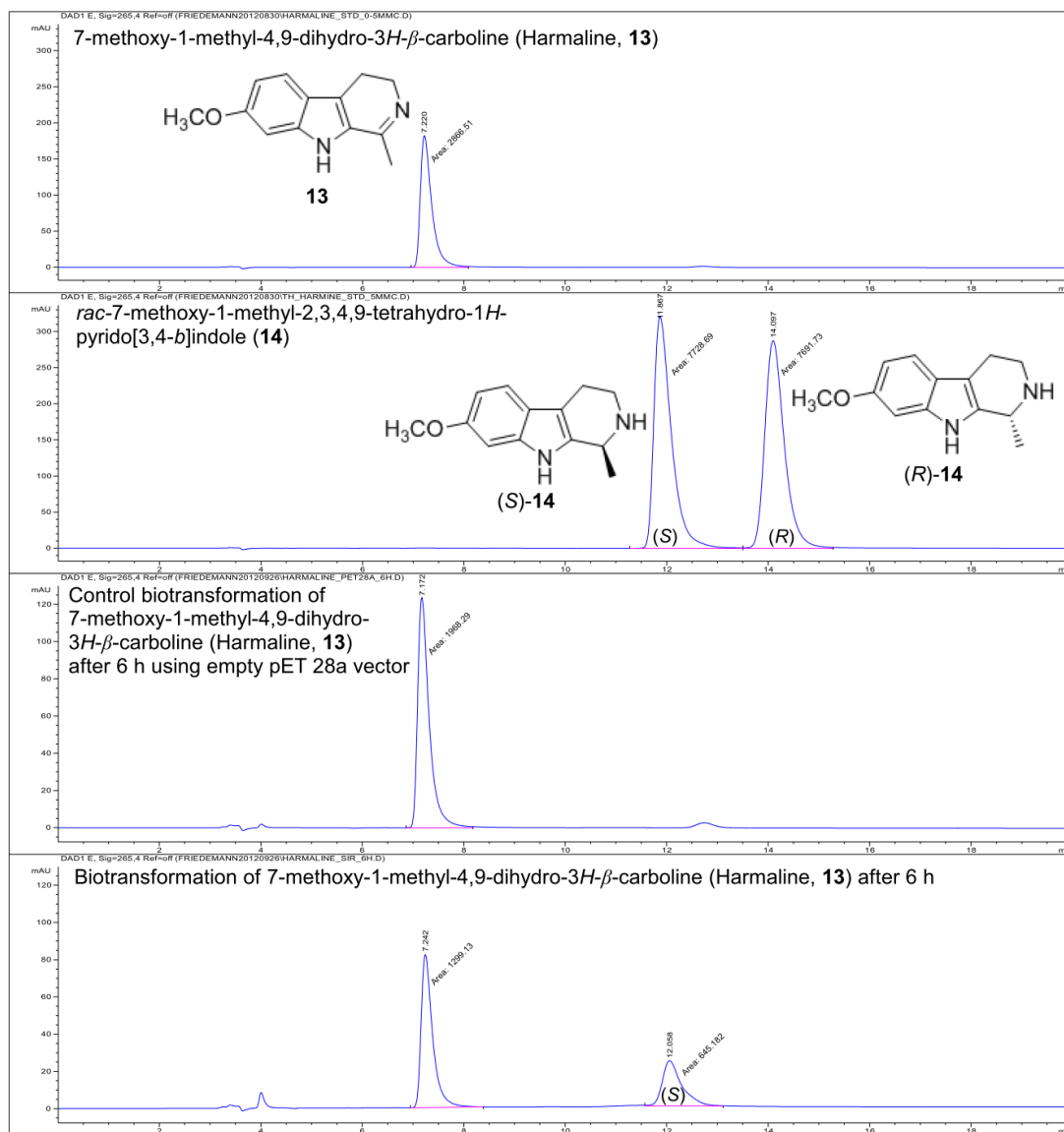
**Figure S21.** Chiral phase HPLC trace (Daicel CHIRALPAK<sup>®</sup> IC 250 mm × 4.6 mm, 5 μm, solvent: hexane/isopropanol/diethylamine = 90/10/0.1, 1 mL/min, 265 nm) of a standard solution of **11b** (top), the signals of the two enantiomers of **12b** (middle) and of a biotransformation of **11b** using (S)-imine reductase (bottom). The biotransformation using cells expressing the (S)-imine reductase fully converted **11b** into the enantiopure (S)-**12b**



**Figure S22.** Chiral phase HPLC trace (Daicel CHIRALPAK<sup>®</sup> IC 250 mm × 4.6 mm, 5 μm, solvent: hexane/isopropanol/diethylamine = 95/05/0.1, 1 mL/min, 265 nm) of a standard solution of **11c** (top), the signals of the two enantiomers of **12c** (middle) and of a biotransformation of **11c** using (*S*)-imine reductase (bottom). The biotransformation using cells expressing the (*S*)-imine reductase led to a conversion of 50% after 6 h with 98% e.e.



**Figure S23.** Chiral phase HPLC trace (Daicel CHIRALPAK<sup>®</sup> IC 250 mm × 4.6 mm, 5 μm, solvent: hexane/isopropanol/diethylamine = 90/10/0.1, 1 mL/min, 265 nm) of a standard solution of **11d** (top), the signals of the two enantiomers of **12d** (upper middle), an empty vector control biotransformation of **11d** (lower middle) and of a biotransformation of **11d** using (*S*)-imine reductase (bottom). The biotransformation using cells expressing the (*S*)-imine reductase led to a conversion of 97% after 6 h in enantiopure form.



**Figure S24.** Chiral phase HPLC trace (Daicel CHIRALPAK<sup>®</sup> IC 250 mm × 4.6 mm, 5 μm, solvent: hexane/isopropanol/diethylamine = 80/20/0.1, 1 mL/min, 265 nm) of a standard solution of **13** (top), the signals of the two enantiomers of **14** (upper middle), an empty vector control biotransformation of **13** (lower middle) and of a biotransformation of **13** using (*S*)-imine reductase (bottom). The biotransformation using cells expressing the (*S*)-imine reductase led to a conversion of 50% after 6 h in enantiopure form.



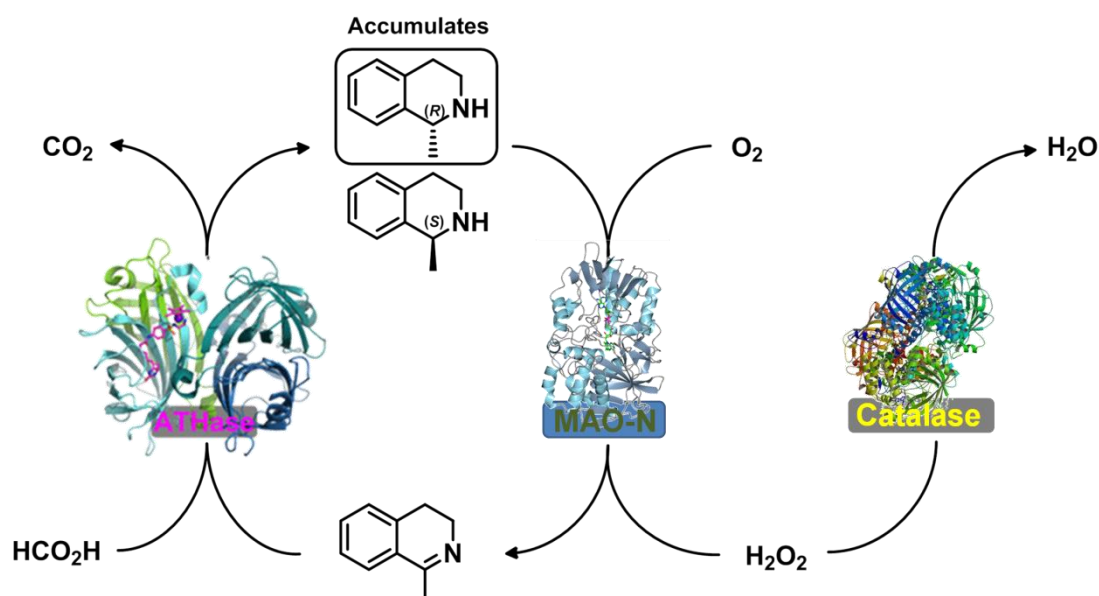
## References

- [1] K. M. Jones, P. Karier, M. Klussmann, *Chemcatchem* **2012**, *4*, 51.
- [2] J. S. Wu, F. Wang, Y. P. Ma, X. C. Cui, L. F. Cun, J. Zhu, J. G. Deng, B. L. Yu, *Chem. Commun.* **2006**, 1766.
- [3] I. Ivanov, S. Nikolova, S. Statkova-Abeghe, *Heterocycles* **2005**, *65*, 2483.
- [4] P. Bernhardt, A. R. Usera, S. E. O'Connor, *Tetrahedron Lett.* **2010**, *51*, 4400.
- [5] B. Schonenberger, A. Brossi, *Helv. Chim. Acta* **1986**, *69*, 1486.
- [6] J. M. Crosthwaite, V. A. Farmer, J. P. Hallett, T. Welton, *J. Mol. Cat. A*, **2008**, *279*, 148-152

# SYNTHETIC CASCADES ARE ENABLED BY COMBINING BIOCATALYST WITH ARTIFICIAL METALLOENZYMES

*Nature Chemistry* **5**, 93-99 (2013) doi:10.1038/nchem.1498

V. Koehler, Y. M. Wilson, M. Durrenberger, D. Ghislieri, E. Churakova, T. Quinto, L. Knorr, D. Haussinger, F. Hollmann\*, N. J. Turner\* and T. R. Ward\*



The combination of two or more catalytic systems to complete a series of cascade reactions is considered particularly appealing as well as a challenge the chemist in the new millennium. We have developed a concurrent redox cascade for the deracemisation racemic amines using our monoamine oxidase-N in combination with a biotinylated Ir-complex within streptavidin (SAV) and catalase to reduce the hydrogen peroxide product in the oxidation. To achieve the final goal it was necessary to shield the metal inside a host to avoid the mutual inactivation of the two catalysts.

In this project D.G., after having collecting preliminary data about the feasibility of the project in Manchester, moved to Basel to complete the experiments using MAO-N/ATHase catalytic system. D.G. co-wrote the MAO-N experimental part.

# New Synthetic Cascades by Combining Biocatalysts with Artificial Metalloenzymes

V. Köhler,<sup>1</sup> Y. M. Wilson,<sup>1</sup> M. Dürrenberger,<sup>1</sup> D. Ghislieri,<sup>2</sup> E. Churakova,<sup>3</sup> T. Quinto,<sup>1</sup> L. Knörr,<sup>1</sup> D. Häussinger,<sup>1</sup> F. Hollmann,<sup>\*,3</sup> N. J. Turner,<sup>\*,2</sup> and T. R. Ward<sup>\*,1</sup>

<sup>1</sup>Department of Chemistry, University of Basel, Spitalstrasse 51, CH-4056 Basel, Switzerland

<sup>2</sup>School of Chemistry, University of Manchester, Manchester Interdisciplinary Biocentre, 131 Princess Street, Manchester, M1 7DN, United Kingdom

<sup>3</sup>Department of Biotechnology, Delft University of Technology, Julianalaan 136, 2628BL Delft, The Netherlands

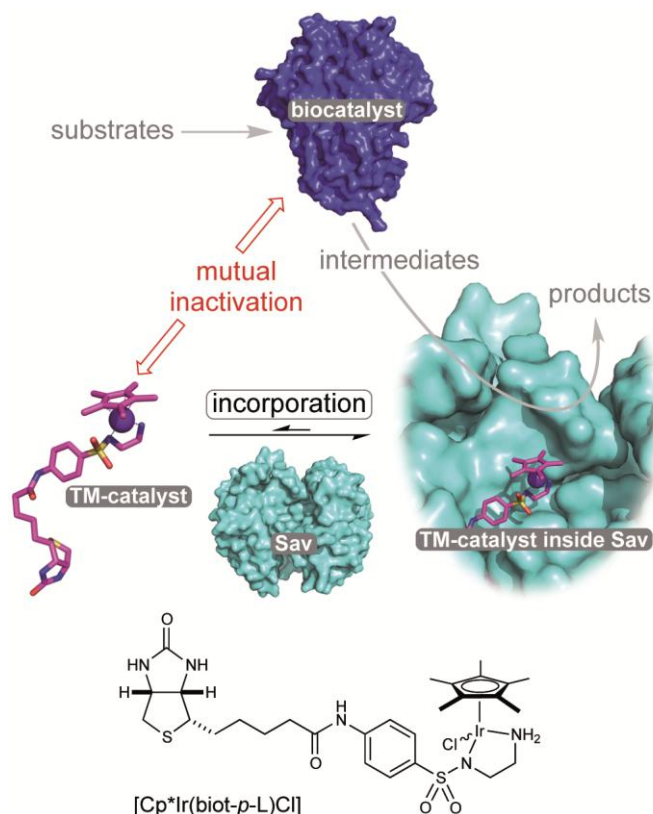
*F.Hollmann@tudelft.nl, Nicholas.Turner@manchester.ac.uk, thomas.ward@unibas.ch*

## Abstract

Enzymatic- and homogeneous catalysis offer complementary means to address synthetic challenges, both in chemistry and in biology. Despite its attractiveness, the implementation of concurrent cascade reactions which combine an organometallic catalyst with an enzyme has proven challenging, due to the mutual inactivation of both catalysts. To address this, we show that incorporation of a d<sup>6</sup>-piano stool complex within a host protein affords an artificial transfer hydrogenase (ATHase) which is fully compatible and complementary with natural enzymes, thus enabling efficient concurrent tandem catalysis. To illustrate the generality of the approach, the ATHase was combined with various NADH-, FAD- and heme-dependent enzymes resulting in orthogonal redox cascades. Up to three enzymes were integrated in the cascade and combined with the ATHase towards i) a double stereoselective amine deracemisation, ii) an horseradish peroxidase-coupled (HRP-coupled) read-out of the transfer hydrogenase activity towards its genetic optimization iii) the formation of L-pipecolic acid from L-lysine and iv) regeneration of NADH to promote a monooxygenase-catalyzed oxyfunctionalization reaction.

## Introduction

Cellular biochemistry requires the orchestration of metabolic pathways in which many enzyme-catalysed processes are able to function simultaneously, resulting in the production of a wide range of primary and secondary metabolites within the cell. In the attempt to construct artificial cells, by employing the principles of synthetic biology, such compartmentalization of cellular processes will need to be mimicked in order to allow cascade reactions to take place in parallel in an efficient manner [1-6]. Whereas enzymes have evolved in concert and in complex media and thus are well suited for cascade reactions, compatibility problems and mutual inactivation are often encountered upon combining chemo- with biocatalysts [7-9]. Such incompatibility may be circumvented by performing cascades in sequential steps or by site-isolation of the individual catalysts through immobilization, heterogeneous- or biphasic reaction conditions, encapsulation etc. [10-24]. Recently, we have described one approach to cellular compartmentalization in which an *E. coli* cell was engineered to simultaneously express an intracellular enzyme (monoamine oxidase) and also bind palladium nanoparticles in its outer membrane, thereby allowing efficient chemo-enzymatic deracemisation of amines [24]. Artificial metalloenzymes which result from encapsulation of an organometallic catalyst within a protein scaffold have been shown to combine attractive features of both chemo- and biocatalysts for single step transformations [25-32]. In the context of concurrent cascade reactions, we reasoned that the artificial cofactor may be effectively shielded by its host protein, thus preventing the mutual inactivation commonly encountered upon combining an organometallic catalyst with an enzyme, Figure 1. To test the validity of the concept, we have examined the combination of an artificial transfer-hydrogenase (ATHase) with an oxidase, a catalase, an amino acid oxidase and a monooxygenase, Figure 2. For this purpose, we rely on the incorporation of a biotinylated  $[\text{Cp}^*\text{Ir}(\text{Biot-}p\text{-L})\text{Cl}]$  complex within streptavidin (Sav hereafter) as ATHase using formic acid as hydride source, Figure 1 and 2.



**Figure 1. Reaction cascades resulting from combining an artificial transfer hydrogenase (ATHase) with a biocatalyst.** The organometallic transfer-hydrogenation catalyst  $[\text{Cp}^*\text{Ir}(\text{biot-}p\text{-L})\text{Cl}]$  and biocatalyst suffer from mutual inactivation thus precluding the implementation of reaction cascades. Relying on the strength of the biotin-streptavidin interaction, incorporation of the biotin-bearing complex  $[\text{Cp}^*\text{Ir}(\text{biot-}p\text{-L})\text{Cl}]$  within streptavidin (Sav) affords an ATHase which is fully compatible and complementary with a variety of natural enzymes thus leading to the development of concurrent orthogonal redox cascades.

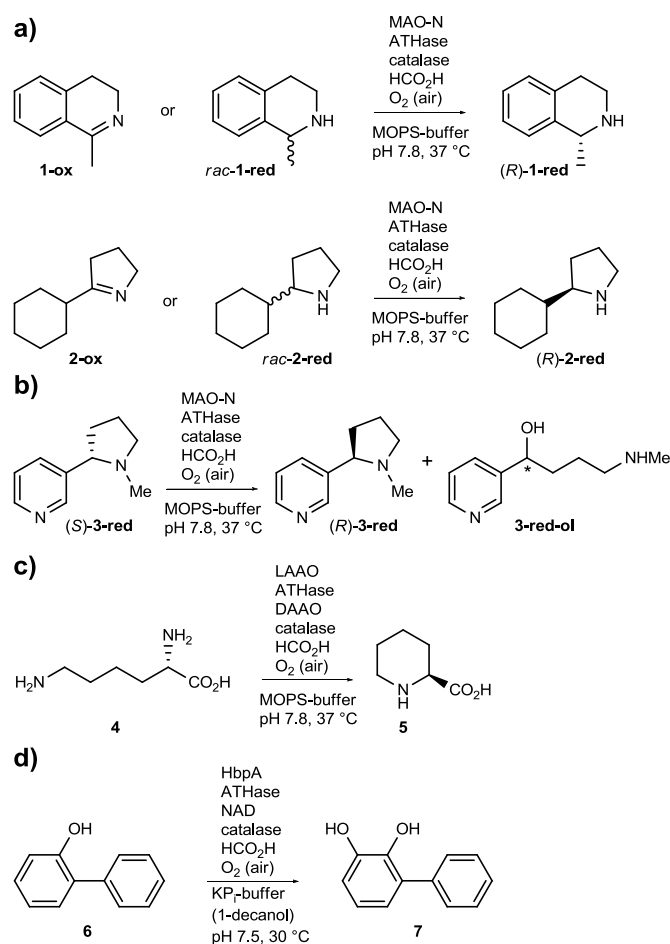
## Results and Discussion

### Double stereoselective deracemisation of amines

In recent years, evolved monoamine oxidases (MAO-N from *Aspergillus niger*) have found widespread applications for the synthesis of enantiopure amines [33,34]. For this purpose, a highly (*S*)-selective MAO is combined with a stoichiometric reducing agent (*e.g.*  $\text{BH}_3\text{-NH}_3$ ), [34] or with a heterogeneous reduction catalyst [24]. Efforts to combine MAO with an homogeneous imine reduction catalyst have proven challenging thus far: upon combining the transfer hydrogenation catalyst  $[\text{Cp}^*\text{Ir}(\text{Biot-}p\text{-L})\text{Cl}]$  with MAO, we observed mutual inactivation, Figure 1. Only traces of amine could be detected starting from the imine nor could imine be detected in significant amounts starting from the racemic amine, Table 1, entries 1, 2. These

observations suggest that biocatalyst and chemocatalyst are incompatible. In the chemo-enzymatic dynamic kinetic resolution of alcohols and amines, as pioneered by Bäckvall, inactivation may be circumvented by performing the cascade reaction in an organic solvent [21,22]. This strategy effectively provides a phase separation between the highly robust and enantioselective enzyme (*eg.* CALB) and the organometallic racemisation catalyst.

In a biomimetic spirit, we speculated that molecular compartmentalization of the organometallic imine reduction catalyst within a protein scaffold may shield it from the biocatalyst, thus preventing mutual inactivation. With this goal in mind, we set out to investigate the potential of cascade reactions in the presence of an artificial transfer hydrogenase (ATHase) based on the supramolecular incorporation of a catalytically active [Cp\*Ir(biot-*p*-L)Cl] complex within streptavidin, Figure 1 and 2. Initially, the individual reaction steps were performed with the **1-red** and **1-ox** (1-methyl-1,2,3,4-tetrahydroisoquinoline, 1-methyl-3,4-dihydroisoquinoline) couple. This led to the identification of [Cp\*Ir(Biot-*p*-L)Cl]·Sav S112T (59% e.e. (*R*)-**red-1**) and [Cp\*Ir(Biot-*p*-L)Cl]·Sav S112K (46% e.e. (*S*)-**red-1**) as well as MAO-N D9 for the oxidation of (*S*)-**red-1** (Table 1, entries 3, 4 and SI) [35,36].



**Figure 2 Overview of reaction cascades scrutinized in this study.** a) (Reduction of prochiral imines with subsequent) deracemization of cyclic amines. b) Stereoinversion of natural nicotine, which leads partially to the formation of the chiral alcohol **3-red-ol**. c) Formation of L-pipecolic acid from L-lysine. d) Hydroxylation of 2-hydroxybiphenyl coupled to an ATHase catalyzed NADH regeneration process. MAO-N stands for a monoamine oxidase variant from *Aspergillus niger*; ATHase stands for an artificial transfer hydrogenase variant, formed by incorporation of  $[\text{Cp}^*\text{Ir}(\text{Biot-}p\text{-L})\text{Cl}]$  into a streptavidin variant; LAO is L-aminoacid oxidase from *crotalus atrox*, DAAO is D-aminoacid oxidase from porcine kidney; HbpA stands for 2-hydroxybiphenyl monooxygenase from *Pseudomonas azaleica*.

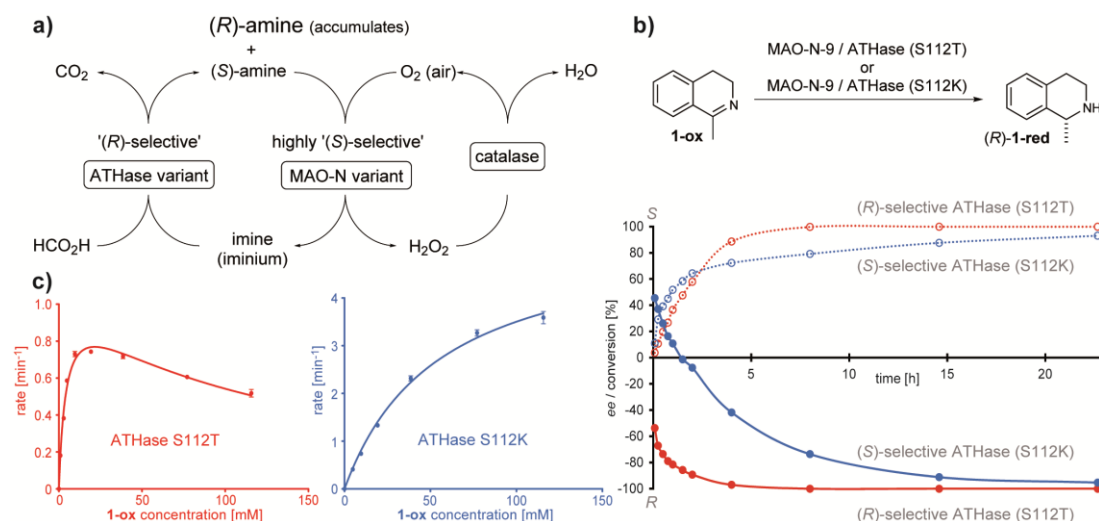
Upon incorporation of  $[\text{Cp}^*\text{Ir}(\text{Biot-}p\text{-L})\text{Cl}]$  in Sav, only modest ATH activity was observed in the presence of MAO-N D9 (See SI). We speculated that the  $\text{H}_2\text{O}_2$  produced by MAO as side product may poison the Ir-catalyst (See SI) [37]. Upon addition of a catalase (from bovine liver), quantitative conversion and 99% e.e. in favour of (*R*)-**1-red** was obtained using 0.5 mol% of  $[\text{Cp}^*\text{Ir}(\text{Biot-}p\text{-L})\text{Cl}] \cdot \text{Sav S112T}$  with 0.19 mg MAO/mL. The orthogonal redox cascade yielded identical results starting either from the racemic amine ((*rac*)-**1-red**) or from the prochiral imine (**1-**

ox; Figure 2 and 3, Table 1 compare entries 5, 6). In stark contrast, only negligible MAO-activity could be observed with  $[\text{Cp}^*\text{Ir}(\text{Biot-}p\text{-L})\text{Cl}]$ , in the presence of catalase, highlighting the beneficial effect of the Sav host protein, effectively site-isolating the reductase and the oxygenase (See SI).

Next, we investigated the influence of the Sav isoform on the rate of the cascade reaction. For this purpose, a moderately (*S*)-selective  $[\text{Cp}^*\text{Ir}(\text{Biot-}p\text{-L})\text{Cl}] \cdot \text{Sav S112K}$  ATHase was combined with MAO-N D9. Although the reaction with Sav S112K showed a faster initial rate, it took significantly longer to reach high enantiomeric excess in favour of the (*R*)-enantiomer: 93% e.e. after 23 hours with S112K vs. 99% e.e. after 8 hours with S112T, Figure 3b, Table 1, entries 6, 7. The kinetic profile reflects a combined effect of  $k_{\text{cat}}$ ,  $K_{\text{M}}$ ,  $K_{\text{inhib}}$  and selectivity ( $k_{\text{cat}(\text{app})}$  5.4  $\text{min}^{-1}$  ( $\pm 0.2 \text{ min}^{-1}$ ),  $K_{\text{M}(\text{app})}$  55 mM ( $\pm 5 \text{ mM}$ )) compared to the (*R*)-selective ATHase S112T ( $k_{\text{cat}(\text{app})}$  1.09  $\text{min}^{-1}$  ( $\pm 0.05 \text{ min}^{-1}$ ),  $K_{\text{M}(\text{app})}$  4.5 mM ( $\pm 0.4 \text{ mM}$ ) with a  $K_{\text{inhibition}}$  of 104 mM ( $\pm 12 \text{ mM}$ ), Figure 3c. These data highlight the versatility of the double stereoselective cascade whereby both ATHase and MAO work in concert to expediently produce the enantiopure amine.

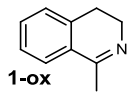
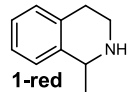
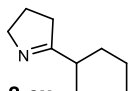
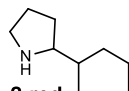
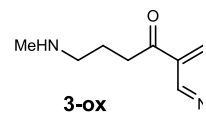

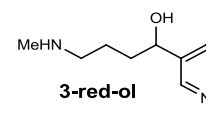
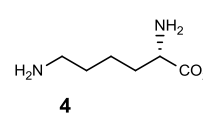
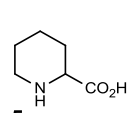
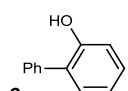
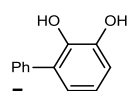
These results demonstrate that: i) the MAO determines the overall enantioselectivity of the reaction ii) a synergistic effect for the matched (*R*)-selective ATHase – (*S*)-selective MAO-N – catalase cascade is operative; iii) the stereoselectivity of the ATHase is unaffected by the presence of both MAO and catalase, as highlighted by the enantioselectivities at the start of the reaction (samples taken after 5 minutes, See SI) and iv) the presence of a His-tag on the MAO-N D9 does not influence the performance of the ATHase as judged by the initial rates.





**Figure 3. Enzyme-cascade for the double stereoselective deracemization of amines.** a) Schematic representation of the double stereoselective deracemisation with MAO-N/ATHase (See SI for experimental details). b) Reaction scheme for the production of (R)-1-red via a reaction cascade and time plot evolution of conversion (dotted lines, empty circles) and enantioselectivity (solid lines, filled circles) for [Cp\*Ir(Biot-*p*-L)Cl]·Sav S112T ATHase (red) and [Cp\*Ir(Biot-*p*-L)Cl]·Sav S112K ATHase (blue). c) Saturation kinetic curves for [Cp\*Ir(Biot-*p*-L)Cl]·Sav S112T ATHase (red trace) and [Cp\*Ir(Biot-*p*-L)Cl]·Sav S112K ATHase (blue trace); error bars indicate standard deviations in the measurement. Although the ATHase rate of the (R)-selective ATHase (S112T variant) is significantly lower than that of the (S)-selective variant (S112K) at the beginning of the reaction, the matched enzyme cascade (ie. S112T MAO-N D9) reaches a high enantiomeric excess in favour of the (R)-amine **1** more rapidly than the mismatched case (ie. S112K MAO-N D9).

<sup>a</sup>The most relevant entries are highlighted in bold. <sup>b</sup>Conversion determined by HPLC or GC (See SI);

entry	substrate	product	Sav-mutant	oxidase/oxygenase	catalase	Conv. <sup>b</sup> [%]	e.e. [%] (abs.config)
1	 <b>1-ox</b>	 <b>1-red</b>	-	MAO-N D9	yes	36	<i>rac.</i>
2	<b>(rac)-1-red</b>	<b>1-red</b>	-	MAO-N D9	no	<1	<i>rac.</i>
3	<b>1-ox</b>	<b>1-red</b>	S112T	-	no	>99	59 ( <i>R</i> )
4	<b>1-ox</b>	<b>1-red</b>	S112K	-	no	>99	46 ( <i>S</i> )
5	<b>(rac)-1-red</b>	<b>1-red</b>	<b>S112T</b>	<b>MAO-N D9</b>	<b>yes</b>	<b>&gt;99</b>	<b>&gt;99 (<i>R</i>)</b>
6	<b>1-ox</b>	<b>1-red</b>	<b>S112T</b>	<b>MAO-N D9</b>	<b>yes</b>	<b>&gt;99</b>	<b>&gt;99 (<i>R</i>)<sup>c</sup></b>
7	<b>1-ox</b>	<b>1-red</b>	S112K	MAO-N D9	yes	98	99 ( <i>R</i> ) <sup>d</sup>
8	 <b>2-ox</b>	 <b>2-red</b>	S112A	-	no	84 <sup>e</sup>	86 ( <i>R</i> )
9	<b>2-ox</b>	<b>2-red</b>	S112A-K121N	-	no	>99 <sup>e</sup>	63 ( <i>R</i> )
10	<b>2-ox</b>	<b>2-red</b>	<b>S112A</b>	<b>MAO-N D9</b>	<b>yes</b>	<b>98<sup>e</sup></b>	<b>99 (<i>R</i>)</b>
11	<b>(rac)-2-red</b>	<b>2-red</b>	<b>S112A-K121N</b>	<b>MAO-N D9</b>	<b>yes</b>	<b>99<sup>e</sup></b>	<b>&gt;99 (<i>R</i>)</b>
12	 <b>3-ox</b>	 <b>3-red</b>	S112A-K121T	-	no	76 <sup>f</sup>	79 ( <i>R</i> )
13	<b>3-ox</b>	 <b>3-red-ol</b>	S112G	-	no	79 <sup>g</sup>	30 (n.d.)
14	<b>(S)-3-red</b>	<b>3-red</b>	<b>S112A-K121T</b>	<b>MAO-N D5</b>	<b>yes</b>	<b>65<sup>h</sup></b>	<b>&gt;99 (<i>R</i>)</b>
15	 <b>4</b>	 <b>5</b>	-	LAAO	yes	20	1 ( <i>R</i> )
16	<b>4</b>	<b>5</b>	S112A	LAAO	yes	89	29 ( <i>S</i> )
17	<b>(S)-4</b>	<b>5</b>	<b>S112A</b>	<b>LAAO + DAAO</b>	<b>yes</b>	<b>88<sup>i</sup></b>	<b>86 (<i>S</i>)</b>
18	 <b>6</b>	 <b>7</b>	-	HbpA	no	3	n.a.
19	<b>6</b>	<b>7</b>	<b>S112A</b>	<b>HbpA</b>	<b>no</b>	<b>&gt;99</b>	<b>n.a.</b>

<sup>c</sup>after 8 hours reaction time; <sup>d</sup>after 65 hours reaction time; <sup>e</sup>yield determined by response of **2-ox** vs. **2-red**; <sup>f</sup>ratio of **3-red** to **3-red-ol** = 6.6 : 1, conversion refers to **3-red** only; <sup>g</sup>ratio of **3-red** to **3-red-ol** = 1 : 22.8, conversion refers to **3-red-ol** only; <sup>h</sup>additionally ~10% of **3-red-ol** were formed; <sup>i</sup>determined by 2D-NMR, see SI. See Methods and SI for full experimental details.

**Table 1. Orthogonal redox cascades combining ATHase with oxidases or oxygenase.<sup>a</sup>**

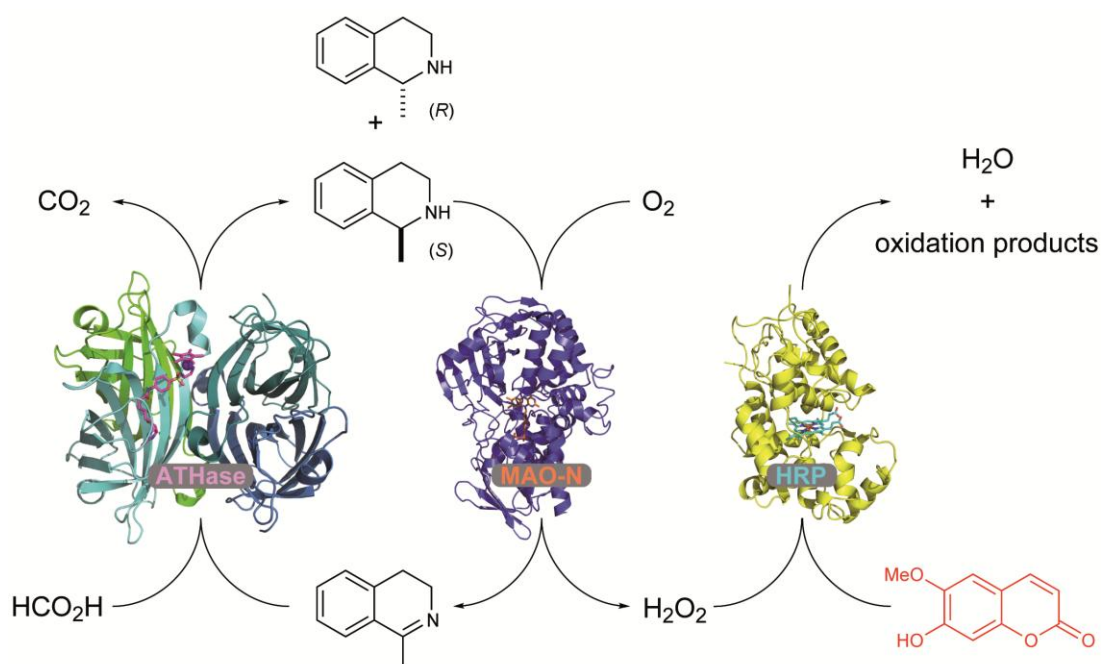
**Other amine-imine couples.** To investigate the scope of the concurrent cascade reaction, a secondary amine with purely aliphatic substituents (*(rac)*-**2-red**) and a tertiary amine (*(S)*-**3-red**) and their respective oxidation products (**2-ox**, **3-ox**) were subjected to the above enzyme-cascade including the ATHase. Prior to this, suitable enzymes for the individual reaction steps (reduction and oxidation) were identified (see Table 1, entries 8, 9 and SI).

In the cascade reaction, the conversion of *(rac)*-**2-red** or **2-ox** into the *(R)*-**red-2** was achieved by combining the MAO-N-9 with [Cp\*Ir(Biot-*p*-L)Cl]·Sav S112A and a catalase, to afford *(R)*-**red-2** (e.e. of 99% *(R)*, Table 1, entries 10, 11). On a preparative deracemisation reaction, nearly quantitative yields of **red-2** were isolated in 95 % e.e. (*R*).

In the case of nicotine **red-3**, we found that mutations on Sav had a significant influence on the product distribution. As reported by Brandänge *et al.*, the tertiary iminium generated upon oxidation of the tertiary amine **red-3** exists in equilibrium with the keto-amine **ox-3** in aqueous solution [38]. The relative rate of keto-amine vs. iminium reduction by the ATHase determines the product distribution **3-red** vs. **3-red-ol**, Table 1, entries 12, 13. For the reduction step alone, [Cp\*Ir(Biot-*p*-L)Cl]·Sav S112A-K121T led to the highest e.e. for nicotine **red-3** (79 % e.e. (*R*)) with a nicotine **red-3** to alcohol **red-3-ol** ratio of 6.6 : 1.

For the stereoinversion of (*S*)-nicotine **red-3** using the cascade reaction, MAO-N D5 was combined with [Cp\*Ir(biot-*p*-L)Cl]·Sav S112A-K121T and a catalase. After 14 hours, *(R)*-nicotine was formed from (*S*)-nicotine in >99% e.e. (*R*) at 65% yield with ~10% yield of alcohol **3-red-ol** (35% e.e.; Table 1, entry 14).

**Activity screen of ATHases by a coupled colorimetric assay** Horse-Radish Peroxidase (HRP) has found broad use in coupled assays both in medicine and in biotechnology [39]. In this context, a (pro)-dye is rapidly oxidized by HRP, consuming H<sub>2</sub>O<sub>2</sub> and leading to an optical signal. We speculated that substitution of the catalase by HRP may allow to estimate the performance of the ATHase in the cascade reaction, Figure 4.

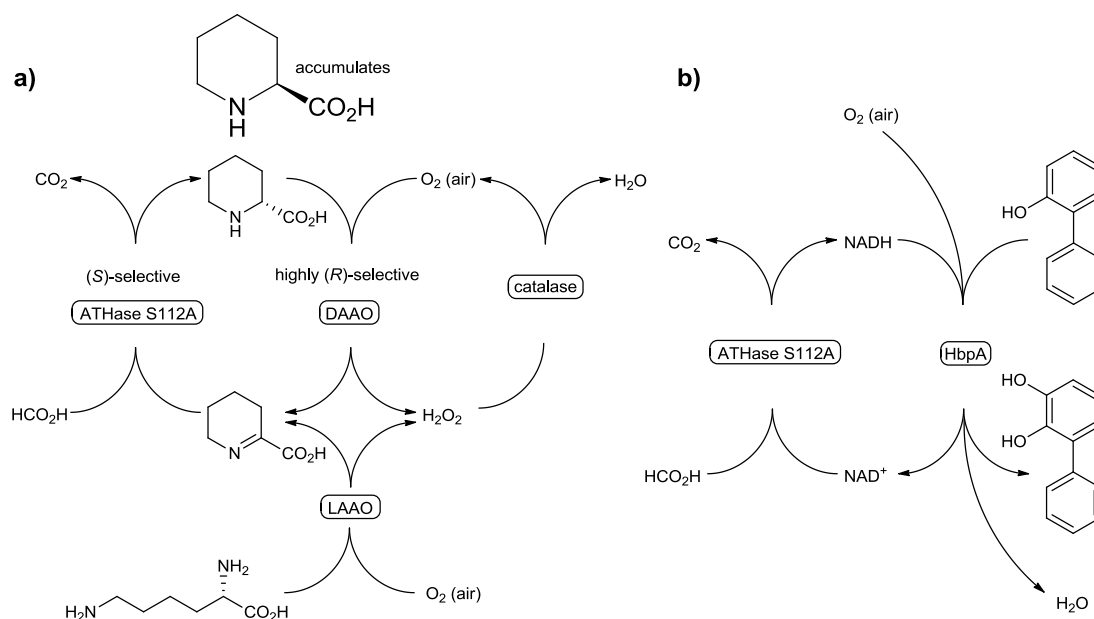


**Figure 4. Colorimetric assay for the determination of the ATHase activity in an enzyme cascade.** The activity of the ATHase in the enzyme cascade is revealed by Horse-Radish Peroxidase (HRP): the H<sub>2</sub>O<sub>2</sub> generated by MAO-N reacts with a dye (scopoletin, red) in the presence of HRP and leads to bleaching of scopoletin.

Comparison of the kinetic constants ( $k_{\text{cat}} > 250 \text{ min}^{-1}$ ,  $K_{\text{M}} < 1 \text{ mM}$  for MAO-N D9) indicate that the ATHase step is rate limiting in the enzyme cascade under the considered reaction conditions (see SI). Thus, the HRP-generated optical signature allows to compare the relative ATHase activities depending on the Sav isoform.

After screening several dyes/prodyes, we identified scopoletin as a suitable substrate which loses its fluorescence upon oxidation: As the MAO-N variant is highly (*S*)-selective, the optical readout generated by the oxidation of scopoletin correlates to the production of (*S*)-**red-1**. As the ATHases display modest selectivities ( $E$  values  $\leq 4$ ), sufficient (*S*)-**red-1** is produced, allowing the implementation of the coupled assay. By following the decrease in fluorescence of scopoletin in the ATHase / MAO / HRP coupled-assay, imine-reductases with strongly increased activity (compared to S112T) could be identified. The ATHase [Cp\*Ir(biot-*p*-L)Cl]-K121A displayed kinetic constants of  $k_{\text{cat}(\text{app})} 20 \text{ min}^{-1}$  ( $\pm 3 \text{ min}^{-1}$ ),  $K_{\text{M}(\text{app})} 12 \text{ mM}$  ( $\pm 3 \text{ mM}$ ),  $K_{\text{i}} 20 \text{ mM}$  ( $\pm 4 \text{ mM}$ ). The relative order of activities in the assay was in good agreement with the rates as determined by HPLC, albeit for high activities the relative activity was underestimated by the assay.

**Combination of ATHase with AAOs for the formation of L-pipecolic acid**  
 Encouraged by the results with MAO, we sought to combine ATHases in more complex cascades with other oxidases. For this purpose, we selected L-lysine (**4**) which, upon oxidation with an L-aminoacid oxidase (LAAO) and reduction with the ATHase, yields pipecolic acid (**5**). The enantiomeric excess of **5** can be upgraded by combining the LAAO / ATHase / catalase with a D-selective aminoacid oxidase (DAAO), Figure 5a [40,41].



**Figure 5. Expanding the concept of orthogonal redox cascades to include other enzymes.** a) Production of L-pipecolic acid from L-lysine requires the combination of an ATHase with an (L)- and a (D)-aminoacid oxidase (AAO). Catalase is added to decompose the  $\text{H}_2\text{O}_2$  generated by the AAOs. b) Concurrent regeneration of NADH by the ATHase in the presence of a monooxygenase.

In a first round of screening, the performance of a range of ATHase mutants was screened for the reduction of  $\Delta^1$ -piperidine-2-carboxylic acid generated *in situ* by oxidation of L-Lysine with LAAO (from snake venom, *Crotalus atrox*). The Ir-cofactor  $[\text{Cp}^*\text{Ir}(\text{Biot-}p\text{-L})\text{Cl}]$  in the absence of Sav showed only little conversion (TON = 11) and led to *racemic* product, highlighting again the inactivation of the naked catalyst by LAAO, Table 1, entry 15. The ATHase in contrast showed promising conversions (up to 90%; TON = 48), albeit with low enantioselectivity. The most (S)-selective mutant (Sav S112A; TON = 47; 29% e.e.) was selected for further studies, Table 1, entry 16 and SI. Combining the system with a DAAO (from porcine kidney) allowed to upgrade the enantiomeric excess of the L-pipecolic acid

by re-oxidizing the D-enantiomer: under the chosen conditions, 86% e.e. in favour of the L-4 was obtained, Figure 5a, Table 1, entry 17. The formation of pipecolic acid was unambiguously established by 2D-NMR analysis of the reaction mixtures using L-Lysine-2-<sup>13</sup>C as substrate (Table 1, entries 15-17 and SI).

**NADH regeneration for monooxygenases** The chemical- and electrochemical recycling of NAD(P)H and analogues has been intensively investigated as an alternative to enzymatic regeneration [12, 42-49]. In this context, [Cp\*Rh(bipy)Cl] has emerged as redox mediator or catalyst of choice. However, in the presence of the downstream enzyme, mutual inactivation is commonly encountered [44,45]. To test the validity of the molecular compartmentalization concept outlined in Figure 1, we investigated the regeneration of NADH in the presence of an NADH-dependent enzyme using an ATHase. Although significantly more active than [Cp\*Rh(bipy)Cl] for the NADH regeneration in the absence of an NADH-dependent enzyme, [Cp\*Ir(Biot-*p*-L)Cl] was rapidly deactivated in the presence of 2-hydroxybiphenyl monooxygenase (HbpA from *Pseudomonas azaleica*, EC1.14.13.44, an NADH- and flavin dependent enzyme). In the presence of Sav, however, the mutual inactivation of [Cp\*Ir(Biot-*p*-L)Cl] and HbpA was efficiently prevented and robust hydroxylation activity was achieved (Table 1, compare entries 18, 19, Figure 5b). We conclude that Sav shields the ATHase from the downstream enzyme, allowing the NADH regeneration with formate as hydride source ( $K_{M(\text{app})} = 165 \mu\text{M}$  ( $\pm 6 \mu\text{M}$ ),  $k_{\text{cat}(\text{app})} = 1.37 \text{ min}^{-1}$  ( $\pm 0.01 \text{ min}^{-1}$ ). Full conversion of 2-hydroxybiphenyl (**6**) to 2,3-dihydroxybiphenyl (**7**) was accomplished in 2 h with a crude enzyme extract, Figure 5b and Table 1, entries 18, 19 and SI.

The system could be run either in pure aqueous phase or as a biphasic system with 1-decanol functioning as a substrate reservoir and product sink, thereby highlighting the applicability of the ATHase under a variety of reaction conditions. The biphasic system displayed again strong inactivation in the absence of Sav, whereas a TON of > 100 (vs. [Cp\*Ir(Biot-*p*-L)Cl]) was achieved when Sav was present.

**Outlook** We have demonstrated herein that an ATHase consisting of [Cp\*Ir(Biot-*p*-L)Cl] anchored within a streptavidin isoform is complementary and compatible with a variety of redox enzymes relying on NADH, FADH<sub>2</sub> and heme cofactors. Such artificial metalloenzymes displays attractive features which are reminiscent of both bio- and chemocatalysts: precious metal reactivity, genetic optimization potential and well-defined second coordination sphere provided by a protein scaffold. This

latter feature could be further exploited towards the immobilization of the entire enzyme cascade.

In order to optimize such cascades, directed evolution protocols are highly desirable. With this goal in mind, we have shown that the ATHase can be integrated with a colorimetric coupled assay, leading to the identification of a genetically improved ATHase. These proof-of-principle examples open fascinating perspectives towards complementing bio-catalytic cascades with molecularly compartmentalized organometallic catalysts.

## Methods

### Typical procedure for a double stereoselective deracemisation with MAO-N/ATHase (analytical scale)

The following stock solutions were prepared: Catalase from bovine liver (50 kU/mL) was dissolved in MOPS/sodium formate buffer (0.6 M in MOPS, 1.5 M in sodium formate, pH adjusted with aq. KOH to pH 7.8). Sav S112T (16.44 mg/mL, 0.75 mM free binding sites, assuming 3 free binding sites per tetramer) was dissolved in the catalase containing buffer. [IrCp\*(Biot-*p*-L)Cl] was dissolved in DMF (37.5 mM). Affinity purified MAO-N D9 (buffer exchange with MOPS, 0.6 M, pH adjusted with KOH to 7.8) was diluted in MOPS buffer (0.6 M, pH adjusted with KOH to 7.8) to a concentration of 0.38 mg/mL. Substrate stock was prepared by dissolving the hydrochloride of **1-ox** in H<sub>2</sub>O (1M). The ATHase was prepared by adding [IrCp\*(Biot-*p*-L)Cl]-stock (10 μL/mL) to the Sav-stock solution. MAO-N-stock was placed in 1.5 mL PP-tubes (100 μL) and ATHase was added (100 μL). The reactions were initiated by addition of substrate stock solution (7.5 μL) and incubated at 37 °C and 250 rpm. For work-up aq. NaOH-solution was added (50 μL of a 10 M solution) and the mixture extracted with CH<sub>2</sub>Cl<sub>2</sub> (1 × 1 mL). The organic phase was dried over Na<sub>2</sub>SO<sub>4</sub> and analysed by HPLC (see SI).

## Acknowledgments

This work was generously supported by a Marie Curie ITN (Biotrains FP7-ITN-238531) in addition, TRW thanks the SNF (grant 200020\_126366) as well as the NCCR Nano for financial support. NJT thanks the Royal Society for a Wolfson Research Merit Award, FH thanks Prof. Andreas Schmid, Dortmund University of Technology, for the kind provision of HbpA. We thank M. Corbett and S. Willies for

helpful advice, R. Pfalzberger for help with the graphic material and Umicore for a precious metal loan.

### Author contributions

V. K., F. H., N. T. and T. W. conceived the catalytic cascades. V. K., F. H., N. T. and T. W. supervised the project. V. K., Y. W., M. D., D. G., E. C. and T. Q. performed the experiments. V. K., Y. W., M. D., D. G., E. C., T. Q., F. H., N. T. and T. W. analyzed the data. V. K., F. H., N. T. and T. W. co-wrote the paper. V. K., Y. W., M. D., D. G. and L. K. contributed materials. D.H. analysed the conversion of  $^{13}\text{C}$ -labelled lysine by 2D NMR.

**Supplementary information** is available free of charge under...

### References

- [1] Wörsdörfer, B., Woycechowsky, K. J. & Hilvert, D. Directed evolution of a protein container. *Science*, **331**, 589-592 (2011).
- [2] Choudhary, S., Quin, M. B., Sanders, M. A., Johnson, E. T. & Schmidt-Dannert, C. Engineered protein nano-compartments for targeted enzyme localization. *PLoS ONE*, **7**, e33342 (2012).
- [3] Dueber, J. E. *et al.* Synthetic protein scaffolds provide modular control over metabolic flux. *Nat. Biotechnol.* **27**, 753-759 (2009).
- [4] Keasling, J. D. Synthetic biology for synthetic chemistry. *ACS Chem. Biol.* **3**, 64-76 (2008).
- [5] Bromley, E. H. C., Channon, K., Moutevelis, E. & Woolfson, D. N. Peptide and protein building blocks for synthetic biology: from programming biomolecules to self-organized biomolecular systems. *ACS Chem. Biol.* **3**, 38-50 (2008).
- [6] Weissman, K. J. & Leadlay, P. F. Combinatorial biosynthesis of reduced polyketides. *Nat. Rev. Microbiol.* **3**, 925-936 (2005).
- [7] Mutti, F. G. *et al.* Simultaneous iridium catalysed oxidation and enzymatic reduction employing orthogonal reagents. *Chem. Commun.* **46**, 8046-8048 (2010).
- [8] Haak, R. M. *et al.* Dynamic kinetic resolution of racemic  $\beta$ -haloalcohols: direct access to enantioenriched epoxides. *J. Am. Chem. Soc.* **130**, 13508-13509 (2008).
- [9] Maid, H. *et al.* Iron catalysis for in situ regeneration of oxidized cofactors by activation and reduction of molecular oxygen: a synthetic metalloporphyrin as a biomimetic NAD(P)H oxidase. *Angew. Chem. Int. Ed.* **50**, 2397-2400 (2011).



- [10] Wasilke, J.-C., Obrey, S. J., Baker, R. T. & Bazan, G. C. Concurrent tandem catalysis. *Chem. Rev.* **105**, 1001-1020 (2005).
- [11] Zhou, J., Recent advances in multicatalyst promoted asymmetric tandem reactions. *Chem. Asian J.* **5**, 422-434 (2010).
- [12] Betanzos-Lara, S. *et al.* Organometallic ruthenium and iridium transfer-hydrogenation catalysts using coenzyme NADH as a cofactor. *Angew. Chem. Int. Ed.* **51**, 3897-3900 (2012).
- [13] Wingstrand, E., Laurell, A., Fransson, L., Hult, K. & Moberg, C. Minor enantiomer recycling: metal catalyst, organocatalyst and biocatalyst working in concert. *Chem. Eur. J.* **15**, 12107-12113 (2009).
- [14] Simons, C., Hanefeld, U., Arends, I. W. C. E., Maschmeyer, T. & Sheldon, R. A. Towards catalytic cascade reactions: asymmetric synthesis using combined chemo-enzymatic catalysts. *Top. Catal.* **40**, 35-44 (2006).
- [15] Wieczorek, B., Covalent anchoring of a racemization catalyst to CALB-beads: towards dual immobilization of DKR catalysts. *Tetrahedron Lett.* **52**, 1601-1604 (2011).
- [16] Rocha-Martín, J., de las Rivas, B., Muñoz, R., Guisán, J. M. & López-Gallego, F. Rational co-immobilization of bi-enzyme cascades on porous supports and their applications in bio-redox reactions with in situ recycling of soluble cofactors. *ChemCatChem*, doi: 10.1002/cctc.201200146 (2012).
- [17] Hanfeld, U., Gardossi, L. & Magner, E. Understanding enzyme immobilisation. *Chem. Soc. Rev.* **38**, 453-468 (2009).
- [18] Brady, D. & Jordaan, J. Advances in enzyme immobilisation. *Biotechnol. Lett.* **31**, 1639-1650.
- [19] Mateo, C., Palomo, J. M. Fernandez-Lorente, G., Guisan, J. M. & Fernandez-Lafuente, R. Improvement of enzyme activity, stability and selectivity via immobilization techniques. *Enzyme Microb. Tech.* **40**, 1451-1463 (2007).
- [20] Lopez-Gallego, F. & Schmidt-Dannert, C. Multi-enzymatic synthesis. *Curr. Opin. Chem. Biol.* **14**, 174-183 (2010).
- [21] Pàmies, O. & Bäckvall, J.-E. Combination of enzymes and metal catalysts. A powerful approach in asymmetric catalysis. *Chem. Rev.* **103**, 3247-3261 (2003).
- [22] Kim, Y., Park, J. & Kim, M.-J. Dynamic kinetic resolution of amines and amino acids by enzyme-metal cocatalysis. *ChemCatChem.* **3**, 271-277 (2011).
- [23] Yusop, R. M., Unciti-Broceta, A., Johansson, E. M. V., Sánchez-Martin, R. M. & Bradley, M. Palladium-mediated intracellular chemistry. *Nat. Chem.* **3**, 239-243 (2011).
- [24] Foulkes, J. M., Malone, K. J., Coker, V. S., Turner, N. J. & Lloyd, J. R. Engineering a biometallic whole cell catalyst for enantioselective deracemization

reactions. *ACS Catal.* **1**, 1589-1594 (2011).

[25] Lu, Y., Yeung, N., Sieracki, N. & Marshall, N. M. Design of functional metalloproteins. *Nature* **460**, 855-862 (2009).

[26] Ward, T. R. Artificial metalloenzymes based on the biotin-avidin technology: enantioselective catalysis and beyond. *Acc. Chem. Res.* **44**, 47-57 (2011).

[27] Bos, J., Fusetti, F., Driessen, A. J. M. & Roelfes, G. Enantioselective artificial metalloenzymes by creation of a novel active site at the protein dimer interface. *Angew. Chem. Int. Ed.* **51**, 7472-7475 (2012).

[28] Jing, Q. & Kazlauskas, R. J. Regioselective hydroformylation of styrene using rhodium-substituted carbonic anhydrase. *ChemCatChem* **2**, 953-957 (2010).

[29] Podtetenieff, J., Taglieber, A., Bill, E., Reijerse, E. J. & Reetz, M. T. An artificial metalloenzyme: creation of a designed copper binding site in a thermostable protein. *Angew. Chem. Int. Ed.* **49**, 5151-5155 (2010).

[30] Deuss, P. J., den Heeten, R., Laan, W. & Kamer, P. C. J. Bioinspired catalyst design and artificial metalloenzymes. *Chem. Eur. J.* **17**, 4680-4698 (2011).

[31] Ueno, T., Abe, S., Yokoi, N. & Watanabe, Y. Coordination design of artificial metalloproteins utilizing protein vacant space. *Coord. Chem. Rev.* **251**, 2717-2731 (2007).

[32] Matsuo, T. *et al.* Meso-Unsubstituted iron corrole in hemoproteins: remarkable differences in effects on peroxidase activities between myoglobin and horseradish peroxidase, *J. Am. Chem. Soc.* **131**, 15124-15125 (2009).

[33] Turner, N. J. Directed evolution drives the next generation of biocatalysts. *Nat. Chem. Biol.* **5**, 567-573 (2009).

[34] Turner, N. J. Enantioselective oxidation of C-O and C-N bonds using oxidases. *Chem. Rev.* **111**, 4073-4087 (2011).

[35] Dürrenberger, M. *et al.* Artificial transfer hydrogenases for the enantioselective reduction of cyclic imines. *Angew. Chem. Int. Ed.* **50**, 3026-3029 (2011).

[36] Rowles, I., Malone, K. J., Etchells, L. L., Willies, S. C. & Turner, N. J. Directed evolution of the enzyme monoamine oxidase (MAO-N): highly efficient chemo-enzymatic deracemisation of the alkaloid ( $\pm$ )-crispine A. *ChemCatChem* doi: 10.1002/cctc.201200202 (2012).

[37] Heiden, Z. M. & Rauchfuss, T. B. Homogeneous catalytic reduction of dioxygen using transfer hydrogenation catalysts. *J. Am. Chem. Soc.* **129**, 14303-14310 (2007).

[38] Brandänge, S., Lindblom, L., Pilotti, Å. & Rodriguez, B. Ring-chain tautomerism of pseudooxynicotine and some other iminium compounds. *Acta Chem. Scand. B* **37**, 617-622 (1983).

- [39] Truppo, M. D., Escalettes, F. & Turner, N. J. Rapid determination of both the activity and enantioselectivity of ketoreductases. *Angew. Chem. Int. Ed.* **47**, 2639-2641 (2008).
- [40] Yasuda, M., Ueda, M., Muramatsu, H., Mihara, H. & Esaki, N. Enzymatic synthesis of cyclic amino acids by *N*-methyl-L-amino acid dehydrogenase from *Pseudomonas putida*. *Tet. Asymm.* **17**, 1775-1779 (2006).
- [41] Gatto, G. J., Boyne, M. T., Kelleher, N. L. & Walsh, C. T. Biosynthesis of pipercolic acid by RapL, a lysine cyclodeaminase encoded in the rapamycin gene cluster. *J. Am. Chem. Soc.* **128**, 3838-3847 (2006).
- [42] Hollmann, F., Hofstetter, K. & Schmid, A. Non-enzymatic regeneration of nicotinamide and flavin cofactors for monooxygenase catalysis. *Trends Biotechnol.* **24**, 163-171 (2006).
- [43] Hollmann, F., Arends, I. W. C. E. & Buehler, K. Biocatalytic redox reactions for organic synthesis: nonconventional regeneration methods. *ChemCatChem* **2**, 762-782 (2010).
- [44] Poizat, M., Arends, I. W. C. E. & Hollmann, F. On the nature of mutual inactivation between  $[\text{Cp}^*\text{Rh}(\text{bpy})(\text{H}_2\text{O})^{2+}]$  and enzymes – analysis and potential remedies. *J. Mol. Catal. B* **63**, 149-156 (2010).
- [45] Hildebrand, F. & Lütz, S. Stable electroenzymatic processes by catalyst separation. *Chem. Eur. J.* **15**, 4998-5001 (2009).
- [46] Haquette, P. *et al.* Chemically engineered papain as artificial formate dehydrogenase for NAD(P)H regeneration. *Org. Biomol. Chem.*, **9**, 5720–5727 (2011).
- [47] Maenaka, Y., Suenobu, T. & Fukuzumi, S. Efficient catalytic interconversion between NADH and  $\text{NAD}^+$  accompanied by generation and consumption of hydrogen with a water-soluble iridium complex at ambient pressure and temperature. *J. Am. Chem. Soc.* **134**, 367-374 (2012).
- [48] Canivet, J., Süß-Fink, G. & Štěpnička, P. Water-soluble phenanthroline complexes of rhodium, iridium and ruthenium for the regeneration of NADH in the enzymatic reduction of ketones. *Eur. J. Inorg. Chem.* 4736-4742 (2007).
- [49] Ryan, J. D. Fish, R. H. & Clark, D. S. Engineering cytochrome P450 enzymes for improved activity towards biomimetic 1,4-NADH cofactors. *ChemBioChem* **9**, 2579-2582 (2008).

# **New Synthetic Cascades by Combining Biocatalysts with Artificial Metalloenzymes**

V. Köhler, Y. M. Wilson, M. Dürrenberger, D. Ghislieri, E. Churakova, T. Quinto, L.

Knörr, D. Häussinger, F. Hollmann,\* N. J. Turner,\* and T. R. Ward\*

**Supplementary information**

## General Information

Chemicals were purchased from Sigma-Aldrich, Acros, Fluka and TCI and used as received. Streptavidin (Sav) mutants were produced, purified and characterised as previously described [1]. The Sav used in this work and on which all variants were based was T7-tagged core Sav described by Gallizia et al. [2] and here we refer to this as wild-type Sav. The corresponding ATHase is also referred to as wild-type (WT). For a detailed synthesis procedure of [Cp\*Ir(Biot-*p*-L)Cl] see reference [3]. Commercial enzyme preparations were purchased from Sigma. MAO-N mutants used in this study are described elsewhere [4,5]. (*rac*)-1-Methyl-1,2,3,4-tetrahydroisoquinoline was prepared from 1-methyl-3,4-dihydroisoquinoline hydrochloride hydrate by reduction with NaBH<sub>4</sub> in MeOH. 2-Cyclohexyl-1-pyrroline was prepared according to literature procedures [6]. (*rac*)-2-Cyclohexylpyrrolidine was prepared from 2-cyclohexyl-1-pyrroline by reduction with NaBH<sub>4</sub> in MeOH. Pseudoxyntocine was prepared as described in reference [7]. 2,3-Dihydroxybiphenyl was a kind gift from Prof. Dr. Andreas Schmid (TU Dortmund, Dortmund, Germany). L-lysine-<sup>13</sup>C<sub>2</sub> HCl (99% <sup>13</sup>C) was obtained from Sigma. NMR experiments were performed at 25°C (MeOH calibration) on Bruker Avance III NMR spectrometers operating at 600, 500 or 400 MHz proton frequency. All were equipped with direct (600 and 400 MHz) or inverse (500 MHz) dual channel, broadband probe-heads with *z*-gradients. Chemical shifts were referenced to residual proton solvent peaks (4.773 ppm for H<sub>2</sub>O, 7.26 for CHCl<sub>3</sub>). The quantitative constant time HSQC experiment was performed using 2048 data points in the F2 and 1024 data points in the F1 dimension, corresponding to acquisition times of 155 ms in F2 and 34 ms in F1. Each increment was recorded with 8 scans resulting in a total experiment time of 2 h 45 min. HPLC measurements were performed on Agilent (or hp) machines equipped with modules from the 1100 and 1200 series and diode array detectors, if not indicated otherwise. HPLC columns were used with the appropriate guard columns, if not indicated otherwise. Column and conditions are indicated for each compound separately. GC measurements were performed on Agilent GCs of the 6890 series equipped with FIDs.

## MAO-N Protein expression

Aqueous solutions of dithiothreitol (8 μL, 200 mM) followed by pET-16b plasmid DNA containing the MAO-N gene variant (2 μL, 49-138 ng/μL) were added to ultra

competent BL21(DE3)pLysS *E. coli* cells (produced in-house) (100  $\mu$ L). The mixture was stored on ice for 15 min and the transformed cells were plated onto LB-Lennox agar plates containing ampicillin (279  $\mu$ M), chloramphenicol (100  $\mu$ M) and glucose (111 mM), and incubated overnight at 37 °C. The culture and preculture media were composed of bactotryptone (from BD, 20 g/L), Na<sub>2</sub>HPO<sub>4</sub> (9.16 mM), KH<sub>2</sub>PO<sub>4</sub> (7.35 mM), NaCl (136.9 mM) and bacto yeast extract (from Merck, 15 g/L). A single colony was inoculated to the preculture medium (50 mL), which contained ampicillin (279  $\mu$ M), chloramphenicol (100  $\mu$ M), and glucose (55.5 mM), and was incubated overnight on an orbital shaker (37 °C, 250 rpm). The preculture was diluted 1 to 1000 into fresh media (600 mL), containing ampicillin (279  $\mu$ M), chloramphenicol (100  $\mu$ M) and glucose (1.1 mM). The cells were grown at 30 °C until an OD<sub>600</sub> of 2–3 was reached. Expression was induced by addition of isopropyl  $\beta$ -D-1-thiogalactopyranoside (600  $\mu$ L, 1 M). The cells were harvested approximately 10 hours after induction by centrifugation (3600  $\times$  g, 10 min, 4 °C). The supernatant was discarded and the pellet was frozen at -20 °C until purification. Protein expression was confirmed by SDS-PAGE analysis.

### **MAO-N Protein purification**

The cell pellet was thawed on ice and resuspended in potassium phosphate buffer (100 mM, pH 7.7, 20 mL/g wet cell pellet) containing DNase I (from Roche, 20 U/mL), lysozyme (40 kU/mL) and phenylmethylsulfonyl fluoride (1 mM). The resuspended cells were incubated at 30 °C, 100 rpm for 30-60 min. The proteic extract was centrifuged (18 000  $\times$  g, 30 min, 4 °C) to remove cell debris and filtered (0.2  $\mu$ m filters, Sarstedt). The buffers for purification by nickel affinity column (1 mL HiTrap Chelating HP, GE Healthcare) were: buffer A: potassium phosphate buffer (100 mM, pH 7.7) containing sodium chloride (300 mM) and buffer B: potassium phosphate buffer (100 mM, pH 7.7) containing sodium chloride (300 mM) and imidazole (1 M). The column was pre-equilibrated with buffer A before loading of the protein sample. The bound protein was washed with buffer A (minimum wash volume 30 mL), followed by 20 % buffer B (minimum wash volume 10 mL) and eluted in 35 % buffer B. The eluted sample was concentrated to 2.5 mL using a centrifugal filter unit (Amicon Ultra-15, 30000 MWCO, from Millipore, 3600  $\times$  g, 2-5 min) and desalted on a PD-10 desalting column (GE Healthcare) pre-equilibrated with MOPS buffer (25 mL, 0.6 M, pH 7.8). Concentration and filtration were

repeated using a fresh filter unit and PD-10 column. The absorbance of the sample at 280 nm was measured using a Nanodrop 1000 (Witec AG). The following factors were used to correct the concentration values obtained from the Nanodrop measurement: 1.691 for MAO-N D9 and 1.787 for MAO-N D5 (calculated from the amino acid sequence using the ExpASy ProtParam tool from the Swiss Institute of Bioinformatics). This corresponds to molar extinction coefficients of  $99350 \text{ M}^{-1}\text{cm}^{-1}$  for MAO-N-5 and  $93850 \text{ M}^{-1}\text{cm}^{-1}$  for MAO-N D9, assuming all cysteine residues are reduced.

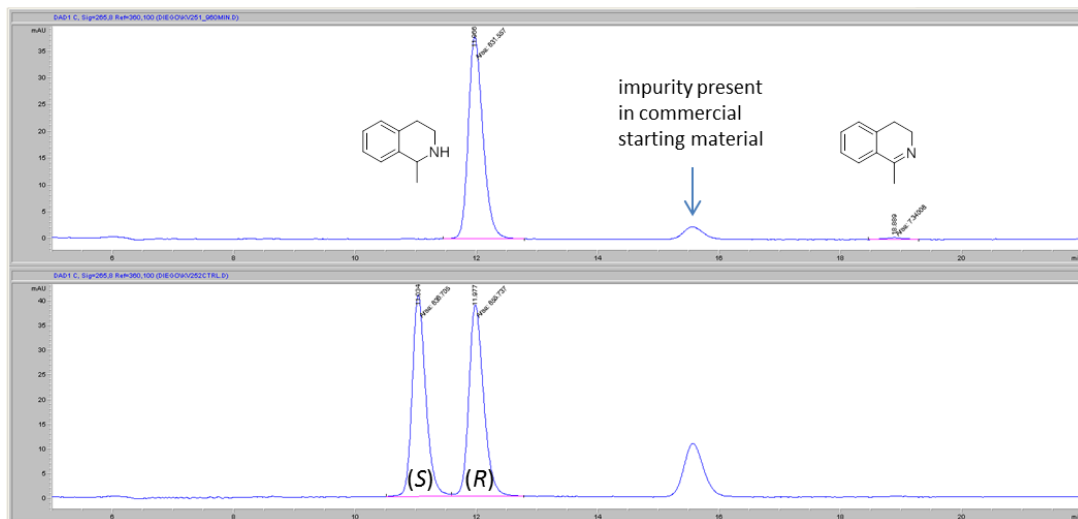
## **Concurrent catalysis reactions with MAO-N/ATHase**

### **Reactions on a preparative scale**

#### Reduction of 1-methyl-3,4-dihydroisoquinoline (**1-ox**) with MAO-N D9/ATHase (S112T)

The following stock solutions were prepared: Buffer A: 0.6 M MOPS, 3 M  $\text{NaHCO}_2$ , pH adjusted with aqueous KOH to 7.8. Buffer B: 0.6 M MOPS, pH adjusted with aqueous KOH to 7.8. Buffer C: Catalase (from bovine liver, 11 kU/mg, Sigma C40) was dissolved to a final concentration of 12.5 kU/mL in buffer A; note: in all later experiments referring to buffer C and described below, 50 kU/mL catalase were used.  $[\text{Cp}^*\text{Ir}(\text{Biot-}p\text{-L})\text{Cl}]$  (1.78 mg, 2.22  $\mu\text{mol}$ ) was dissolved in DMF (59.1  $\mu\text{L}$ ) resulting in a final concentration of approximately 37.5 mM. Preparation of ATHase: S112T (42.3 mg Sav S112T, 643 nmol tetramer by weight; note: three free binding sites per tetramer were assumed to ensure the presence of sufficient free binding sites - the actual number of free binding sites is usually higher, *vide infra*) was dissolved in buffer C (2.573 mL), the solution of  $[\text{Cp}^*\text{Ir}(\text{Biot-}p\text{-L})\text{Cl}]$  (25.7  $\mu\text{L}$ ; corresponds to two free binding sites per biotinylated iridium complex) was added and the mixture gently agitated. The ATHase was prepared immediately before addition to the MAO-N preparation. MAO-N D9 solution (2.5 mL of a solution of 0.38 mg/mL in 0.6 M MOPS (pH 7.8) was placed in a 50 mL Falcon tube. ATHase (2.5 mL) was added, followed by 1-methyl-3,4-dihydroisoquinoline hydrochloride (187.5  $\mu\text{L}$  of a 1 M solution in  $\text{H}_2\text{O}$ ). The Falcon tube was incubated in a lying position at 250 rpm and 37 °C. A 100  $\mu\text{L}$  sample was taken after 16 hours, treated with aq. NaOH (50  $\mu\text{L}$  of a 10 N solution) and extracted with  $\text{CH}_2\text{Cl}_2$  (1  $\times$  1 mL). The extracts were dried with  $\text{Na}_2\text{SO}_4$  and analysed by chiral phase HPLC, showing a conversion of 99 %

(considering the experimentally determined response factor) and an e.e. of > 99 % (Figure S1; Daicel IC 250 × 4.6 mm, 5 μm; hexane/*i*-PrOH/HNEt<sub>2</sub> = 97/3/0.03—0.06, 1 mL/min, 25 °C, 265 nm; T<sub>R</sub> 11.0 min (*R*)-1-methyl-1,2,3,4-tetrahydroisoquinoline), 12.0 min (*S*)-1-methyl-1,2,3,4-tetrahydroisoquinoline), 18.9 min (1-methyl-3,4-dihydroisoquinoline). Workup was performed after 17 hours incubation: The solution was transferred to a separating funnel, the reaction container rinsed with water (3 × 2 mL) and the washings were combined with the reaction mixture. *tert*-Butyl methyl ether (10 mL, abbreviated TBME in the following) was added, followed by aqueous NaOH (1.2 mL of a 10 N solution). Phase separation after shaking was incomplete and the formation of an additional gel-like layer was observed. Extraction was repeated (4 × 10 mL). The combined organic extracts were washed with brine, which did not improve phase separation. The aqueous layer and the gel-like part of the organic layer were therefore centrifuged in 2 mL PP-tubes for 2 min at 21100 x *g*. The organic layers were combined and dried with Na<sub>2</sub>SO<sub>4</sub>. Volatiles were removed at the rotary evaporator to afford a nearly colourless liquid (25.8 mg, which contained 1.7 weight % DMF (determined by <sup>1</sup>H NMR, Figure S2), 93.8 % yield after correction.



**Figure S1.** Chiral phase HPLC trace of 1-methyl-3,4-dihydroisoquinoline reduction with ATHase (Sav S112T) and MAO-N D9 showing the signals for 1-methyl-1,2,3,4-tetrahydroisoquinoline (top) after 16 hours reaction time and, for comparison, a racemic sample (bottom).



## Reactions with MAO-N /ATHase on an analytical scale

(rac)-1-Methyltetrahydroisoquinoline (rac)-1-red and 1-methyl-3,4-dihydroisoquinoline (1-ox)

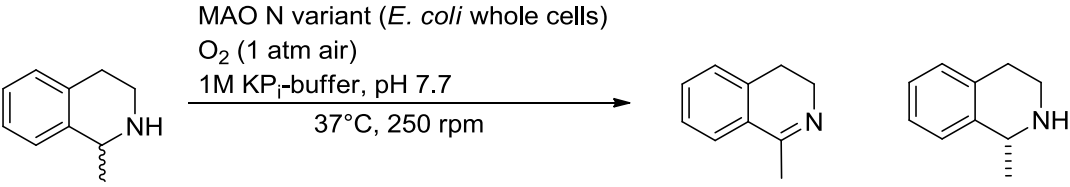
The analytical reactions were carried out with the same buffer (consider note regarding buffer C, on page 5 of the SI) and substrate concentrations as described above. (Initially concentrations were varied to find the optimal reaction conditions.) Analytical reactions were conducted in the following format: 100  $\mu$ L ATHase preparation was added to 100  $\mu$ L MAO-N preparation in a 1.5 mL PP-tube and the reactions were initiated by the addition of substrate (7.5  $\mu$ L of either a 1 M 1-methyl-3,4-dihydroisoquinoline hydrochloride hydrate in H<sub>2</sub>O, or a 1 M 1-methyl-1,2,3,4-tetrahydroisoquinoline (solution prepared in 1 N HCl). The tubes were incubated in a lying position at 250 rpm and 37 °C for the appropriate time. Subsequently the tube was removed from the incubator and aqueous NaOH (50  $\mu$ L of a 10 N solution) was added, immediately followed by CH<sub>2</sub>Cl<sub>2</sub> (1 mL). Mixing was achieved by means of a vortex mixer. The organic phase was separated, dried with Na<sub>2</sub>SO<sub>4</sub> and analysed by chiral phase HPLC. The experiment cited in the main text in Table 1, entry 5 was carried out with 0.5 mol% ATHase and analysed after 24 hours. For experiments cited in the main text in Table 1, entries 6, 7, see >Time course of concurrent catalysis reactions with MAO-N D9/ATHase (Sav S112T or Sav S112K) in the reduction of 1-methyl-3,4-dihydroisoquinoline (1-ox).

## Evaluation of MAO-N mutants as whole cell biocatalysts

In the initial stages of the project a suitable MAO-N variant for the oxidation of (*S*)-1-methyl-1,2,3,4-tetrahydroisoquinoline was identified by performing biotransformations with (*rac*)-1-methyl-1,2,3,4-tetrahydroisoquinoline, where the biocatalyst was employed in the form of wet *E. coli* cells expressing the respective MAO-N variant. (*rac*)-1-methyl-1,2,3,4-tetrahydroisoquinoline (5 mg in 3.5 mL KP<sub>i</sub> buffer (1M, pH 7.7) was placed in a 15 mL PP-tube containing cell pellet of *E. coli* cells expressing MAO-N (500 mg of cell pellet). The reactions were incubated in a lying position in a shaking incubator at 37 °C and 250 rpm. For HPLC analysis, samples (300  $\mu$ L) were taken in 30 minute intervals and treated as follows: Aqueous NaOH-solution (20  $\mu$ L, 10 M) was added to the aliquot in a 1.5 mL PP-tube followed by *tert*-butyl methyl ether (1  $\times$  1 mL). After vigorous mixing by means of a vortex

mixer the sample was centrifuged at  $16100 \times g$  rpm for 1 minute. The organic phase was separated, dried with  $\text{MgSO}_4$  and analysed by chiral HPLC. These tests, which do not take the concentration of active enzyme in the whole cell biocatalyst into account, suggested variant MAO-N D9 as a good starting point for further investigations (Table S5).

**Table S5.** Catalysis results for the kinetic resolution of (*rac*)-**1-red**. Conversion was calculated by comparison of the area of **1-red** to **1-ox** by chiral HPLC analysis under consideration of the experimentally determined response factor.



MAO-N variant	time [h]	conversion [%]	e.e. [%]
MAO-N D5	2	43	85
MAO-N D9	0.5	50	>99

### Kinetic studies of MAO-N (part not included in the published paper)

Chromatogenic solutions for kinetic determination:

**1) Substrate mix:**

(*rac*)-MTQ and (*S*)-MTQ stock solutions were prepared in water to cover a substrate range between 0.02 and 40 mM.

**2) Colourimetric mix:**

2 mg Horseradish Peroxidase

60  $\mu\text{L}$  1 M aminoantipyrine in water

200  $\mu\text{L}$  1M tribromohydroxybenzoic acid in DMSO

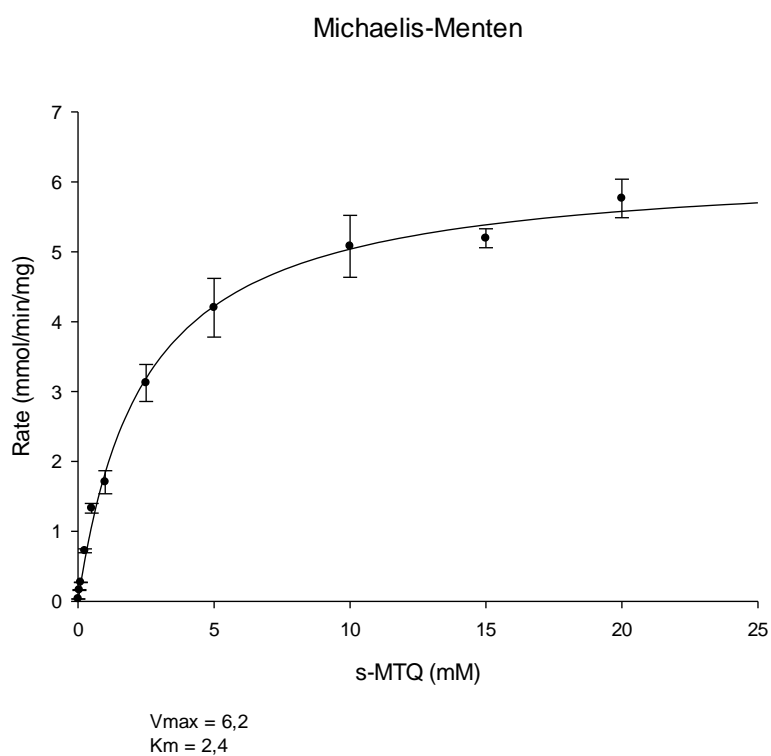
adjust volume to 10 mL with 1.8 M MOPS buffer pH 7.8

100  $\mu\text{L}$  of solution **1**) was mixed with 50  $\mu\text{L}$  of solution **2**) directly in the 96 well plates. To the preformed mixture, 50 $\mu\text{L}$  of MAO-N in 0.6 M MOPS Buffer pH 7.8 was added resulting in a final volume of 200  $\mu\text{L}$ . Dye formation was followed at  $\lambda=510$  nm and  $37^\circ\text{C}$  for 1 hour.

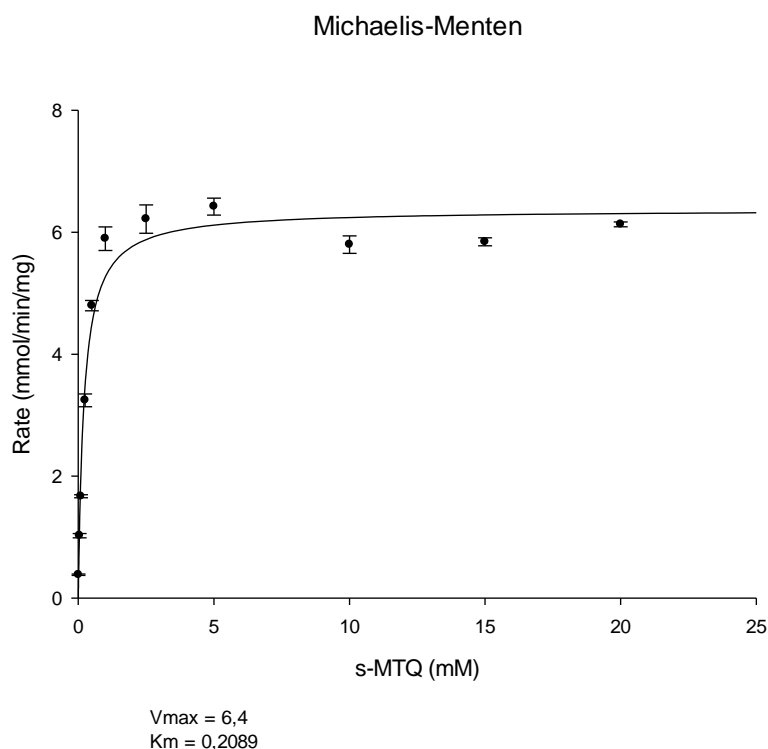
Analysis of steady-state kinetic data was performed by fitting initial velocity data to Michaelis-Menten or substrate inhibition equations using the Sigma Plot Enzyme Kinetics Module to determine turnover numbers ( $k_{cat}$ ), Michaelis-Menten constants ( $K_m$ ) and inhibition constants ( $K_i$ ).

**Table S6.** MAO-N D5 and MAO-N D9 kinetic data

	MAO-N D5				MAO-N D9			
	Vmax (U/mg)	$K_m$ (mM)	$K_{cat}$ ( $s^{-1}$ )	$K_{cat}/K_m$ ( $mM^{-1}s^{-1}$ )	Vmax (U/mg)	$K_m$ (mM)	$K_{cat}$ ( $s^{-1}$ )	$K_{cat}/K_m$ ( $mM^{-1}s^{-1}$ )
(S)-MTQ	6.24	2.39	1.29	0.54	5.48	0.23	1.13	4.93
(±)-MTQ	3.70	3.42	0.77	0.22	4.50	0.32	0.93	2.91



**Figure S2.** MAO-N D5 MM kinetic curve for (S)-MTQ.



**Figure S3.** MAO-N D9 MM kinetic curve for (*S*)-MTQ.

**Time course of concurrent catalysis reactions with MAO-N D9/ATHase (Sav S112T or Sav S112K) for the reduction of 1-methyl-3,4-dihydroisoquinoline (1-ox)**

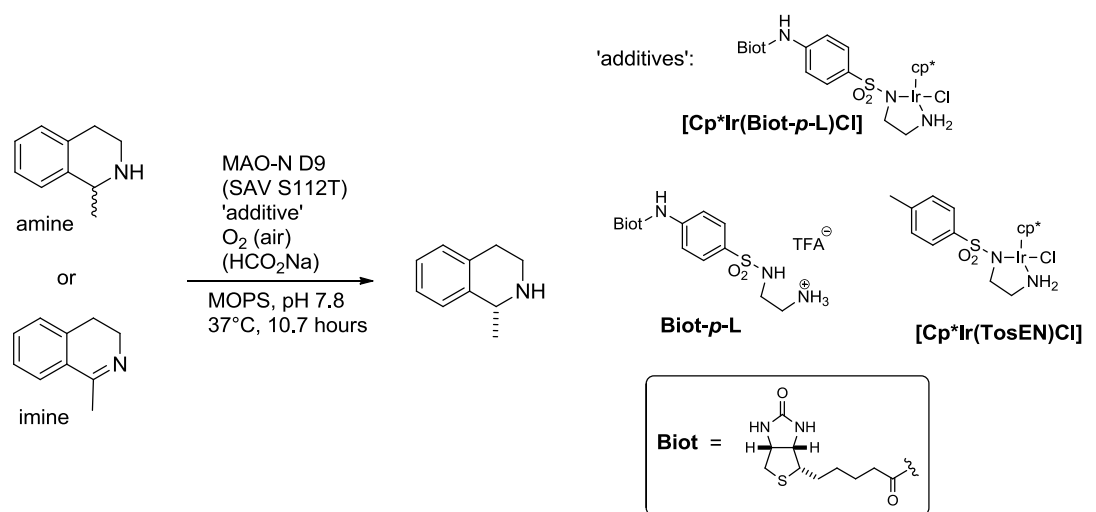
The reactions were carried out and analysed as described in the protocol for reactions on an analytical scale with 1 mol % ATHase. Each time point depicted in Figure 2a of the main text corresponds to an individual experiment. The reactions for both ATHase preparations (Sav S112T and S112K) were run simultaneously using the same MAO-N preparation and reaction buffers. All reactions were initiated within 5 minutes and work up was performed at the indicated time points.

**Controls**

**Inhibition of MAO-N**

In order to investigate the observation of MAO-N inhibition in the absence of Sav a series of control experiments was performed. The reactions were performed according to the protocol for reactions on an analytical scale. Results are summarized in Table S7.

**Table S7.**



entry	substrate	Sav S112T <sup>a)</sup>	'additive'	formate	catalase	amine [%] <sup>b)</sup>	e.e. [%]
1	amine	1.0 mol %	0.5 mol % $[\text{Cp}^*\text{Ir}(\text{Biot-}p\text{-L})\text{Cl}]$	yes	yes	> 99	> 99 (R)
2	amine	-	0.5 mol % $[\text{Cp}^*\text{Ir}(\text{Biot-}p\text{-L})\text{Cl}]$	no	no	> 99	0
3	amine	-	0.5 mol % $\text{Biot-}p\text{-L}$	yes	yes	53 <sup>c)</sup>	> 99 (R)
4	imine	1.0 mol %	0.5 mol % $[\text{Cp}^*\text{Ir}(\text{Biot-}p\text{-L})\text{Cl}]$	yes	yes	97 <sup>d)</sup>	> 99 (R)
5	imine	-	0.5 mol % $[\text{Cp}^*\text{Ir}(\text{Biot-}p\text{-L})\text{Cl}]$	yes	yes	36	0
6	imine	-	1.0 mol % $[\text{Cp}^*\text{Ir}(\text{TosEN})\text{Cl}]$	yes	yes	99	0

All reactions were performed in parallel with the same MAO-N D9 preparation (100  $\mu\text{L}$  of a solution with 0.38  $\text{mg mL}^{-1}$ ) to which the respective buffer (0.6 M MOPS, 3.0 M  $\text{HCO}_2\text{Na}$  (except entry 2), 50  $\text{kU/mL}$  catalase (except entry 2) with the respective additive (dissolved in DMF to a concentration of 37.5  $\text{mM}$ , except for entry 6 (75  $\text{mM}$ ) and with or without Sav S112T was added (100  $\mu\text{L}$ ). Reactions were initiated by addition of the substrate stock solution (7.5  $\mu\text{L}$  of a 1 M solution). a) Free binding sites; three free binding sites per tetramer were assumed. b) Amine [%] = (amine  $\times$  100)/(amine + imine); determined by normal phase HPLC after extraction; the relative response was corrected by the experimentally determined response factor. c) Excess of 50 % caused by inaccuracies in the determination of the response factor and/or the integration of chromatography trace and/or distortion due to extraction. d) > 99 % conversions were observed after 24 hours.

## References

- [1] Köhler, V. *et al.*  $\text{OsO}_4$ -Streptavidin: A tunable hybrid catalyst for the enantioselective *cis*-dihydroxylation of olefins. *Angew. Chem. Int. Ed.* **50**, 10863-10866 (2011).
- [2] Gallizia, A. *et al.* Production of a soluble and functional recombinant streptavidin in *Escherichia coli*. *Protein Expres. Purif.* **14**, 192–196 (1998).
- [3] Wilson, Y. M., Dürrenberger, M. & Ward, T. R. Organometallic chemistry in protein scaffolds. *Protein Engineering Handbook*, Volume III, Eds. S. Lutz, U. T.

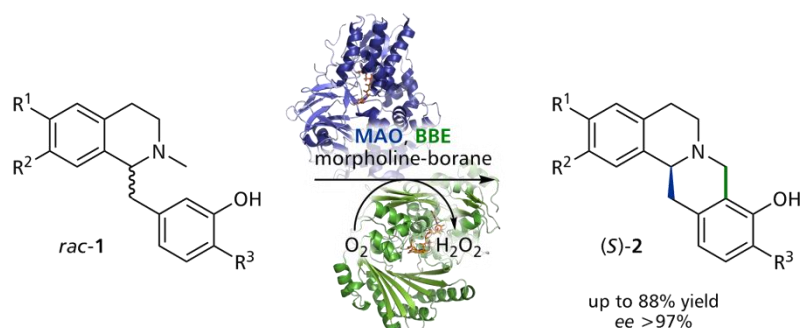
Bornscheuer, Wiley VCH, Weinheim (2012).

- [4] Atkin K. E. *et al.* The structure of monoamine oxidase from *Aspergillus niger* provides a molecular context for improvements in activity obtained by directed evolution. *J. Mol. Biol.* **384**, 1218–1231 (2008).
- [5] Rowles, I., Malone, K. J., Etchells, L. L., Willies, S. C. & Turner, N. J. Directed evolution of the enzyme monoamine oxidase (MAO-N): highly efficient chemo-enzymatic deracemisation of the alkaloid (±)-crispine A. *ChemCatChem*, **4**, 1259-1261 (2012).
- [6] Starr, D. F., Bulbrook, H. & Hixon, R. M. Electron sharing ability of organic radicals VI. Alpha-substituted pyrrolines and pyrrolidines. *J. Am. Chem. Soc.* **54**, 3971-3976 (1932).
- [7] Dunsmore, C. J., Carr, R., Fleming, T. & Turner, N. J. A chemo-enzymatic route to enantiomerically pure cyclic tertiary amines. *J. Am Chem. Soc.* **128**, 2224-2225 (2006).
- [8] Kada, G., Kaiser, K., Falk, H. & Gruber, H. Rapid estimation of avidin and streptavidin by fluorescence quenching or fluorescence polarization. *Biochim. Biophys. Acta, Gen. Subj.* **1427**, 44-48 (1999).
- [9] Michaelis, L. & Menten, M. L. Die kinetik der invertinwirkung. *Biochem. Z.* **49**, 333–369 (1913).
- [10] Haldane, J. *Enzymes*. Longmans, Green and Co., New York (1930).
- [11] Vuister, G. W. & Bax, A. Resolution enhancement and spectral editing of uniformly <sup>13</sup>C enriched proteins by homonuclear broadband <sup>13</sup>C decoupling. *J. Magn. Reson.* **98**, 428–435 (1992).
- [12] Schmid, A., Vereyken, V., Held, M. & Witholt, B. Preparative regio- and chemoselective functionalization of hydrocarbons by cell free preparations of 2-hydroxybiphenyl 3-monooxygenase. *J. Mol. Catal. B.* **11**, 455-462 (2001).
- [13] Suske, W. A., *et al.* Purification and characterization of 2-hydroxybiphenyl 3-monooxygenase, a novel NADH-dependent, flavin-containing, aromatic hydroxylase from *Pseudomonas azelaica*, HBP1. *J. Biol. Chem.* **272**, 24257-24265 (1997).
- [14] Dawson, R. M. C., Elliott, D. C., Elliott, W. H. & Jones, K. M. *Data for Biochemical Research*, 3rd Ed., Clarendon Press, Oxford, 122-123 (1986).

# CHEMO/BI-ENZYMATIC REDOX CASCADE FOR THE ENANTIOCONVERGENT TRANSFORMATION OF ( $\pm$ )-BENZYLISOQUINOLINES INTO (*S*)-BERBINES

Manuscript ready for submission

J. H. Schrittwieser, B. Groenendaal, V. Resch, D. Ghislieri, S. Wallner,  
E. M. Fischereder, E. Fuchs, B. Grischek, J. H. Sattler,  
P. Macheroux, Nicholas J. Turner, Wolfgang Kroutil



A novel chemo/bi-enzymatic cascade system for the enantioconvergent transformation of racemic benzylisoquinolines (**1**) into (*S*)-berbines (**2**) has been developed. The one-pot combination of monoamine oxidase (MAO) and morpholine-borane leads to deracemisation of (*rac*)-**1**, while concomitant cyclisation of (*S*)-**1** by berberine bridge enzyme (BBE) provides (*S*)-**2** as the final product in up to 98% conversion, up to 88% isolated yield and in enantiomerically pure form (e.e. >97%).

In this project D.G. provided the MAO-N D11 mutant for the chemo/bi-enzymatic cascade system.

# Chemo/Bi-enzymatic Redox Cascade for the Enantio-convergent Transformation of *rac*-Benzylisoquinolines into (*S*)-Berbines

Joerg H. Schrittwieser, Bas Groenendaal, Verena Resch, Diego Ghislieri, Silvia Wallner, Eva-Maria Fischereeder, Elisabeth Fuchs, Barbara Grischek, Johann H. Sattler, Peter Macheroux, Nicholas J. Turner, Wolfgang Kroutil\*

† Department of Chemistry, Organic & Bioorganic Chemistry, University of Graz  
Heinrichstrasse 28, 8010 Graz (Austria)

‡ School of Chemistry, University of Manchester, Manchester Interdisciplinary Biocentre, 131 Princess Street, Manchester, M1 7DN (UK)

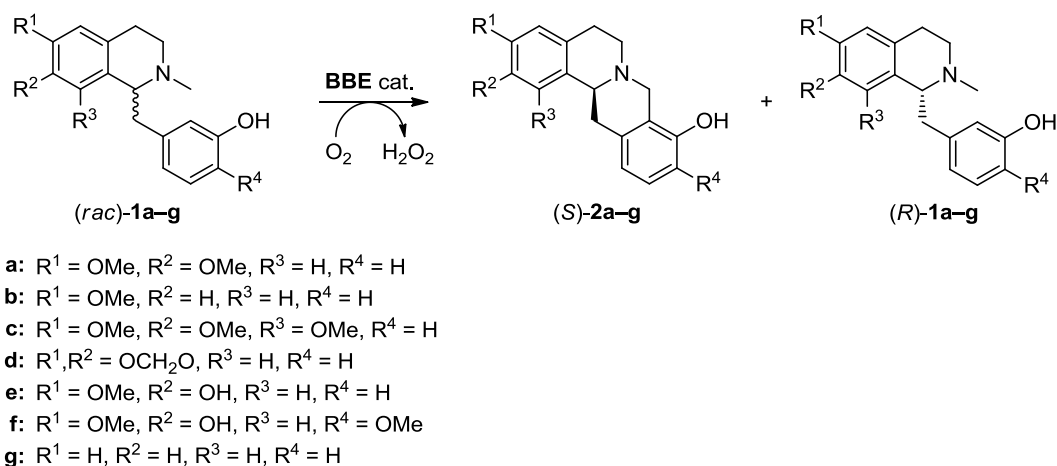
\* wolfgang.kroutil@uni-graz.at

Berbines (tetrahydroprotoberberines) represent a sub-class of isoquinoline alkaloids found in various plant families (*e.g.*, papaveraceae, fumariaceae) and comprising more than 100 known structures.[1] Diverse biological activities have been reported for these secondary metabolites, ranging from sedative and analgesic effects to spasmolytic and anti-inflammatory properties.[2] Recently, two berbine alkaloids – (*S*)-stepholidine and (*S*)-12-chloroscoulerine – have attracted increased attention because of their unique effect on the dopaminergic system, making them highly promising drug candidates for the treatment of schizophrenia and Alzheimer's disease.[3]

Although most naturally occurring berbines contain only one stereogenic centre, their enantioselective synthesis remains a challenge. Even today, the vast majority of asymmetric syntheses relies on the use of chiral auxiliaries, and often these approaches are plagued by limited yields and e.e. values, as well as regioselectivity issues in the formation of the berbine C-ring.[4] Recently, we have reported on the biocatalytic asymmetric synthesis of berbines employing the berberine bridge



enzyme (BBE) from *Eschscholzia californica* (California poppy) for enantioselective oxidative C–C bond formation in a kinetic resolution (Scheme 1).[5]

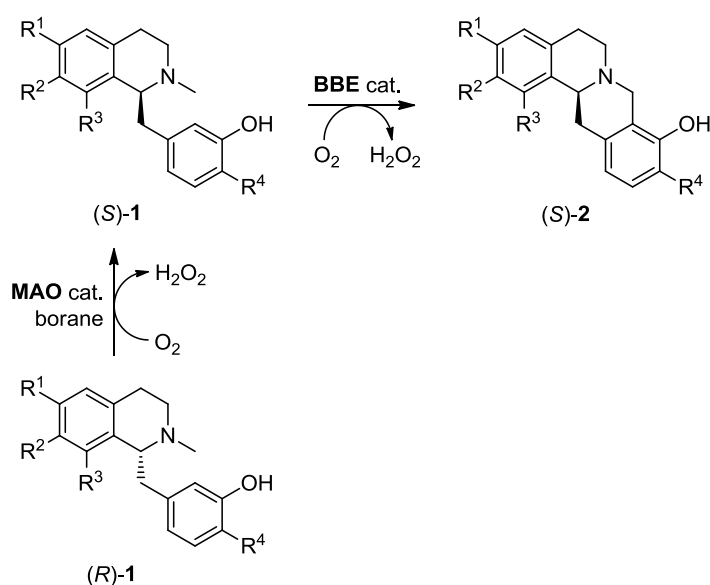


**Scheme 1.** Kinetic resolution of racemic benzyliso-quinolines employing berberine bridge enzyme (BBE).

The kinetic resolution of racemic substrates (*rac*)-**1** proceeded with excellent enantio- and regioselectivity, such that the products (*S*)-**2** and the remaining substrates (*R*)-**1** were isolated in good yield and optically pure form. This outstanding biotransformation was applied to the chemo-enzymatic total synthesis of seven different berbine alkaloids;[5c] however, the yield in the BBE-catalyzed key step was obviously always limited to 50%. Herein, we describe how this limitation was overcome by implementation of a chemo/bi-enzymatic cascade reaction system. The most straightforward approach for overcoming the 50% yield limit in a kinetic resolution is to integrate *in situ* substrate racemisation, leading to a dynamic kinetic resolution (DKR) process. While this strategy is now very well-established and broadly employed,[6] it proved problematic in our particular case: Amongst the published procedures for amine racemisation – relying on homogeneous[7] or heterogeneous[8] metal catalysis, or thiol radical-mediated reversible H-abstraction[9] – we could not identify a system that was active exclusively on the benzylisoquinoline substrates, while leaving the berbine products untouched. For example, we found that Shvo’s diruthenium-complex,[10] when employed under previously described reaction conditions,[7g] readily racemised benzyl-isoquinolines and berbines alike.[5a] Raney nickel, on the other hand, led to degradation of the complex alkaloids, while palladium on char-coal did not show any detectable racemisation activity at all.

Enzymes might offer a chemoselectivity and substrate specificity high enough for

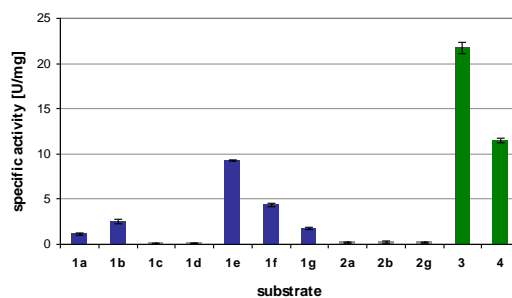
our purpose. However, benzyloquinoline racemases are not known, and while the interconversion of reticuline enantiomers does occur in nature, it represents a one-way process that strictly leads from the (*S*)-configured to the (*R*)-configured alkaloid.[11] Fortunately, an alternative has recently become available: A novel variant of monoamine oxidase (MAO) from *Aspergillus niger* (MAO-N variant D11) has been shown to oxidize benzyloquinolines with high (*R*)-selectivity in most cases.[12] The one-pot combination of MAO-N D11 with ammonia-borane as reducing agent thus establishes a “cyclic deracemisation” system,[6c,g] yielding (*S*)-benzyloquinolines from the corresponding racemates. We hence anticipated that a cascade system comprising MAO-N D11, BBE and a borane source would allow the complete conversion of (*rac*)-benzyloquinolines into (*S*)-berbines (Scheme 2). While this sequence could also possibly be run in a step-wise fashion, a concurrent cascade would represent a more elegant and efficient solution.



**Scheme 2.** Conversion of (*rac*)-benzyloquinolines to (*S*)-berbines by a MAO/BBE/borane redox cascade.

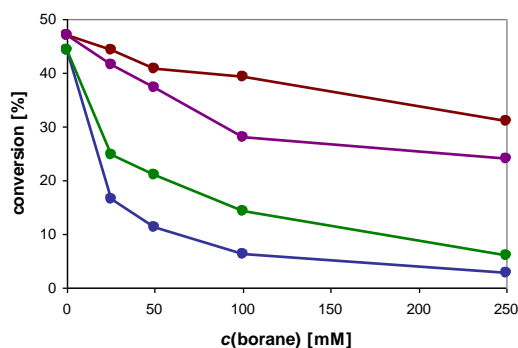
The first step in putting this concept into practice was the evaluation of the substrate scope of MAO-N variant D11. Ideally, the amine oxidase should show good activity on benzyl-isoquinolines that are known substrates for BBE, while being inactive on the corresponding berbines. Thus, MAO-N D11 was screened against a panel of seven known BBE substrates and three BBE reaction products. As shown in Figure 1, activity on five of the tested benzyloquinolines was detected, while none of the berbines was turned over by the enzyme. Additional studies revealed that **1a**, **1b**, **1e**, and **1f** were oxidized with a strong preference for the (*R*)-enantiomer ( $E > 200$ ),

while the enantioselectivity for substrate **1g** was low ( $E = 6.5$ ).[12]



**Figure 1.** Results of substrate screening with MAO-N variant D11. Activity (criterion: mean > 5 SD) was found for substrates **1a**, **1b**, and **1e–g** (light grey) as well as the positive controls (*rac*)-1-phenylethylamine **3** and (*rac*)-crispine A **4** (both dark grey). Error ranges represent standard deviations of triplicate experiments.

Next, we investigated the activity of BBE under the MAO reaction conditions. Since BBE is known to be inhibited by reducing agents,[13] the presence of boranes was expected to have a detrimental effect on the enzyme. Indeed, BBE was strongly inhibited by borane-ammonia complex, the standard reducing agent employed in deracemisation systems with MAO-N: already at a concentration of 25 mM, the apparent activity dropped below 50% of the value observed under borane-free conditions, while at 250 mM less than 10% of activity remained (Figure 2).

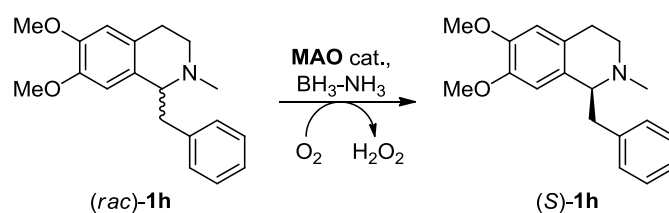


**Figure 2.** Conversion of (*rac*)-**1a** by BBE in the presence of varied amounts of amine-borane complexes BH<sub>3</sub>-NH<sub>3</sub> (blue), BH<sub>3</sub>-*t*BuNH<sub>2</sub> (green), BH<sub>3</sub>-morpholine (red), or BH<sub>3</sub>-Me<sub>3</sub>N (purple). Reaction time: 2 h.

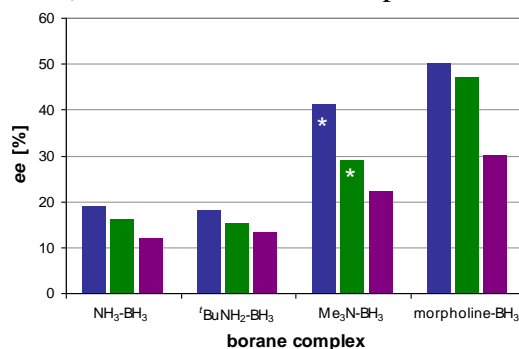
We speculated that more bulky or less water-soluble borane complexes should have less effect on BBE reactivity, since they would be hindered to enter the active site of the enzyme or since their effective concentration should be lower (BH<sub>3</sub>-Me<sub>3</sub>N, for instance, was not entirely soluble at concentrations >50 mM, resulting in a suspension). We thus tested BH<sub>3</sub>-*t*BuNH<sub>2</sub>, BH<sub>3</sub>-Me<sub>3</sub>N and BH<sub>3</sub>-morpholine as alternative borane sources. While the *tert*-butylamine complex gave only marginally better results than BH<sub>3</sub>-NH<sub>3</sub>, BH<sub>3</sub>-Me<sub>3</sub>N and BH<sub>3</sub>-morpholine proved to be more

compatible with the enzyme. In the presence of 250 mM of either of these amine-boranes, BBE retained more than 50% of its activity (Figure 2). The trimethylamine complex gave the best results, which we attribute to its low aqueous solubility.

We also investigated the effect of the borane source on the efficiency of MAO-N-catalyzed deracemisation reactions. Benzylisoquinoline derivative **1h** (Scheme 3) was used in this study, since its oxidation product[14] can be extracted and quantified by GC-FID analysis.[12] Hence, incomplete reduction of the MAO-generated prochiral intermediate by the borane complex can easily be detected.



**Scheme 3.** Deracemisation of benzylisoquinoline derivative **1h** by a combination of monoamine oxidase (MAO) and amine-borane complexes.



**Figure 3.** Deracemisation of benzylisoquinoline derivative **1h** in the presence of varied amounts of amine-borane complexes. Blue bars...50 mM, green bars...100 mM, purple bars...250 mM. Reaction time: 20 h. The asterisk indicates samples where in-complete reduction was observed (50 mM BH<sub>3</sub>-Me<sub>3</sub>N: 5.1% oxidation product, 100 mM BH<sub>3</sub>-Me<sub>3</sub>N: 2.8% oxidation product). Reaction time: 20 h.

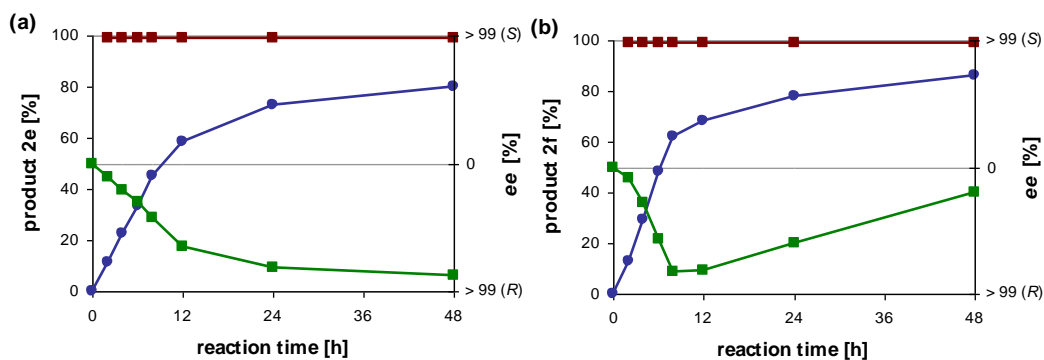
**Table 1.** Stepwise combination of MAO and BBE for the conversion of (*rac*)-benzylisoquinolines to (*S*)-berbines.<sup>[a]</sup>

substrate	procedure	time <sup>[b]</sup> [h]	( <i>S</i> )- <b>2</b> <sup>[c]</sup> [%]	e.e. ( <b>2</b> ) <sup>[d]</sup> [%]
<b>1b</b>	A	72 + 24	79.4 <sup>[e]</sup>	>97
<b>1b</b>	B	72 + 24	79.0 <sup>[f]</sup>	>97
<b>1e</b>	A	48 + 24	92.6	>97
<b>1e</b>	B	48 + 24	90.3	>97
<b>1f</b>	A	48 + 24	97.4	>97
<b>1f</b>	B	48 + 24	94.7	>97
<b>1b</b>	A	72 + 24	79.4 <sup>[e]</sup>	>97

[a] Reactions were performed in buffer/DMSO = 90/10, pH 7.7, at a substrate concentration of 10 mM, 100 g L<sup>-1</sup> lyophilized *E. coli* cells expressing MAO-N D11, 0.1 g L<sup>-1</sup> BBE, 100 mM morpholine-borane, 37 °C. Procedure A: direct addition of BBE to the reaction mixture after complete deracemisation. Procedure B: addition of BBE to the supernatant of centrifuged reaction mixture after complete deracemisation (for details, see *Supporting Information*). [b] Reaction time for complete deracemisation + reaction time for BBE-catalyzed ring-closure. [c] Conversion to product **2** determined by HPLC analysis on an achiral C18 phase. [d] Enantiomeric excess determined by HPLC analysis on a chiral phase. [e] 4.3% of regioisomeric product formed. [f] 4.1% of regioisomeric product formed.

As shown in Figure 3, BH<sub>3</sub>-NH<sub>3</sub> and BH<sub>3</sub>-*t*BuNH<sub>2</sub> performed very similar in the deracemisation system, while the trimethylamine and the morpholine complex both gave superior results. In the reactions with BH<sub>3</sub>-Me<sub>3</sub>N, however, incomplete reduction was observed when the borane source was applied in concentrations lower than 250 mM. Hence, we chose to use morpholine-borane in all further experiments.

As a first approach to combine the two enzymatic transformations we carried out a stepwise deracemisation/ring-closure sequence. Thus, deracemisation of substrates **1b**, **1e**, and **1f**[15] by the MAO/borane-system was run to completion before aliquots were withdrawn and BBE was added to the reaction mixture. The BBE-catalyzed ring-closure was either carried out after removal of the cell mass by centrifugation or directly in the reaction mixture from the deracemisation stage. In both cases, the transformations proceeded nicely, resulting in high conversion to the berbine **2** (Table 1). In addition, chiral-phase HPLC analysis of the products showed that all compounds were obtained in enantiomerically pure form (e.e. >97%), thus indicating that BBE's enantioselectivity was not impaired by the extended reaction system.



**Figure 4.** Time-study of the conversion of (*rac*)-benzylisoquinolines to (*S*)-berbines by a MAO/BBE/ borane redox cascade, using (a) (*rac*)-**1e**, and (b) (*rac*)-**1f** as substrate. The plot shows the conversion to product (*S*)-**2** (blue), as well as substrate e.e. (green) and product e.e. (red) as a function of reaction time.

We therefore went on to combine the MAO and BBE reactions in a concurrent one-pot cascade. Time-study experiments were carried out and the BBE amount added was adjusted in such a way that the C–C coupling reaction would not quickly run out of the (*S*)-benzylisoquinoline substrate. The transformations of **1e** and **1f** proceeded smoothly and the berbine products were formed in 80% and 86% conversion, respectively, after 48 h (Figure 4). It is noteworthy that in contrast to our previous studies on BBE,<sup>[5b]</sup> where catalase was required to protect the enzyme from oxidative inactivation by hydrogen peroxide, the cascade system did not profit from the addition of catalase. Apparently, the presence of a chemical reducing agent and the natural catalase activity of the *E. coli* cells lead to a sufficiently fast degradation of any H<sub>2</sub>O<sub>2</sub> formed.

As indicated by the continuous rise of substrate e.e. in favour of the (*R*)-enantiomer, the MAO-catalyzed deracemisation is the limiting factor in the cascade transformation. This situation becomes more severe when **1b** and **1g** are used as substrates. In these cases, prolonged reaction times were required and undesired side reactions were observed, such that the HPLC yield of **2** never exceeded 65% (for further information, see *Supporting Information*).

To demonstrate the synthetic applicability of the cascade system, we scaled the transformations of **1e** and **1f** to a preparative batch size (150–165 mg, 0.5 mmol). Pleasingly, the reactions proceeded even better on large scale, such that higher conversions (92% and 98%, respectively) were attained. The biotransformation of **1f** even ran to completion within 24 h, as opposed to 48 h in the small-scale experiments (Table 2). This difference can most likely be attributed to an increased

availability of oxygen in the 250 mL Erlenmeyer flasks used as reaction vessels (for 50 mL of reaction volume). The reaction products (*S*)-**2e** and (*S*)-**2f** were isolated in 88% and 80% yield, respectively, and in enantiomerically pure form (e.e. >97%).

**Table 2.** Preparative-scale conversion of (*rac*)-benzyl-isoquinolines to (*S*)-berbines by a MAO/BBE/borane redox cascade.<sup>[a]</sup>

substrate	time [h]	<i>c</i> ( <b>2</b> ) <sup>[b]</sup> [%]	yield ( <i>S</i> )- <b>2</b> <sup>[c]</sup> [%]	e.e. ( <b>2</b> ) <sup>[d]</sup> [%]
<b>1e</b>	48	92	88	>97
<b>1f</b>	24	98	80	>97

[a] Reactions were performed in buffer/DMSO = 90/10, pH 7.7, at a substrate concentration of 10 mM, 100 g L<sup>-1</sup> lyophilized *E. coli* cells expressing MAO-N D11, 0.05 g L<sup>-1</sup> BBE (**1e**) or 0.02 g L<sup>-1</sup> BBE (**1f**), 100 mM morpholine-borane, 37 °C (for details, see *Supporting Information*). [b] Conversion to product **2** determined by HPLC analysis on an achiral C18 phase. [c] Isolated yield after column chromatography. [d] Enantiomeric excess determined by HPLC analysis on a chiral phase.

In summary, we have developed a chemo/bi-enzymatic redox cascade<sup>[16]</sup> that allows the conversion of racemic benzylisoquinolines **1** to (*S*)-berbines **2** in 100% maximum theoretical yield. As demonstrated in preparative-scale transformations, near-quantitative conversions were obtained, and two (*S*)-berbine alkaloids were produced in good yield and optically pure form. In combination with the previously reported synthesis of the racemic benzylisoquinoline substrates,<sup>[5c]</sup> the cascade transformation allows the efficient asymmetric total synthesis of the berbine alkaloids (*S*)-**1e** and (*S*)-**1f**, in overall yields of 18% and 13%, respectively, over nine steps. Besides, the present work also introduces a conceptually novel approach: It employs two flavin-dependent oxidases that act on different sites of opposite substrate enantiomers, yet leading to the formation of a single, enantiomerically pure product. We therefore expect our findings to stimulate further developments in the field of biocatalytic cascade transformations for the synthesis of bioactive target compounds.

## Experimental Section

*Representative MAO/BBE cascade transformation on preparative scale:* In an Erlenmeyer flask (250 mL), lyophilized cells of *E. coli* C43(DE3) expressing MAO-N D11 (5.0 g) were resuspended in phosphate buffer (45 mL; 100 mM K-phosphate, pH 7.7). BH<sub>3</sub>-Morpholine (505 mg, 5 mmol), BBE solution (105 μL of a 354 μM

preparation; final concentration: 0.05 g/L) and a solution of substrate (*rac*)-**1e** (150 mg, 0.5 mmol; final concentration 10 mM) in DMSO (5 mL) were added and the mixture was shaken at 37 °C and 150 rpm. After 24 h, further morpholine·BH<sub>3</sub> (250 mg, 2.5 mmol) and BBE solution (105 μL) were added and shaking continued. After 48 h, a sample (250 μL) was taken, extracted with EtOAc and analyzed for conversion. HPLC analysis showed 92% product formation, and the reaction mixture was aliquoted into Falcon tubes (50 mL) and centrifuged (4000 rpm, 1 h, rt) to remove the cell mass. The supernatant was extracted with EtOAc (3 × 20 mL), whereby phase separation was accelerated by centrifugation; the cell pellets were suspended in EtOAc, centrifuged again (4000 rpm, 10 min, rt) and the EtOAc phase was combined with the extracts. The combined organic phases were dried over Na<sub>2</sub>SO<sub>4</sub> and the solvent was evaporated under reduced pressure to give 0.60 g of a yellowish liquid. Column chromatography (silica; CH<sub>2</sub>Cl<sub>2</sub>/MeOH/NH<sub>3</sub>(aq) = 96/3/1) afforded 131 mg (88%) of (*S*)-**2e** as a white solid foam (for product characterization, see *Supporting Information*).

## Reference

- [1] a) K. W. Bentley, *The Isoquinoline Alkaloids*. (Harwood Academic Publishers, Amsterdam, 1998); b) M. Shamma, *The Isoquinoline Alkaloids. Chemistry and Pharmacology*. (Academic Press, New York/London, 1972).
- [2] a) S. I. Jang, B. H. Kim, W.-Y. Lee, S. J. An, H. G. Choi, B. H. Jeon, H.-T. Chung, J.-R. Rho, Y.-J. Kim, K.-Y. Chai, *Arch. Pharm. Res.* **2004**, *27*, 923–929; b) C. Halbsguth, O. Meissner, H. Haerberlein, *Planta Med.* **2003**, *69*, 305–309; c) D. S. Bhakuni, R. Chaturvedi, *J. Nat. Prod.* **1983**, *46*, 466–470; d) J. Yamahara, T. Konoshima, Y. Sakakibara, M. Ishiguro, T. Sawada, *Chem. Pharm. Bull.* **1976**, *24*, 1909–1912; e) J. Yamahara, *Folia Pharmacol. Jpn.* **1978**, *27*, 909–927.
- [3] For reviews, see: a) J. Mo, Y. Guo, Y.-S. Yang, J.-S. Shen, G.-Z. Jin, X. Zhen, *Curr. Med. Chem.* **2007**, *14*, 2996–3002; b) K. Yang, G. Jin, J. Wu, *Curr. Neuropharmacol.* **2007**, *5*, 289–294; c) G.-Z. Jin, Z.-T. Zhu, Y. Fu, *Trends Pharmacol. Sci.* **2002**, *23*, 4–7; d) J. Li, G. Jin, J. Shen, R. Ji, *Drugs Fut.* **2006**, *31*, 379–384.
- [4] For reviews on the asymmetric synthesis of isoquinoline alkaloids, including berbines, see: a) M. Chrzanowska, M. D. Rozwadowska, *Chem. Rev.* **2004**, *104*, 3341–3370; b) M. D. Rozwadowska, *Heterocycles* **1994**, *39*, 903–931. For recent examples, see: c) V. M. Mastranzo, F. Yuste, B. Ortiz, R. Sánchez-Obregón, R. A. Toscano, J. L. García Ruano, *J. Org. Chem.* **2011**, *76*, 5036–5041; d) A. L. Zein, L. N. Dawe, P. E. Georghiou, *J. Nat. Prod.* **2010**, *73*, 1427–1430; e) T. Fukuda, M.



Iwao, *Heterocycles* **2007**, *74*, 701–720; f) M. Chrzanowska, A. Dreas, *Heterocycles* **2006**, *69*, 303–310; g) D. Mujahidin, S. Doye, *Eur. J. Org. Chem.* **2005**, 2689–2693; h) M. Boudou, D. Enders, *J. Org. Chem.* **2005**, *70*, 9486–9494; i) M. Chrzanowska, A. Dreas, M. D. Rozwadowska, *Tetrahedron: Asymmetry* **2004**, *15*, 1113–1120; j) L. Liu, *Synthesis* **2003**, 1705–1706; k) F. A. Davis, P. K. Mohanty, *J. Org. Chem.* **2002**, *67*, 1290–1296; l) P. S. Cutter, B. Miller, N. E. Schore, *Tetrahedron* **2002**, *58*, 1471–1478.

[5] a) J. H. Schrittwieser, V. Resch, J. H. Sattler, W.-D. Lienhart, K. Durchschein, A. Winkler, K. Gruber, P. Macheroux, W. Kroutil, *Angew. Chem. Int. Ed.* **2011**, *50*, 1068–1071; *Angew. Chem.* **2011**, *123*, 1100–1103; b) V. Resch, J. H. Schrittwieser, S. Wallner, P. Macheroux, W. Kroutil, *Adv. Synth. Catal.* **2011**, *353*, 2377–2383; c) J. H. Schrittwieser, V. Resch, S. Wallner, W.-D. Lienhart, J. H. Sattler, J. Resch, P. Macheroux, W. Kroutil, *J. Org. Chem.* **2011**, *76*, 6703–6714.

[6] For reviews, see: a) H. Pellissier, *Tetrahedron* **2011**, *67*, 3769–3802; b) J. H. Lee, K. Han, M.-J. Kim, J. Park, *Eur. J. Org. Chem.* **2010**, 999–1015; c) N. J. Turner, *Curr. Opin. Chem. Biol.* **2010**, *14*, 115–121; d) A. H. Kamaruddin, M. H. Uzir, H. Y. Aboul-Enein, H. N. A. Halim, *Chirality* **2009**, 449–467; e) Y. Ahn, S.-B. Ko, M.-J. Kim, J. Park, *Coord. Chem. Rev.* **2008**, *252*, 647–658; f) H. Pellissier, *Tetrahedron* **2008**, *64*, 1563–1601; g) N. J. Turner, *Curr. Opin. Chem. Biol.* **2004**, *8*, 114–119; h) O. Pàmies, J.-E. Bäckvall, *Chem. Rev.* **2003**, *103*, 3247–3261; i) H. Pellissier, *Tetrahedron* **2003**, *59*, 8291–8327.

[7] For examples using ruthenium complexes, see: a) L. K. Thalén, M. H. Hedberg, J.-E. Bäckvall, *Tetrahedron Lett.* **2010**, *51*, 6802–6805; b) L. K. Thalén, D. Zhao, J.-B. Sortais, J. Paetzold, C. Hoben, J.-E. Bäckvall, *Chem. Eur. J.* **2009**, *15*, 3403–3410; c) C. E. Hoben, L. Kanupp, J.-E. Bäckvall, *Tetrahedron Lett.* **2008**, *49*, 977–979; d) M. A. J. Veld, K. Hult, A. R. A. Palmans, E. W. Meijer, *Eur. J. Org. Chem.* **2007**, 5416–5421; e) C. Roengpithya, D. A. Patterson, A. G. Livingston, P. C. Taylor, J. L. Irwin, M. R. Parrett, *Chem. Commun.* **2007**, 3462–3463; f) J. Paetzold, J. E. Bäckvall, *J. Am. Chem. Soc.* **2005**, *127*, 17620–17621; g) O. Pàmies, A. H. Éll, J. S. M. Samec, N. Hermanns, J.-E. Bäckvall, *Tetrahedron Lett.* **2002**, *43*, 4699–4702. For examples using iridium complexes, see: h) T. Jerphagnon, A. J. A. Gayet, F. Berthiol, V. Ritleng, N. Mršić, A. Meetsma, M. Pfeffer, A. J. Minnaard, B. L. Feringa, J. G. de Vries, *Chem. Eur. J.* **2009**, *15*, 12780–12790; i) A. J. Blacker, M. J. Stirling, M. I. Page, *Org. Process Res. Dev.* **2007**, *11*, 642–648; j) M. Stirling, J. Blacker, M. I. Page, *Tetrahedron Lett.* **2007**, *48*, 1247–1250.

[8] For examples using palladium on various supports, see: a) A. N. Parvulescu, P. A. Jacobs, D. E. De Vos, *Appl. Catal. A* **2009**, *368*, 9–16; b) L. H. Andrade, A. V. Silva, E. C. Pedrozo, *Tetrahedron Lett.* **2009**, *50*, 4331–4334; c) A. N. Parvulescu, E. Van der Eycken, P. A. Jacobs, D. E. De Vos, *J. Catal.* **2008**, *255*, 206–212; d) A. N. Parvulescu, P. A. Jacobs, D. E. De Vos, *Chem. Eur. J.* **2007**, *13*, 2034–2043; e) A. Parvulescu, D. De Vos, P. Jacobs, *Chem. Commun.* **2005**, 5307–5309; f) M. T. Reetz, K. Schimossek, *Chimia* **1996**, *50*, 668–669. For examples using palladium

nanoparticles, see: g) Y. Kim, J. Park, M.-J. Kim, *Tetrahedron Lett.* **2010**, *51*, 5581–5584; h) M.-J. Kim, W.-H. Kim, K. Han, Y. K. Choi, J. Park, *Org. Lett.* **2007**, *9*, 1157–1159. For an example using Raney metals, see: A. N. Parvulescu, P. A. Jacobs, D. E. De Vos, *Adv. Synth. Catal.* **2008**, *350*, 113–121.

[9] a) F. Poulhès, N. Vanthuyne, M. P. Bertrand, S. Gastaldi, G. Gil, *J. Org. Chem.* **2011**, *76*, 7281–7286; b) L. El Blidi, N. Vanthuyne, D. Siri, S. Gastaldi, M. P. Bertrand, G. Gil, *Org. Biomol. Chem.* **2010**, *8*, 4165–4168; c) L. El Blidi, M. Nechab, N. Vanthuyne, S. Gastaldi, M. P. Bertrand, G. Gil, *J. Org. Chem.* **2009**, *74*, 2901–2903; d) L. Routaboul, N. Vanthuyne, S. Gastaldi, G. Gil, M. Bertrand, *J. Org. Chem.* **2008**, *73*, 364–368; e) S. Gastaldi, S. Escoubet, N. Vanthuyne, G. Gil, M. P. Bertrand, *Org. Lett.* **2007**, *9*, 837–839; f) S. Escoubet, S. Gastaldi, N. Vanthuyne, G. Gil, D. Siri, M. P. Bertrand, *J. Org. Chem.* **2006**, *71*, 7288–7292; g) S. Escoubet, S. Gastaldi, N. Vanthuyne, G. Gil, D. Siri, M. P. Bertrand, *Eur. J. Org. Chem.* **2006**, 3242–3250.

[10] For reviews, see: a) M. C. Warner, C. P. Casey, J. E. Bäckvall, *Top. Organomet. Chem.* **2011**, *37*, 85–125; b) R. Karvembu, R. Prabhakaran, K. Natarajan, *Coord. Chem. Rev.* **2005**, *249*, 911–918. For the original report, see: Y. Shvo, D. Czarkie, Y. Rahamim, D. F. Chodosh, *J. Am. Chem. Soc.* **1986**, *108*, 7400–7402.

[11] a) K. Hirata, C. Poeaknapo, J. Schmidt, M. H. Zenk, *Phytochemistry* **2004**, *65*, 1039–1046; b) W. De-Eknamkul, M. H. Zenk, *Phytochemistry* **1992**, *31*, 813–821; c) W. De-Eknamkul, M. H. Zenk, *Tetrahedron Lett.* **1990**, *31*, 4855–4858.

[12] J. H. Schrittwieser, B. Groenendaal, S. C. Willies, D. Ghislieri, I. Rowles, V. Resch, J. H. Sattler, E.-M. Fischereder, B. Grischek, W.-D. Lienhart, N. J. Turner, W. Kroutil, *manuscript in preparation*.

[13] P. Steffens, N. Nagakura, M. H. Zenk, *Tetrahedron Lett.* **1984**, *25*, 951–952.

[14] In view of the proposed mechanism for MAOs, the oxidation product is most likely the corresponding 3,4-dihydroisoquinolinium ion. See: D. E. Edmondson, A. Mattevi, C. Binda, M. Li, F. Hubálek, *Curr. Med. Chem.* **2004**, *11*, 1983–1993. However, this species can interconvert with the corresponding enamine in basic aqueous solution. See: X.-S. He, *J. Nat. Prod.* **1993**, *56*, 973–975.

[15] Substrates **1a** and **1g** were not investigated in these experiments because the former is turned over too slowly by MAO-N, while the latter is converted with too little enantioselectivity. Thus, in both cases, no complete deracemization can be achieved within a reasonable time frame.

[16] For recent reviews on biocatalytic (redox) cascade reactions, see: a) J. H. Schrittwieser, J. Sattler, V. Resch, F. G. Mutti, W. Kroutil, *Curr. Opin. Chem. Biol.* **2011**, *15*, 249–256; b) E. Ricca, B. Brucher, J. H. Schrittwieser, *Adv. Synth. Catal.* **2011**, *353*, 2239–2262.

**Chemo/Bi-enzymatic Redox Cascade  
for the Enantioconvergent  
Transformation of *rac*-  
Benzylisoquinolines into (*S*)-  
Berbines**

Joerg H. Schrittwieser, Bas Groenendaal, Verena Resch, Diego Ghislieri, Silvia Wallner, Eva-Maria Fischereeder, Elisabeth Fuchs, Barbara Grischek, Johann H. Sattler, Peter Macheroux, Nicholas J. Turner, Wolfgang Kroutil

**Supplementary information**

## General Methods

$^1\text{H}$  and  $^{13}\text{C}$ -NMR spectra were recorded using a 300 MHz instrument. Chemical shifts are given in parts per million (ppm) relative to TMS ( $\delta = 0$  ppm) and coupling constants ( $J$ ) are reported in Hertz (Hz). Melting points were determined on a Gallenkamp MPD350 apparatus in open capillary tubes and are uncorrected. Thin layer chromatography was carried out on silica gel 60 F<sub>254</sub> plates and compounds were visualized either by UV. Unit resolution GC-MS analyses were performed using electron impact (EI) ionisation at 70 eV and quadrupole mass selection. High resolution MS analyses were performed using electron impact (EI) ionisation at 70 eV and TOF mass selection. Optical rotation values  $[\alpha]_{\text{D}}^{20}$  were measured at 589 nm (Na line) on a Perkin-Elmer Polarimeter 341 using a cuvette of 1 dm path length, and are given in  $^{\circ} \text{L g}^{-1} \text{m}^{-1}$ .

Unless otherwise noted, reagents and organic solvents were obtained from commercial sources and used without further purification.

## Protein Expression and Purification

Expression and purification of berberine bridge enzyme [1] and MAO-N D11[2] were carried out as previously described.

## Substrate Screening of MAO-N D11

Stock solutions of the test substrates (20 mM; final concentration after dilution 1 mM) in DMSO were prepared. For each colorimetric reaction, the substrate stock solution (5  $\mu\text{L}$ ) was mixed with MAO reaction buffer (20  $\mu\text{L}$ ; 100 mM K-P<sub>i</sub>, pH 7.7), pyrogallol red solution (50  $\mu\text{L}$ ; 0.3 mM in MAO reaction buffer), horseradish peroxidase solution (5  $\mu\text{L}$ ; 1 mg/mL in MAO reaction buffer) and purified MAO-N D11 solution (20  $\mu\text{L}$ ; 0.53 mg/mL) in a 96-well microtiter plate. In addition, reactions with (*rac*)-1-phenylethylamine (1 mM) and (*rac*)-crispine A (1 mM) as well as negative controls (lacking substrate and MAO, respectively) were set up. All reactions, including the blanks, were performed in triplicate. Reactions were followed by measuring the absorbance at 550 nm every minute for a period of 4 h using a *Molecular Devices* SpectraMax M2 plate reader. Slopes were determined by applying a linear fit to the linear range of the absorbance curve using the built-in function of the plate reader's *Molecular Devices* Softmax Pro v5.0 software. Slopes were corrected for spontaneous decolorisation of pyrogallol red (rate obtained from

the blank samples) and the specific MAO activity was calculated using formula (1) given below.

$$A = \frac{\Delta OD \cdot Y}{\varepsilon \cdot L \cdot c_p} \quad (1)$$

where  $A$  [ $\text{U} \cdot \text{mg}^{-1}$ ] ... MAO activity;  $\Delta OD$  [ $\text{min}^{-1}$ ] ... slope of absorbance decrease;  $Y$  ... dilution factor of MAO solution (5 in this case);  $\varepsilon$  [ $\text{L} \cdot \text{mmol}^{-1} \cdot \text{cm}^{-1}$ ] ... extinction coefficient of pyrogallol red (30.9 at 550 nm);  $L$  [cm] ... path length of sample (0.31 in this case);  $c_p$  [ $\text{mg} \cdot \text{mL}^{-1}$ ] ... protein concentration of MAO stock solution.

## Biotransformations

**MAO/BBE cascade transformation (time study).** In Falcon tubes (15 mL), lyophilized cells of *E. coli* C43(DE3) expressing MAO-N D11 (250 mg) were resuspended in phosphate buffer (2.25 mL; 100 mM K-phosphate, pH 7.7).  $\text{BH}_3$ -morpholine (25.3 mg, 250  $\mu\text{L}$ ; final concentration 100 mM), BBE solution (**1b**: 21  $\mu\text{L}$ , **1e**: 5.3  $\mu\text{L}$ , **1f**: 2.1  $\mu\text{L}$ , **1g**: 42  $\mu\text{L}$  of a 354  $\mu\text{M}$  preparation, final concentration: **1b**: 0.2 g/L, **1e**: 0.05 g/L, **1f**: 0.02 g/L, **1g**: 0.4 g/L) and a solution of substrate **1** (25  $\mu\text{mol}$ ; final concentration 10 mM) in DMSO (250  $\mu\text{L}$ ) were added and the mixture was shaken at 37 °C and 150 rpm. Additional  $\text{BH}_3$ -morpholine (6.3 mg) was added after 24 h, and in the case of **1b** and **1g** also after 48 h. Fresh BBE solution was added after 24 h (**1b**: 10  $\mu\text{L}$ , **1e**: 2.5  $\mu\text{L}$ , **1f**: 1.0  $\mu\text{L}$ , **1g**: 21  $\mu\text{L}$ ) and 48 h (**1b**: 5  $\mu\text{L}$ , **1g**: 10  $\mu\text{L}$ ). Samples were taken after 2, 4, 6, 8, 12, 24, and 48 h, and in the case of **1b** and **1g** also after 72 h. The samples were extracted with EtOAc ( $2 \times 500 \mu\text{L}$ ) and the extract was dried over  $\text{Na}_2\text{SO}_4$ . The solvent was evaporated under a stream of air, the samples were re-dissolved in HPLC-grade methanol (700  $\mu\text{L}$ ) and conversion as well as substrate and product *ee* were determined by HPLC analysis.

## References

- [1] a) Resch, V.; Schrittwieser, J. H.; Wallner, S.; Macheroux, P.; Kroutil, W. *Adv. Synth. Catal.* **2011**, 353, 2377–2383; b) Schrittwieser, J. H.; Resch, V.; Wallner, S.; Lienhart, W.-D.; Sattler, J. H.; Resch, J.; Macheroux, P.; Kroutil, W. *J. Org. Chem.* **2011**, 76, 6703–6714.
- [2] J. H. Schrittwieser, B. Groenendaal, S. C. Willies, D. Ghislieri, I. Rowles, V. Resch, J. H. Sattler, E.-M. Fischereder, B. Grischek, W.-D. Lienhart, N. J. Turner, W. Kroutil, *manuscript in preparation*.

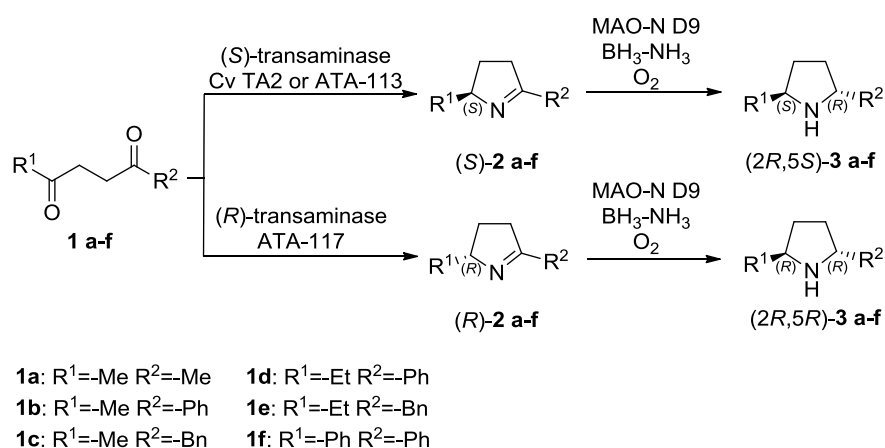


Chiral amines, such as 2,5-disubstituted pyrrolidines, were developed in 1977 by Whitesell.[1] Since then they have been widely applied to different types of enantioselective syntheses and a number of procedures using these as chiral auxiliaries have been proposed.[2] Classic syntheses of 2,5-disubstituted pyrrolidines include kinetic resolution[3] or metal catalysed enantioselective hydroamination.[4] The Turner group have previously reported the MAO-N catalysed deracemisation of a number of 2-substituted pyrrolidines, such as nicotine, with high enantiomeric excess.[5] Recently, Kroutil and co-workers demonstrated the regio- and enantioselective monoamination of 2,6 diketones for the synthesis of 1,5 disubstituted piperidines. They used transaminases for the enantioselective amination of the starting ketones followed by spontaneous cyclisation to give  $\Delta$ 1-piperidines. Pd-catalysed enantioselective hydrogenation yielded to final piperidines.[6]

In this project we investigated the combination of  $\omega$ -transaminases and monoamine oxidase-N (MAO-N) for the enantioselective synthesis of 2,5 disubstituted pyrrolidines. After synthesising a panel of 1,4 diketones,[7] they were subjected to a transamination reaction with two enantiocomplementary mutants ((*S*)-selective CvTA2 and (*R*)-selective ATA-117), to give access to both the enantiomers of the corresponding  $\Delta$ 1-pyrrolines. We then coupled MAO-N with a non-selective reducing agent ( $\text{BH}_3\text{-NH}_3$ ) to enantioselectively synthesize the final disubstituted pyrrolidines.

In an attempt to determine the substrate scope of each enzyme we decided to carry out the biotransformations in two subsequent steps. The first step was the transamination reaction, the second the MAO-N catalysed deracemisation. As shown in Table 1, the transaminases prefer small aliphatic substituents in the  $\alpha$  position to the ketone whereas monoamine oxidases prefer aromatic substituents in the  $\alpha$  position to the amine. In particular we showed that MAO-Ns have a good regioselectivity avoiding the racemisation of the stereocenter previously set in the transamination reaction. After converting **1** into **2** we decided to investigate the influence of the stereocenter on the reduction of the imine. Therefore, we subjected the  $\Delta$ 1-pyrrolines to different non-selective reducing agents such as  $\text{NaBH}_4$  and  $\text{BH}_3\text{-NH}_3$  or Pd-catalysed hydrogenation, detecting only little enantioselectivity (e.e. <10%) with  $\text{NaBH}_4$  and  $\text{BH}_3\text{-NH}_3$  or decomposition after the hydrogenation. Unfortunately, due to the substrate limitations of each enzyme, we only managed to synthesize both two enantiomers of **2b** and **2c** in good conversion and diastereomeric

excess. Only the (*S*)-selective transaminase was able to convert **1d** into **2d** (Table 1).



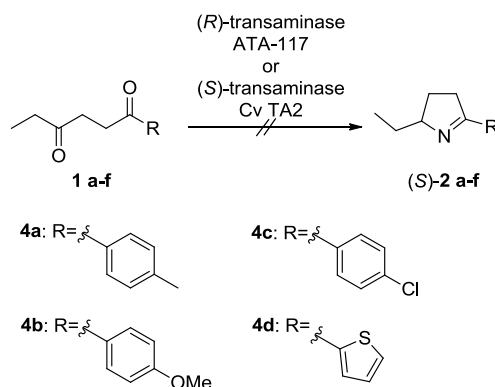
Substrate	Transaminase	e.e. <b>2</b> (%) <sup>[1]</sup>	d.e. <b>3</b> (%) <sup>[1]</sup>
<b>1a</b>	Cv TA2	n.r.	n.r. <sup>[2]</sup>
<b>1a</b>	ATA-117	n.r.	-
<b>1b</b>	Cv TA2	>99 ( <i>S</i> )	90 ( <i>2R</i> , <i>5S</i> )
<b>1b</b>	ATA-117	>99 ( <i>R</i> )	98 ( <i>2R</i> , <i>5R</i> )
<b>1c</b>	Cv TA2	>99 ( <i>S</i> )	80 ( <i>2R</i> , <i>5S</i> )
<b>1c</b>	ATA-117	>99 ( <i>R</i> )	99 ( <i>2R</i> , <i>5R</i> )
<b>1d</b>	Cv TA2	>99 ( <i>S</i> )	94 ( <i>2R</i> , <i>5S</i> )
<b>1d</b>	ATA-117	n.r.	-
<b>1e</b>	Cv TA2	n.r.	-
<b>1e</b>	ATA-117	n.r.	-
<b>1f</b>	Cv TA2	n.r.	n.r. <sup>[2]</sup>
<b>1f</b>	ATA-117	n.r.	-

**Table 1.** TA/MAO-N catalysed cascade reaction for the synthesis of 2,5-disubstituted pyrrolidines. <sup>[1]</sup>e.e. and d.e. were determined by GC analysis, n.r. is no reaction. <sup>[2]</sup>Deracemisation starting from the racemate.

Considering the good results obtained in the transamination of **1b** and the subsequent deracemisation of **2b**, we decided to scale the reaction up and carry out a biotransformation on preparative scale (50 mg), obtaining both the enantiomers of the corresponding pyrrolidine in good diastereomeric excess (Table 1). Moreover, we combined the two enzymes (*S*)-selective transaminase Cv TA2 and MAO-N D9 in a one-pot, two-steps synthesis of (*2S,5R*)-**3b** (99% d.e. after 48 h).

During this project, a few more diketones were synthesized but none of them were successfully converted to the corresponding  $\Delta^1$ -pyrroline (Scheme 1).





**Scheme 1.** Transamination of different 1,4 diketones.

In addition, 2,5-diphenyl pyrrolidine **3f** was chemically synthesised[8] and subjected to deracemisation but no reaction was detected by HPLC (Table 1).

This work is still ongoing and further experiments are being done to expand the substrate scope and optimise the reaction parameters.

## References

- [1] Whitesell, J. K.; Felman, S. W. *J. Org. Chem.* **1977**, *42*, 1663.
- [2] a) Porter, N. A.; Lacher, B.; Chang, V. H.-T.; Magnin, D. R. *J. Am. Chem. Soc.* **1989**, *111*, 8309. b) Porter, N. A.; Scott, D. M.; Lacher, B.; Giese, B.; Zeitz, H. G.; Lindner, H. J. *J. Am. Chem. Soc.* **1989**, *111*, 8311. c) Stafford, J. A.; Heathcock, C. H. *J. Org. Chem.* **1990**, *55*, 5433. d) Defoin, A.; Brouillard-Poichet, A.; Streith, J. *Helv. Chim. Acta* **1991**, *74*, 103. e) Yamazaki, T.; Welch, J. T.; Plummer, J. S.; Gimi, R. *Tetrahedron Lett.* **1991**, *32*, 4267. f) Honda, T.; Kimura, N.; Tsubuki, M. *Tetrahedron: Asymmetry* **1993**, *4*, 21.
- [3] a) D. V. Gribkov, K. C. Hultsch, *Chem. Commun.* **2004**, 730-731; b) A. Viso, N. E. Lee, S. L. Buchwald, *J. Am. Chem. Soc.* **1994**, *116*, 9373-9374.
- [4] a) M. R. Crimmin, M. Arrowsmith, A. G. M. Barrett, I. J. Casely, M. S. Hill, P. A. Procopiu, *J. Am. Chem. Soc.* **2009**, *131*, 9670-9685; b) A. L. Reznichenko, K. C. Hultsch, *Organometallics* **2010**, *29*, 24-27.
- [5] Dunsmore C. J., Carr R., T. Fleming, Turner N. J., *J. Am. Chem. Soc.* **2006**, *128*, 2224.
- [6] Simon R. C., Grischek B., Zepeck F., Steinreiber A., Belaj F., Kroutil W., *Angew. Chem. Int. Ed.* **2012**, *51*, 6713.
- [7] a) L. G. Stetter H., *Chem. Ber.* **1985**, *118*, 1115-1125; b) Z.-L. Shen, K. K. K. Goh, H.-L. Cheong, C. H. A. Wong, Y.-C. Lai, Y.-S. Yang, T.-P. Loh, *J. Am. Chem. Soc.* **2010**, *132*, 15852-15855
- [8] Sato M., Gunji Y., Ikeno T., Yamada T., *Synthesis* **2004**, 1434.

**Transaminases/monoamine oxidases  
biocatalytic cascade for the  
deracemisation of chiral  
pyrrolidines**

D. Ghislieri, J. Hopwood and E. O'Really

**Supplementary information**

## General Experimental Information and Materials

Starting materials were purchased from Acros and Sigma-Aldrich and used as received. Solvents were analytical or HPLC grade and dried over molecular sieves when necessary. Column chromatography was performed on silica gel (Sigma, 220-440 mesh).

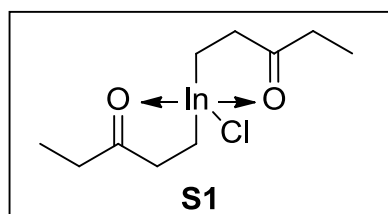
$^1\text{H}$  and  $^{13}\text{C}$  NMR spectra were recorded on a Bruker Avance 400 (400.1 MHz or 399.9 MHz for  $^1\text{H}$  and 100.6 MHz for  $^{13}\text{C}$ ) without additional internal standard. Chemical shifts are reported in  $\delta$  values (ppm) and are calibrated against residual solvent signal. The following abbreviations were used to define the multiplicities: s, singlet; d, doublet; t, triplet; q, quartet; m, multiplet; b, broad.

GC-MS spectra were recorded on a Hewlett Packard HP 6890 equipped with a HP-1MS column, a HP 5973 Mass Selective Detector and an ATLAS GL FOCUS sampling robot. GC analysis was performed on Agilent 6850 GCs equipped with a Gerstel Multipurposesampler MPS2L.

## MAO-N transformation and expression

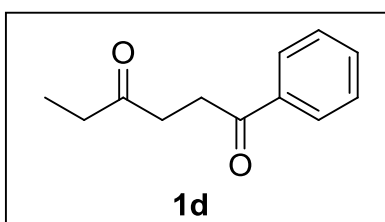
Chemically competent cells, *E. coli* strains C43(DE3), were transformed according to the manufacturer's protocol. 5 mL of LB medium (containing 100  $\mu\text{g}/\text{mL}$  of ampicillin) was inoculated from a single colony of *E. coli* C43(DE3) harbouring the [pET16b MAO-N (D9)] plasmid and the culture was grown to saturation at 30  $^\circ\text{C}$  and 120 rpm. This culture was used to inoculate 600 mL of autoinduction medium (4ZY-LAC-SUC; containing 100  $\mu\text{g}/\text{mL}$  of ampicillin) and the new culture was grown at 25  $^\circ\text{C}$  and 150 rpm for 72 h. The cells were harvested by centrifugation (8000 rpm, 20 min), resuspended in phosphate buffer (100 mM K-Pi, pH 7.7) and centrifuged again (4000 rpm, 20 min). The cell pellets were stored at  $-20$   $^\circ\text{C}$  until use.

## Synthesis of racemic intermediates and standards



**Indium homoenolate complex (S1).**[1] Under vigorously stirring, to a solution of 1-penten-3-one (1.68 g, 20 mmol) in a mixture 1:1  $\text{CH}_3\text{CN}:\text{H}_2\text{O}$  (100 mL) was added indium (1.84 g, 16 mmol) and  $\text{InCl}_3$  (1.77 g, 8 mmol). After 24 hours, the mixture was extracted with  $\text{CH}_2\text{Cl}_2$  (3 x 20 mL) and dried over  $\text{MgSO}_4$ . The organic phase was then concentrated under

vacuum to give compound **S1** (2.85 g, 17.8 mmol, 89% yield).

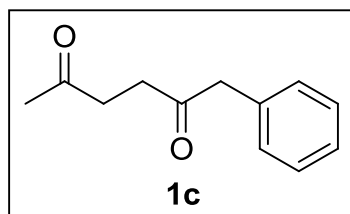


**1-phenylhexane-1,4-dione**.<sup>[1]</sup> Under nitrogen atmosphere, to a solution of **S1** (960 mg, 3 mmol) in anhydrous THF (30 mL), benzoyl chloride (700 mg, 5 mmol) and PdCl<sub>2</sub>(PPh<sub>3</sub>)<sub>2</sub> (180 mg, 0.25 mmol) were

added. The reaction mixture was stirred at reflux for 6 hours. Solvent was removed under vacuum and the residue was purified by silica gel column chromatography using Cyclohexane/EtOAc 9:1 as eluant giving compound **1d** (79 mg, 4.20 mmol, 84% yield). Analytical data matches with the literature.<sup>[1]</sup>

<sup>1</sup>H NMR (400 MHz, CDCl<sub>3</sub>) δ ppm: 8.03-7.99 (m, 2H, ArH), 7.61-7.55 (m, 1H, ArH), 7.51-7.45 (m, 2H, ArH), 3.32 (t, *J* = 6.8 Hz, 2H, COCH<sub>2</sub>CH<sub>2</sub>COAr), 2.88 (t, *J* = 6.3 Hz, 2H, COCH<sub>2</sub>CH<sub>2</sub>COAr), 2.59 (q, *J* = 7.3 Hz, 2H, CH<sub>3</sub>CH<sub>2</sub>CO), 1.12 (t, *J* = 7.3 Hz, 2H, CH<sub>3</sub>CH<sub>2</sub>CO).

<sup>13</sup>C NMR (100 MHz, CDCl<sub>3</sub>): δ ppm 210.2 (COCH<sub>2</sub>), 198.8 (COAr), 136.6 (ArC), 133.3 (ArC), 128.6 (ArC), 128.1 (ArC), 36.0 (COCH<sub>2</sub>), 35.8 (COCH<sub>2</sub>), 32.5 (COCH<sub>2</sub>), 7.9 (CH<sub>3</sub>CH<sub>2</sub>).

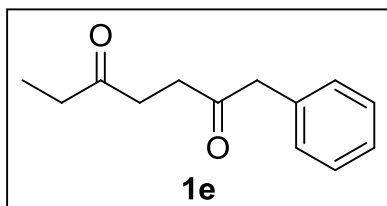


**1-phenylhexane-2,5-dione (1c)**.<sup>[2]</sup> Under nitrogen atmosphere, to a solution of phenylpyruvic acid (1 g, 6.09 mmol) in EtOH (10 mL) was added triethylamine (1.2 mL, 9.74 mmol), 1-buten-3-one (0.74 mL, 9.13

mmol) and 3-benzyl-5-(2-hydroxyethyl)-4-methylthiazolium chloride (165 mg, 0.61 mmol). The mixture was stirred at reflux for 4 hours. The solvent was removed under vacuum, then CH<sub>2</sub>Cl<sub>2</sub> (50 mL) was added and the organic phase washed with 10% H<sub>2</sub>SO<sub>4</sub> (2 x 50 mL). Solvent was removed under vacuum to give the crude compound **1c** (980 mg, 85% yield). Analytical data matches with the literature.<sup>[2]</sup>

<sup>1</sup>H NMR (400 MHz, CDCl<sub>3</sub>) δ ppm: 7.35-7.27 (m, 3H, ArH), 7.21-7.18 (m, 2H, ArH), 3.75 (s, 2H, COCH<sub>2</sub>Ph), 2.75-2.66 (m, 4H, COCH<sub>2</sub>CH<sub>2</sub>COBn), 2.17 (s, 3H, CH<sub>3</sub>CO).

<sup>13</sup>C NMR (100 MHz, CDCl<sub>3</sub>) δ ppm: 207.2 (COCH<sub>2</sub>), 207.0 (COCH<sub>2</sub>), 134.2 (ArC), 129.5 (ArC), 128.7 (ArC), 127.0 (ArC), 50.1 (CH<sub>2</sub>Ph), 37.0 (COCH<sub>2</sub>), 35.5 (COCH<sub>2</sub>), 29.9 (COCH<sub>3</sub>).

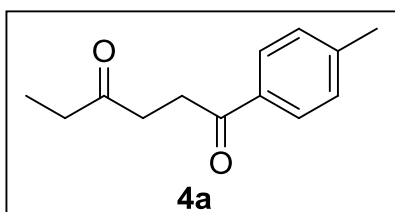


**1-phenylheptane-2,5-dione (1e).**[2] Under nitrogen atmosphere, to a solution of phenylpyruvic acid (1 g, 6.09 mmol) in EtOH (10 mL) was added triethylamine (1.2 mL, 9.74 mmol), 1-penten-3-one

(0.91 mL, 9.13 mmol) and 3-benzyl-5-(2-hydroxyethyl)-4-methylthiazolium chloride (165 mg, 0.61 mmol). The mixture was stirred at reflux for 4 hours. The solvent was removed under vacuum, then CH<sub>2</sub>Cl<sub>2</sub> (50 mL) was added and the organic phase washed with 10% H<sub>2</sub>SO<sub>4</sub> (2 x 50 mL). Solvent was removed under vacuum to give the crude compound **1e** (1.12 g, 90% yield). Analytical data matches with the literature.[2]

<sup>1</sup>H NMR (400 MHz, CDCl<sub>3</sub>) δ ppm: 7.35-7.27 (m, 3H, ArH), 7.23-7.18 (m, 2H, ArH), 3.75 (s, 2H, COCH<sub>2</sub>Ph), (2.72 (t, *J* = 6.6 Hz, 2H) and 2.65 (t, *J* = 5.7 Hz, 2H) COCH<sub>2</sub>CH<sub>2</sub>COBn), 2.45 (q, *J* = 7.3 Hz, 2H, CH<sub>3</sub>CH<sub>2</sub>CO), 1.04 (t, *J* = 7.3 Hz, 3H, CH<sub>3</sub>CH<sub>2</sub>CO).

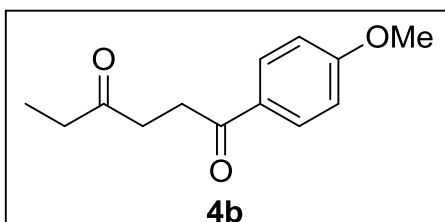
<sup>13</sup>C NMR (100 MHz, CDCl<sub>3</sub>) δ ppm: 210.0 (COCH<sub>2</sub>), 207.1 (COBn), 134.2 (ArC), 129.5 (ArC), 128.7 (ArC), 127.0 (ArC), 50.1 (CH<sub>2</sub>Ph), 35.9 (COCH<sub>2</sub>), 35.7(COCH<sub>2</sub>), 35.5 (COCH<sub>2</sub>), 7.8 (CH<sub>3</sub>CH<sub>2</sub>).



**1-(p-tolyl)hexane-1,4-dione (4a).** [1] Under nitrogen atmosphere, to a solution of **S1** (190 mg, 0.6 mmol) in anhydrous THF (6 mL), 4-methylbenzoyl chloride (132 μL, 1.0 mmol) and

PdCl<sub>2</sub>(PPh<sub>3</sub>)<sub>2</sub> (36 mg, 0.25 mmol) were added. The reaction mixture was stirred at reflux for 18 hours. Solvent was removed under vacuum and the residue was purified by silica gel column chromatography using Cyclohexane/EtOAc 9:1 as eluant giving compound **4a** (143 mg, 0.70 mmol, 70% yield). Analytical data matches with the literature.[1]

<sup>1</sup>H NMR (400 MHz, CDCl<sub>3</sub>) δ ppm: 7.90 (m, 2H, ArH), 7.27 (d, *J* = 7.5 Hz, 2H, ArH), 3.29 (t, *J* = 6.3 Hz, 2H, COCH<sub>2</sub>CH<sub>2</sub>COAr), 2.87 (t, *J* = 6.3 Hz, 2H, COCH<sub>2</sub>CH<sub>2</sub>COAr), 2.59 (q, *J* = 7.3 Hz, 2H, CH<sub>3</sub>CH<sub>2</sub>CO), 2.43 (s, 3H, CH<sub>3</sub>Ar), 1.12 (t, *J* = 7.3 Hz, 3H, CH<sub>3</sub>CH<sub>2</sub>CO)

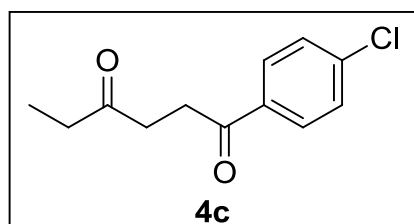


**1-(p-methoxyphenyl)hexane-1,4-dione (4b).**[1] Under nitrogen atmosphere, to a solution of **S1**

(190 mg, 0.6 mmol) in anhydrous THF (6 mL), benzoyl chloride (, 0.5 mmol) and  $\text{PdCl}_2(\text{PPh}_3)_2$  (36 mg, 0.25 mmol) were added. The reaction mixture was stirred at reflux for 18 hours. Solvent was removed under vacuum and the residue was purified by silica gel column chromatography using Cyclohexane/EtOAc 9:1 as eluant giving compound **4b** (122 mg, 0.55 mmol, 55% yield). Analytical data matches with the literature.[1]

$^1\text{H}$  NMR (400 MHz,  $\text{CDCl}_3$ )  $\delta$  ppm: 7.91 (d,  $J = 8.8$  Hz, 2H, ArH), 6.86 (d,  $J = 8.7$  Hz, 2H, ArH), 3.80 (s, 3H,  $\text{ArOCH}_3$ ), 3.18 (t,  $J = 6.3$  Hz, 2H,  $\text{COCH}_2\text{CH}_2\text{COAr}$ ), 2.78 (t,  $J = 6.4$  Hz, 2H,  $\text{COCH}_2\text{CH}_2\text{COAr}$ ), 2.50 (q,  $J = 7.3$  Hz, 2H,  $\text{CH}_3\text{CH}_2\text{CO}$ ), 1.03 (t,  $J = 7.3$  Hz, 3H,  $\text{CH}_3\text{CH}_2\text{CO}$ ).

$^{13}\text{C}$  NMR (100 MHz,  $\text{CDCl}_3$ ):  $\delta$  210.3 ( $\text{COCH}_2$ ), 197.3 ( $\text{COAr}$ ), 163.5 (ArC), 130.3 (ArC), 129.8 (ArC), 113.7 (ArC), 55.5 ( $\text{CH}_2\text{Ph}$ ), 36.1 ( $\text{COCH}_2$ ), 35.9 ( $\text{COCH}_2$ ), 32.1 ( $\text{COCH}_2$ ), 7.9 ( $\text{CH}_3\text{CH}_2$ ).

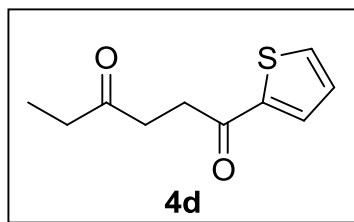


**1 - (4 - chlorophenyl) hexane -1,4 - dione (4c).**[1]

Under nitrogen atmosphere, to a solution of **S1** (190 mg, 0.6 mmol) in anhydrous THF (6 mL), 4-chlorobenzoyl chloride (129  $\mu\text{L}$ , 1.0 mmol) and  $\text{PdCl}_2(\text{PPh}_3)_2$  (36 mg, 0.25 mmol) were added. The reaction mixture was stirred at reflux for 18 hours. Solvent was removed under vacuum and the residue was purified by silica gel column chromatography using Cyclohexane/EtOAc 9:1 as eluant giving compound **4c** (210 mg, 0.95 mmol, 95% yield). Analytical data matches with the literature.[1]

$^1\text{H}$  NMR (400 MHz,  $\text{CDCl}_3$ )  $\delta$  ppm: 7.95 (d,  $J = 8.6$  Hz, 2H, ArH), 7.45 (d,  $J = 8.6$  Hz, 2H, ArH), 3.27 (t,  $J = 5.8$  Hz, 2H,  $\text{COCH}_2\text{CH}_2\text{COAr}$ ), 2.98 (t,  $J = 6.3$  Hz, 2H,  $\text{COCH}_2\text{CH}_2\text{COAr}$ ), 2.59 (q,  $J = 7.3$  Hz, 2H,  $\text{CH}_3\text{CH}_2\text{CO}$ ), 1.12 (t,  $J = 7.3$  Hz, 3H,  $\text{CH}_3\text{CH}_2\text{CO}$ ).

$^{13}\text{C}$  NMR (100 MHz,  $\text{CDCl}_3$ )  $\delta$  ppm: 210.0 ( $\text{COCH}_2$ ), 197.5 ( $\text{COAr}$ ), 139.6(ArC), 135.0 (ArC), 129.5 (ArC), 128.9 (ArC), 36.0 ( $\text{COCH}_2$ ), 35.7 ( $\text{COCH}_2$ ), 32.4 ( $\text{COCH}_2$ ), 7.8 ( $\text{CH}_3\text{CH}_2$ ).



**1-(thiophen - 2-yl) hexane -1,4 - dione (4d).**[1] Under nitrogen atmosphere, to a solution of **S1** (190 mg, 0.6 mmol) in anhydrous THF (6 mL), 2-thiophenecarbonyl chloride (107  $\mu$ L, 1.0 mmol) and PdCl<sub>2</sub>(PPh<sub>3</sub>)<sub>2</sub> (36 mg, 0.25 mmol) were added. The reaction mixture was

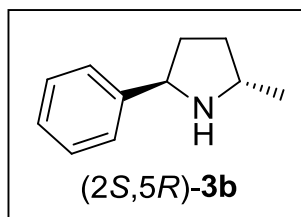
stirred at reflux for 18 hours. Solvent was removed under vacuum and the residue was purified by silica gel column chromatography using Cyclohexane/EtOAc 9:1 as eluant giving compound **4d** (151 mg, 0.84 mmol, 84% yield). Analytical data matches with the literature.[1]

<sup>1</sup>H NMR (400 MHz, CDCl<sub>3</sub>)  $\delta$  ppm: 7.77 (dd,  $J$  = 3.8, 1.1 Hz, 1H, ArH), 7.63 (dd,  $J$  = 4.9, 1.1 Hz, 1H, ArH), 7.13 (dd,  $J$  = 4.9, 3.8 Hz, 1H, ArH), 3.24 (t,  $J$  = 6.4 Hz, 2H, COCH<sub>2</sub>CH<sub>2</sub>COAr), 2.85 (t,  $J$  = 6.4 Hz, 2H, COCH<sub>2</sub>CH<sub>2</sub>COAr), 2.55 (q,  $J$  = 7.3 Hz, 2H, CH<sub>3</sub>CH<sub>2</sub>CO), 1.09 (t,  $J$  = 7.3 Hz, 3H, CH<sub>3</sub>CH<sub>2</sub>CO).

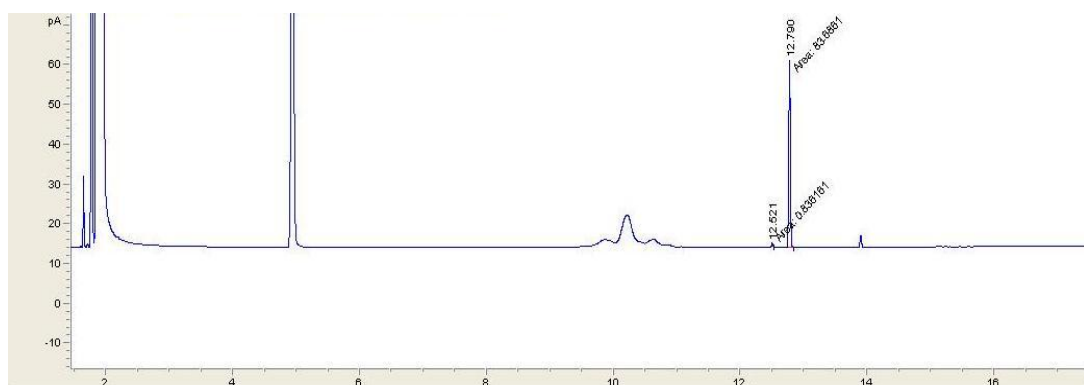
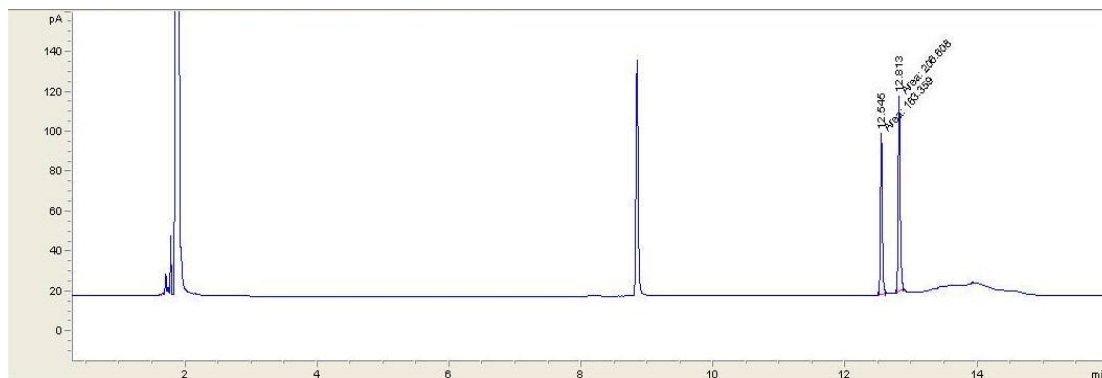
<sup>13</sup>C NMR (100 MHz, CDCl<sub>3</sub>)  $\delta$  ppm: 209.8 (COCH<sub>2</sub>), 191.7 (COAr), 143.7 (ArC), 133.5 (ArC), 132.0 (ArC), 128.1 (ArC), 36.1 (COCH<sub>2</sub>), 35.8 (COCH<sub>2</sub>), 33.0 (COCH<sub>2</sub>), 7.8 (CH<sub>3</sub>CH<sub>2</sub>).

#### **MAO-N deracemisation general procedure: Analytical Scale**

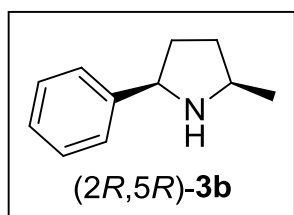
In a 2 mL Eppendorf tube, the 2,5 disubstituted pyrrolines (4.5  $\mu$ L of 1M solution in DMF), BH<sub>3</sub>-NH<sub>3</sub> (18  $\mu$ L of 1M solution in 1M KPO<sub>4</sub>-buffer, pH = 7.8) and cell pellet of MAO-N D9 from *E. coli* cultures (280  $\mu$ L of a solution 100 mg/mL in 1 M KPO<sub>4</sub>-buffer, pH = 7.8) were mixed. If necessary, the pH of the solution was adjusted to 7.8 by addition of HCl. The tube was placed in a shaking incubator and shaken at 37 °C and 250 rpm. In total 5 reactions were set up for each pyrroline. The reactions were monitored by GC with one reaction taken and worked up every 1, 3, 6, 24 and 48 hours. GC samples were prepared as follows: aqueous NaOH-solution (10  $\mu$ L, 10 M) was added to the reaction mixture in the Eppendorf tube, followed by 1 mL of CH<sub>2</sub>Cl<sub>2</sub>. After vigorous mixing, by means of a vortex mixer, the sample was centrifuged at 13200 rpm for 1 minute. The organic phase was separated, dried with MgSO<sub>4</sub> and analysed by GC.



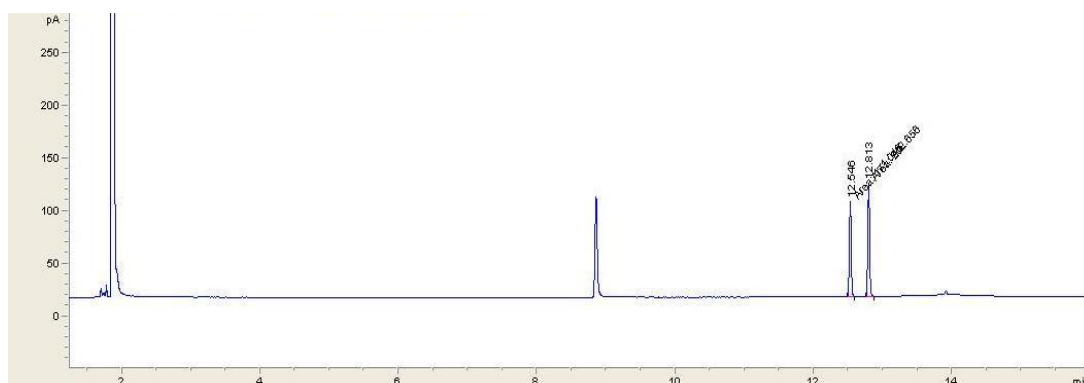
**(2S,5R)-2-methyl-5-phenylpyrrolidine (3b).** The reaction was set up as described in the general procedure using MAO-N D9 as biocatalyst. After 24 hours GC analysis showed 98% d.e.



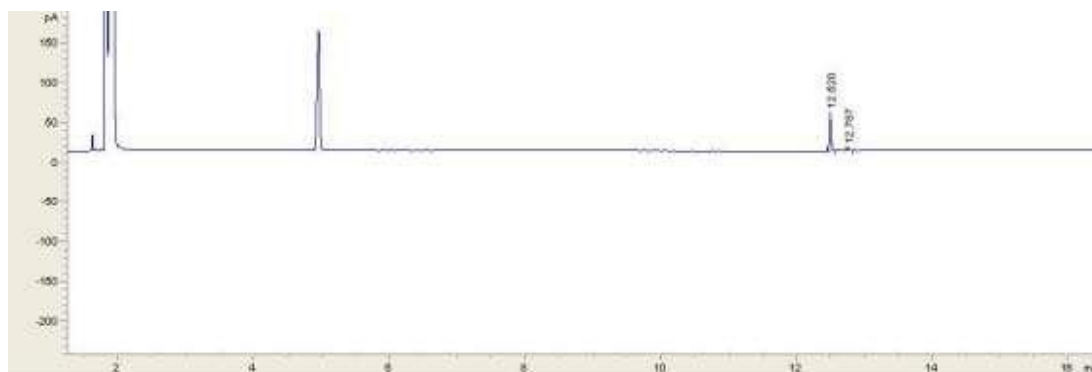
**Figure S1.** GC traces (CAM Column) of (2R,5R)-3b and (2S,5R)-3b after reduction (R)-2b with BH<sub>3</sub>-NH<sub>3</sub> (top) and after reduction with MAO-N and BH<sub>3</sub>-NH<sub>3</sub> (bottom).



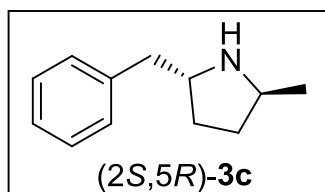
**(2R,5R)-2-methyl-5-phenylpyrrolidine (3b).** The reaction was set up as described in the general procedure using MAO-N D9 as biocatalyst. After 48 hours GC analysis showed 90% d.e.



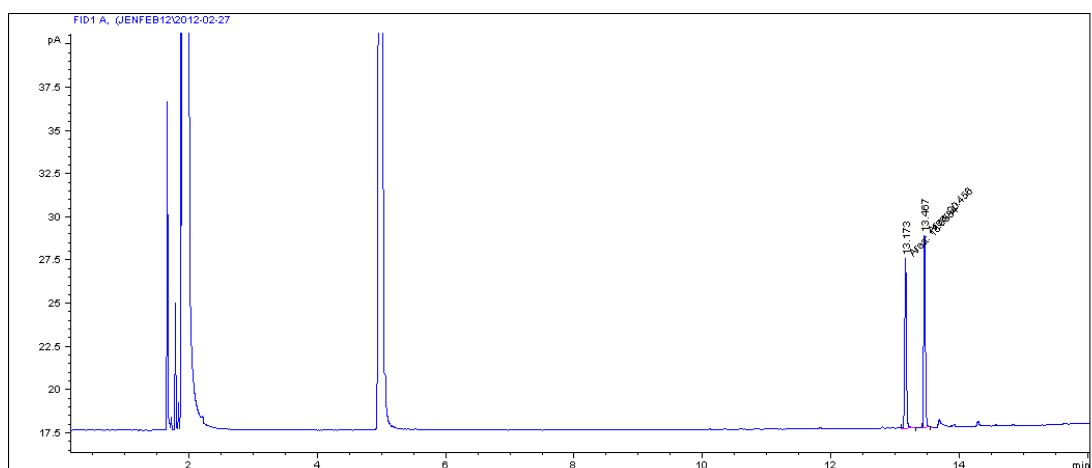


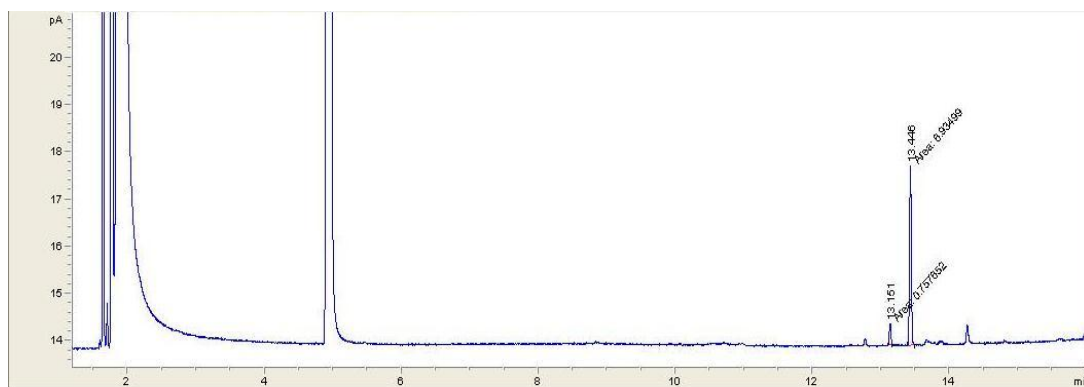


**Figure S2.** GC traces (CAM Column) of (2*R*,5*R*)-**3b** and (2*S*,5*R*)-**3b** after reduction (*S*)-**2b** with BH<sub>3</sub>-NH<sub>3</sub> (top) and after reduction with MAO-N and BH<sub>3</sub>-NH<sub>3</sub> (bottom).

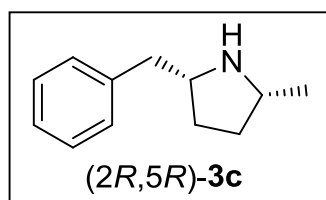


(2*S*, 5*R*) - 2 - methyl - 5 - benzylpyrrolidine (**3c**). The reaction was set up as described in the general procedure using MAO-N D9 as biocatalyst. After 6 hours GC analysis showed 80% d.e.

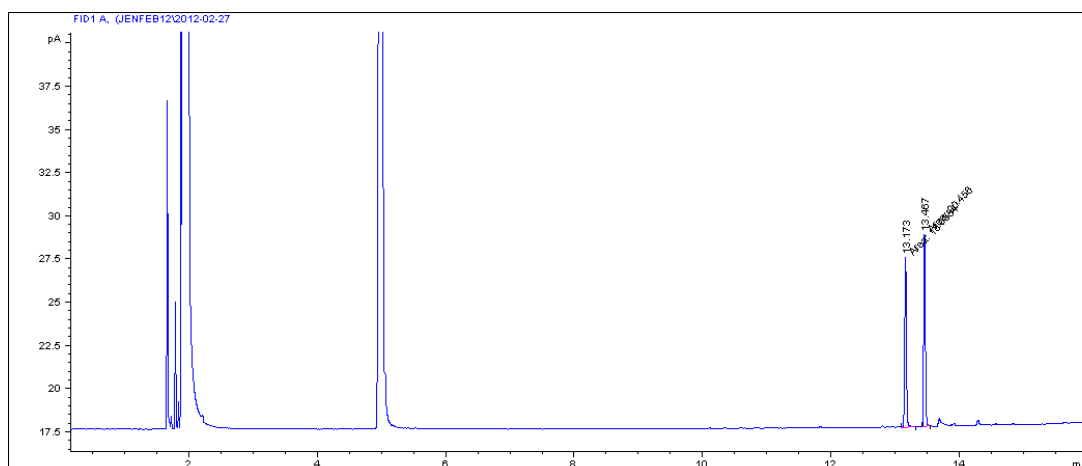


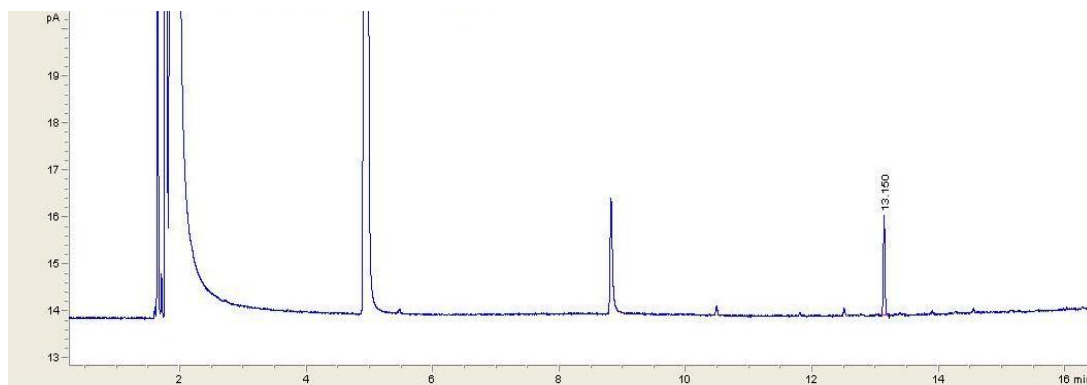


**Figure S3.** GC traces (CAM Column) of (2*R*,5*R*)-**3c** and (2*S*,5*R*)-**3c** after reduction with MAO-N and BH<sub>3</sub>-NH<sub>3</sub>.

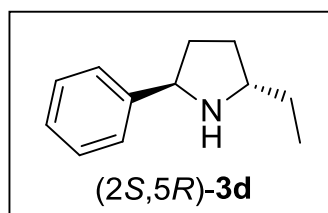


(2*R*, 5*R*) - 2 - methyl - 5 - benzylpyrrolidine (**3c**). The reaction was set up as described in the general procedure using MAO-N D9 as biocatalyst. After 3 hours GC analysis showed 99% d.e.

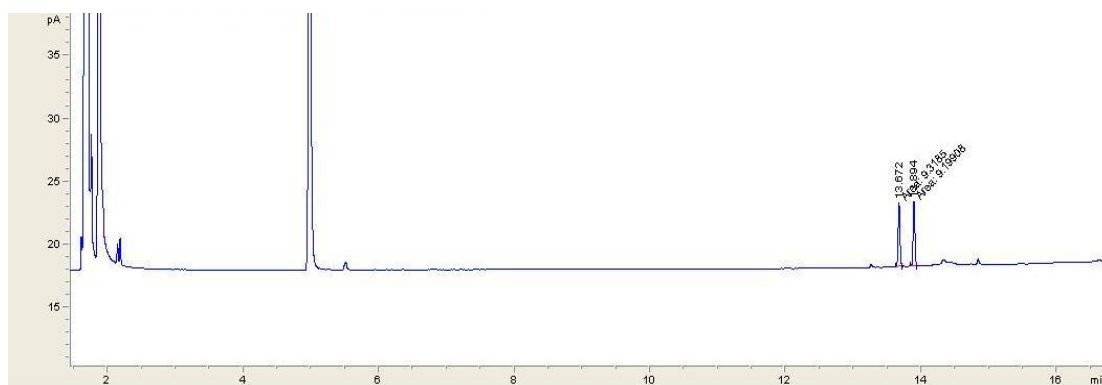


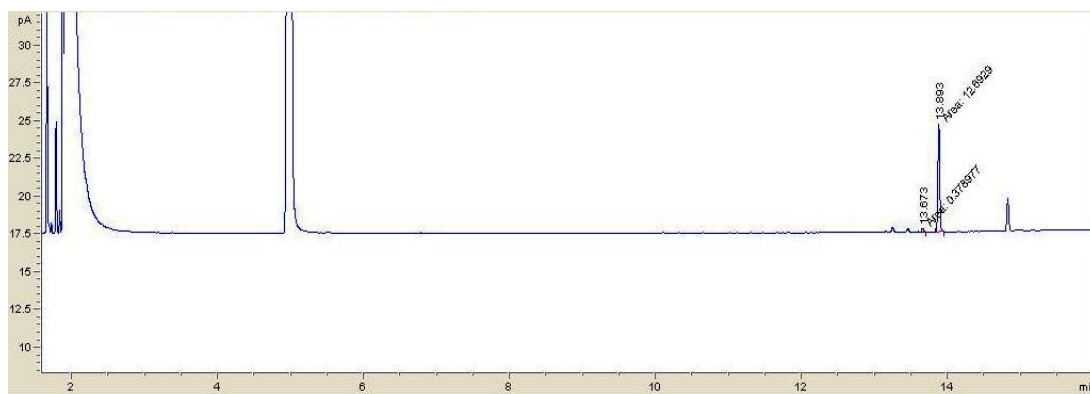


**Figure S3.** GC traces (CAM Column) of (2*R*,5*R*)-**3c** and (2*S*,5*R*)-**3c** after reduction with MAO-N and  $\text{BH}_3\text{-NH}_3$ .



**(2*S*,5*R*)-2-ethyl-5-phenylpyrrolidine (**3d**).** The reaction was set up as described in the general procedure using MAO-N D9 as biocatalyst. After 24 hours GC analysis showed 94% d.e.

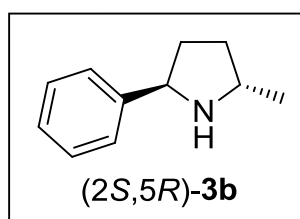




**Figure S4.** GC traces (CAM Column) of (2*R*,5*R*)-**3d** and (2*S*,5*R*)-**3d** after reduction (*S*)-**2b** with BH<sub>3</sub>-NH<sub>3</sub> (top) and after reduction with MAO-N and BH<sub>3</sub>-NH<sub>3</sub> (bottom).

#### MAO-N deracemisation of (2-methyl-5-phenyl)pyrrolidine: Preparative Scale

In a 50 mL Falcon tube, **2b** (135  $\mu$ L of 1M solution in DMF), BH<sub>3</sub>-NH<sub>3</sub> (540  $\mu$ L of 1 M solution in 1M KPO<sub>4</sub>-buffer, pH = 7.8) and cell pellet from *E. coli* cultures (8.4 mL of a solution 100 mg/mL in 1 M KPO<sub>4</sub>-buffer, pH = 7.8) were mixed. If necessary, the pH of the solution was adjusted to 7.8 by addition of HCl. The tube was placed in a shaking incubator and shaken at 37 °C and 250 rpm. After 24 hours the work up was performed in the following way, aqueous NaOH-solution (100  $\mu$ L, 10 M) and CH<sub>2</sub>Cl<sub>2</sub> (20 mL) were added. The reaction mixture was vigorously mixed and the two layers separated by centrifugation at 4000 rpm and 4 °C for 5 minutes. The aqueous phase was extracted again with CH<sub>2</sub>Cl<sub>2</sub> (20 mL). The combined organic phases were dried with MgSO<sub>4</sub> and concentrated at the rotary evaporator.

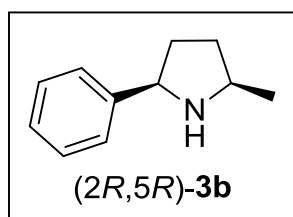


**(2*S*,5*R*)-2-methyl-5-phenylpyrrolidine (**3b**).** The reaction was set up as described in the general procedure using MAO-N D9 as biocatalyst. After work-up (2*S*,5*R*)-**3b** was obtained as colourless liquid (18 mg, 82% yield).  $[\alpha]_{\text{D}}^{20}$ : -32.9 ° ( $c = 1.0$ , CH<sub>2</sub>Cl<sub>2</sub>). The analytical data matched with the literature.[3]

<sup>1</sup>H NMR, 400 MHz, CDCl<sub>3</sub>  $\delta$  ppm: 7.37-7.32 (m, 2H, ArH), 7.31-7.25 (m, 2H, ArH), 7.20-7.15 (m, 1H, ArH), 4.27 (t,  $J = 7.5$  Hz, 1H, -CHPh), 3.40-3.31 (m, 1H, CHCH<sub>3</sub>), 3.30 (bs, 1H, NH), 2.22 (ddd,  $J = 11.8, 7.6, 3.7$  Hz, 1H, -CHHCHPh), 1.97 (ddd,  $J = 14.8, 9.6, 3.2$  Hz, 1H, -CHHCHPh), 1.61-1.48 (m, 1H, -CHHCHCH<sub>3</sub>), 1.37-1.24 (m, 1H, -CHHCHCH<sub>3</sub>), 1.12 (d,  $J = 6.3$  Hz, 3H, -CH<sub>3</sub>).

<sup>13</sup>C NMR, 100 MHz, CDCl<sub>3</sub>  $\delta$  ppm: 145.9 (ArC), 128.3 (ArC), 126.5 (ArC), 126.2

(ArC), 61.5 (CHPh), 54.0 (CHCH<sub>3</sub>), 35.5 (CH<sub>2</sub>), 34.8 (CH<sub>2</sub>), 22.2 (CH<sub>3</sub>).

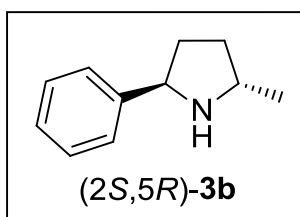


**(2R,5R)-2-methyl-5-phenylpyrrolidine (3b).** The reaction was set up as described in the general procedure using MAO-N D9 as biocatalyst. After work-up (2R,5R)-**3b** was obtained as a colorless liquid (14 mg, 64% yield).  $[\alpha]_D^{20}$ : +30.7 ° (c = 1.0, CH<sub>2</sub>Cl<sub>2</sub>) The analytical data matched with the literature.[4]

<sup>1</sup>H NMR, 400 MHz, CDCl<sub>3</sub> δ ppm: 7.38-7.34 (m, 2H, ArH), 7.31-7.25 (m, 2H, ArH), 7.21-7.16 (m, 1H, ArH), 4.04 (t, J = 7.9 Hz, 1H, -CHPh), 3.28-3.13 (m, 1H, CHCH<sub>3</sub>), 2.13-2.00 (m, 1H, -CHHCHPh), 1.91-1.81 (m, 1H, -CHHCHPh), 1.57-1.40 (m, 1H, -CHHCHCH<sub>3</sub>), 1.37-1.27 (m, 1H, -CHHCHCH<sub>3</sub>), 1.14 (d, J = 6.1 Hz, 3H, -CH<sub>3</sub>).

<sup>13</sup>C NMR, 100 MHz, CDCl<sub>3</sub> δ ppm: 145.0 (ArC), 128.5 (ArC), 126.9 (ArC), 126.8 (ArC), 63.2 (CHPh), 54.9 (CHCH<sub>3</sub>), 34.4 (CH<sub>2</sub>), 33.7 (CH<sub>2</sub>), 21.8 (CH<sub>3</sub>).

#### TA/MAO-N tandem biocatalytic reaction



**(2S,5R)-2-methyl-5-phenylpyrrolidine (3b).** In a 50 mL Falcon tube, 1-Phenylpentane-1,4-dione (100 mg, 0.57 mmol) was dissolved in DMSO (3 mL) and added to a solution containing CvTA2 and the GDH recycling system (100 mM HEPES-buffer, pH = 7.8, 12 mL). The tube was placed in a shaking incubator and shaken at 37 °C and 250 rpm. After 24 hours BH<sub>3</sub>-NH<sub>3</sub> (78 mg, 2.28 mmol) and cell pellet from *E. coli* cultures (2.4 g) were added and the tube was placed in a shaking incubator for further 24 hours. Aqueous NaOH-solution (100 μL, 10 M) and CH<sub>2</sub>Cl<sub>2</sub> (20 mL) were added. The reaction mixture was vigorously mixed and the two layers separated by centrifugation at 4000 rpm and 4 °C for 5 minutes. The aqueous phase was extracted again with CH<sub>2</sub>Cl<sub>2</sub> (20 mL). The combined organic phases were dried with MgSO<sub>4</sub> and concentrated at the rotary evaporator to give (2S,5R)-**3b** as a colorless liquid (27 mg, 29% yield).

#### References

- [1] Z.-L. Shen, K. K. K. Goh, H.-L. Cheong, C. H. A. Wong, Y.-C. Lai, Y.-S. Yang, T.-P. Loh, *J. Am. Chem. Soc.* **2010**, *132*, 15852-15855.
- [2] L. G. Stetter H., *Chem. Ber.* **1985**, *118*, 1115-1125.
- [3] D. V. Gribkov, K. C. Hultsch, F. Hampel, *J. Am. Chem. Soc.* **2006**, *128*,

3748-3759.

[4] D.-S. Wang, Z.-S. Ye, Q.-A. Chen, Y.-G. Zhou, C.-B. Yu, H.-J. Fan, Y. Duan, *J. Am. Chem. Soc.* **2011**, *133*, 8866-8869.

## METHODS

### **Preparation of plasmid DNA from *E. coli***

Plasmid DNA was isolated from a 5 mL *E. coli* (XL1-Blue, BL21 or C43) overnight culture using the QIA miniprep kit as described by the manufacturer's protocol. Routinely 30-50  $\mu\text{L}$  of ddH<sub>2</sub>O was used to elute the plasmid from the column.

### **DNA concentration determination**

DNA concentration was estimated from the absorbance at 260 nm. DNA purity was determined from the control measurement at  $\lambda = 280$  nm. For pure DNA the 260/280 value is 1.8. Values significantly lower than this indicate contamination of the sample.

### **DNA sequencing**

Plasmid DNA was isolated and the concentration determined. Then, the isolated plasmid DNA was sent to GATC Biotech (<http://www.gatc-biotech.com>) for sequencing.

### **QuikChange site-directed mutagenesis**

**Primer sequences:** The mutagenic oligonucleotide primers containing the NNS site(s) were diluted to a concentration of 100 ng/ $\mu\text{L}$  in water. The final concentration in the reaction was 2.6 ng/ $\mu\text{L}$ .

**Mutant strand synthesis PCR:** The reaction was prepared in thin walled PCR tubes containing the reagents shown in Table 1. For the PCR reaction, plasmid DNA was freshly isolated from *E. coli* XL1-Blue cells.

Reagents	Volume
10x Reaction buffer	5 $\mu$ L
ds DNA template (50 ng)	0.5-2 $\mu$ L
Oligonucleotide primer #Forward	3 $\mu$ L
Oligonucleotide primer #Reverse	3 $\mu$ L
dNTP mix (10 mM each)	1 $\mu$ L
ddH <sub>2</sub> O	Adjust to a final volume of 50 $\mu$ L
<i>Pfu</i> Turbo DNA polymerase (2.5 U/ $\mu$ L)	1 $\mu$ L -added immediately before PCR started

**Table 1.** Site-directed mutagenesis PCR reaction mix

The PCR cycle program was as follows:

95°C	1 min	1x
95°C	1 min	
55°C	1 min	30x
68°C	16 min	
4°C	hold	

**DNA digestion:** The *Dpn*I endonuclease is specific for methylated and hemimethylated DNA and is used to digest the parental DNA template and to select for mutation-containing synthesised DNA. DNA isolated from almost all *E. coli* strains is methylated and therefore susceptible to *Dpn*I digestion.

1  $\mu$ L of *Dpn*I restriction enzyme was added to the mixture of DNA, according to the manufacturer's protocol. The digestion of methylated, nonmutated parental DNA template was performed at 37°C for 60 min.

**Nick repair after transformation of XL1-Blue competent cells:** After transformation, the XL1-Blue cells repaired the nicks in the mutated plasmid DNA after site-directed mutagenesis PCR and digestion with *Dpn*I. The 200  $\mu$ L shot was divided into 50  $\mu$ L samples in pre-chilled falcon tubes and 1  $\mu$ L of *Dpn*I digested PCR product was added to each tube. The tube was gently tapped to mix the contents and incubated on ice for 10 min. The tubes were placed at 42 °C for 30 seconds (s) and incubated on ice for 2 min. 900  $\mu$ L of pre-warmed SOC medium (37 °C) was added to each tube and the samples were shaken at 225 rpm and 37 °C for 1 hour (h). 100  $\mu$ L of the saturation library transformation was spread onto LB/Amp agar plates



and incubated at 37 °C overnight.

**Verification of representation of mutagenesis:** To verify the success of the mutagenesis experiment, 10 colonies were randomly picked from the XL1-Blue library and grown overnight in 5 mL LB/Amp at 225 rpm and 37 °C. The plasmid was isolated and the DNA was sent for sequencing.

**Isolation of plasmid DNA from multiple colonies on agar plates:** 5 mL of LB was added to a plate containing the transformed clones. With a spreader the colonies were directly resuspended on the plate, transferred into a falcon tube and centrifuged at 4000 rpm for 20 min. The supernatant was discarded and the plasmid DNA was isolated and stored at -20°C.

### **Transformation protocols**

**XL1-Blue chemically competent cells:** One Shot XL-1 Blue competent cells (50 µL of cells) were thawed on ice and mixed directly with 0.5-2 µL of plasmid DNA. The mixture was stored on ice for 2-5 min, then incubated for 30 s at 42 °C and returned to ice for 2 min. 250 µL of SOC medium (at room temperature) was added. The vials were left shaking at 37 °C for 1 h at 225 rpm. 100 µL of each transformation was spread onto LB/Amp agar plates and incubated overnight at 37°C.

A single colony was picked and plasmid DNA for saturation mutagenesis PCR reactions was isolated from an overnight culture.

**E. coli BL21 chemically competent cells:** One Shot BL21 competent cells were used to produce MAO-N. 1-2 µL of plasmid DNA and a single shot (50 µL) of *E. coli* BL21 chemically competent cells were thawed on ice. The transformation was carried out in the same way as described for *E. coli* XL1-Blue.

**E. coli C43 chemically competent cells:** One Shot C43 competent cells were used to produce MAO-N. 1-2 µL of plasmid DNA and a single shot (50 µL) of *E. coli* C43 chemically competent cells were thawed on ice. The transformation was carried out in the same way as described for *E. coli* XL1-Blue.

### **Purification of MAO-N**

All subsequent steps were performed at 4°C.

**Preparation of cell-free extracts:** 5 g of frozen cell paste was thawed on ice and resuspended in 25 mL of phosphate buffer (100 mM K-Pi, pH 7.7; containing 1

mg/mL of lysozyme) and incubated at 30 °C for 30 min. The suspension was cooled to 4 °C and cells were lysed by ultrasonication (30 s pulse, 30 s pause; 15 cycles). Cell debris was removed by centrifugation (20000 rpm, 40 min). Subsequently, the cell-free extracts were filtered through a syringe filter with a 0.22 µm pore size.

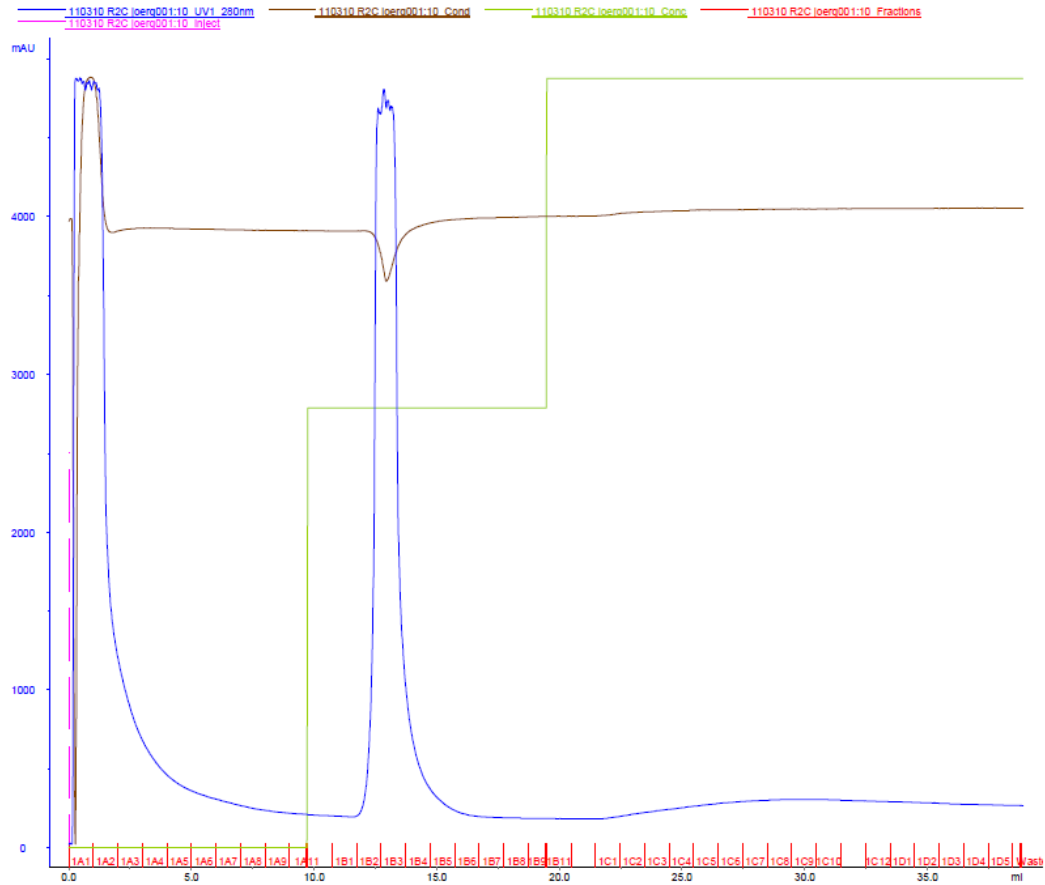
**Ni-chelating protein purification system:** Recombinant MAO-N contains a 10x His-tag and can therefore be purified by Ni chelating chromatography, which is based on the interaction between a transition Ni<sup>2+</sup> ion immobilized on a matrix and the histidine side chains. The tag enables purification of the recombinant protein product.

Before the purification, the following stock solutions were prepared:

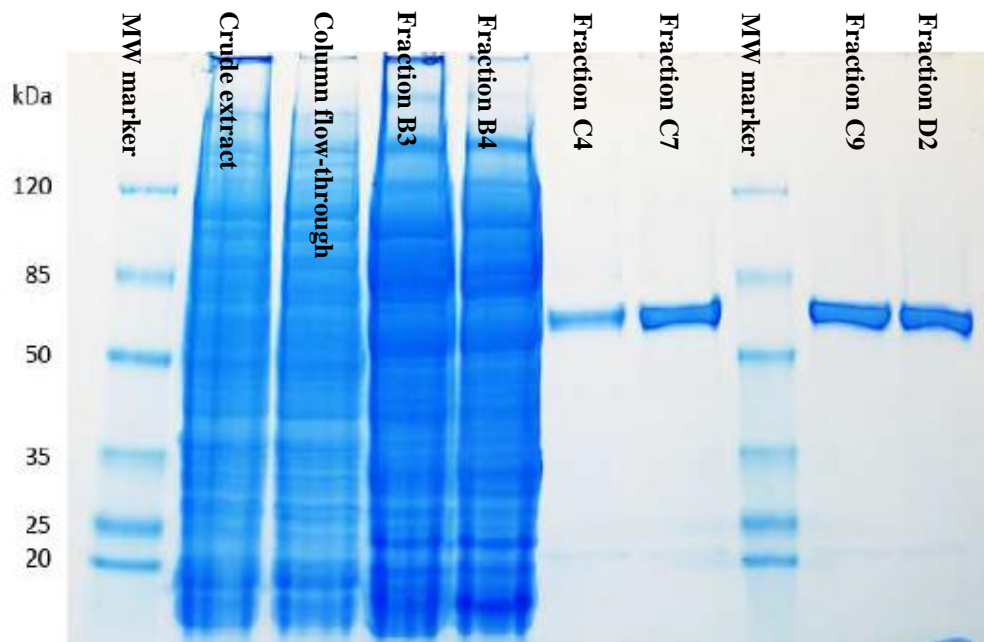
Buffer A: 100 mM K-Pi, pH 7.7, 300 mM NaCl

Buffer B: 100 mM K-Pi, pH 7.7, 300 mM NaCl, 1 M imidazole

The cell free extract, after filtration, was loaded onto a HisTrap Ni-sepharose column (1 mL, *GE Healthcare*) pre-equilibrated with buffer A. The column was loaded in the Äkta explorer system from GE Healthcare and the proteins were step-eluted using buffer A (10 mL), buffer A / buffer B = 80/20 (10 mL) and buffer A / buffer B = 65/35 (10–30 mL); collecting 1 mL fractions. The MAO-containing fractions (from the 35% buffer B step) were pooled and concentrated using a *Sartorius Vivaspin 6* spin column (30 kDa mass cut-off), the volume was adjusted to 2.5 mL and the protein solution was desalted using a PD-10 column.



**Figure 1.** FPLC-chromatogram from Ni-affinity purification of MAO-N variant D11C. Blue line is the absorbance at 280 nm; green line is the Buffer B concentration; brown line is the conductivity. MAO-N eluted in fractions C1–D6.

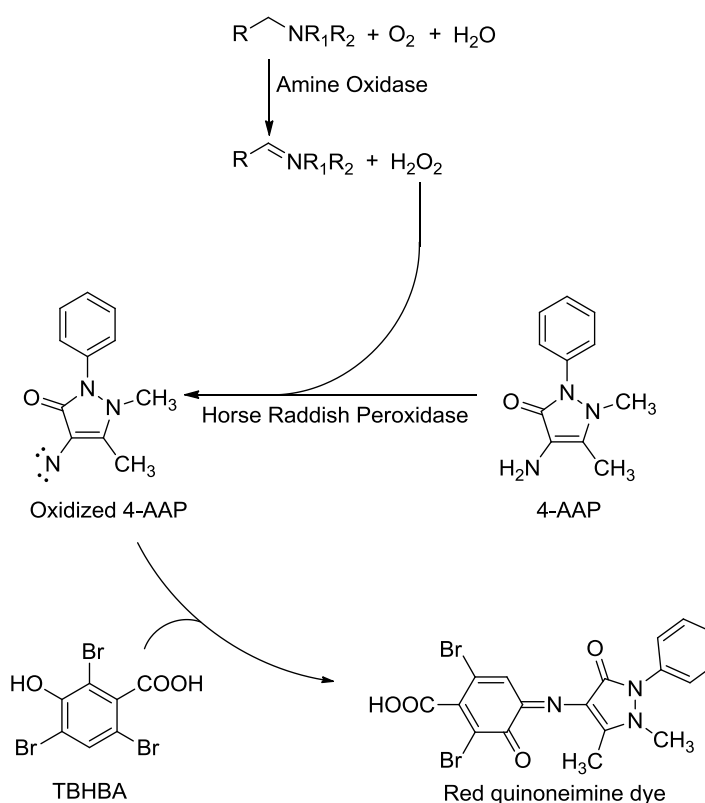


**Figure 2:** SDS-gel of MAO-N variant D11C purification.

**PD-10 protein desalting:** The concentrated fractions that had eluted at 350 mM imidazole concentration were desalted using PD-10 Sephadex columns. Per column, 2.5 mL protein sample could be desalted. Each column was pre equilibrated by washing with 25 mL of buffer A. 2.5 mL protein sample was then applied and the flow through was discarded. The desalted protein sample was eluted with 3.5 mL buffer A.

### Liquid phase screening of MAO-N variants

A coupled assay was used in order to evaluate which MAO-N variant was active toward the different compounds and to determine relative reaction rate. This assay is robust rapid, highly quantitative, reasonably sensitive, inexpensive and suitable for automation. In the presence of a suitable amine substrate, amine oxidase enzymes generate hydrogen peroxide, which then drives the peroxidase-dependent oxidation of 4-aminoantipyrine (4-AAP). A subsequent interaction with 2,4,6-tribromo-3-hydroxybenzoic acid (TBHBA) generates stoichiometric amounts of a red quinoneimine dye, the formation of which is monitored at 510 nm (Scheme 1).[1]



**Scheme 1.** MAO-N/HRP coupled assay mechanism

With this colorimetric assay, taking the linear and early part of the graphs ( $V_{max}$ , where there is no limiting substrate) it is possible to know if the monoamine oxidases are active toward a certain substrate and subsequently calculate the relative activities.

### **Reference**

- [1] A. Holt, M. M. Palcic, *Nat. Protoc.* **2006**, *1*, 2498-2505.

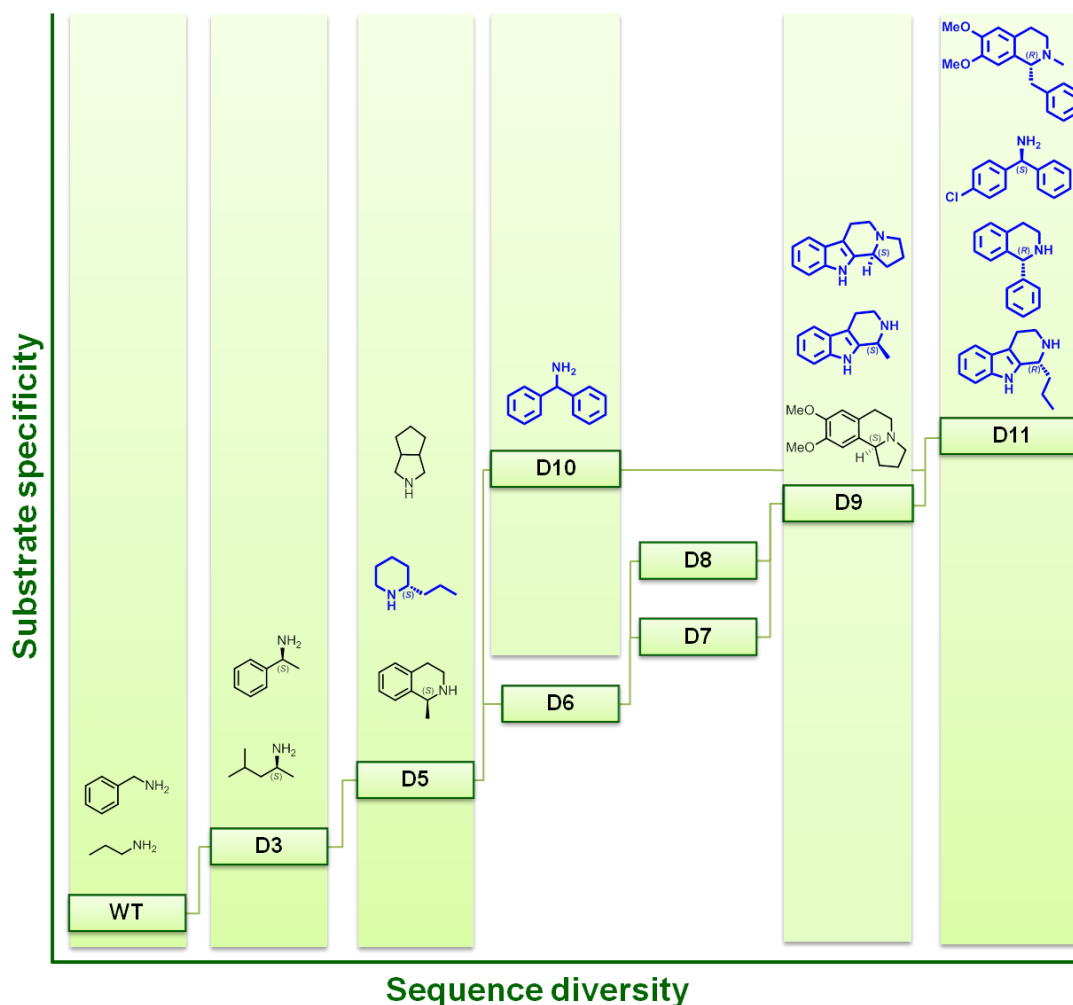
## CONCLUSIONS AND OUTLOOK

### Conclusions

The aim of this project was to address the limitation of MAO-N in substrate specificity, find novel classes of substrates which could be deracemised, and, then, combine the MAO-N mutants with other bio/chemo-catalysts for the synthesis of chiral amines.

To achieve this goal, we engineered a new MAO-N variant with increased substrate scope and enhanced tolerance for bulky substrates such as aminodiphenylmethane and 1-phenyltetrahydroisoquinoline. Application of these engineered biocatalysts was highlighted by the asymmetric synthesis of the generic drugs Solifenacin and Levocetirizine. It was also demonstrated that the panel of MAO-N variants developed in our laboratory is able to mediate the deracemisation of primary, secondary and tertiary amines which are included in important classes of biologically active alkaloid natural products (tetrahydroisoquinolines, tetrahydro- $\beta$ -carboline and piperidines). We have also explored a novel method, distinct from deracemisation and desymmetrisation, to use MAO-N for the synthesis of chiral amines. In particular, we developed a MAO-N mediated asymmetric oxidative Pictet-Spengler approach for the synthesis of (*R*)-harmicine, which employs the MAO-N catalyzed formation of a reactive iminium ion that undergoes spontaneous cyclisation.

In this work a new MAO-N mutant (D11) showed (*R*)-selectivity toward a certain class of compounds, therefore we synthesized a broad range of 1-substituted tetrahydro- $\beta$ -carboline in order to investigate the switch in enantioselectivity. Experimental and modelling data highlighted a relation between lipophilicity of the substituents and enantiopreference of the enzyme.



**Figure 1.** Representative examples of structural classes that can be oxidised/deracemised by different MAO-N mutants. Substrates highlighted in blue represent previously unreported compounds which are oxidised by MAO-N.

We then demonstrated the broad applicability of our biocatalyst in cascade reactions, combining MAO-N with other biocatalysts. In this thesis, is reported a concurrent redox cascade for the deracemisation of pyrrolidines and tetrahydroisoquinolines using our MAO-N with a biotinylated Ir-complex within streptavidin (SAV). To achieve the final goal it was necessary to shield the metal inside a host to avoid the mutual inactivation of the two catalysts. Having demonstrated the ability of MAO-N to deracemise 1-benzyl-tetrahydroisoquinoline and berberine bridge enzyme (BBE) to catalyze the synthesis of tetrahydroprotoberberines, we have described the combination of MAO-N with BBE for the one-pot synthesis of berbines, which represent a sub-class of tetrahydro-isoquinoline alkaloids found in various plants. This bi-enzymatic cascade allowed the synthesis of these structures achieving a theoretical 100% yield instead of the 50% given by the kinetic resolution using BBE

itself. Still ongoing is the combination of MAO-N with transaminases; preliminary results have shown the possibility of combining these two enzymes in a one-pot two-step biotransformation but more substrates have to be synthesized in order to explore the substrate scope of this cascade reaction.

## Outlook

The recent application of MAO from *Aspergillus sp.* in an industrial manufacturing process developed by Codexis and Merck for the desymmetrisation of a prochiral amine to produce a key intermediate in the synthesis of the Hepatitis C drug Boceprevir, highlighted the application of MAO-N in an industrial manufacturing process. The increasing demand for enhanced efficiency and 'green technologies' in the pharmaceutical and fine chemical industries will help the widespread application of these enzymes for chiral amine synthesis both in industrial and academic laboratories. Further development of this project could be on the discovery of new monoamine oxidases with opposite enantioselectivity either by identifying novel activities, possibly by exploring other species of organisms, or by using protein engineering to attempt to switch the selectivity of one of our mutants.

Moreover, we have shown that monoamine oxidases have great potential to become the catalysts of choice in synthetic laboratories for the generation of imines and iminium ions from amines, a transformation which is often challenging using traditional chemical reagents. Regarding this application, a lot of work was done on the MAO-N catalyzed synthesis of cyclic imines (building blocks for the synthesis of Hepatitis C drugs), but the generation of reactive iminium ions for a Pictet-Spengler reaction is still a relatively unexplored field.

MAO-Ns were successfully combined with other chemo- and biocatalysts with the aim to synthesize chiral amines starting from racemic or achiral compounds. The next step in this project could be the combination of our enzymes with imine reductase (IRED) avoiding the use of a non-selective reducing agent in the deracemisation process. In addition it may be possible to co-produce different enzymes (MAO-N and IRED or BBE) in *E.coli* leading to a more efficient biocatalytic cascade.